U.S. DEPARTMENT OF THE INTERIOR
U.S. GEOLOGICAL SURVEY

Laboratory Studies Of Selected Core Samples From A/M area, Savannah River Site, South Carolina.

by
Robert J. Horton

USGS Branch of Geophysics
Box 25046, MS 964
Denver Federal Center, Denver, CO.

USGS Open-File Report 96-699

Executive Summary

Laboratory investigations were conducted to determine the composition and electrical properties of clay bearing sediments present in the A/M area at the Department of Energy Savannah River Site (SRS) in South Carolina. Manufacturing operations at the SRS facility have resulted in the release of DNAPL (dense non-aqueous phase liquids) into the subsurface. The laboratory studies included X-ray diffraction (XRD) measurements, clay-organic reaction experiments and complex resistivity (CR) measurements. This work is part of a USGS project to determine the applicability of geophysical methods in subsurface DNAPL detection. The clay minerals present in the subsurface at A/M area play an important role in the migration, distribution, and geophysical detection of the DNAPL.

Twenty two core samples from the A/M area were analyzed using x-ray diffraction methods to determine the type and distribution of clay minerals present. The core samples, thought to be representative of typical of A/M area near surface sediments, were obtained from 4 drillholes including MSB-3B, MHT-17C, MHT-20C and MSB-79C. Clay minerals identified in the core samples include smectite, kaolinite, illite, and possibly vermiculite. Halloysite, although reported at SRS, was not observed in these SRS samples.

Kaolinite and illite were the most commonly observed clays in the SRS samples. Kaolinite was observed in all 22 core samples, and was generally the most abundant clay in a given sample. Illite was observed in 21 of the samples, and is thought to occur in relatively small amounts.

Swelling clays were observed in 9 samples. Swelling clays are significant because of their unique chemical and electrical properties. The swelling clays present are thought to include smectite and vermiculite, however, analytical methods to specifically identify vermiculite have not been applied to the SRS samples. In 6 of the samples the swelling clay represents a significant component of the clay minerals present. In 3 of the samples, the swelling clay appeared to be a minor component.

The XRD data indicates that the clays present in the Upland Unit and the Tobacco Road Sand include kaolinite and illite. The clay minerals identified in the Dry Branch, Santee and Warley Hill Formations include smectite, kaolinite, and illite. The "tan clay zone" is composed of a swelling clay, possibly vermiculite, and kaolinite with minor amounts of illite. The "green clay zone" is composed of smectite, kaolinite, and minor illite.

Clay-organic experiments were conducted to determine if the clay minerals present at A/M area react with PCE and TCE.

Reference clay standards and clay sediment samples from A/M area cores were exposed to PCE and TCE and analyzed using XRD to determine if clay-organic complexes had formed. In addition, halloysite was exposed to isopropyl alcohol to determine if it would modify the clays crystal structure.

Reference clay samples of illite, kaolinite and Ca- and Na-montmorillonite were exposed to PCE and TCE. These experiments were performed using 100% pure clay sample saturated with 100% organic solvent. The illite and kaolinite samples did not appear to form clay-organic complexes. However, both montmorillonites, Na and Ca, appeared to react with the solvents, forming clay-organic complexes.

Six A/M area core samples containing swelling clay (smectite and/or vermiculite) were exposed to the vapor phase of TCE and PCE. Four samples reacted with TCE vapor, as indicated by an increase in d-spacing. One sample swelled due to PCE exposure, another appears to have dehydrated during the experiment. Two samples have inconclusive results. The kaolinite and illite clay present in the A/M area samples were not affected by the solvent exposures.

Complex resistivity (CR) measurements were made on splits of the same A/M area samples used for the XRD measurements. The purpose of the CR measurements was to characterize the electrical properties of the SRS A/M area sediments, and determine if CR measurements could be used to differentiate DNAPL contaminated sediments from non-contaminated sediments. The samples were measured in their "as received" condition. In addition, the resistivity of some samples were measured as a function of water weight percent. The "as received" measurements provide baseline CR data for comparison with water saturated and DNAPL exposed measurements.

The resistivities of the SRS samples ranged from 30 to 18,500 ohm-m. The "as received" resistivities vary due to the amount of water present in the samples and due to different sediment composition. In general, dry sandy samples had the highest resistivities where as moist clayey sediments had the lowest resistivities. The CR data indicates that samples containing swelling clay minerals (smectite and/or vermiculite) generally have lower resistivities than samples composed of non-swelling clays (kaolinite and illite). The CR data also indicates that the resistivity is not dependent upon the amount of clay present in the samples. Additional CR measurements are required to determine if the electrical properties of the SRS sediments are modified by clay-organic reactions with the solvents present at A/M area.

Section 1

X-Ray Diffraction Studies of Selected Core Samples From A/M area, Savannah River Site, South Carolina.

Introduction

This section of the report describes the results of x-ray diffraction (XRD) studies to determine the type and distribution of clay mineral present in the A/M area at the Department of Energy Savannah River Site in South Carolina. Manufacturing operations at the SRS facility have resulted in the release of organic solvents known as DNAPL (dense non-aqueous phase liquid) into the subsurface. This work is part of a USGS project to determine the applicability of geophysical methods in subsurface DNAPL detection at the SRS facility.

Clay minerals reported at SRS include kaolinite, halloysite, smectite, vermiculite, illite and glauconite (Segall, 1992, and Looney and others, 1992). Clay minerals are important factors in determining the hydrologic, geophysical and geochemical properties of the subsurface. The hydrogeologic properties of sediments are effected by the amount of clay present. Hydraulic conductivies of sediments generally decrease with increasing clay content. Due to their small grain size, clay bearing units form aquitards. At A/M area, clay units act a barriers to prevent the downward migration of DNAPL's. Once DNAPL has penetrated the pore spaces of clayey sediments, it is difficult to remove or remobilize due to the small size of the pore spaces.

Geophysical surveys may provide a means of detecting the subsurface distribution of DNAPL. Clays have distinctive geophysical properties that can be important in the planning and interpretation of geophysical surveys. Clays generally have higher seismic velocities that other sediments, making them relatively good seismic targets.

The electrical properties of clays makes them important factors in electrical geophysical surveys (Olhoeft, 1978). Due to the surface charge on clay particles, even small concentrations of suspended clay colloids can significantly increase the conductivity of ground water. Clayey units are generally more electrically conductive that non-clay bearing sediments, making them relatively easy to detect using electrical geophysical methods. However, due to their high conductivity, clay bearing units attenuate the propagation of electromagnetic waves, severely limiting the effective range of electromagnetic geophysical surveys.

Many clay minerals are known to react with organic molecules forming clay-organic complexes. Numerous clay-organic reactions have been observed, however, the reaction mechanism(s) are poorly understood. As organic solvents migrate through the subsurface they may react with clay minerals. Some clay-organic reactions are known to change the electrical properties of the clay (King and Olhoeft, 1989, and Sadowski, 1988). Clay-organic reactions may demobilize the organic molecules by adsorption to the clay mineral surface. The clay minerals can also act as catalysts or initiation sites for a variety of chemical reactions (Theng, 1974 and 1979). Clay-organic reactions involving the solvents present at SRS (TCE and PCE) have been reported (Anderson and others, 1985; Brown and Thomas, 1984; Rogers and McFarlane, 1981; Rao and others, 1988; and Karickhoff, 1981).

The clay minerals present in the subsurface at A/M area play an important role in the migration, location, and detection of the DNAPL. Therefore, knowledge of the type and distribution of clay minerals in the A/M area subsurface is important. To determine the type and distribution of clay minerals present at A/M area, core samples were collected and analyzed using x-ray diffraction (XRD) methods. This paper describes the XRD studies of the A/M area core samples.

Clay Mineralogy

Clay minerals are a subset of the phyllosilicate minerals known as hydrous sheet silicates. Clay minerals are composed of layered sheets. There are two basic types of sheets in clay minerals, the tetrahedral sheet and the octahedral sheet. Tetrahedral sheets are composed of silica tetrahedrons linked together to form a hexagonal sheet network. Octahedral sheets are composed of aluminum or magnesium octahedrons linked together to form a hexagonal sheet network.

All clay minerals are formed by an assemblage of two-layer or three-layer sheets. In two-layer clays, each layer is composed of a tetrahedral and an octahedral sheet. The two-layer clays are referred to as T-O (Tetrahedral sheet-Octahedral sheet) or 1:1 clays. Three-layer clays are composed of one octahedral sheet sandwiched between two tetrahedral sheets. Three-layer clays are referred to as T-O-T (Tetrahedral sheet-Octahedral sheet-Tetrahedral sheet) or 2:1 clays. T-O-T clays can be divided into two broad groups, expanding and non-expanding. Expanding clays adsorb water into their interlayer spaces and swell. Non-expanding clays do not swell in water.

Different clay mineral species are created by substitutions of one atom for another in the tetrahedral and octahedral sheets, resulting in a different chemical composition and structure. In the tetrahedral sheet, tetravalent silicon is often replaced by trivalent aluminum or iron. When substitution replaces an atom with one of lower valence, a net negative charge is produced within

the clay structure. The negative charge is balanced by the addition of a positive cation. Sodium and potassium are common charge balancing cations. Due to their size, these large atoms cannot substitute into the tetrahedral or octahedral structure. However, they do fit between adjacent T-O-T layers, filling holes within the hexagonal sheet network.

The clay minerals reported at SRS include kaolinite, halloysite, smectite, vermiculite, illite, and glauconite (Segall, 1992, and Looney and others, 1992). Kaolinite and halloysite are T-O clays. The composition of kaolinite is $Al_2Si_2O_7*2(H_20)$. Halloysite has the same chemical composition as kaolinite, however it contains a layer of water between adjacent T-O sheets. This water is irreversibly dehydrated at relatively low temperatures forming metahalloysite. Kaolinite and halloysite do not have interlayer cations.

Smectite, vermiculite, illite, and glauconite are T-O-T clays. Smectite clay is an expandable T-O-T clay. There are two basic types of smectite clays known as Wyoming type and the Cheto, or Chambers, type. Other common smectite clays include nontronite, hectorite, beidellite, and saponite. Montmorillonite is the most common smectite. The chemical composition of a Wyoming type smectite is $Na_2\ Fe^{3+}\ Al_6\ Mg\ (Al\ Si_{15})O_{44}\ *4(H_2O)$. The composition of a Cheto type smectite is $Ca_{1.5}\ Mg_2\ Al_6\ (Al_{0.5}\ Si_{15.5})O_{44}\ *4(H_2O)$. In smectites, layer charge is balanced by exchangeable cations including sodium, calcium, potassium and magnesium.

Vermiculite is an expanding T-O-T clay mineral. The silicate sheets are separated by a layer of water molecules. There are two basic types of vermiculites, differing by the composition of their octahedral sheet. The composition of dioctahedral vermiculite is $Al_2(Si_{3.2}Al_{0.8})O_{10}(OH)_2Mg_4*nH_2O$. Trioctahedral vermiculite has a composition of $Mg_3(Si_3Al)O_{10}(OH)_2Mg_{0.5}*nH_2O$. In vermiculite layer charge is balanced by an exchangeable cation, generally magnesium.

Illite and glauconite are non-expanding T-O-T clays. Within the crystal structure, some silicon is replaced by aluminum resulting in a charge deficiency (Grim, 1968). The charge is balanced by interlayer potassium atoms. The chemical composition of common illite is $K_3\ Fe^{3+}\ Mg\ Al_6\ (Al_2\ Si_{14})O_{44}\ *4(H_2O)$. The chemical composition of glauconite is $K_3\ Fe^{3+}{}_3\ Fe\ Mg\ Al_3\ (Al_2\ Si_{14})O_{44}\ *4(H_2O)$. In illite and glauconite, layer charge is balanced by a potassium cation.

Methods

Core samples were collected from the A/M area and analyzed using XRD methods to determine the type and distribution of clay minerals present. The sampling strategy was to collect samples representative of the different lithologies within the A/M project

area. The core samples, thought to be typical near surface (upper 200 feet) sand and clay sediments, were obtained from 4 drillholes. The four drillholes are MSB-3B, MHT-17C, MHT-20C and MSB-79C (figure 1). SRS personnel were consulted in the selection of drillholes for sampling.

Drillhole MHT-17C was selected for sampling of the representative lithologies in the project area. Typical sand and clay units were sampled from MHT-17C. There are two shallow clay units that are discontinuous throughout the project area. Representative samples of these clay units were sampled from drillhole MHT-20C, as they were not well represented in MHT-17C. Drillhole MSB-79C was selected for uncontaminated control samples. Drillhole MSB-79C is located relatively close to the project area, has a similar lithology, and contains no (or extremely low) DNAPL concentrations. Typical sand and clay was collected from drillhole MSB-3B. In addition, a sample was taken from the MSB-3B screened interval, where a proposed surfactant test is planed.

Sampling technique

Twenty two core samples were collected. A list of the cores sampled is given in table 1. All samples collected were splits of the core samples, leaving at least 50% of the original core in the box and intact. The core was usually split using a small hand trowel, however, some of the hard clay samples had to be split with a knife. Core samples were collected in 500 ml plastic Nalgene mason jars. Typically a sample volume of 250 to 400 ml was collected.

Each sample consists of core material from a 1 or 2 foot interval. For the small diameter spoon samples (2 inch), a two foot sample interval was required to obtain the 250 to 400 ml volume. Care was taken to get a "representative" sample. If a color, textural, or lithologic change was observed within a given two foot section, it was not sampled to prevent mixing of different lithologies within the sample jar. When color or texture variations were observed, they were sampled individually.

Laboratory XRD Procedures

The clay samples were analyzed using a Scintag 2000 X-ray diffractometer (XRD). The clay samples were generally scanned from 2° to 40° 2θ. The scan rate used was 4 per second with a step interval of 0.03 degrees. For the XRD measurements, a copper lamp with a wavelength of 1.54Å was used. The XRD slits were always set at the following:

Source inner 1.0
Source outer 2.0
Detector outer 0.5
Detector inner 0.3

XRD identification of clay minerals is accomplished by examination of diffraction peak position, intensity, and width. The peak position or d-spacing, is determined by Bragg's Law ($2d\sin\theta=n\lambda$). Peak intensity is determined by chemical composition and position of atoms in the lattice, and sample and slit characteristics. Peak breath or width is dependant on the mean optical coherent dimension. Well crystalline minerals like quartz have large dimensions and produce sharp peaks with narrow widths. Clays have small dimensions, resulting in wide peaks. Peak width is important for qualitative analysis because peaks from clays can be easily identified from peaks of other minerals like quartz, calcite and pyrite.

In clay minerals the position of distinctive XRD peaks is characteristic of the distance between the T-O and T-O-T layers. Because this distance represents the C axis of the crystal structure, it is called the c-spacing or the 001 spacing referring to the crystal indices. The T-O layer clays generally have a 001 spacing of 7.1 to 7.2 Å. The T-O-T layer clays generally have a minimum 001 spacing of 9.2 Å.

A common identification procedure is to examine the clay XRD patterns before and after various treatments that may alter the diffraction patterns. The most common treatment is to glycolate the sample, which will cause many clays to expand. Another common practice is to heat the sample, which will collapse the layers by dehydration. Higher temperatures will have different effects on the dehydration and crystal structure of clay minerals.

Sample Preparation

Oriented XRD mounts were prepared by placing a few grams of sample into a test tube with a few milliliters of distilled water. The clay-water mixture was vigorously shaken for approximately one minute. The clay-water mixture was then allow to sit undisturbed to allow the large, non-clay particles to settle. The fine-grained clay particles remained in suspension. A sample of the water/clay suspension was drawn off and applied to a glass slide. The samples was allow to dry by evaporation at room temperature. To prevent the samples from completely dehydrating, the prepared mounts were stored in a bell jar containing water vapor until they were analyzed using x-ray diffraction.

To glycolate the oriented mounts, they were placed in a bell jar containing ethylene glycol vapor at room temperature. The oriented mounts were generally allow to glycolate over night (>12 hours) before being run on the XRD. Moore and Reynolds (1989) suggest glycolating for at least 8 hours at 60°C for maximum swelling. Individual samples were removed from the glycolator and immediately analyzed on the XRD to minimize collapse of layers due to the evaporation of glycol from the sample into the air.

The qualitative identification of clay minerals using XRD patterns is based on comparison of XRD features from the unknown sample with XRD features of known minerals. Typically, clay minerals are identified by using basal or 001 diffraction peaks. An estimate of the abundance of the clay minerals present in a sample can be made from the relative size and area of the diffraction peaks. However, many factors influence the character of the XRD pattern including sample preparation techniques, x-ray diffractometer settings and the nature of the clay bearing sample. Therefore, statements about the abundance or dominance of clays based on the XRD patterns should be regarded only as an estimate.

XRD Results

In this section of the report, the individual XRD patterns are discussed. Plots of the XRD patterns are given in appendix A. The discussion includes a brief sample description, the file name of the samples XRD plots, the type of clays present, and an estimate of the dominant clay(s) present in the sample. Table 1 gives a summary of the type and distribution of clays identified in the SRS samples.

The grain size distribution information given here was taken from lithology logs obtained from C. Eddy-Dilek, Westinghouse Savannah River Company. The grain size distribution is given in percent gravel (>2.0mm), percent sand (2.0 - 0.065mm), and percent mud (<0.0625mm). The percent mud grain size can be used to estimate the amount of clay in the sample, keeping in mind that clay-size particles are those less than 0.0039mm.

The XRD techniques used for this study did not include sample preparation methods to identify vermiculite, such as Mg saturation and glycerol exposure. Normally hydrated vermiculite and smectite can both produce 14Å peaks. Therefore, samples that produce 14Å XRD peaks could be either smectite or vermiculite. For the purposes of the following discussions, 14Å XRD peaks that expanded due to glycol exposure will be identified as a "swelling clay", possibly vermiculite.

MHT-17C 16-18 feet

This sample is a reddish clayey sand, thought to represent the upper most sand unit (Upland Unit). The sampled interval average grain size distribution is 5% gravel, 80% sand and 15% mud.

The XRD analysis of the oriented mount (m17c16or.rd) indicates the sample contains kaolinite and illite. The 7.19Å peak suggests kaolinite is the dominate clay mineral in the sample. The illite peaks indicate a minor amount of illite is present.

The XRD analysis of the glycolated sample (m17c16g.rd) show no

significant peak shifts, indicating the sample does not contain swelling clays (i.e. smectite).

MHT-17C 36-38

This sample is a hard purple clay, thought to represent one of the upper most clay layers (325-foot clay zone?) in the Upland Unit. The sampled interval grain size distribution is 0% gravel, 20% sand and 80% mud.

The XRD analysis of the oriented mount (m17c36or.rd) indicates the sample contains kaolinite and illite. The 7.23Å peak suggests kaolinite is the dominate clay mineral in the sample. The illite peaks indicate a minor amount of illite is present.

The XRD analysis of the glycolated sample (m17c36og.rd) shows no significant peak shifts, indicating the sample does not contain swelling clays.

MHT-17C, 52-54 feet

This sample is a yellow sand containing small clay balls, thought to be representative of a typical sand of the Tobacco Road Sand unit. The sampled interval average grain size distribution is 0% gravel, 93% sand and 7% mud.

The XRD analysis of the oriented mount (m17c52or.rd) indicates the sample contains kaolinite and illite. The 7.19Å peak suggests kaolinite is the dominate clay mineral in the sample.

The XRD analysis of the glycolated sample (m17c52g.rd) show no significant peak shifts, indicating the sample does not contain swelling clays.

MHT-17C, 54-56 feet

This sample is a purple sand, also thought to be a typical sand of the Tobacco Road Sand unit. The sampled interval average grain size distribution is 0.1% gravel, 92% sand and 8% mud.

The XRD analysis of the oriented mount (m17c54or.rd) indicates the sample contains kaolinite and illite. The 7.19Å peak suggests kaolinite is the dominate clay mineral in the sample. The narrow, low-intensity illite peaks suggest illite is a minor component.

The XRD analysis of the glycolated sample (m17c54g.rd) shows no significant peak shifts, indicating the sample does not contain swelling clays.

MHT-17C, 56-58 feet

This sample is a purple clayey sand, also thought to be part of the Tobacco Road Sand unit. The sampled interval average grain size distribution is 0.1% gravel, 93% sand and 7% mud.

The XRD analysis of the oriented mount (m17c56or.rd) indicates

the sample contains kaolinite and illite. The 7.19Å peak suggests kaolinite is the dominate clay mineral in the sample. The narrow, low-intensity illite peaks suggest illite is only a minor component.

The XRD analysis of the glycolated sample (m17c56g.rd) show no significant peak shifts, indicating the sample does not contain swelling clays.

MHT-17C, 82-84 feet

This sample is a yellow-brown sand, thought to be part of the Dry Branch Formation. The sampled interval average grain size distribution is 0% gravel, 95% sand and 5% mud.

The XRD analysis of the oriented mount (m17c82w.rd) indicates the sample contains kaolinite and only minor illite. The 7.14Å peak suggests kaolinite is the dominate clay mineral. The extremely low-intensity illite peaks, just above background, suggest illite is a only a minor component.

The XRD analysis of the glycolated sample (m17c82.rd) show no significant peak shifts, indicating the sample does not contain swelling clays.

MHT-17C, 121-123 feet

This sample is a yellow-brown clayey sand, thought to be part of the Santee Formation. The sampled interval average grain size distribution is 1% gravel, 91% sand and 8% mud.

The XRD analysis of the oriented mount (m17c121o.rd) indicates the sample contains minor kaolinite and minor illite. The narrow, low-intensity 7.23Å peak suggests only a small amount of kaolinite is present. The low-intensity illite peaks, suggest very little illite is present in this sample. The relatively high-intensity peaks at 4.25Å and 3.34Å are quartz peaks, suggesting the sample may have a high concentration of clay-size quartz.

The XRD analysis of the glycolated sample (m17c121g.rd) show no peak shifts, indicating the sample does not contain swelling clays.

MHT-17C, 145-146 feet

This sample is a yellow-tan clayey sand, thought to represent the Warley Hill Formation. The sampled interval average grain size distribution is 2% gravel, 88% sand and 10% mud.

The XRD analysis of the oriented mount (m17c145o.rd) indicates the sample contains a swelling clay and kaolinite. The peak at 14.86Å suggests the sample may contain vermiculite. The narrow, low-intensity 7.19Å peak, just above background, suggests only a small amount of kaolinite is present. A very small amount of illite may be present producing the extremely low-intensity peaks at 9.97Å

and 4.96Å.

The XRD analysis of the glycolated sample (m17c145g.rd) shows the 14.86Å peak has shifted to 16.76Å, indicating the samples contains a swelling clay. The broad, low-intensity peak may be produced by vermiculite.

MHT-17C, 158 feet

This sample is a yellow-tan clayey sand, thought to represent the sand unit (Warley Hill) directly above the "green clay". The sampled interval average grain size distribution is 0% gravel, 98% sand and 2% mud.

The XRD analysis of the oriented mount (m17c158o.rd) indicates the sample contains smectite, kaolinite and illite. The broad, low-intensity peak at 12.50Å indicates the sample contains a smectite clay. The 12.50Å position of the 001 peak suggests the sample may have dehydrated during drying. The relatively broad, high-intensity 7.19Å peak suggests a relatively large amount of kaolinite is present. The intensity of the illite 001 peak is relatively high compared to other sampled intervals, suggesting a relatively large amount of illite may also be present.

The XRD analysis of the glycolated sample (m17c158g.rd) shows the smectite has peak shifted to 16.89Å, indicating glycol has been drawn into the interlayer spaces of the smectite. Glycolation caused the smectite peak to become much better defined with a higher intensity and narrower peak. The clay present in this interval is interpreted to be a mixed layer smectite-illite with a random stacking pattern.

MHT-17C, 163 feet

This sample is a tan clayey sand, thought to represent the top of the "green clay" layer. The sampled interval average grain size distribution is 0.1% gravel, 85% sand and 15% mud.

The XRD analysis of the oriented mount (m17c163o.rd) indicates the sample contains kaolinite and illite. The width and high-intensity of the 7.23Å peak suggests kaolinite is the dominate clay mineral. The narrow, low-intensity illite peaks, suggest a relatively low amount of illite. This sample has relatively low-intensity quartz peaks, compared to other SRS samples, suggesting a somewhat lower quartz clay-size fraction.

The XRD analysis of the glycolated sample (m17c163.rd) show no significant peak shifts, indicating the sample does not contain swelling clays.

MHT-17C, 164 feet

This sample is a tan clay, thought to represent the middle of the "green clay" layer. The sampled interval average grain size distribution is 0.1% gravel, 85% sand and 15% mud.

The XRD analysis of the oriented mount (m17c164o.rd) indicates the sample contains kaolinite and illite. The width of the 7.23Å peak suggests kaolinite is the dominate clay mineral. The narrow, low-intensity illite peaks, suggest a relatively low amount of illite.

The XRD analysis of the glycolated sample (m17c164g.rd) show no significant peak shifts, indicating the sample does not contain swelling clays.

MSB-3B, 40 feet

This sample is a purple clayey sand, thought to represent the upper most sand unit (Upland Unit). The sampled interval grain size distribution is 5% gravel, 80% sand and 15% mud.

The XRD analysis of the oriented mount (m3b40or.rd) indicates the sample contains kaolinite and minor illite. The strong peak at 7.10 suggests kaolinite is the dominate clay mineral in the sample. The extremely low-intensity illite peak, just above background, suggest very little illite is present.

The XRD analysis of the glycolated sample (M3B40og.rd) shows no significant peak shifts, indicating the sample does not contain swelling clays.

MSB-3B, 98 feet

This sample is a yellow-brown clayey sand, thought to represent the "tan clay". The sampled interval average grain size distribution is 10% gravel, 65% sand and 25% mud.

The XRD analysis of the oriented mount (msb3b98o.rd) indicates the sample contains a swelling clay and kaolinite. The broad, low-intensity peak (just above background) at indicates the sample contains a swelling clay, possibly vermiculite. The broad, low-intensity nature of the peak makes it difficult to identify. The kaolinite peak at 7.19Å has a relatively low-intensity compared to other samples, suggesting a relatively low amount of kaolinite is present.

The XRD analysis of the glycolated sample (m3b98og.rd) shows the 14.66Å peak has shifted to 15.25Å. The shift indicates the sample has swelled, due to glycol being drawn into the interlayer spaces of the clay. The relatively small shift suggests the swelling clay may be vermiculite.

MSB-3B, 113 feet

This sample is a light tan sand, thought to be a typical sand below the "tan clay zone" (Santee Formation). The sampled interval average grain size distribution is 3% gravel, 87% sand and 10% mud.

The XRD analysis of the oriented mount (m3b113or.rd) indicates the sample contains kaolinite and illite. The 7.19Å peak suggests

kaolinite is the dominant clay in this interval.

The XRD analysis of the glycolated sample (m3b113g.rd) indicates the sample also contains a swelling clay. The broad, low-intensity (just above background) peak at 16.98Å suggests the clay present in this interval may be a mixed layer smectite-illite with a random stacking.

MSB-3B, 138 feet

This sample is a yellow-tan sand,thought to represent the sand interval above the "green clay zone"(Warley Hill Formation). The sampled interval average grain size distribution is 7% gravel, 83% sand and 10% mud.

The XRD analysis of the oriented mount (m3b138or.rd) indicates the sample contains smectite, kaolinite, and illite. The broad, low-intensity peak at 12.90Å indicates the sample contains a smectite clay. The broad, low-intensity nature of the peak suggests a layered smectite-illite clay with a random stacking pattern. The broad peak at 7.19Å indicates a relatively large amount of kaolinite is present. The intensity of the illite 001 peak is relatively high compared to other sampled intervals, suggesting a relatively large amount of illite may be present.

The XRD analysis of the glycolated sample (m3b138g.rd) shows the smectite peak shifted to 16.98Å. The broad, low-intensity peak suggests the clay present in this interval is a mixed layer smectite-illite with a random stacking pattern.

MSB-3b, 162 feet

This sample is a tan clay, thought to represent the "green clay zone". The sampled interval average grain size distribution is 1% gravel, 79% sand and 20% mud.

The XRD analysis of the oriented mount (ms3b162o.rd) indicates the sample contains kaolinite and illite. The broad, high-intensity 7.19Å peak suggests kaolinite is the dominate clay mineral. The peaks at 10.05Å and 5.00Å indicate illite is present in this sample. This sample has relatively low-intensity quartz peaks, compared to other SRS samples, suggesting a somewhat lower quartz clay-size fraction.

The XRD analysis of the glycolated sample (m3b162og.rd) show no significant peak shifts, indicating the sample does not contain swelling clays.

MHT-20C, 7-8 feet

This sample is a reddish clay, thought to represent the upper most or shallowest clay layer in the Upland Unit. The red color appears to be a surficial oxide coating on a gray-white clay. The sampled interval grain size distribution is 1% gravel, 15% sand and 84% mud.

The XRD analysis of the oriented mount (mh20c7o.rd) indicates the sample contains kaolinite and illite. The 7.23Å peak indicates kaolinite is the dominate clay mineral in the sample. The narrow, low-intensity illite peaks indicate a minor amount of illite is present.

The XRD analysis of the glycolated sample (m20c7og.rd) show no significant peak shifts, indicating the sample does not contain swelling clays.

MHT-20C, 36-38 feet

This sample is a purple clay. This sample represents the second clay layer (Upland Unit). The sampled interval grain size distribution is 0% gravel, 40% sand and 60% mud.

The XRD analysis of the oriented mount (mh20c36o.rd) indicates the sample contains kaolinite and illite. The broad peak at 7.14Å suggests kaolinite is the dominate clay mineral in the sample. The narrow, low-intensity illite peaks indicate illite is present but in a relatively minor amount.

The XRD analysis of the glycolated sample (m20c36og.rd) show no significant peak shifts, indicating the sample does not contain swelling clays.

MSB-79C, 80 feet

This sample is a yellow-tan sand, thought to represent a typical aquifer sand (Dry Branch Formation) above the "tan clay zone". The sampled interval average grain size distribution is 3% gravel, 92% sand and 5% mud.

The XRD analysis of the oriented mount (m79c80or.rd) indicates the sample contains smectite, kaolinite and illite. The broad, peak at 12.63Å indicates the sample contains a smectite clay. The 12.63Å position, and the broad, asymmetric shape of the 001 smectite peak suggests the sample may have dehydrated during drying. The 7.19Å peak indicates kaolinite is present. The narrow peaks at 10.05Å and 5.00Å indicate illite is present in the sample.

The XRD analysis of the glycolated sample (m79c80g.rd) shows the smectite has peak shifted to 16.89Å, indicating glycol has been drawn into the interlayer spaces of the smectite. Glycolation caused the smectite peak to become much better defined with a higher intensity and narrower peak. The width at the base of the smectite peak suggest smectite is a significant component of the clay minerals present in this interval.

MSB-79C, 120-121 feet

This sample is a yellow-brown sandy clay, thought to represent the "tan clay zone" at the base of the Dry Branch Formation. The sampled interval average grain size distribution is 0% gravel, 50% sand and 50% mud.

The XRD pattern of the oriented mount (m79c120o.rd) shows no well defined clay peaks. Low-intensity peaks, just above background, suggest a swelling clay, kaolinite and illite may be present. Extremely low-intensity peaks at 10.05Å and 7.10Å suggest the sample contains a very minor amount of illite and kaolinite. A very broad, low-intensity peak centered at 14.86Å suggests the presence of a swelling clay, possibly vermiculite. This sample also has relatively low-intensity quartz peaks, compared to other SRS samples, possibly indicating a lower quartz clay-size fraction.

The XRD analysis of the glycolated sample (m79c120g.rd) shows the broad, low-intensity peak centered at 14.86Å may have shifted slightly to a larger d-spacing. The low-intensity illite and kaolinite peaks, while still just above background, are somewhat better defined in the glycolated XRD pattern. However, only a small amount of illite and kaolinite are present in this sample.

MSB-79C, 167 feet

This sample is a red-brown sand, thought to represent a typical aquifer sand (Warley Hill Formation?) above the "green clay zone". The sampled interval average grain size distribution is 5% gravel, 91% sand and 4% mud.

The XRD analysis of the oriented mount (m79c167o.rd) indicates the sample contains smectite, kaolinite and illite. The broad, peak at 12.50Å indicates the sample contains a smectite clay. The 12.50Å D-spacing, and the broad, asymmetric shape of the 001 smectite peak suggests the sample may have dehydrated during drying. The 7.19Å peak indicates kaolinite is present. The narrow peaks at 9.97Å and 4.98Å indicate illite is also present in the sample.

The XRD analysis of the glycolated sample (m79c167g.rd) shows the smectite has peak shifted to 17.09Å (Δ+4.59Å), indicating the presence of a swelling clay. Glycolation caused the smectite peak to become much better defined with a higher intensity and narrower peak. However, the broad smectite peak suggest a layered smectite-illite clay with a random stacking pattern may be present.

MSB-79C, 206 feet

This sample is a yellow-brown to white clay, thought to represent the "green clay zone". The sampled interval average grain size distribution is 3% gravel, 50% sand and 47% mud.

The XRD analysis of the oriented mount (m79c206o.rd) indicates the sample contains kaolinite and illite. The broad 7.23Å peak suggests kaolinite is the dominate clay mineral. The peaks at 10.05Å and 5.00Å indicate illite is present in this sample.

The XRD analysis of the glycolated sample (m79c206g.rd) shows the sample also contains a swelling clay. The low-intensity, poorly defined peak at 16.98Å suggests the presence of a layered smectite-

illite clay with a random stacking pattern.

Discussion

Clay minerals identified in the core samples include smectite, vermiculite, kaolinite and illite. Kaolinite and illite were the most commonly observed clays in the SRS samples. Halloysite was not observed in these SRS samples, however, XRD sample preparation techniques to specifically identify halloysite were not used in this study of the SRS core samples.

Kaolinite was the most commonly observed clay in the SRS samples. Kaolinite was observed in all 22 core samples, and is generally thought to be the most abundant clay in a given sample. Illite was observed in 21 of the samples, although it is thought to occur in relatively small amounts.

Swelling clays, smectite and or vermiculite, were observed in 9 samples. In 6 of the samples the swelling clay was a significant component of the clay minerals present. In 3 of the samples, the swelling clay appeared to be a minor component. The smectite is thought to be present as both smectite, and as a mixed layer smectite-illite clay.

XRD patterns indicative of halloysite were not observed. However, sample preparation methods to specifically identify halloysite, such as exposure to hydrazine-water-glycerol, were not preformed on the SRS samples. Mixtures of 7Å metahalloysite and kaolinite can be mistakenly identified as disordered kaolinite (Brindley and Brown, 1980).

Most of the XRD patterns of the SRS core samples contained a 10Å peak, which is indicative of both illite and halloysite. The narrow nature of the observed 10Å peaks suggests illite. In order to determine if the 10Å peak was illite or halloysite, 10 SRS samples containing a 10Å peak were oven dried at 85°C for 48 hours. If the 10Å peak was produced by halloysite, the dehydration effect of the heating process would drive off the interlayer water, collapsing the 10Å peak to about 7.2Å (Brindley and Brown, 1980). The following list of samples were oven dried at 85°C to observe the effect of heat on the 10Å peak.

MHT-17C, 16-18
MHT-17C, 36-38
MHT-17C, 52-54
MHT-17C, 56-58
MHT-17C, 158
MHT-17C, 164
MSB-3B, 113
MSB-3B, 138
MSB-79C, 80
MSB-79C, 167

Analysis of the XRD patterns show the heating had no significant effect on the position or intensity of the 10Å peaks. This observation, and the fact the XRD patterns also have a 5Å peak

(illite 0.02) indicates the 10Å peaks are produced by illite.

One possible reason no 10Å halloysite was observed in the XRD patterns, is that the samples dehydrated, collapsing to a 7Å metahalloysite form. The dehydration could have taken place as a result of core storage or during sample preparation. Although wrapped in plastic, it is possible that the core samples dehydrated in storage. During the preparation of oriented mounts the clay-water suspension was allowed to dry through evaporation. It is possible that the low humidity in the laboratory dehydrated the halloysite.

To determine if 10Å halloysite was present in the SRS cores but had collapsed due to dehydration, eight oriented mounts were prepared from core samples known to be partially hydrated. Some of the SRS samples were still moist, forming drops of condensation on the inside of the plastic sample jars. The oriented sample mounts were prepared from sample jars containing visible condensation. The eight moist samples include:

MHT-17C 82	MSB-3B 98
MHT-17C 121-123	MSB-3B 113
MHT-17c 145-146	MSB-138
MHT-17C 163	MSB-79C 120-121

These oriented mounts were allowed to settle and "dry" in a bell jar containing water vapor to keep the samples from dehydrating completely. The XRD patterns of these "moist" samples show no 10Å peaks thought to represent halloysite. When the 10Å peaks are observed, the XRD pattern also has a 5Å peak indicating the presence of illite (001 and 002 respectively).

Based on the above observations, 10Å halloysite is not thought to be present in the SRS core samples in any significant amounts. However, to determine the presence of 7Å halloysite, additional XRD analysis is required.

There is some question about the identity of the swelling clays identified in three samples. MHT-17C 145, MSB-3B 98, and MSB-79C 120, have broad peaks located between 14.66 and 14.86Å, that are indicative of hydrated vermiculite. If the SRS samples do contain vermiculite, the vermiculite is assumed to be normally hydrated because the samples have not been heated and were prepared by settling in water. However, normally hydrated vermiculite can be difficult to distinguish from smectite because they both produce 14Å peaks. In addition, sample preparation methods to specifically identify vermiculite, such as Mg saturation and glycerol exposure, were not preformed on the SRS samples. Based on the current laboratory results, it is not possible to conclusively identify these swelling clays. For the purposes of this report, the clay identified in these three samples, MHT-17C 145, MSB-3B 98, and MSB-79C 120, will be referred to as a swelling clay, possibly

vermiculite.

Conclusions

Based on the XRD results conclusions can be made as to what clays are present in the different formations and units present at A/M area. At least two core samples were analyzed for each of the major mapped units in the near surface (upper 200 feet) at A/M area. Some A/M area units are represented by samples from more than one drillhole. Following is an interpretation of the type of clays present in the different formations, and or units, based on the XRD analysis. Figure 2, from Looney and others (1992), gives a stratigraphic column for the study area to aid in the discussion. Table 2 summarizes the type of clays minerals present by formation-unit, in order of increasing depth.

Upland Unit

Samples representative of sand from the Upland Unit include MHT-17c 16-18, and MSB-3B 40. The grain size distribution indicates these sands are composed of 15% mud. The clay minerals identified in the Upland Unit sands include kaolinite and illite. Kaolinite is the most abundant clay present in the sands of the Upland Unit.

Samples representative of the clay layers from the Upland Unit include MHT-20c 7-8, MHT-20c 36-38, and MHT-17c 36-38. The grain size distribution indicates these samples are composed of 60 to 84 percent mud. The clay minerals identified in the Upland Unit clays include kaolinite and illite. Clay layers of the Upland Unit are composed primarily of kaolinite.

Tobacco Road Sand

Samples representative of sand from the Tobacco Road Sand include MHT-17c 52-52, MHT-17c 54-56, and MHT-17c 56-58. The grain size distribution indicates these sand samples contain between 5 and 8 percent mud. The clay minerals identified in the Tobacco Road Sands include kaolinite and illite. Kaolinite is the most abundant clay present in the Tobacco Road Sand.

Dry Branch Formation

Samples representative of sand from the Dry Branch Formation include MSB-79c 80 and MHT-17c 82-84. The grain size distribution indicates these sand samples contain 5 percent mud. The clay minerals identified in the sands of the Dry Branch Formation include smectite, kaolinite and illite. Smectite was only observed in one of the Dry Branch sand samples (MSB-79c 80).

Tan Clay Zone

Samples representative of "tan clay zone" include MSB-3B 98 and MSB-79C 120-121. The grain size distribution indicates the mud content of these samples ranges from 25 to 50 percent. The clay

minerals identified in the "tan clay zone" include a swelling clay, kaolinite and illite. The XRD data suggest that the swelling clay may be vermiculite. Kaolinite is the most abundant clay present in sample MSB-3B 98. The XRD patterns for MSB-79C 120-121 have no well defined clay peaks to make a qualitative estimate of the dominant clay mineral.

Santee Formation

Samples representative of the Santee Formation include MHT-17C 121-123 and MSB-3B 113. The grain size distribution indicates the mud content of these samples ranges from 8 to 10 percent. The clay minerals identified in these sand samples include a swelling clay, kaolinite and illite. The swelling clay was observed only in one Santee sample, MSB-3B 113. The XRD data suggest the clay is smectite, present as a layered smectite-illite mineral.

Warley Hill Formation

Samples representative of sands of the Warley Hill Formation include MSB-3B 138, MHT-17c 145-146, MHT-17c 158 and MSB-79c 167. The grain size distribution indicates the mud content of these samples ranges from 2 to 10 percent. The clay minerals identified in these sand samples include smectite, vermiculite, kaolinite and illite. Swelling clay, smectite and or vermiculite was observed in all the Warley Hill samples. The XRD data suggest the smectite present in these samples is as a layered smectite-illite mineral. Kaolinite and illite were observed in all the Warley Hill samples, however, sample MHT-17C 145-146 only has a very small amount of kaolinite and only a trace of illite.

Green Clay Zone

Samples representative of "green clay zone" include MSB-3B 162. MHT-17C 163, MHT-17C 164 and MSB-79c 206. The grain size distribution indicates the mud content of these samples ranges from 15 to 47 percent. The clay minerals identified in the "green clay zone" include kaolinite, illite and smectite. Kaolinite is the most abundant clay present. Smectite was identified in only one of the "green clay zone" samples (MSB-79c 206), and may be present in minor amounts.

XRD Summary

Twenty two SRS core samples from the A/M area were analyzed using x-ray diffraction methods to determine what clay minerals were present. The samples, from 4 different drillholes, were thought to be representative of typical A/M area near surface (upper 200 feet) sand and clay sediments. Clay minerals identified in the core samples include smectite, possibly vermiculite, kaolinite and illite. Halloysite, although reported in the literature, was not observed in these SRS samples.

Kaolinite and illite were the most commonly observed clays in

the SRS samples. Kaolinite was observed in all 22 core samples, and is generally thought to be the most abundant clay in a given sample. Illite was observed in 21 of the samples, although it is thought to occur in relatively small amounts.

Swelling clays, smectite and or vermiculite, were observed in 9 samples. In 6 of the samples swelling clays were a significant component of the clay minerals present, in 3 samples swelling clays appeared to be a minor component. The smectite clays are thought to be present as both smectite, and as a mixed layer smectite-illite clay.

The XRD data indicates that the clays present in the Upland Unit and the Tobacco Road Sand include kaolinite and illite. The clay minerals identified in the Dry Branch and Santee Formations include smectite, kaolinite, and illite. Clay minerals identified in the Warley Hill Formation include smectite, vermiculite, kaolinite, and illite. The "tan clay zone" clay minerals are composed of swelling clay and kaolinite with minor amounts of illite. The "green clay zone" clay minerals are composed of smectite, kaolinite, and illite.

Section 2

X-Ray Diffraction Studies of Clay-organic Reactions

Introduction

This section of the report describes the preliminary results of x-ray diffraction (XRD) studies to determine if the clay minerals present in the A/M area react with PCE and TCE. Experiments were also conducted to determine if exposure to isopropyl alcohol, a proposed surfactant, would modify the crystal structure of halloysite.

Numerous clay-organic reactions have been observed, including: cation exchange, anion exchange, cation-dipole effects, adsorption by proton transfer, hydrogen bonding, water bridge complexes, ligand exchange and chelation, van der Waals attraction, polymerization, and catalyzed and initiation reactions (Theng 1974 and 1979; Grim, 1968; and van Olphen, 1977). These reactions are poorly understood, little is known about the specific reaction mechanisms or which organic compounds react with what clays (Lucius and others, 1989, and Fitch, 1990). Clay-organic reactions involving PCE have been reported (Anderson and others, 1985; Brown and Thomas, 1984; Rogers and McFarlane, 1981; Rao and others, 1988; and Karickhoff, 1981). These studies indicate that PCE reacts with clay minerals, but do not identify specific reaction mechanisms.

PCE and TCE are non-polar organic molecules. Very little is known about the behavior of non-polar species at the clay surface interface (Theng, 1974). Non-polar organic molecules are believed to be adsorb on to clay surfaces by van der Waals attraction. Van der Waals attractions are weak forces produced by intermolecular attractions between non-polar molecules. In general, larger organic molecules are more strongly adsorbed to clay mineral because of a greater surface areas for Van der Waals attractions (Theng, 1974). PCE and TCE are short aliphatic chain molecules, therefore the van der Waals attractions would be relatively weak.

Experimental Approach

XRD has been applied to numerous clay-organic reaction studies (Bradley, 1945; MacEwan, 1944 and 1946; Grim, 1968; Theng, 1974; Greenland and Quirk, 1962). XRD is applicable to clay-organic research because the adsorption of organic compounds is not limited to the exterior surface of the clay minerals. Interlamellar adsorption of organic compounds results in a change in the d-spacing of the clays which is measured using the XRD method.

Using XRD analysis Bradley (1945) and MacEwan (1944 and 1946) demonstrated that numerous polar organic compounds adsorbed on the basal surfaces of both montmorillonite and halloysite. The d-spacing varies dependent on the organic molecule adsorbed. The adsorption of polar organic molecules on the clay surface does not appear to displace the inorganic cations present on the surface (Grim, 1968). The XRD results of clay-organic reaction studies are generally published in tabulated form, giving Δvalues for the change in d-spacing resulting from the intercalation of organic molecules (Talibudeen, 1954; Grim, 1968; Brindley and Brown, 1980; Theng, 1974 and 1979; and Greenland and Quirk, 1962).

Three different types of clay-organic XRD experiments were conducted including: 1. exposure of reference clays to solvents, PCE and TCE, present at A/M area, 2. exposure of A/M area swelling clay samples to solvents present at SRS, and 3. exposure of halloysite to isopropyl alcohol.

Sample Preparation

The clay samples were exposed to either vapor phase or liquid phase. The type of exposure, and length of exposure was varied depending on the purpose of the experiment. For vapor phase exposures hydrated clay samples, prepared as oriented mounts described in section 1, were placed in a bell jar containing the solvent vapor at room temperature. The atmosphere inside the bell jar was filled with solvent vapor due to the high vapor pressure of the solvent(s) used. Vapor phase exposures ranged from 12 hours to two months, depending on the individual exposure experiments. Individual samples were removed from the bell jar and immediately analyzed on the XRD to minimize any collapse of layers due to evaporation of the solvent from the sample into the air.

Three different techniques were used for liquid phase exposures. The most common method of liquid phase exposure was to place three drops of solvent on an oriented mount using an eye dropper. To keep the liquid phase from evaporating, the sample mount was then placed in a bell jar containing the same solvent in vapor form. The liquid-exposed, oriented mounts were kept in the bell jar for at least 1 hour before XRD analysis.

Another liquid-phase-exposure method was to place approximately one cm^3 of clay sample on a watch glass. The clay was saturated with solvent then stirred into a paste having the consistency of drywall mud. The clay-solvent "mudball" was allowed to dry by evaporation in a fume hood. The drying process took about 15 minutes. The dried clay was scraped off the watch glass onto a sheet of paper with a stainless steel spatula then chopped into a fine powder using a glass slide. The powdered sample was mounted as a bulk sample for XRD analysis. Samples prepared using this technique are referred to as "mudball" mounts.

The third liquid-phase-exposure technique used was to place approximately one cm^3 of sample into a test tube with a few milliliters of solvent. The tube was sealed with a rubber stopper and vigorously shaken for about 1 minute. Clay-solvent mixtures were generally allowed to settle over night before XRD analysis. For XRD analysis, a sample of the clay was removed from the test tube using a stainless steel spatula and smeared on a glass slide. This method of liquid phase exposure was used the least because it generated the most waste solvent and produced relatively poor XRD patterns with high background counts and low intensity peaks.

Reference Clays

Clay minerals reported at SRS include kaolinite, halloysite, smectite, vermiculite, illite and glauconite (Segall, 1992, and Looney and others, 1992). Reference clay samples of illite (IMt-1), kaolinite (KGa-1 and KGa-2), and Ca- and Na-montmorillonite (STx-1 and Swy-1), were exposed to PCE and TCE. The exposed clays were then analyzed on the XRD for changes in their d-spacings that would indicate the possible formation of clay-organic complexes. Vermiculite and glauconite clays were not included in this experiment. Samples of the reference clays were obtained from the Clay Mineral Society, Source Clay Minerals Repository, University of Missouri, Columbia, MO.

Kaolinite

Two samples of kaolinite reference clay were exposed to liquid phase solvents and analyzed on the XRD. Two kaolinite mudball mounts were prepared using PCE and isopropyl alcohol. A TCE exposure was not performed. The two XRD patterns were compared with a bulk kaolinite XRD pattern on the video monitor. No shift in the position of the solvent exposed kaolinite peaks were observed suggesting no clay-organic complex forms with these solvents and kaolinite.

Illite

Three samples of the illite reference clay, IMt-1, were exposed to liquid phase solvents and analyzed on the XRD. Three illite mudball mounts were prepared using PCE, TCE, and isopropyl alcohol. The three XRD patterns were compared with a bulk IMt-1 XRD pattern on the video monitor. No shift in the position of the illite d(001) and d(002) peaks were observed, suggesting no clay-organic complex forms with the solvents and illite clays.

Ca-montmorillonite

Two oriented mounts of a Ca-montmorillonite, STx-1, were prepared and exposed to TCE and PCE vapor for about 12 hours. The XRD analysis indicates that the d-spacing of both samples increased. Figure 3 shows a comparison of the TCE vapor exposed clay and an oriented mount. The d-spacing increased from 14.66 to 18.03Å indicating that TCE reacts with Ca-montmorillonite and enters the interlayer spaces of the crystal structure. Figure 4

shows a comparison of the PCE vapor exposed clay and an oriented mount. The d-spacing increased from 14.66 to 15.44Å indicating that PCE also reacts with Ca-montmorillonite. The PCE exposed sample did not swell as much as the TCE sample, suggesting that TCE may be more reactive that PCE.

Na-montmorillonite

Two oriented mounts of a Na-montmorillonite, SWy-1, were prepared and exposed to TCE and PCE vapor for about 12 hours. A comparison of the oriented mount and the TCE vapor exposed mount showed a d-spacing increase from 12.60 to 14.14Å, suggesting that TCE reacts with Na-montmorillonite. The XRD pattern of the PCE-exposed sample has two peaks at 23.9 and 12.52Å. The double peak suggests that PCE may have entered every other interlayer space of the crystal structure on an ordered basis. The double suggests that PCE does react with Na-montmorillonite.

SRS Swelling Clays

Nine SRS A/M area core samples were determined to contain swelling clay minerals (smectite and or vermiculite, see section 1 of this report). Six of these samples were chosen for the clay-organic XRD experiment. The 6 samples include: MHT-17C 145, MHT-17C 158, MSB-3B 98, MSB-3B 138, MSB-79C 167, and MSB-79C 80. Three of the swelling clay samples had broad, poorly defined, low intensity peaks and were not used in this experiment.

The samples used for this experiment are splits of the core samples used for the XRD analysis reported in section 1 of this report. Two oriented mounts of each clay sample were prepared using the oriented mount technique described in section 1 of this report. For solvent exposure, one mount of each sample was placed in a bell jar with PCE vapor, the other was placed in a bell jar filled with TCE vapor. The samples were exposed to the solvent vapor for at least 10 hours before XRD analysis. After XRD analysis the samples were returned to the respective bell jars for a one month exposure time then reanalyzed using XRD.

MHT-17C 145

This sample is a yellow-tan clayey sand, thought to represent the Warley Hill Formation. XRD analysis indicates the sample contains a swelling clay, possibly vermiculite, and kaolinite and minor illite. Figure 5 shows the results of the 10 hour vapor phase exposures compared with the XRD pattern of the hydrated oriented mount. All the XRD patterns have low intensities. The swelling clay peaks are very broad and difficult to quantify regarding peak position. The 1 month exposure XRD patterns also have low intensities and broad peaks. Based on these data, no interpretation regarding the swelling clay present and clay-organic reactions can be made. The position of the kaolinite and illite peaks have not changed with exposure indicating they do not react with the solvents.

MHT-17C 158

This sample is a yellow-tan clayey sand, thought to represent the sand unit (Warley Hill) directly above the "green clay". XRD analysis indicates the sample contains smectite, kaolinite and illite. Figure 6 shows the results of the 10 hour vapor phase exposures compared with the XRD pattern of the oriented mount. The TCE and PCE XRD patterns have higher intensities, however, there are no significant shifts in the position of the 001 d-spacing. A 10 hour vapor phase exposure does not appear to produce a clay-organic complex with this sample.

A comparison of the 10 hour PCE and 1 month PCE exposures showed no significant change in the d-spacing. A liquid phase PCE exposure was also analyzed. Figure 7 shows a comparison of PCE liquid phase exposed sample and the oriented mount. No significant change in d-spacing has occurred. The XRD data suggests that PCE does not form a clay-organic complex with the clay(s) present in this sample.

Figure 8 shows a comparison of the TCE 10 hour and TCE 1 month exposure. There is a relatively large shift in the position of the 001 peak, from 12.76 to 15.75Å. This increase in the d-spacing indicates that TCE has been drawn into the interlayer space of the smectite, suggesting a clay-organic complex has formed. The position of the kaolinite and illite peaks have not changed indicating these clays do not react with the solvents.

MSB-3B 98

This sample is a yellow-brown clayey sand, thought to represent the "tan clay". XRD analysis indicates the sample contains a swelling clay, possibly vermiculite, and kaolinite. The XRD patterns of the exposed clay sample (not shown) have low intensities, are very broad and difficult to quantify regarding peak position. Based on these data, no interpretation regarding the swelling clay and clay-organic reactions can be made. The position of the kaolinite peak has not changed with exposure indicating it does not react with the solvents.

MSB-3B 138

This sample is a yellow-tan sand, thought to represent the sand interval above the "green clay zone" (Warley Hill Formation). XRD analysis indicates the sample contains smectite, kaolinite, and illite. A comparison of the 10 hour vapor phase exposures with the oriented mount shows no significant shifts in the position of the 001 d-spacing. A 10 hour vapor phase exposure does not appear to produce a clay-organic complex.

Figure 9 shows a comparison of the oriented mount (as received) and PCE 1 month exposure. There is a shift in the position of the 001 peak, from 12.03 to 13.08Å. This increase in the d-spacing indicates that PCE has been drawn into the interlayer space of the smectite, suggesting a clay-organic complex has

formed.

Figure 10 shows a comparison of the oriented mount (as received) and TCE 1 month exposure. There is a relatively large shift in the position of the 001 peak, from 12.08 to 15.63Å. This increase in the d-spacing indicates that TCE has been drawn into the interlayer space of the smectite, suggesting a clay-organic complex has formed.

The position of the kaolinite and illite peaks have not changed with exposure indicating these clays do not react.

MSB-79C 80

This sample is a yellow-tan sand, thought to represent a typical aquifer sand (Dry Branch Formation) above the "tan clay zone". XRD analysis indicates the sample contains smectite, kaolinite and illite. Figure 11 shows the results of the 10 hour vapor phase exposures compared with the XRD pattern of the oriented mount. The TCE and PCE XRD patterns have higher intensities, however, there is no significant shift in the position of the 001 d-spacing. A 10 hour vapor phase exposure does not appear to produce a clay-organic complex.

Figure 12 shows a comparison of the PCE 10 hour and PCE 1 month exposure. The 10 hour XRD pattern has a higher intensity that the 1 month pattern. There is no significant shift in the position of the 001 d-spacing, however, the 1 month XRD pattern may have a slightly smaller d-spacing. Figure 13 shows a comparison of the 1 month exposure with the oriented mount. The PCE d-spacing is slightly smaller that the oriented mount. A possible explanation for the slightly smaller d-spacing is that interlayer water from the PCE exposed clay may have evaporated into the PCE vapor environment inside the bell jar during the month long exposure.

Figure 14 shows a comparison of the TCE 10 hour and TCE 1 month exposure. There is a relatively large shift in the position of the 001 peak, from 12.38 to 15.46Å. This increase in the d-spacing indicates that TCE has been drawn into the interlayer space of the smectite, suggesting a clay-organic complex has formed.

The position of the kaolinite and illite peaks have not changed due to the exposures indicating these clays do not react with the solvents.

MSB-79C 167

This sample is a red-brown sand, thought to represent a typical aquifer sand (Warley Hill Formation?) above the "green clay zone". XRD analysis indicates the sample contains smectite, kaolinite and illite. A comparison of the 10 hour vapor phase exposures with the oriented mount shows no significant shifts in the position of the 001 d-spacing.

Figure 15 shows a comparison of the oriented mount and TCE 1 month exposure. There is a relatively large shift in the position of the 001 peak, from 12.38 to 15.36Å. This increase in the d-spacing indicates that TCE has been drawn into the interlayer space of the smectite, suggesting a clay-organic complex has formed.

The position of the kaolinite and illite peaks have not changed due to the solvent exposures indicating these clays do not react.

Halloysite-isopropyl alcohol

Halloysite has been identified in the near surface sediments at SRS. Halloysite dehydrates easily and known to form organic complexes with some alcohols (Carr and Chin, 1971; MacEwan, 1948; and Brindley and Brown, 1980). This halloysite-alcohol experiment was conducted to determine if halloysite would react with the proposed surfactant, isopropyl alcohol.

Halloysite is a member of the kaolinite group clay minerals. Halloysite is unique among the kaolinite group minerals in that it contains a single layer of water molecules sandwiched between its structural T-O layers. Hydrated has a d(001) spacing of 10Å. Halloysite dehydrates, losing the interlayer of water and the d(001) spacing collapses to about 7.2Å. The 7.2Å form is known as metahalloysite. The dehydration is irreversible and takes place fairly rapidly at room temperature and low relative humidities (Brindley and Brown, 1980).

Metahalloysite (dehydrated 7.2Å halloysite) is known to form complexes with some alcohols. Published studies of alcohol-metahalloysite complexes are given by Carr and Chih (1971) and MacEwan (1948). These studies indicate that metahalloysite reacts with methanol, producing a $+\Delta 2.5$Å shift in the d(001) spacing (Brindley and Brown, 1980). Metahalloysite exposed to ethanol, 1-propanol and 1-butanol produces only a small d(001) spacing shift of $<+\Delta 0.3$Å (Brindley and Brown, 1980).

During a brief review of published clay-organic literature, no reference to 10Å halloysite-isopropyl alcohol organic complexes were located. Therefore, to determine if isopropyl alcohol would produce a clay-organic complex, or possibly dehydrate the 10Å halloysite, the following experiment was preformed:

> A sample of 10Å halloysite was exposed to isopropyl alcohol then analyzed using XRD to observe changes in the d(001) spacing. This experiment was designed to be analogous to a halloysite bearing environment below the water table, exposed to isopropyl alcohol.

Sample preparation

Approximately 1 cm^3 of 10Å halloysite was crushed in a ceramic

mortar with distilled water. The 10Å halloysite sample was obtained from Gene C. Whitney, USGS, Branch of Sedimentary Processes, Lakewood, Colorado. The distilled water was added to prevent the sample from loosing interlayer water through evaporation. The crushed sample rinsed from the mortar into a test tube using distilled water. The halloysite was allowed to settle to the bottom of the test tube for about 1 hour. The distilled water was drawn off with a pipet and 3 to 4 milliliters of 100% isopropyl alcohol was added to the test tube. The tube was sealed with a rubber stopper and vigorously shaken for about 1 minute. The halloysite-alcohol mixture was allowed to sit for 48 hours before XRD analysis.

XRD analysis

A portion of the halloysite-alcohol mixture was removed from the isopropyl bath, using a stainless spatula, and mounted on a glass slide for XRD analysis. The sample mount was then immediately run on the XRD to minimize evaporation effects. During the XRD measurement, the sample dried out due to the evaporation of the alcohol. Figure 16 shows the XRD pattern of the halloysite exposed to isopropyl alcohol for 48 hours.

The XRD pattern (figure 16) of the halloysite exposed to isopropyl alcohol for 48 hours still has a peak at about 10Å. This indicates that the isopropyl alcohol does not cause the halloysite layers to collapse. There is no apparent shift in the position of the d(001) peak. This observation suggests that isopropyl alcohol exposure will produced no measurable physical change in the 10Å halloysite crystal structure.

Clay-organic Summary

Clay samples were exposed to solvents then analyzed using XRD to determine if the clay minerals present at A/M area react with PCE and TCE. The clay samples included reference samples and clay sediment samples from A/M area cores. An experiment was also conducted to determine if exposure to isopropyl alcohol, a proposed surfactant, would modify the crystal structure of halloysite.

Clay minerals reported at SRS include kaolinite, halloysite, smectite, vermiculite, illite and glauconite. Reference clay samples of illite, kaolinite and Ca- and Na-montmorillonite (mono- and divalent cation smectites) were exposed to PCE and TCE. Vermiculite and glauconite clay samples were not included in this experiment. The illite and kaolinite samples did not form clay organic complexes. Both montmorillonites, Na and Ca, appeared to react with the solvents. These experiments were performed using 100% clay and 100% alcohol.

Six A/M area core samples containing swelling clay (smectite and or vermiculite) were chosen for vapor phase solvent exposures.

Samples were analyzed in the XRD after 10 hour exposures and after a 1 month exposure. Two of the samples had broad, low intensity XRD peaks that were not interpretable. Of the 4 remaining samples, all reacted with TCE vapor, as indicated by increased d-spacings. One sample swelled due to PCE exposure, another appears to have dehydrated during the experiment. The kaolinite and illite present in the A/M area samples was not effected by the solvent exposures.

A sample of 10Å halloysite was exposed to isopropyl alcohol to determine if isopropyl alcohol would react with the clay. After a 48 hour liquid phase isopropyl alcohol exposure, no measurable change in the 10Å halloysite crystal structure was observed.

Section 3

Complex Resistivity Measurements of Selected Core Samples From A/M area, Savannah River Site, South Carolina.

Introduction

This section of the report describes the preliminary results of complex resistivity (CR) measurements made on 22 SRS core samples collected from the A/M area. These samples are splits of the samples used for the XRD analysis reported in section 1 of this report. The samples are thought to be representative of typical SRS near surface (upper 200 feet) sand and clay sediments. The purpose of the CR measurements was to characterize the electrical properties of the SRS A/M area sediments, and determine if CR measurements can be used to differentiate DNAPL contaminated sediments from non-contaminated sediments.

Geophysical detection of DNAPL is difficult due to the lack of significant physical contrasts between the contaminated zones and the surrounding sediments. DNAPLs are not magnetic, and therefore cannot be detected by magnetic methods. The amount of DNAPL contamination present in the pore spaces of sediments is generally not large enough to produce detectable gravity or seismic velocity anomalies. Due to their low solubility, DNAPLs do not dissolve and consequently do not produce conductive plumes. Therefore, electrical and electromagnetic methods that detect conductivity anomalies are not applicable to the direct detection of subsurface DNAPL.

However, some clay minerals, notably the montmorillonite group, are know to react with organic solvents which modify the physical and electrical properties of clay. It is possible that clay-organic reactions may provide a means of detecting DNAPL contamination. These laboratory measurements are designed to determine if DNAPL contaminated clays can be differentiated from non-contaminated clays using complex resistivity (CR) measurements.

Three sets of CR measurements were proposed including measuring the samples in their "as received" condition, as a function of water saturation, and as a function of DNAPL exposure. For this interim report, only the "as received" CR measurements have been completed. The water saturation and DNAPL exposed measurements have not been completed at this time. However, several CR measurements as a function of water weight percent have been completed and are presented here. The as received measurements provide baseline data for comparison with measurements of water saturated and DNAPL exposed samples.

Complex Resistivity (CR)

When an electric field is transmitted through the ground, a temporary polarization effect is generated. Polarization effects are produced by current-induced, electron transfer between ions in the groundwater and minerals composing the rock or sediment. Many polarization mechanisms have been reported including electrode, membrane, interfacial, ionic, electronic, orientational, magneto-electric, pyro-electric, piezo-electric, and ferro-electric polarization (Hunt and others, 1979; Sumner, 1976). The dominant polarization mechanisms observed in clay minerals is membrane polarization.

Membrane polarization results from restrictive, non-equilibrium ion transport through electrolytes in contact with minerals having unsatisfied surface charges. These minerals, such as clays with high cation exchange capacities, are surrounded by a diffuse cloud of positive ions. When electric current is applied, ion transfer through the charged ion cloud is restricted, producing polarized zones of ion concentration and ion deficiency.

Resistivity measurements made over a wide band of frequencies are used to produce impedance spectral signatures. In CR measurements, resistivity and phase are measured as a function of frequency. The impedance spectra may exhibit non-linear behavior, and can be characteristic of a particular substance. For two substances, such as clean and contaminated clay, the frequency dependant electrical properties may be different enough that they can be differentiated by their spectral signatures.

The polarization properties of clays have been measured in several laboratory studies (Madden and Marshall, 1959; Olhoeft, 1977, 1978, 1979; Olhoeft and Scott, 1980; and Klein and Sill, 1982). These studies indicate that clays have characteristic polarization effects produced primarily by membrane polarization processes. The polarization properties of montmorillonite result from its large cation exchange capacity (CEC), large surface area, and from water bound between the silicate layers.

Laboratory studies indicate that when some organic solvents react with clays, the polarization properties of the clay are modified (Olhoeft, 1985; King and Olhoeft, 1989; and Sadowski, 1988). In a study of clay-toluene reactions, Olhoeft and King (1991) demonstrated that the resistivity of an uncontaminated clay sample did not show frequency dependent resistivity, however, the contaminated clay shows a strong frequency dependant resistivity. At the lower frequencies, below 10 Hz, the resistivity of the contaminated sample is significantly higher than that of the uncontaminated sample. The contaminated sample also exhibited significantly higher phase angles, indicating a chemically reactive process. These observations indicate that mechanisms that allow

electrical conduction have been modified by the formation of a clay-toluene complex.

The toluene-clay reaction is different than that expected for PCE or TCE and clay. However, the above study demonstrated that clay-organic reactions can be observed geophysically. Based on the results of the above study, these laboratory measurements are being conducted to determine if CR measurements can be used to differentiate clean and PCE and TCE contaminated clays.

Instrumentation

The CR data measurements were made at the USGS petrophysics laboratory using the impedance spectroscopy instrumentation described by Olhoeft (1985). The impedance spectroscopy instrumentation was calibrated at the beginning of each measurement session, to record cable generated inductive and capacitive coupling effects. The calibration data was stored on the data acquisition computer and removed from the data during data processing.

Samples were measured in a cylindrical teflon sample holder, 1 inch in diameter and three inches long. Electrical signal were transmitted to, and received from, the sample through four equally spaced electrodes made from bright platinum mesh. Two electrodes at the ends of the sample holder were used to transmit current through the sample. The voltage response of the sample was measured across two electrodes, spaced 1 inch apart, in the center of the sample holder.

The CR data were collected on a HP 9845C computer using NLCRSM, an unpublished computer program written by Olhoeft, Geophysics Department, Colorado School of Mines, Golden, CO. (information available from the author). The program controls the impedance spectroscopy instrumentation through a HPIB interface. The CR data presented here was collected from 100 to 0.001 Hz with three sample points per decade. Using the sample holder geometry (length and cross-sectional area), transmitted current and received voltage, the program NLCRSM calculates the electric field (V/m) and current density (A/m^2). For each frequency, NLCRSM uses the electric field and current density data to calculate real resistivity and phase angle through Fourier analysis and deconvolution (Sadowski, 1988).

Sample preparation

Twenty two SRS A/M area samples were measured in their "as received" condition. Each sample was loaded into the sample holder, trying to preserve as much of the original texture and compaction as possible. In some of the dry sand samples, no original texture or compaction was preserved. Some of the hard, dry clayey samples had to be pulverized in a mortar in order to be loaded into the sample holder.

After the "as received" measurement was completed, an attempt was made to add water to some samples, to observe resistivity changes as a function of water content. Distilled water was added through small ports in the sample holder. The amount of water added to the sample was determined by weight, and is given as weight percent. The dry sandy samples would generally imbibe water, where as the clayey sediments would not due to their relatively low permeabilities. The samples measured as a function of water weight percent include:

MHT-17C 16-18
MHT-17C 121-123
MSB-3B 98
MSB-3B 113
MSB-3B 138
MSB-3B 162
MSB-79C 120-121

Data display

The CR data are displayed in this report as resistivity and phase angle spectra. The data are plotted from 0.001 to 100 Hz. For the "as received" samples, the resistivities are plotted on a normal scale, where as the phase angle data are plotted on a log scale. Plots of resistivity as a function of weight percent water are plotted on a log scale. The resistivity and phase spectra are given in appendix B.

Complex Resistivity Results

In this section of the report a brief discussion of the individual resistivity and phase spectra is given. The discussion includes a brief description of the sample, grain size distribution, clay mineral(s) present, and spectra characteristics. The grain size distribution information given here was taken from lithology logs obtained from C. Eddy-Dilek, Westinghouse Savannah River Company. The percent mud grain size can be used as an estimate of the maximum possible amount of clay present in the sample. The clay mineral identifications come from the XRD section of this report.

MHT-17C 16-18 feet

This sample is a very dry, reddish clayey sand. The sampled interval average grain size distribution is 5% gravel, 80% sand and 15% mud. XRD analysis indicates the sample contains kaolinite and illite.

The as received resistivity measurement ranges from 13,781 to 18,457 ohm-m (10 to 0.001 Hz respectively). This sample has the highest resistivity of the 22 as received measurements. Data above 10 Hz was edited due to system noise. The resistivity spectrum is fairly linear, showing a gradual decrease in resistivity with

increasing frequency. The phase spectrum also shows a fairly linear response.

Water was added to sample increasing its weight 3.76 percent. The resulting resistivities range from 2,209 to 2,778 ohm-m (50 to 0.001 Hz respectively). Additional water was added to the sample, bringing its water weight percent to 13.53. The resulting resistivities range from 1,882 to 2,352 ohm-m (100 to 0.001 Hz respectively). The three resistivity spectra, as received, 3.76% water and 13.53% water, are similar, showing a gradual decrease in resistivity with increasing frequency.

MHT-17C 36-38

This sample is a hard purple clay. The sampled interval grain size distribution is 0% gravel, 20% sand and 80% mud. XRD analysis indicates the sample contains kaolinite and illite.

The resistivity data indicate the sample ranges from 1,862 to 2,487 ohm-m (100 to 0.001 Hz respectively). The resistivity spectrum has two distinct slopes. from 0.001 to 0.1 Hz the slope is relatively flat compared to above 0.1 Hz. The phase data has a non-linear response with a low amplitude phase peak centered at 1 Hz.

MHT-17C, 52-54 feet

This sample is a very dry, yellow sand containing small clay balls. The sampled interval average grain size distribution is 0% gravel, 93% sand and 7% mud. XRD analysis indicates the sample contains kaolinite and illite.

The resistivity data indicates the sample ranges from 1,267 to 1,427 ohm-m (100 to 0.001 Hz respectively). The resistivity data has a non-linear response, showing a marked decrease in resistivity above 0.2 Hz. The phase data has no significant phase peak.

MHT-17C, 54-56 feet

This sample is a very dry, purple sand. The sampled interval average grain size distribution is 0.1% gravel, 92% sand and 8% mud. XRD analysis indicates the sample contains kaolinite and illite.

The resistivity spectra indicates the sample ranges from 1,206 to 1,370 ohm-m (100 to 0.001 Hz respectively). The resistivity data has a non-linear response, showing a marked decrease in resistivity at about 0.2 Hz. The resistivity spectra has an inflection point at about 1.0 Hz. The phase spectra has no significant phase peak at 1 Hz. The phase data below 0.1 Hz appear to be noisy.

MHT-17C, 56-58 feet

This sample is a moist, purple clayey sand. The sampled interval average grain size distribution is 0.1% gravel, 93% sand and 7% mud. XRD analysis indicates the sample contains kaolinite and illite.

The resistivity spectra indicates the sample ranges from 1,872 to 2,225 ohm-m (100 to 0.001 Hz respectively). The resistivity data has a fairly linear response, showing a gradual decrease in resistivity with increasing frequency. The phase spectra shows no significant phase peak, data below 0.1 Hz appears to be noisy.

MHT-17C, 82-84 feet

This sample is a dry, yellow-brown sand. The sampled interval average grain size distribution is 0% gravel, 95% sand and 5% mud. XRD analysis indicates the sample contains kaolinite and only minor illite.

The resistivity data indicates the sample ranges from 1,230 to 1,332 ohm-m (100 to 0.001 Hz respectively). The resistivity spectrum has a fairly linear response, however, two distinct slopes are present. From 0.001 to 0.2 Hz, the slope is relatively flatter than above 0.2 Hz. The phase spectra shows no significant phase peak, data below 0.5 Hz are noisy.

MHT-17C, 121-123 feet

This sample is a dry, yellow-brown clayey sand. The sampled interval average grain size distribution is 1% gravel, 91% sand and 8% mud. The XRD analysis indicates the sample contains minor kaolinite and minor illite.

The resistivity data indicates the sample ranges from 1,599 to 1,940 ohm-m (100 to 0.001 Hz respectively). The resistivity spectrum shows a non-linear decrease in resistivity, being steeper at the lower frequencies (0.001 to 5 Hz) than at higher frequencies (5 to 100 Hz). The phase spectra shows no well defined phase peaks.

Water was added to sample increasing its weight 8.97% percent. The resulting resistivities range from 1,520 to 1,580 ohm-m (100 to 0.001 Hz respectively). The two resistivity spectra are similar, however, the as received spectrum shows slightly more frequency dependency that the 8.97% water spectrum.

MHT-17C, 145-146 feet

This sample is a moist, yellow-tan clayey sand. The sampled interval average grain size distribution is 2% gravel, 88% sand and 10% mud. XRD analysis indicates the sample contains a swelling clay mineral, kaolinite, and possibly minor illite.

Of the 22 SRS core samples measured, this sample has the lowest resistivity, ranging from 30.2 to 36.3 ohm-m (100 to 0.001 Hz respectively). The resistivity spectra is fairly linear, however, the low frequency response (0.001 to 0.02 Hz) has a steeper slope than at higher frequencies. From 0.5 to 100 Hz, the resistivity spectra has a linear response, showing a gradual decrease in resistivity with increasing frequency. The phase spectra has a low at 0.05 Hz and a low-amplitude peak at 5.0 Hz.

MHT-17C, 158 feet

This sample is a moist, dry yellow-tan clayey sand. The sampled interval average grain size distribution is 0% gravel, 98% sand and 2% mud. The XRD analysis indicates the sample contains a swelling clay mineral, kaolinite and illite.

The resistivity data range from 62.3 to 84.7 ohm-m (100 to 0.001 Hz respectively). The resistivity spectrum is fairly linear, however, there is a slight inflection at 5.0 Hz, above which the slope of the resistivity is more gradual. The phase spectra shows a broad phase peak at 10Hz.

MHT-17C, 163 feet

This sample is a moist, tan clayey sand. The sampled interval average grain size distribution is 0.1% gravel, 85% sand and 15% mud. XRD analysis indicates the sample contains kaolinite and illite.

The resistivity data range from 191 to 217 ohm-m (100 to 0.001 Hz respectively). The resistivity spectrum has a non-linear response, showing three different slopes. The low frequency data, 0.001 to 0.02 Hz, has a relatively steep slope, the middle frequencies, from 0.02 to 2.0 Hz has a relatively flat slope, and the high frequencies (2.0 to 100 Hz) have an intermediate slope. The phase data is relatively noisy, no distinct phase peaks were observed.

MHT-17C, 164 feet

This sample is a moist, tan clay. The sampled interval average grain size distribution is 0.1% gravel, 85% sand and 15% mud. XRD analysis indicates the sample contains kaolinite and illite.

The resistivity data range from 233 to 254 ohm-m (100 to 0.001 Hz respectively). The resistivity spectrum has a non-linear response, showing three different slopes. The low frequency data, 0.001 to 0.005 Hz, has a relatively steep slope. From 0.005 to 0.05 Hz the slope is relatively flat and slightly positive. From 0.05 to 100 Hz, the resistivity has a fairly steep showing a decrease in resistivity. The phase data are relatively noisy, particularly below 0.1 Hz, no distinct phase peaks were observed.

MSB-3B, 40 feet

This sample is a purple clayey sand. The sampled interval grain size distribution is 5% gravel, 80% sand and 15% mud. XRD analysis indicates the sample contains kaolinite and minor illite.

The resistivity data range from 432 to 534 ohm-m (100 to 0.001 Hz respectively). The resistivity spectrum has a non-linear response. The low frequency response, 0.001 to 0.05 Hz is relatively flat. From 0.05 to 100 Hz, the resistivity decreases, there is a slight inflection at 2.0 Hz, above which the slope of

the resistivity begins to flatten out. The phase spectra shows a broad low amplitude peak at 1 Hz.

MSB-3B, 98 feet

This sample is a yellow-brown clayey sand. The sampled interval average grain size distribution is 10% gravel, 65% sand and 25% mud. XRD analysis indicates the sample contains a swelling clay mineral and kaolinite.

The resistivity data range from 328 to 427 ohm-m (100 to 0.001 Hz respectively). The resistivity spectra in non-linear. The low frequency response, 0.001 to 0.1 Hz has a relatively shallow slope. From 0.1 to 100 Hz, the slope becomes steep and the resistivity decreases. There is a slight inflection at 20 Hz, above which the slope of the resistivity begins to flatten out. No phase peaks were observed in the phase spectra.

Water was added to sample increasing its weight 13.97% percent. The resulting resistivities range from 74.6 to 84.3 ohm-m (100 to 0.001 Hz respectively). The two resistivity spectra, as received and 13.97% water, are similar, however, the as received spectrum shows slightly more frequency dependency above 10 Hz.

MSB-3B, 113 feet

This sample is a light tan sand. The sampled interval average grain size distribution is 3% gravel, 87% sand and 10% mud. XRD analysis indicates the sample contains a swelling clay mineral, kaolinite and illite.

The resistivity data range from 308 to 577 ohm-m (100 to 0.001 Hz respectively). The resistivity spectra in non-linear. The low frequency response, 0.001 to 0.1 Hz has a relatively shallow slope. From 0.1 to 10 Hz, the slope becomes steep then at 10 Hz the slope flattens out. The phase spectra shows a broad peak centered at 2 Hz.

Water was added to sample increasing its weight 9.81 percent. The resulting resistivities range from 143 to 185 ohm-m (100 to 0.001 Hz respectively). Additional water was added to the sample, bringing its water weight percent to 14.43. The resulting resistivities range from 88.6 to 94.1 (100 to 0.001 Hz respectively). The three resistivity spectra are similar, however, frequency dependency appears to decrease with increasing water content.

MSB-3B, 138 feet

This sample is a yellow-tan sand. The sampled interval average grain size distribution is 7% gravel, 83% sand and 10% mud. XRD analysis indicates the sample contains a swelling clay mineral, kaolinite, and illite.

The resistivity data range from 417 to 547 ohm-m (100 to 0.001 Hz respectively). The resistivity spectra fairly linear. The

phase spectra shows no significant phase peak, data below 0.02 Hz is noisy.

Water was added to sample increasing its weight 12.3% percent. The resulting resistivities range from 266 to 306 ohm-m (100 to 0.001 Hz respectively). The two resistivity spectra are similar, however, the as received spectrum shows slightly more frequency dependency at the low frequencies.

MSB-3b, 162 feet

This sample is a moist, tan clay. The sampled interval average grain size distribution is 1% gravel, 79% sand and 20% mud. XRD analysis indicates the sample contains kaolinite and illite.

The resistivity data range from 3776 to 627 ohm-m (100 to 0.001 Hz respectively). The resistivity spectra has a non-linear response, with an increase in slope through the middle frequency range (0.02 to 10 Hz). The phase spectra has a peak at 1 Hz.

Water was added to sample increasing its weight 5.64% percent. The resulting resistivities range from 279 to 392 ohm-m (100 to 0.001 Hz respectively). The two resistivity spectra are very similar.

MHT-20C, 7-8 feet

This sample is a dry, reddish clay. The sampled interval grain size distribution is 1% gravel, 15% sand and 84% mud. XRD analysis indicates the sample contains kaolinite and illite.

The resistivity data range from 1,726 to 2,417 ohm-m (100 to 0.001 Hz respectively). The resistivity spectra fairly linear. The phase spectra has a flat slope through the middle frequency range (0.2 to 5 Hz) and shows no phase peak.

MHT-20C, 36-38 feet

This sample is a very hard, purple clay. The sampled interval grain size distribution is 0% gravel, 40% sand and 60% mud. XRD analysis indicates the sample contains kaolinite and illite.

The resistivity data range from 2564 to 3,346 ohm-m (50 to 0.001 Hz respectively). The resistivity spectrum has two distinct slopes. From 0.001 to 0.2 Hz the slope is flatter than above 0.2 Hz. The phase spectra shows no significant phase peaks.

MSB-79C, 80 feet

This sample is a slightly moist, yellow-tan sand. The sampled interval average grain size distribution is 3% gravel, 92% sand and 5% mud. XRD analysis indicates the sample contains a swelling clay mineral, kaolinite and illite.

The resistivity data range from 386 to 460 ohm-m (100 to 0.001 Hz respectively). The resistivity spectrum has a non-linear

response. From 0.001 to 0.02 Hz the slope is positive. Above 0.02 Hz the slope goes negative and the resistivity decreases with increasing frequency. The phase data has a peak 5.0 Hz, below 0.05 Hz the data were noisy and edited from the plot.

MSB-79C, 120-121 feet

This sample is a moist, yellow-brown sandy clay. The sampled interval average grain size distribution is 0% gravel, 50% sand and 50% mud. XRD data suggest the sample contains a swelling clay mineral, kaolinite and illite.

The resistivity data range from 242 to 354 ohm-m (100 to 0.001 Hz respectively). The resistivity spectrum has a fairly linear response. The phase data are fairly flat through the middle frequencies (0.1 to 10 Hz), no significant phase peaks are observed.

Water was added to sample increasing its weight 4.28% percent. The resulting resistivities range from 198 to 238 ohm-m (100 to 0.001 Hz respectively). The two resistivity spectra, as received and water added, are similar, however, the as received spectrum has a slightly steep slope suggesting a decrease in frequency dependency with increasing water content.

MSB-79C, 167 feet

This sample is a moist, red-brown sand. The sampled interval average grain size distribution is 5% gravel, 91% sand and 4% mud. XRD analysis indicates the sample contains a swelling clay mineral, kaolinite and illite.

The resistivity data range from 75 to 124 ohm-m (100 to 0.001 Hz respectively). The resistivity spectrum has a non-linear response. From 0.001 to 0.2 Hz the slope is relatively flat. Above 0.2 Hz the slope becomes steeper, flatting out again above 20 Hz. The phase spectrum has a peak centered between 2.0 and 5.0 Hz.

MSB-79C, 206 feet

This sample is a moist, yellow-brown to white clay. The sampled interval average grain size distribution is 3% gravel, 50% sand and 47% mud. XRD analysis indicates the sample contains kaolinite and illite, and a small amount of a swelling clay mineral.

The resistivity data range from 172 to 213 ohm-m (100 to 0.001 Hz respectively). The resistivity spectrum has a non-linear response. From 0.001 to 0.005 Hz the slope is relatively steep, then flattens out from 0.005 to 0.1 Hz. Above 0.1 Hz the slope increases, flatting out again above 20 Hz. The phase spectrum has a peak centered at 2.0 Hz.

Electrical Measurement Summary

Complex resistivity (CR) measurements were made on 22 SRS core samples collected from the A/M area. The purpose of the CR measurements was to characterize the electrical properties of the SRS A/M area sediments, and determine if CR measurements can be used to differentiate DNAPL contaminated sediments from non-contaminated sediments. The samples were measured in their "as received" condition. The resistivity of some samples were measured as a function of water weight percent. The "as received" measurements provide baseline CR data for comparison with water saturated and DNAPL exposed measurements.

The "as received" resistivities of the SRS samples ranged from 30.2 to 18,457 ohm-m. This range of resistivities is consistent with resistivities observed in the borehole logging data (verbal communication with Philip H. Nelson, USGS; see Nelson and Kibler, 1995). The "as received" resistivities vary due to the different amounts of water present in the sample and due to different sediment composition. Dry sand samples had the highest resistivities where as moist clayey sediments had the lowest resistivities.

Figure 17 shows a plot of resistivity vs phase angle for the "as received" samples. The data presented were measured at a frequency of 1 Hz. The samples are plotted with two different symbols representative of the two clay types; one for samples containing swelling clays (smectite and or vermiculite), and one for samples that contain no swelling clays. The plot shows that at this frequency, the clays have no relationship between resistivity and phase. The figure clearly indicates that the mode of the swelling clay samples has a lower resistivities than the mode of the non-swelling clay samples.

Figure 18 shows a plot of resistivity vs phase angle measured at 100 Hz. The samples are plotted with two different symbols representative of different clay types. The figure indicates that at 100 Hz, resistivity and phase are related. The resistivities observed at 100 Hz are lower than the resistivities measured at 1 Hz. As with the 1 Hz data (figure 17), the 100 Hz data indicates that samples containing swelling clay generally have lower resistivities than non-swelling clay samples.

Figure 19 shows a plot of resistivity vs percent clay, measured at a frequency of 1 Hz. Figure 20 shows a plot of resistivity vs percent clay, measured at a frequency of 100 Hz. The samples are plotted with two different symbols representative of different clay types. The figures indicate that the resistivity of the "as received" samples is not dependent upon clay content. Interestingly, the lowest resistivity samples observed had a low clay content (10 percent or less) and were composed of swelling

clay minerals.

Figure 21 shows a plot of phase angle vs percent clay, measured at a frequency of 1 Hz. Figure 22 shows a plot of phase angle vs percent clay, measured at a frequency of 100 Hz. The samples are plotted with two different symbols representative of different clay types. The figures indicate that the phase response of the "as received" samples is not dependent upon clay content. The 1 Hz phase data suggests that the mode of the swelling clay samples has a higher phase angle than the mode of the non-swelling clay samples. The 100 Hz phase data suggests that swelling clay samples generally have a lower phase angle response than the non-swelling clays.

Addition CR measurements are required to determine if the electrical properties of the SRS sediments are modified by clay-organic reactions with the solvents present at A/M area.

References

Anderson, D,C., Crawley, W., and Zabik, J.D., 1985, Effects of various liquids on clay soil: bentonite slurry mixtures: in Hydrologic barriers in soil and rock, ASTM STP 874, American Society for Testing Materials, pp. 93-101.

Bradley, W.F., 1945, Molecular associations between montmorillonite and some polyfunctional organic liquids: Journal of the American Chemical Society, vol 67, pp. 975-981.

Brindley, G.W., and Brown, G., 1980, Crystal Structures of clay minerals and their X-ray identification: Mineralogical Society Monograph NO.5., Mineralogical Society, 41 Queen's Gate, London, SW7 5HR, 495p.

Brown, K.W., and Thomas, J.C., 1984, Conductivity of three commercially available clays to petroleum products and organic solvents: Hazardous Waste, V.1 PP. 545-553.

Carr, R.M., and Chih, H., 1971, Complexes of halloysite with organic compounds,: Clay Minerals, v.9, pp. 153-166.

Fitch, A., 1990, Clay-modified electrodes: A review: Clays and Clay minerals, v.38, pp. 391-400.

Greenland, D.J., and Quirk, J.P., 1962, Adsorption of 1-n-alkylpyridinium bromides by montmorillonite: Clays and Clay Minerals, vol 9, pp. 484-499.

Grim, R.E., 1968, Clay Mineralogy, McGraw-Hill Book Company, New York, 596 p.

Hunt, G.R., Johnson, G.R., Olhoeft, G.R., Watson, D.E., and Watson, K., 1979, Initial report of the petrophysics laboratory: U.S. Geological Survey Circular 789, 74 p.

Karickhoff, S.W., 1981, Semi-empirical estimates of sorption of hydrophobic pollutants on natural sediments and soils: Chemosphere, v.10, pp. 833-846.

King, T.V.V., and Olhoeft, G.R., 1989, Mapping organic contamination by detection of clay-organic processes: Proceedings, NWWA Conf. on Petroleum hydrocarbon and organic chemicals in groundwater, Prevention, Detection, and Restoration, Houston.

Klein, J.D., and Sill, W.R., 1982, Electrical properties of artificial clay-bearing sandstone: Geophysics, v. 47, no. 11, pp. 1593-1605.

Looney, B.B., Rossabi, J., Tuck, D.M., Jordan, J.E., Bergren, C.L., Van Pelt, R., and Jones, W.E., 1992, Assessing DNAPL contamination, A/M area, Savannah River Site: Phase I Results (U): DE-AC09-89SR180035, Westinghouse Savannah River Company, Aiken, SC.

Lucius, J.E., Olhoeft, G.O., Hill, P.L., and Duke, S.K., 1989, Properties and hazards of 108 selected substances: U.S. Geological Survey Open-File Report 89-491. 536 p.

MacEwan, D.M.C., 1944, Identification of the montmorillonite group minerals by X-rays: Nature, vol 154, pp. 577-578.

MacEwan, D.M.C., 1946, Identification and estimation of the montmorillonite group minerals, with special reference to soil clays: Journal of the Society of the Chemical Industry, London, vol. 65, pp. 298-305.

MacEwan, D.M.C., 1948, Complexes of clays with organic compounds. I. Complex formation between montmorillonite and halloysite and certain organic liquids. Transcripts, Faraday Society, v.44, pp. 349-367

Madden, T.R., and Marshall, D.J., 1959, Electrode and membrane polarization: U.S. Atomic Energy Commission report RME-3160, 113 p.

Moore, D.M., and Reynolds, R.C., 1989, X-ray diffraction and the identification and analysis of clay minerals: Oxford university press, new York, 332 p.

Nelson, P.H., and Kibler, J.E., 1995, Geophysical logs and groundwater chemistry in the A/M area, Savannah River Site, South Carolina: U.S. Geological Survey Open-File Report 95-507, 36p.

Olhoeft, G.R., 1977, Nonlinear complex resistivity: Presented at the 47th. Annual International SEG Meeting, Calgary

Olhoeft, G.R., 1978, Nonlinear complex resistivity in clays: Presented at the 48th. Annual International SEG Meeting in San Francisco

Olhoeft, G.R., 1979, Nonlinear electrical properties: in Nonlinear behavior of molecules, atoms, and ions in electric or electromagnetic fields, Elsevier, pp 395-410.

Olhoeft, G.R., 1985, Low-frequency electrical properties: Geophysics, v. 50, pp. 2492-2503.

Olhoeft, G.R., and King, T.V.V., 1991, Mapping subsurface organic compounds non-invasively by the reactions with clays: U.S. Geological Survey Water Resources Investigation Report 91-4034, pp. 552-557.

Olhoeft, G.R., and Scott, J.H., 1980, Nonlinear complex resistivity logging: 21st. Annual SPWLA Logging Symp. Transactions, p. T1-T8

Rao,P.S., Rhue, R.D., Johnson, C.T., and Oguada, R.A., 1988, Sorption of selected volatile organic constituents of jet fuels and solvents on natural sorbents from gas and solutions phases: AFESC/ESL-TR-88-02, NTIS AD-A204 073/1/WNR, 212 P.

Rogers, R.D., and McFarlane, J.C., 1981, Sorption of carbon tetrachloride, ethylenes, dibromide and trichloroethylene on soils and clay: (USEPA) EPA-600/J-81-560, Environmental Monitoring and Assessment, v.1, pp. 155-162.

Sadowski, R.M., 1988, Clay-organic Interactions: Unpublished Master Thesis, Colorado School of Mines, 209 p.

Segall, M.J., 1992, Clay mineralogy studies: Chapter 4 in Sedimentology and stratigraphy of the Upland Unit, SCUREF Cooperative Agreement Task Order #53, v.1, pp. 19-33.

Sumner, J.S., 1976, Principles of induced polarization for geophysical exploration: Elsevier, 277 p.

Talibudeen, O., 1954, Complex formation between montmorillonoid clays and amino acids and proteins: Transcripts Faraday Society, vol 51, pp. 582-590.

Theng, B.K.G., 1974, The Chemistry of Clay-Organic Reactions: New York, Wiley & Sons, 343 p.

Theng, B.K.G., 1979, formation and properties of clay-polymer complexes: Elsevier scientific Publishing Company, New York, 362 p.

van Olphen, H., 1977, An Introduction to Clay Colloid Chemistry: New York, Wiley-Interscience, 318 p.

Table 1
Summary of the type and distribution of clay minerals

Drillhole	Interval	Unit-composition	Clays Present
MHT-17C	16-18	Upland-sand	+kaolinite, illite
MHT-17C	36-38	Upland-clay	+kaolinite, illite
MHT-17C	52-54	Tobacco-sand	+kaolinite, illite
MHT-17c	54-56	Tobacco-sand	+kaolinite, illite
MHT-17C	56-58	Tobacco-sand	+kaolinite, illite
MHT-17C	82-84	Dry Branch-sand	+kaolinite, -illite
MHT-17C	121-123	Santee-sand	-kaolinite, -illite
MHT-17C	145-146	Warley Hill-sand	vermiculite, -kaolinite, -illite?
MHT-17C	158	Warley Hill-sand	smectite, +kaolinite, illite
MHT-17C	163	Green Clay-clay	+kaolinite, illite
MHT-17C	164	Green Clay-clay	+kaolinite, illite
MSB-3B	40	Upland-sand	+kaolinite, -illite
MSB-3B	98	Tan Clay-clay	vermiculite, kaolinite
MSB-3B	113	Santee-sand	smectite, kaolinite, illite
MSB-3B	138	Warley Hill-sand	smectite, +kaolinite, illite
MSB-3B	162	Green Clay-clay	+kaolinite, illite
MHT-20c	7-8	Upland-clay	+kaolinite, illite
MHT-20C	36-38	Upland-clay	+kaolinite, illite
MSB-79C	80	Dry Branch?-sand	+smectite, kaolinite, illite
MSB-79C	120-121	Tan Clay-clay	-kaolinite, -illite, vermiculite
MHT-79c	167	Warley Hill-sand	smectite, kaolinite, illite
MHT-79C	206	Green Clay-clay	+kaolinite, illite, smectite

Note: + = abundant clay in sample, - = minor amount detected

Table 2
Summary of clays present by unit, in order of increasing depth

Unit-composition	Drillhole	Interval	Clays Present
Upland-clay	MHT-20c	7-8	+kaolinite, illite
Upland-sand	MHT-17C	16-18	+kaolinite, illite
Upland-clay	MHT-17C	36-38	+kaolinite, illite
Upland-clay	MHT-20C	36-38	+kaolinite, illite
Upland-sand	MSB-3B	40	+kaolinite, -illite
Tobacco-sand	MHT-17C	52-54	+kaolinite, illite
Tobacco-sand	MHT-17c	54-56	+kaolinite, illite
Tobacco-sand	MHT-17C	56-58	+kaolinite, illite
Dry Branch?-sand	MSB-79C	80	+smectite, kaolinite, illite
Dry Branch-sand	MHT-17C	82-84	+kaolinite, -illite
Tan Clay-clay	MSB-3B	98	vermiculite, kaolinite
Santee-sand	MSB-3B	113	smectite, kaolinite, illite
Tan Clay-clay	MSB-79C	120-121	-kaolinite, -illite, vermiculite
Santee-sand	MHT-17C	121-123	-kaolinite, -illite
Warley Hill-sand	MSB-3B	138	smectite, +kaolinite, illite
Warley Hill-sand	MHT-17C	145-146	-kaolinite, -illite?, vermiculite
Warley Hill-sand	MHT-17C	158	+kaolinite, illite, vermiculite
Green Clay-clay	MSB-3B	162	+kaolinite, illite
Green Clay-clay	MHT-17C	163	+kaolinite, illite
Green Clay-clay	MHT-17C	164	+kaolinite, illite
Warley Hill-sand	MHT-79c	167	smectite, kaolinite, illite
Green Clay-clay	MHT-79C	206	+kaolinite, illite, smectite

Note: + = abundant clay in sample, - = minor amount detected

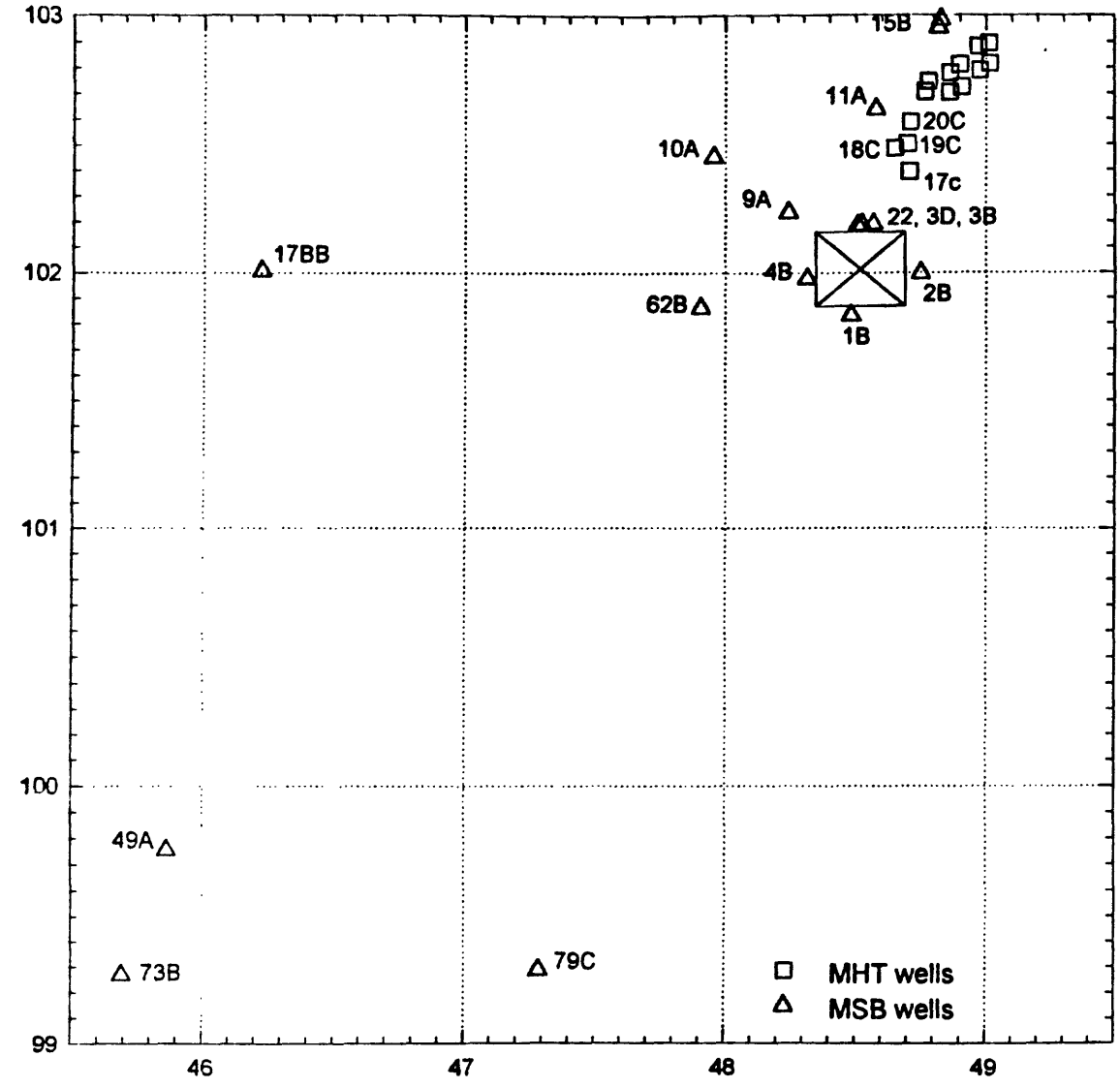

Figure 1. Map of a part of the A/M area showing the location of the MSB and MHT drillholes. The core samples analyzed in this report came from drillholes MHT-17C, MHT-20, MSB-3B, and MHT-79C.

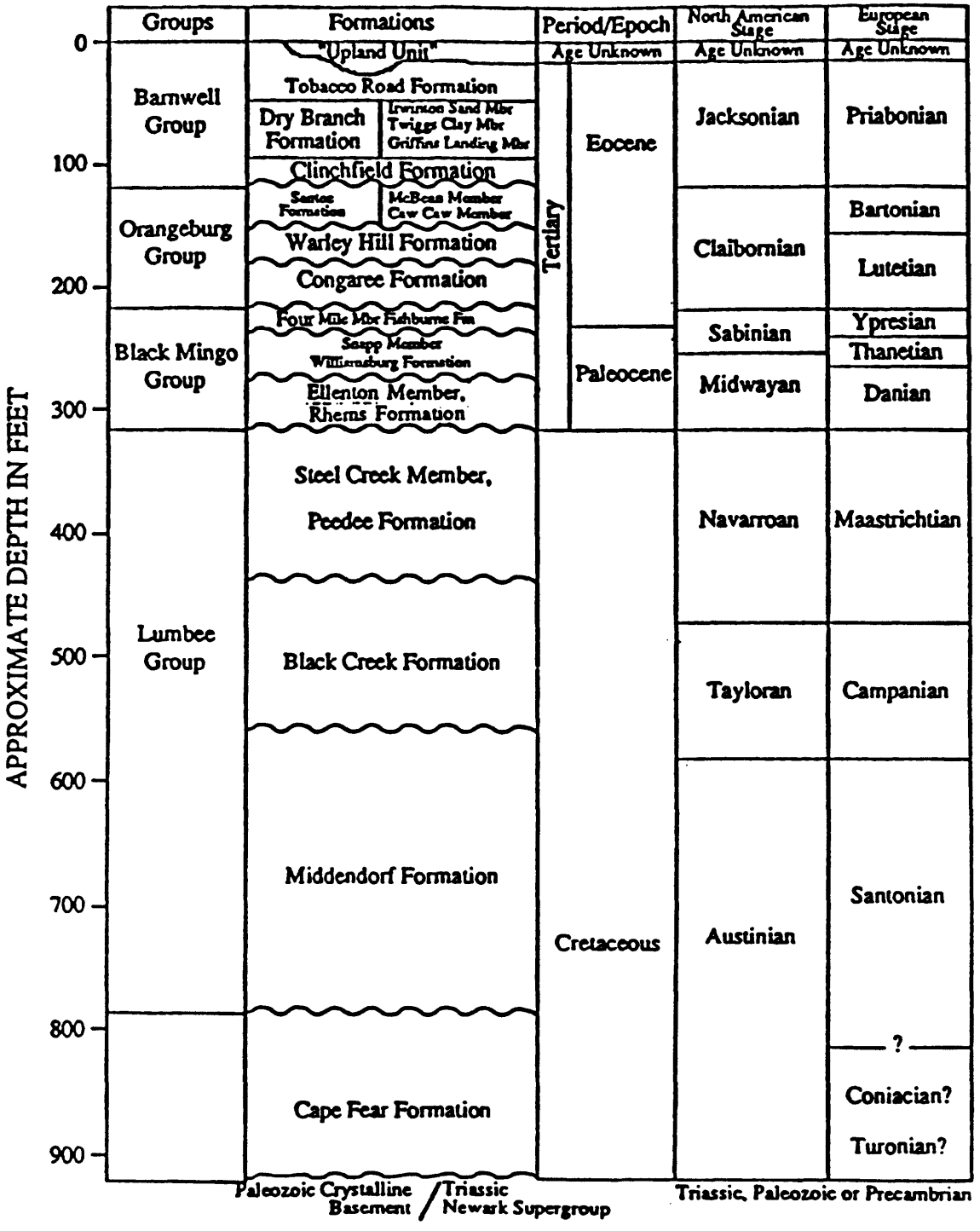

Figure 2. Stratigraphic column for SRS (from Looney and others, 1992).

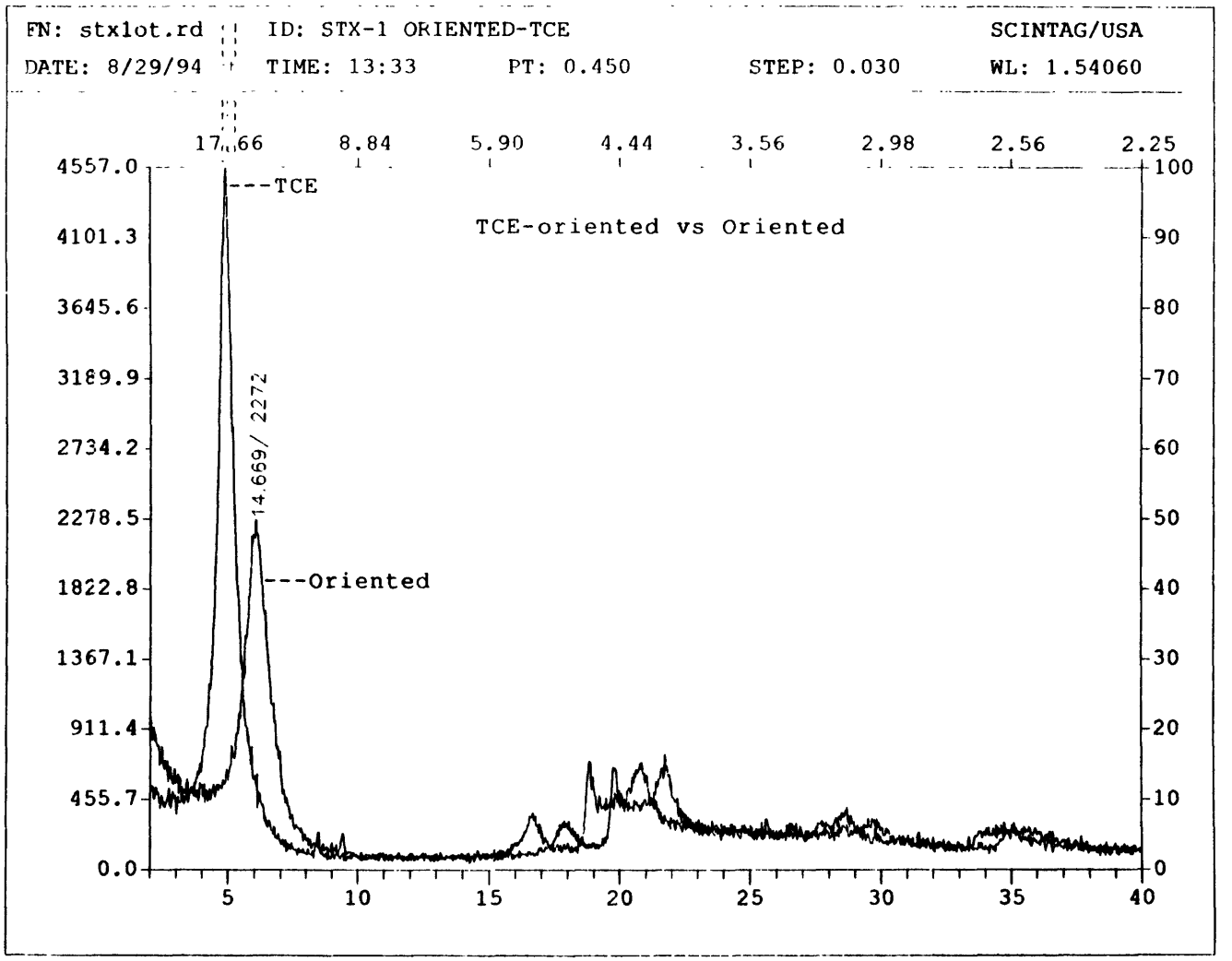

Figure 3. A comparison of the TCE vapor exposed clay and an oriented mount. The d-spacing increased from 14.66 to 18.03Å indicating that TCE reacts with Ca-montmorillonite and enters the interlayer spaces of the crystal structure.

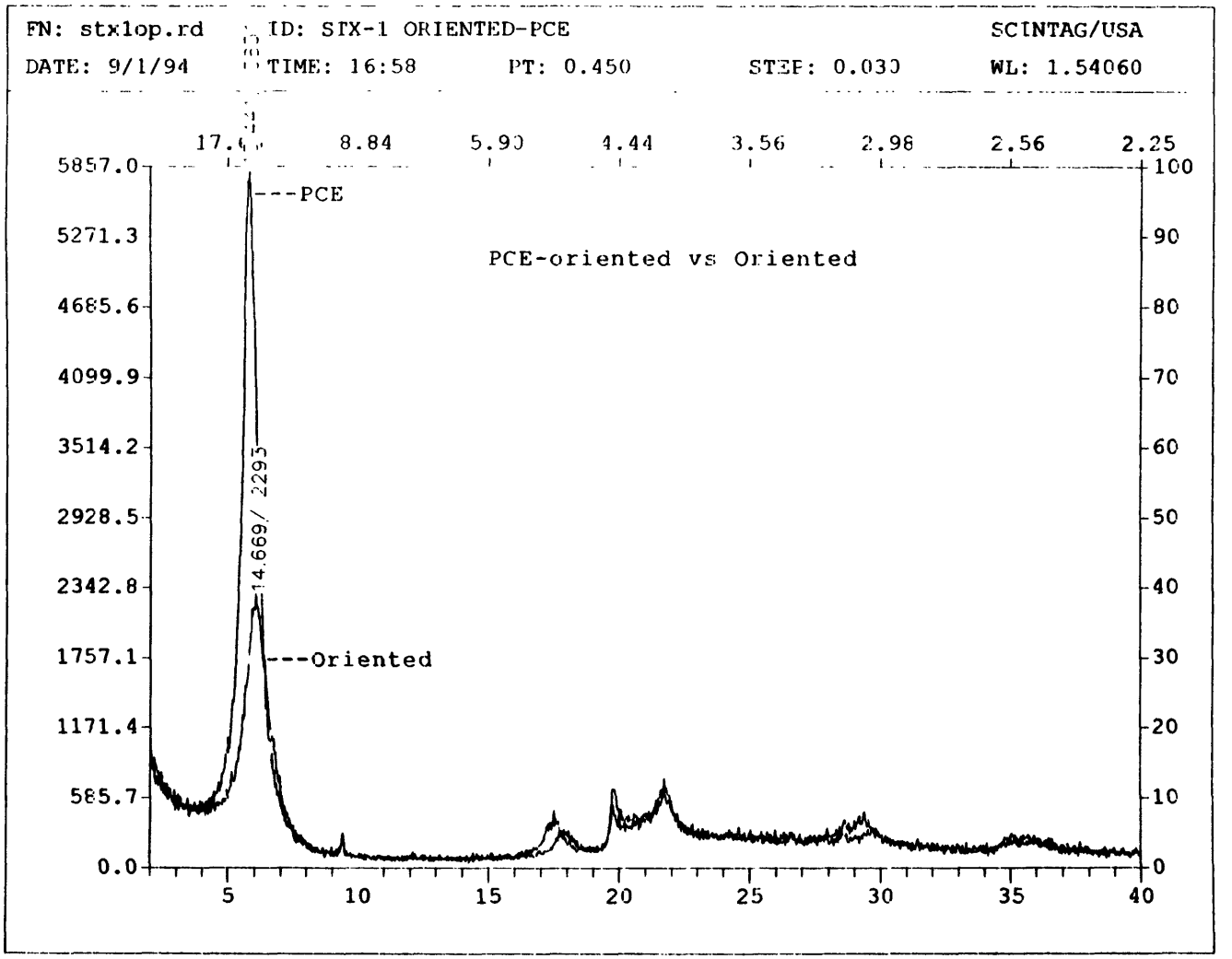

Figure 4 shows a comparison of the PCE vapor exposed clay and an oriented mount. The d-spacing increased from 14.66 to 15.44Å indicating that PCE also reacts with Ca-montmorillonite.

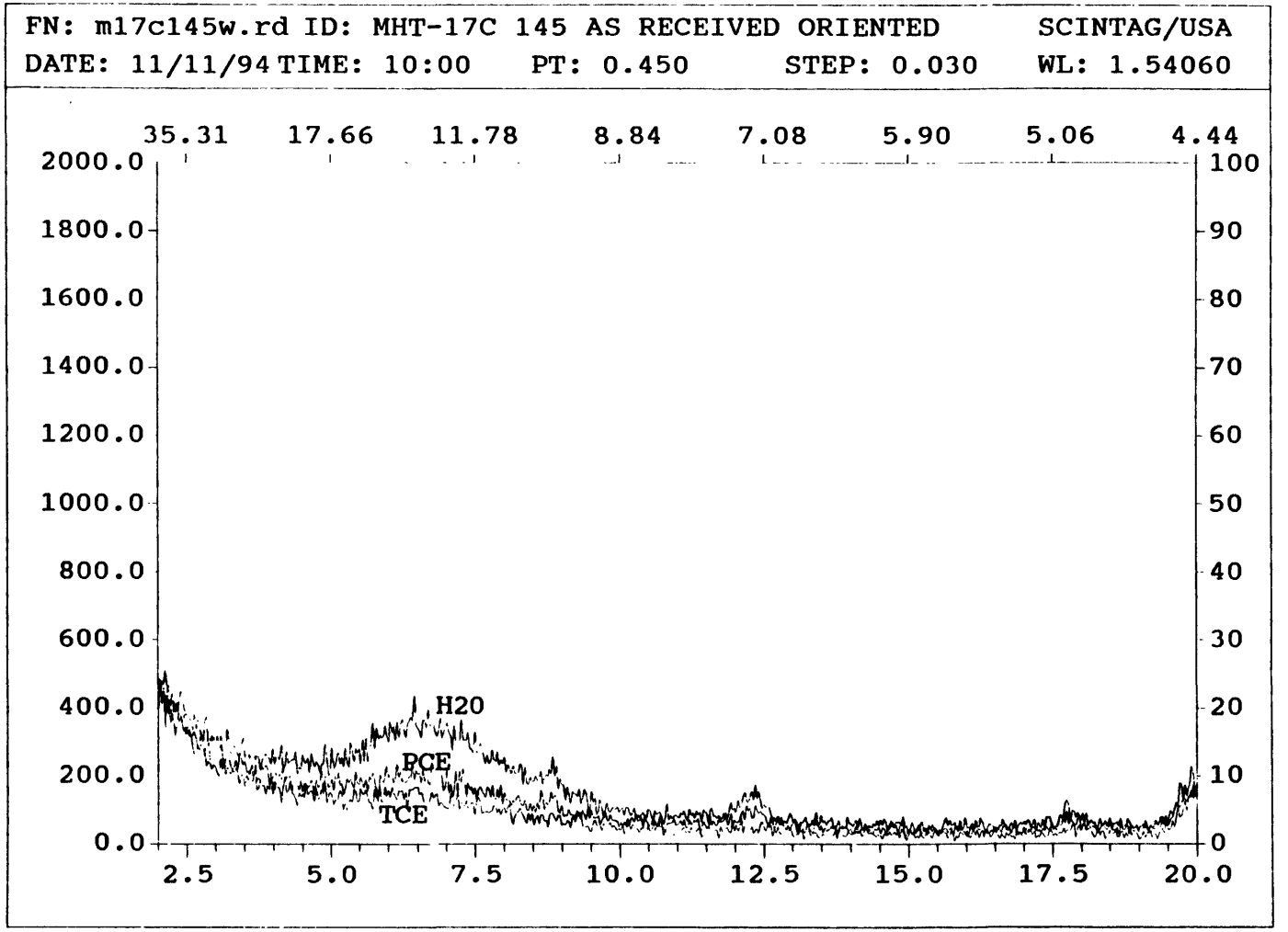

Figure 5. Results of the 10 hour vapor phase exposures compared with the XRD pattern of the hydrated oriented mount for sample MHT-17C 145. All the XRD patterns have low intensities. The swelling clay peaks are very broad and difficult to quantify regarding peak position. Based on these data, no interpretation regarding the swelling clay present and clay-organic reactions can be made.

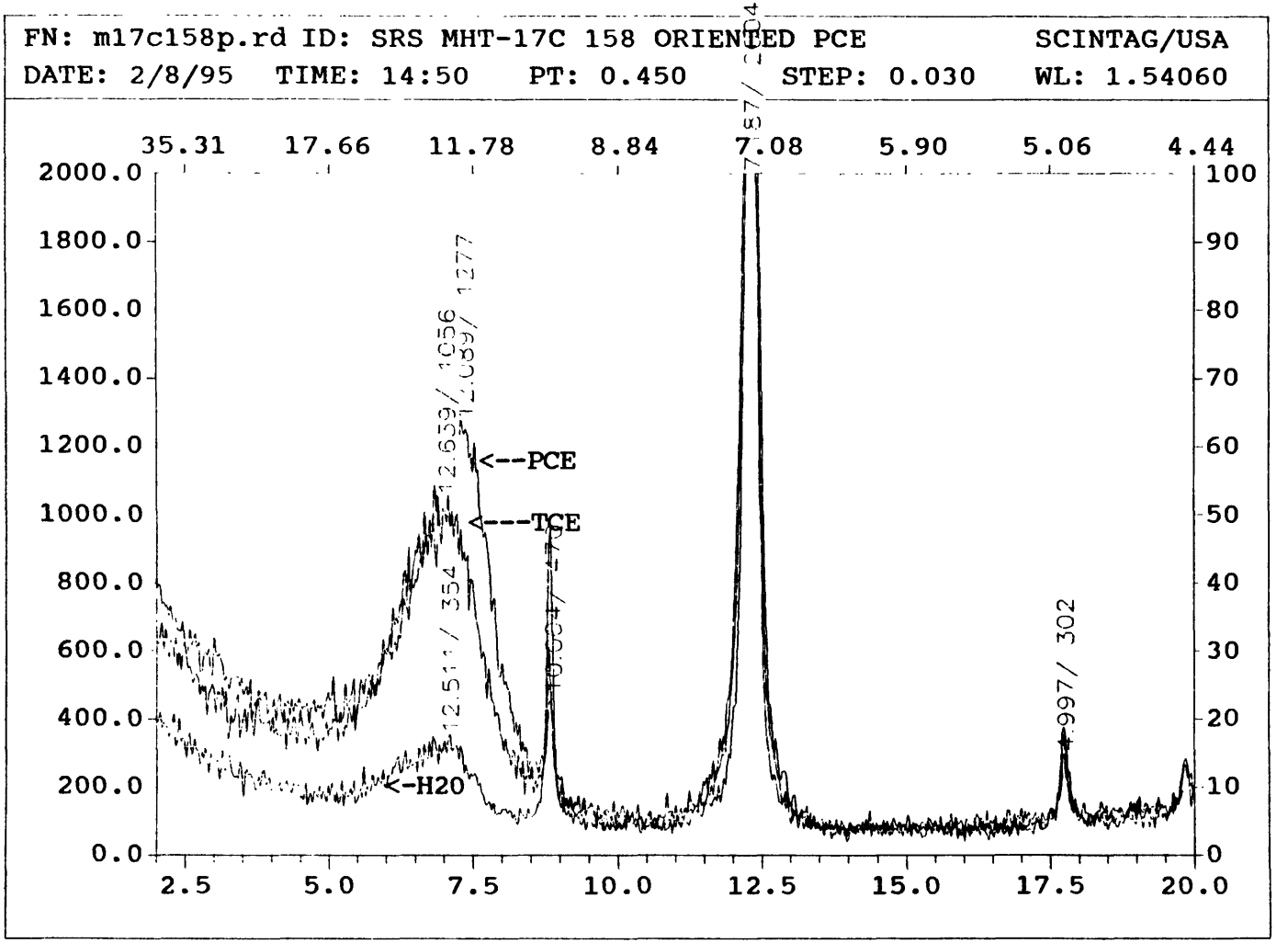

Figure 6. Results of the 10 hour vapor phase exposures compared with the XRD pattern of the oriented mount for sample MHT-17C 158. The 10 hour vapor phase exposure does not appear to produce a clay-organic complex with this sample.

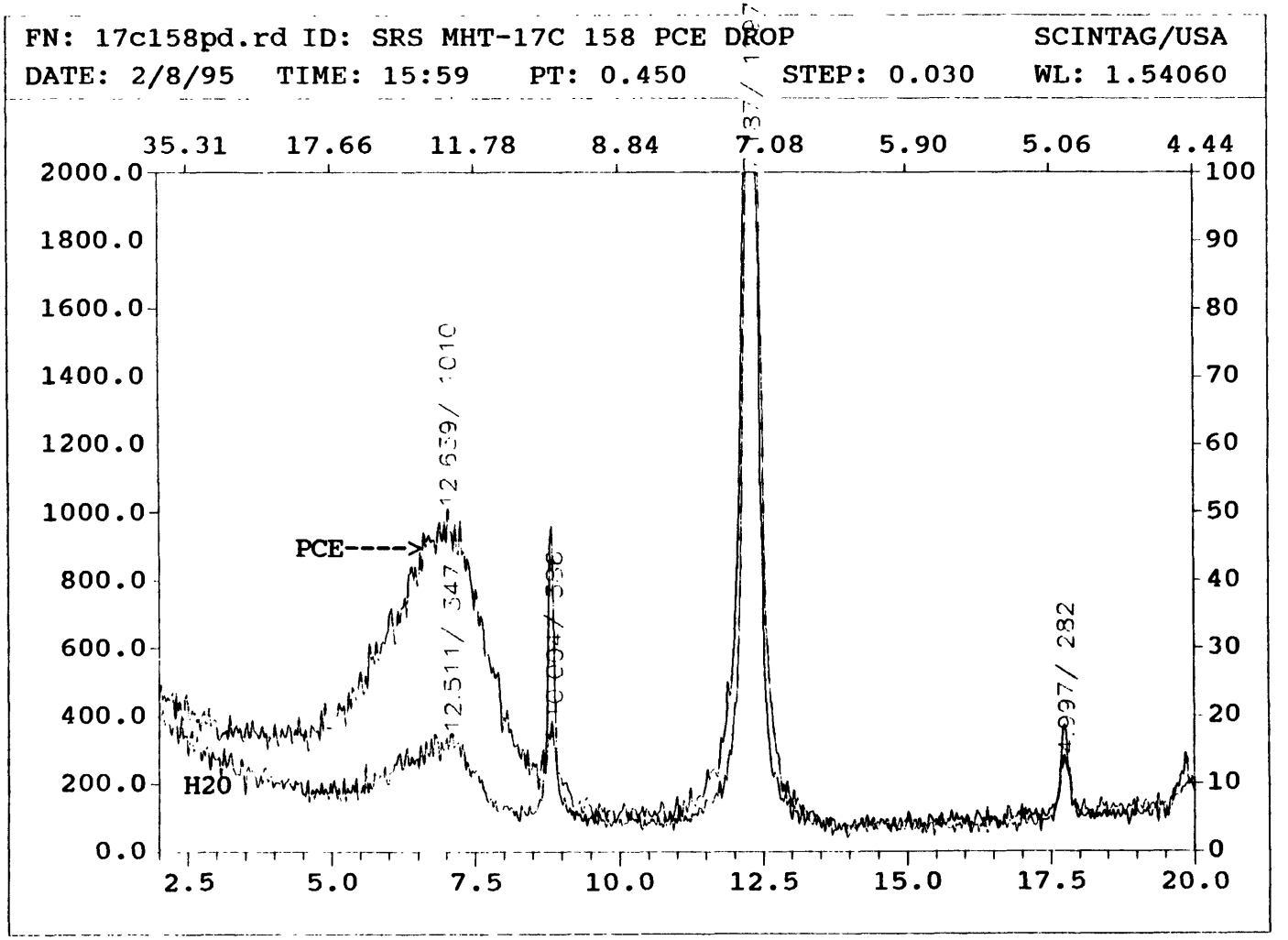

Figure 7. A comparison of PCE liquid phase exposed sample and the oriented mount for sample MHT-17C 158. No significant change in d-spacing has occurred, suggesting that PCE does not form a clay-organic complex with the clay(s) present in this sample.

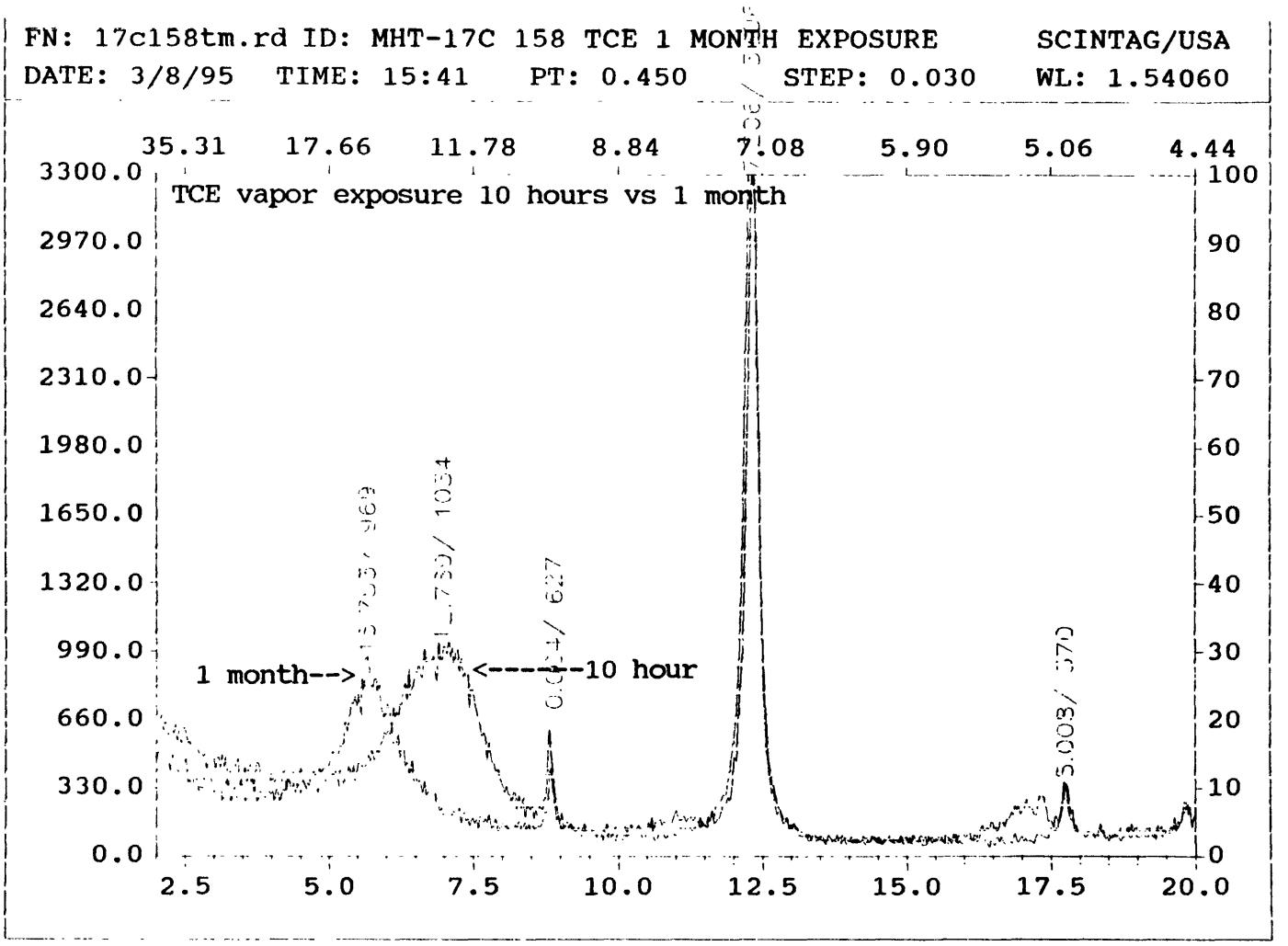

Figure 8. A comparison of the TCE 10 hour and TCE 1 month exposure for sample MHT-17C 158. The relatively large shift in the position of the 001 peak indicates that TCE has been drawn into the interlayer space of the smectite forming a clay-organic complex.

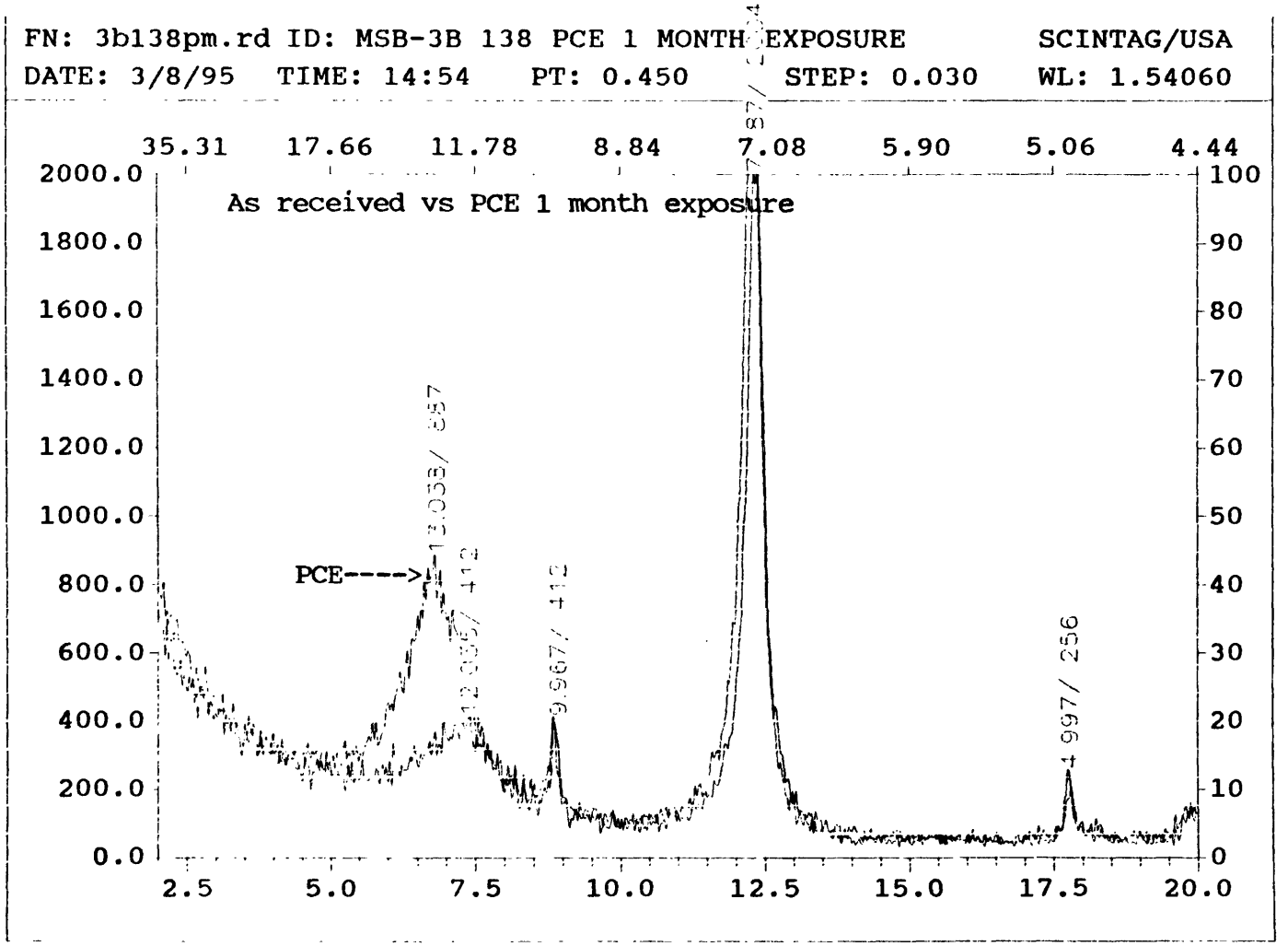

Figure 9. A comparison of the oriented mount (as received) and PCE 1 month exposure for sample MSB-3B 138. The shift in the peak position from 12.03 to 13.08Å indicates that PCE has been drawn into the interlayer space of the clay.

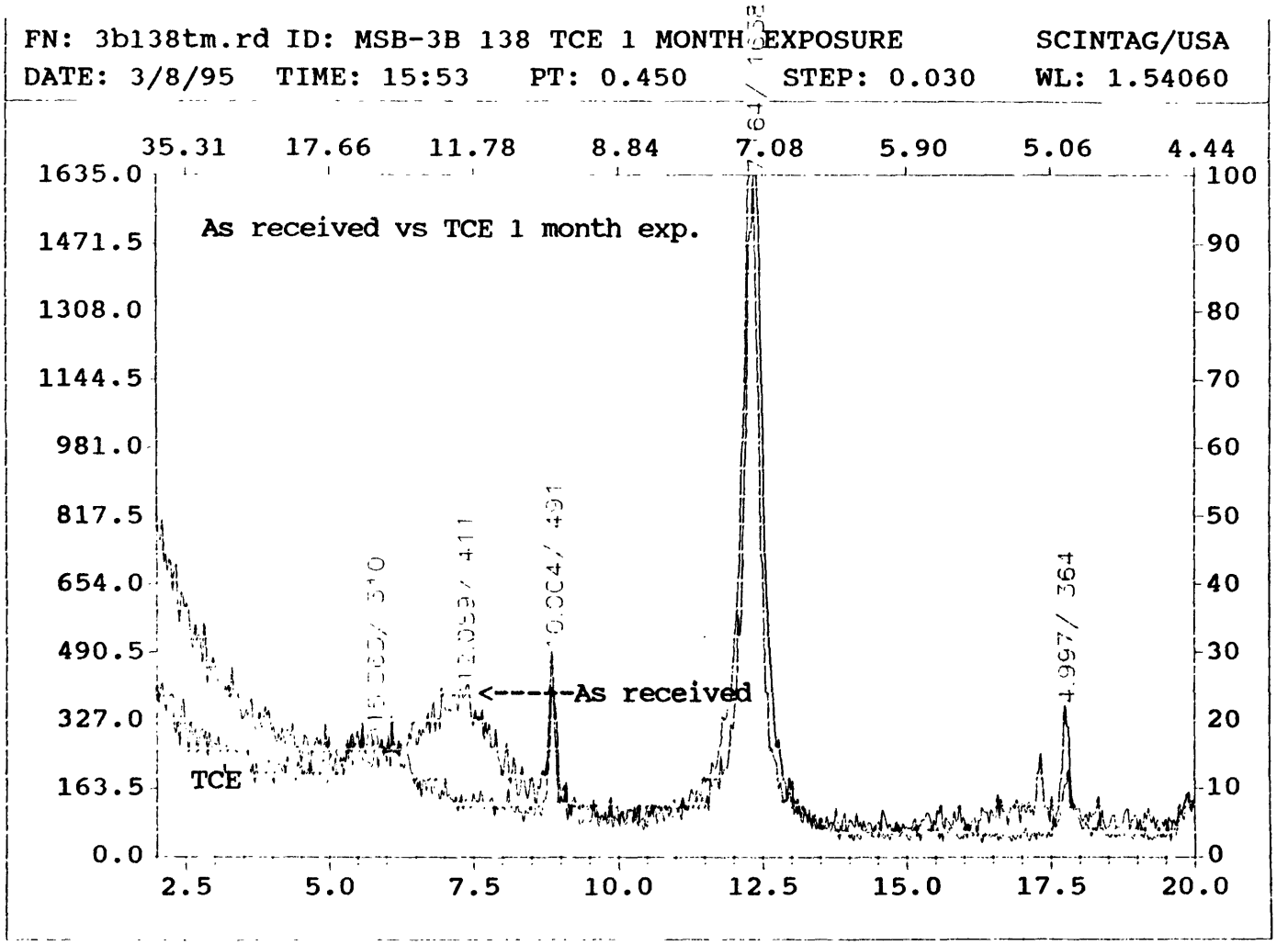

Figure 10. A comparison of the oriented mount (as received) and TCE 1 month exposure for sample MSB-3B 138. The relatively large shift in peak position indicates that TCE has been drawn into the interlayer space of the clay.

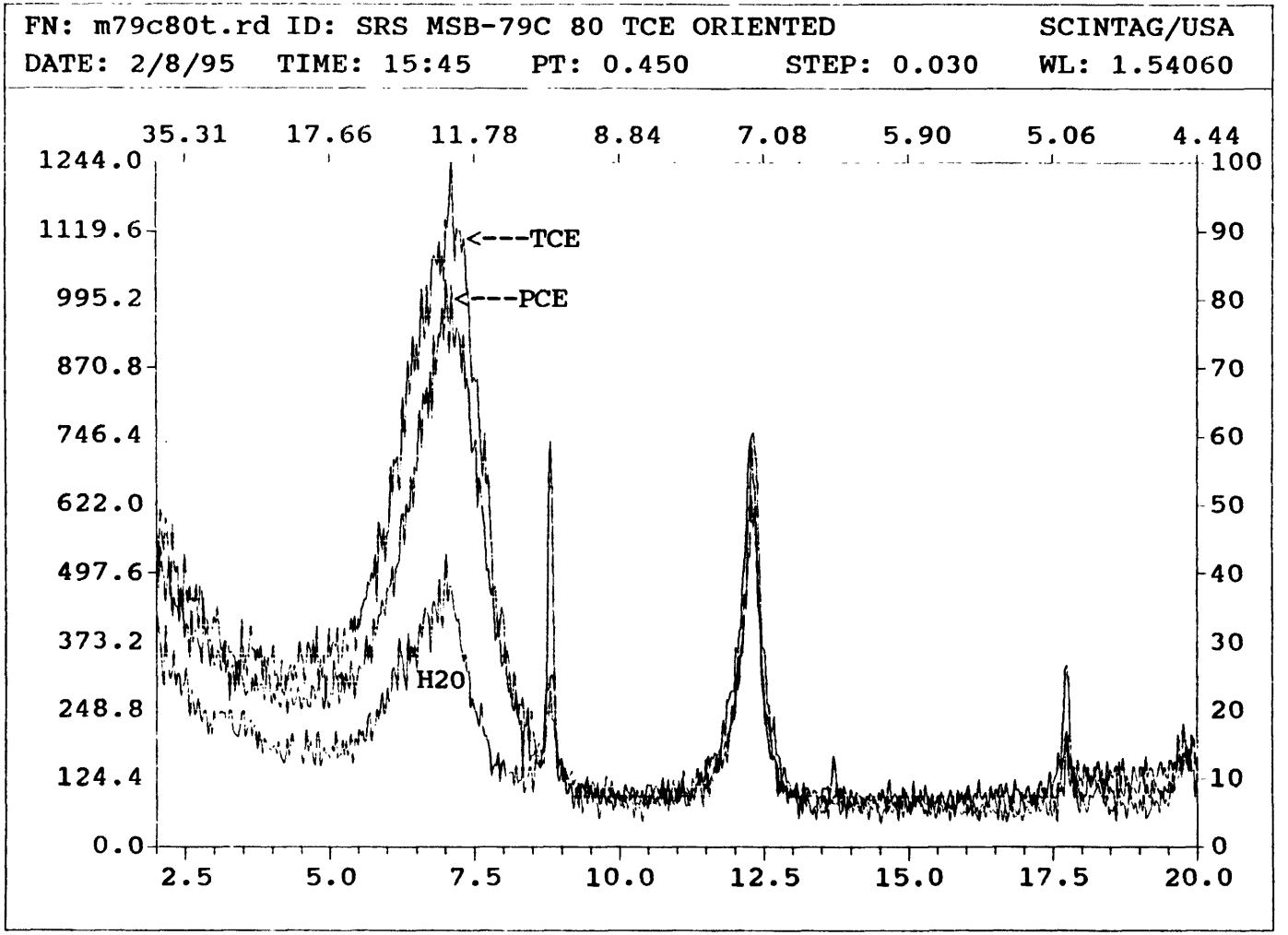

Figure 11. Results of the 10 hour vapor phase exposures compared with the XRD pattern of the oriented mount for sample MSB-79C 80. The TCE and PCE XRD patterns have no significant shift in the position of the 001 d-spacing indicating a 10 hour vapor phase exposure does not produce a clay-organic complex.

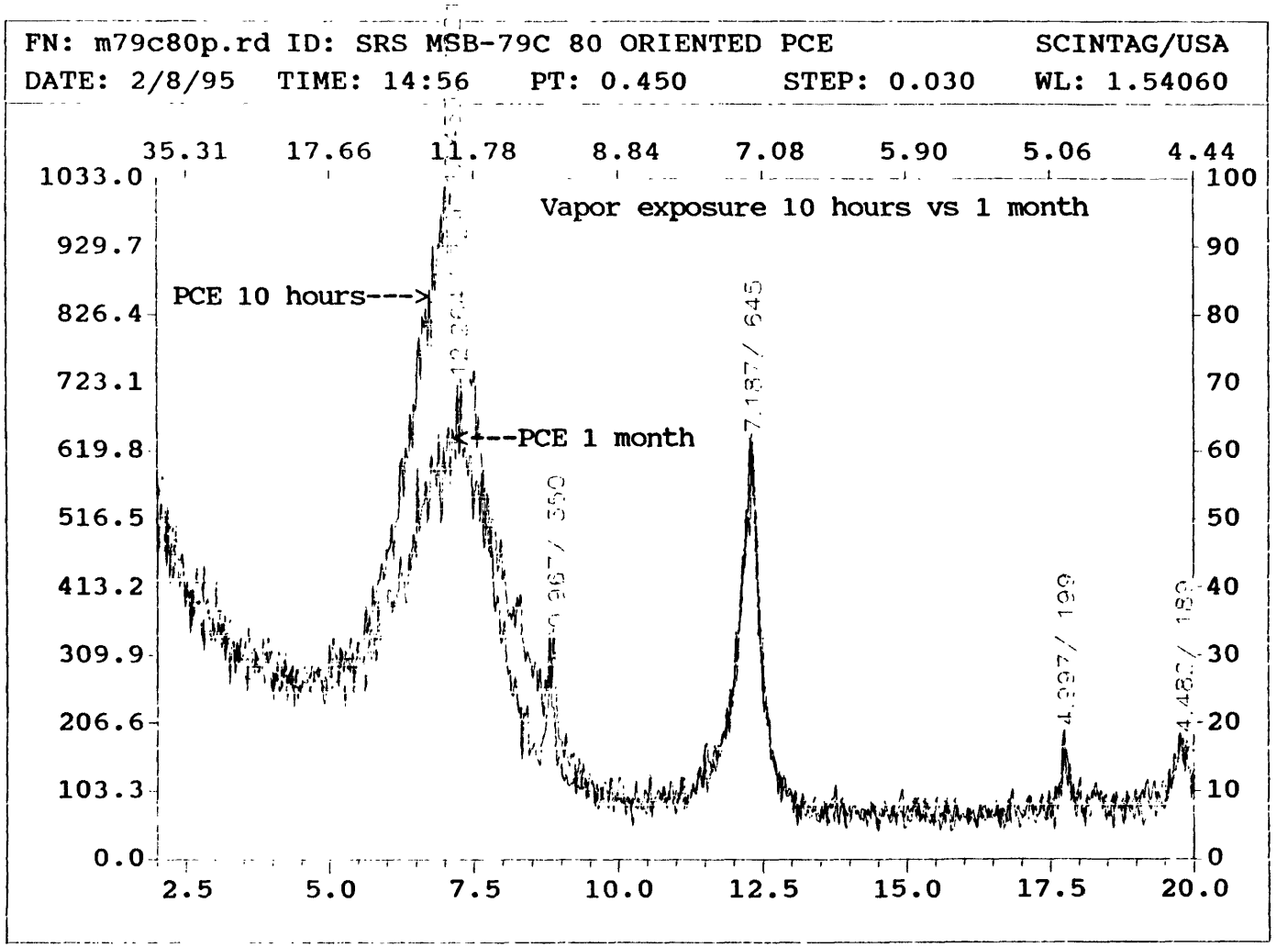

Figure 12. A comparison of the PCE 10 hour and PCE 1 month exposure for sample MSB-79C 80. The 1 month XRD pattern may have a slightly smaller d-spacing.

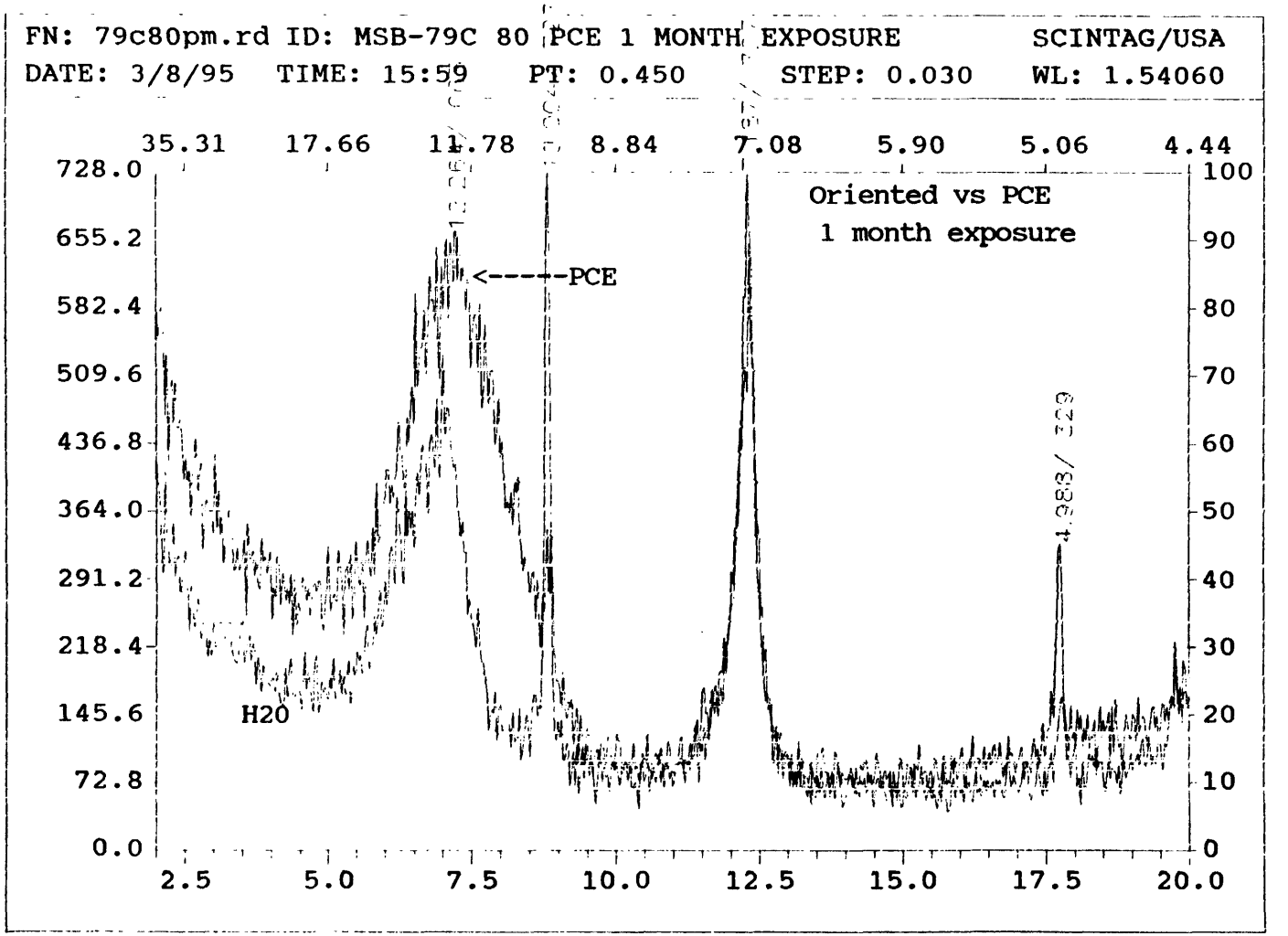

Figure 13. A comparison of the 1 month PCE exposure with the as received oriented mount for sample MSB-79C 80. The PCE d-spacing is slightly smaller that the oriented mount. A possible explanation for the slightly smaller d-spacing is that interlayer water from the PCE exposed clay may have evaporated into the PCE vapor environment inside the bell jar during the month long exposure.

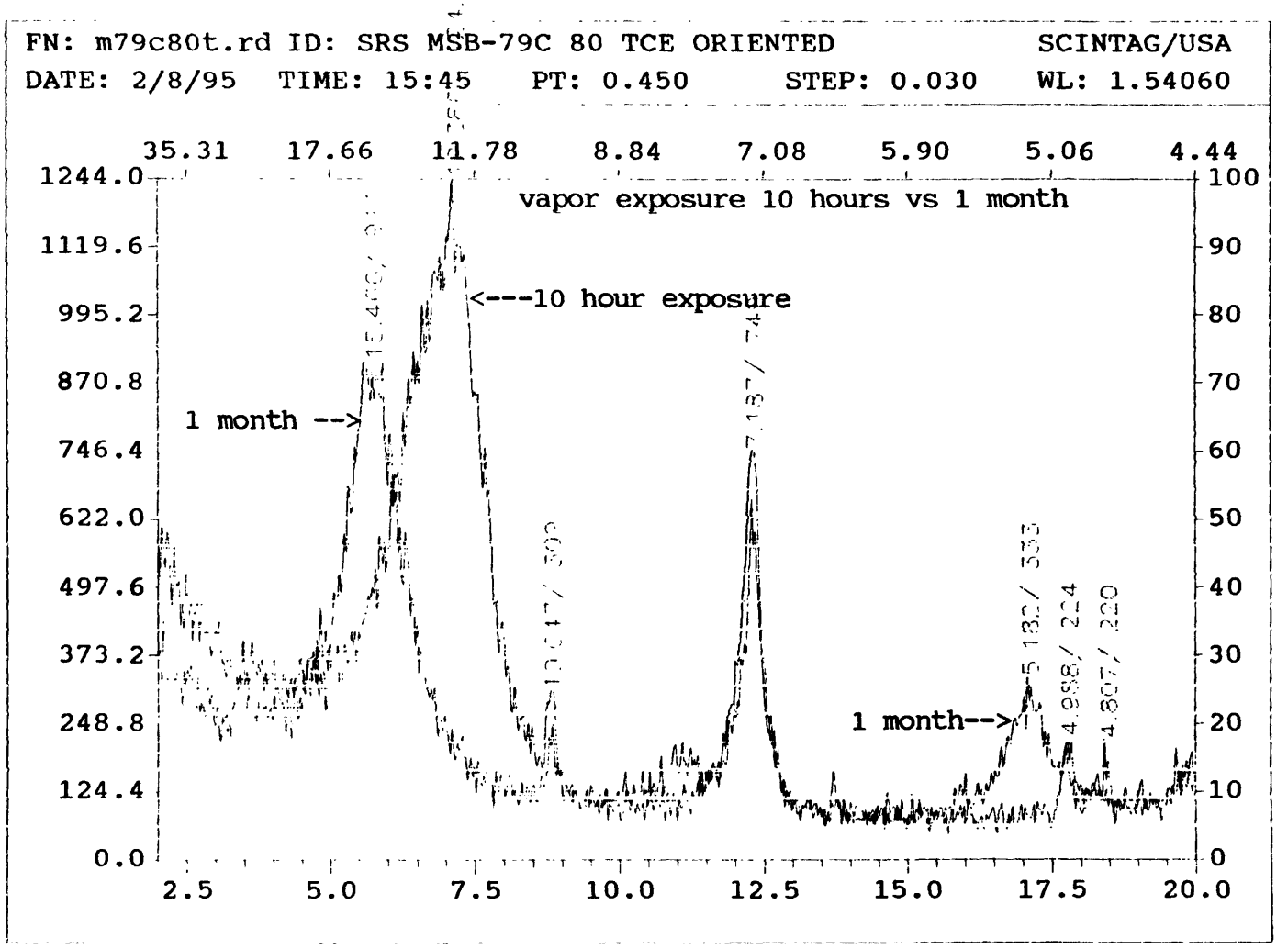

Figure 14. A comparison of the TCE 10 hour and TCE 1 month exposure for sample MSB-79C 80. The relatively large shift in the 001 peak indicates that TCE has been drawn into the interlayer space of the clay.

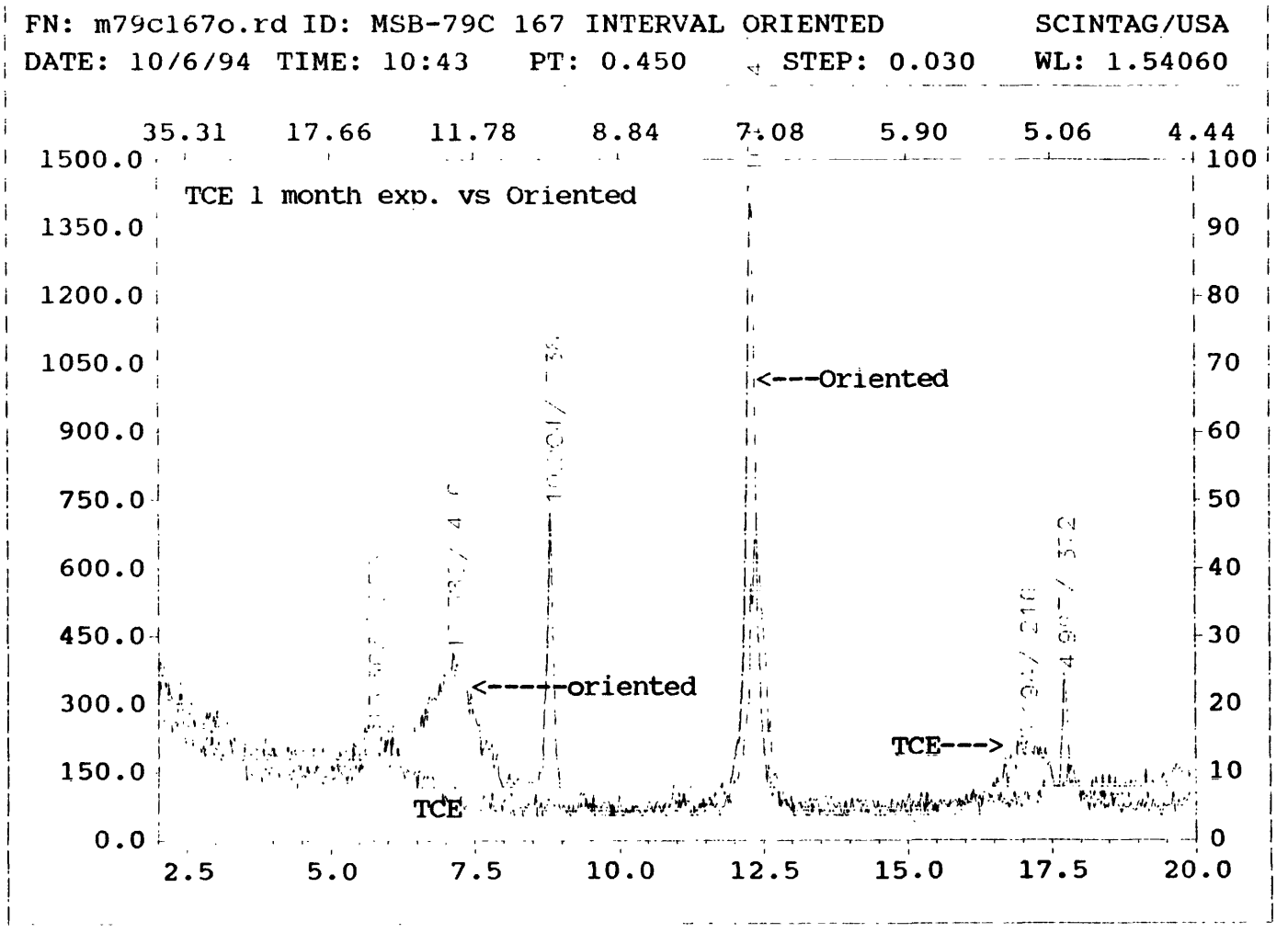

Figure 15. A comparison of the oriented mount and TCE 1 month exposure for sample MSB-79C 167. The shift in peak position indicates that TCE has been drawn into the interlayer space of the clay.

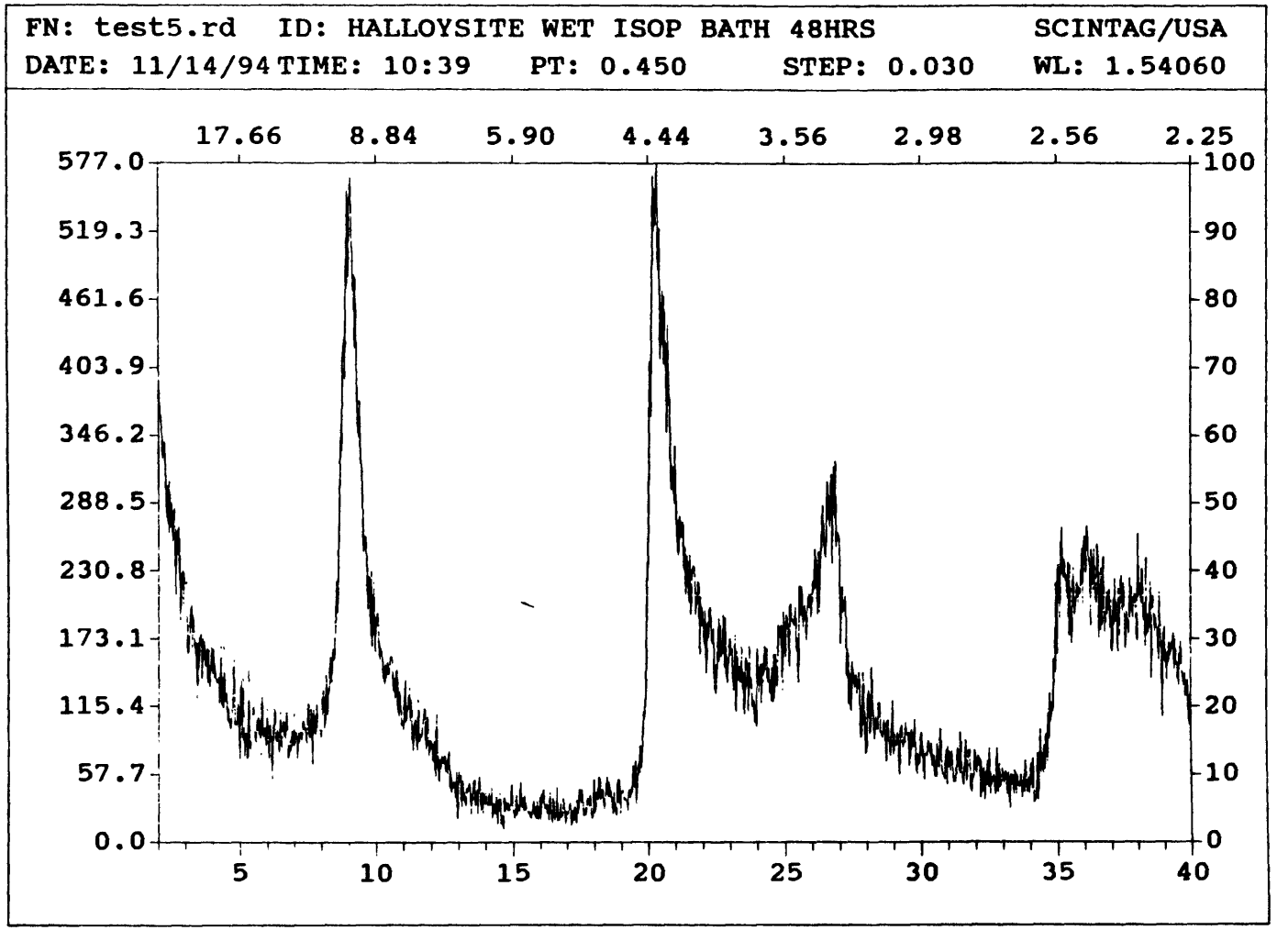

Figure 16. XRD pattern of the halloysite exposed to isopropyl alcohol for 48 hours. The halloysite still has a peak at 10Å indicating that the isopropyl alcohol does not cause the halloysite layers to collapse.

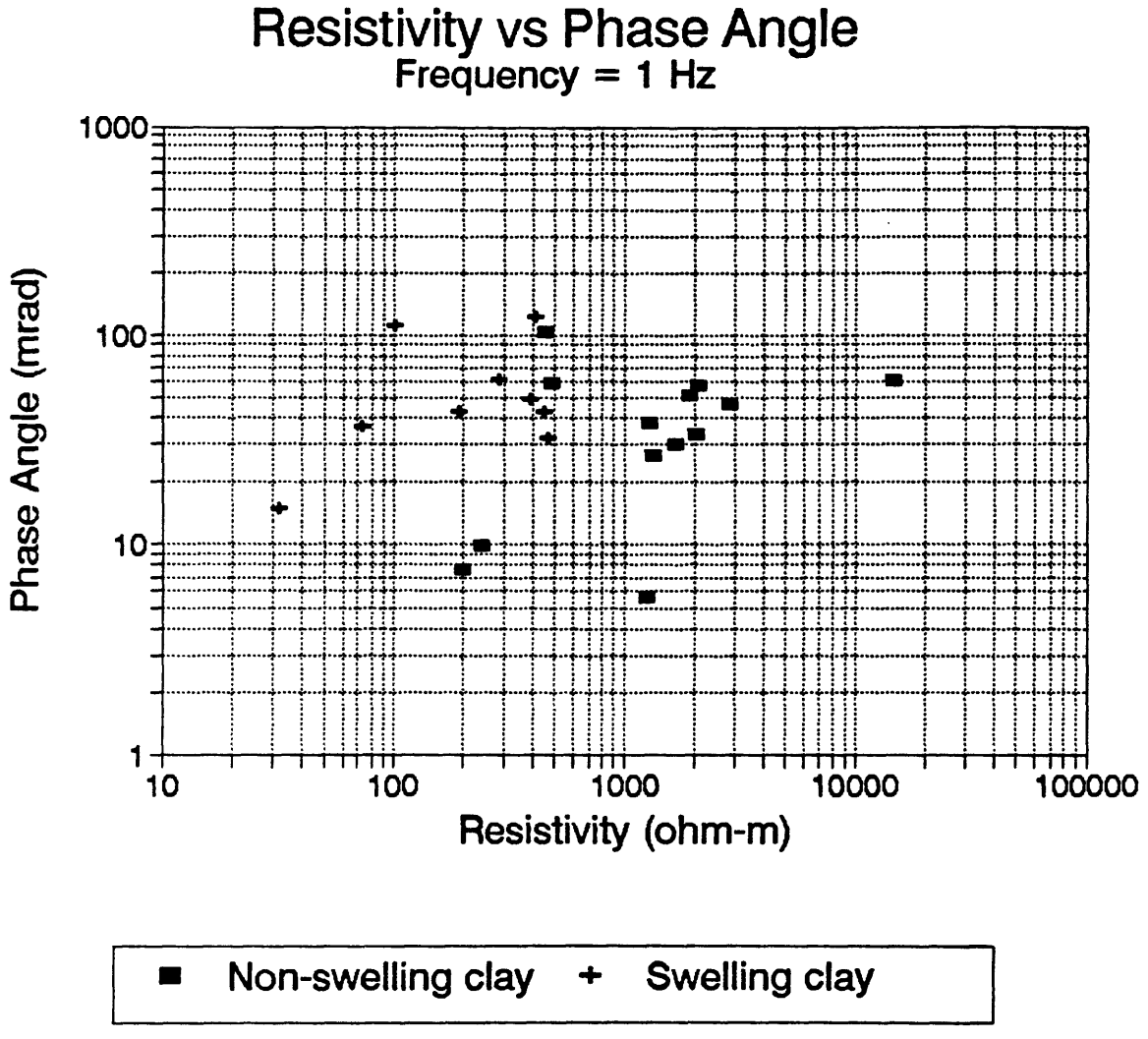

Figure 17. A plot of resistivity vs phase angle for the "as received" samples measured at 1 Hz. The plot shows no relationship between resistivity and phase. Swelling clay samples generally have lower resistivities than non-swelling clay samples.

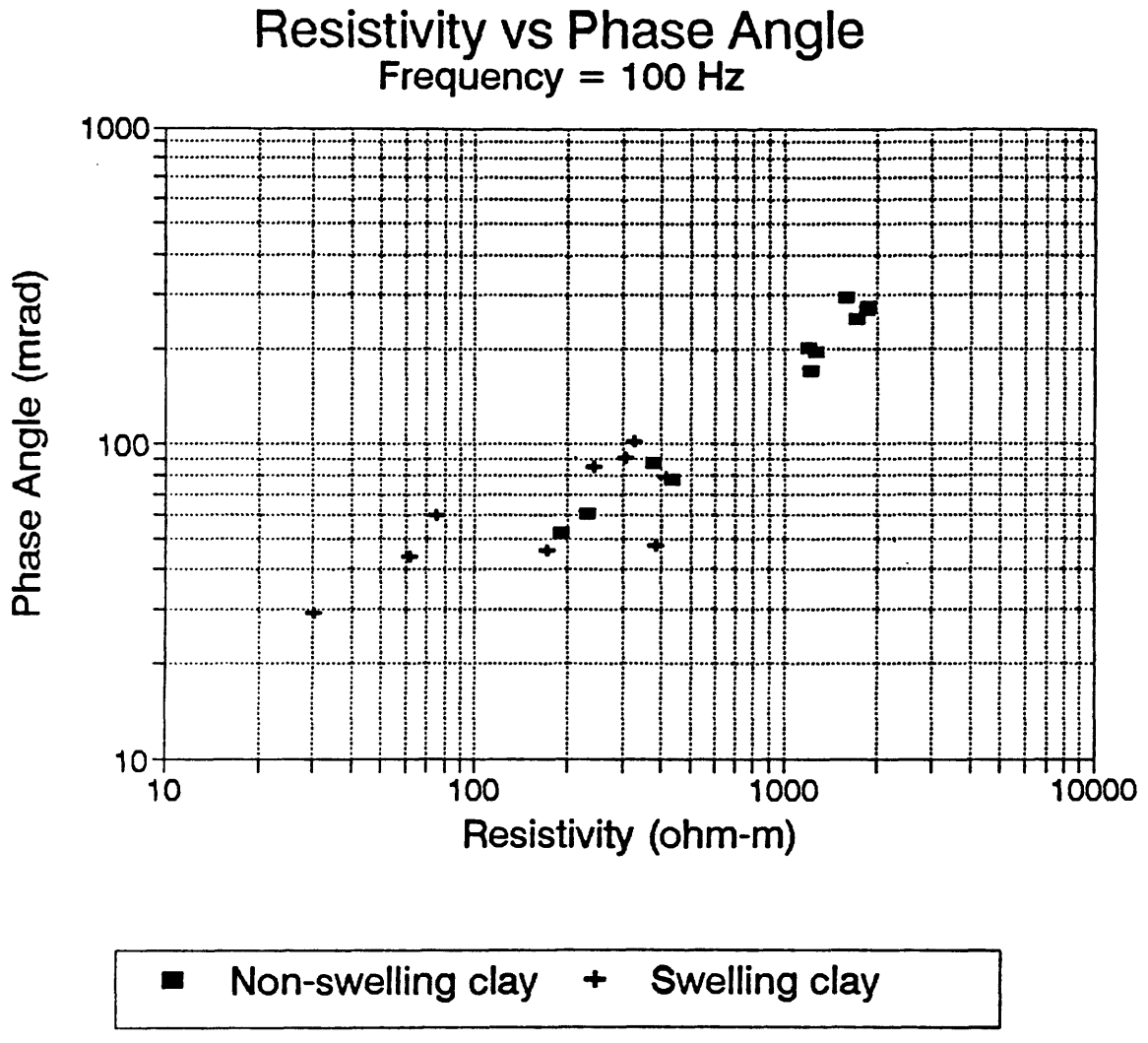

Figure 18. A plot of resistivity vs phase angle measured at 100 Hz. The plot indicates that at 100 Hz, resistivity and phase are related.

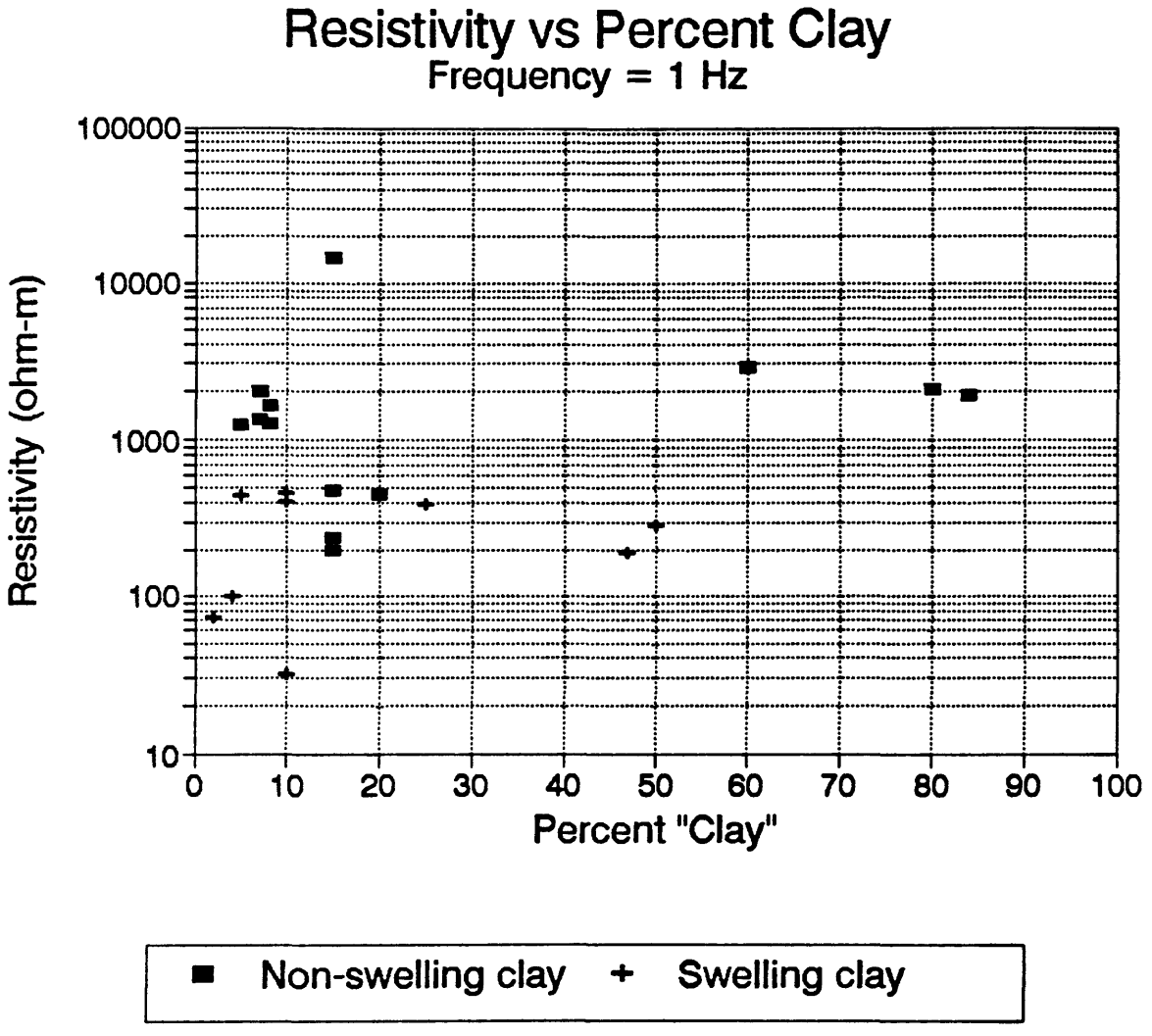

Figure 19. shows a plot of resistivity vs percent clay, measured at a frequency of 1 Hz. The plot indicates that the resistivity of the "as received" samples is not dependent upon clay content.

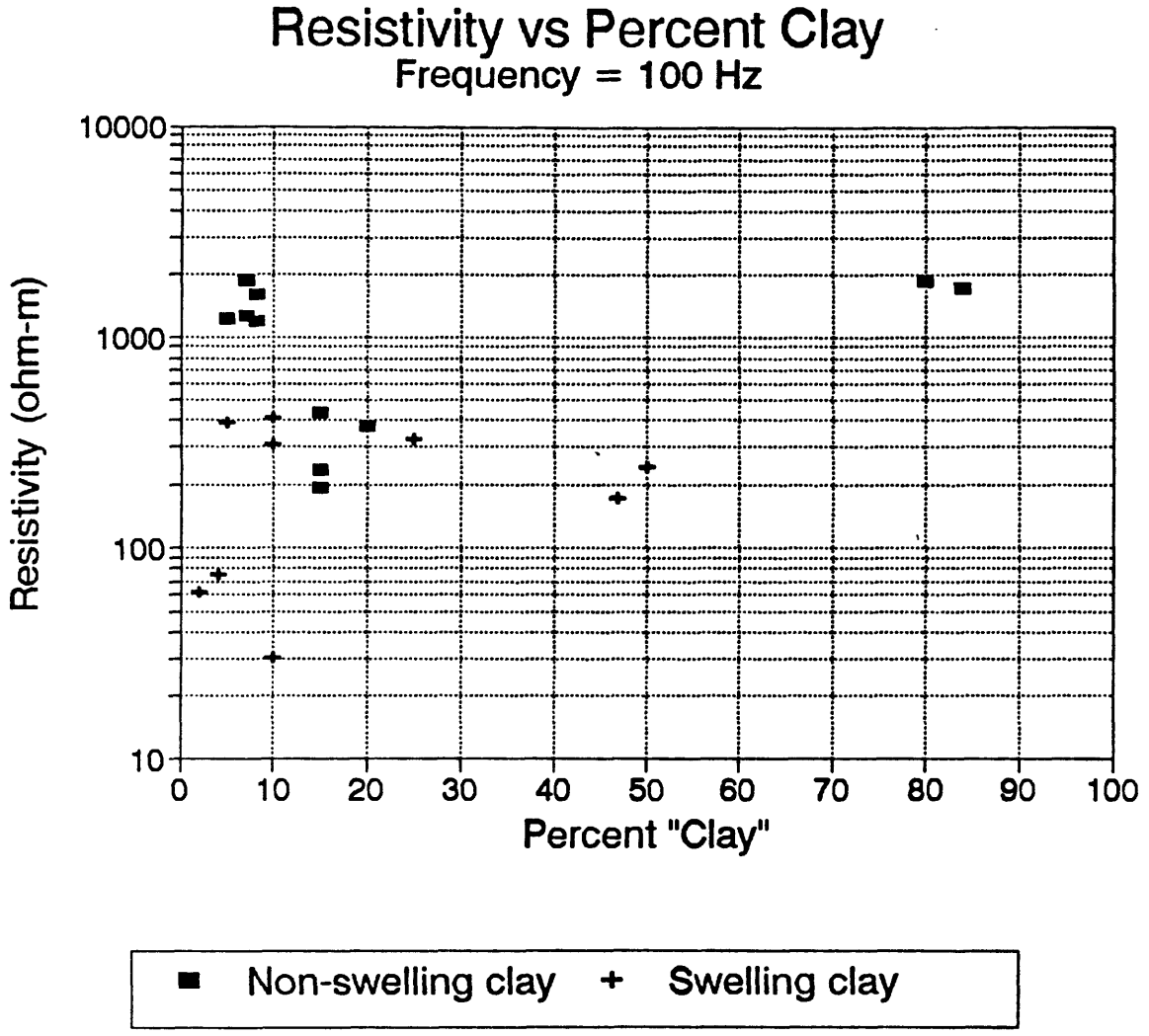

Figure 20. shows a plot of resistivity vs percent clay, measured at a frequency of 100 Hz. The plot indicates that the resistivity of the "as received" samples is not dependent upon clay content.

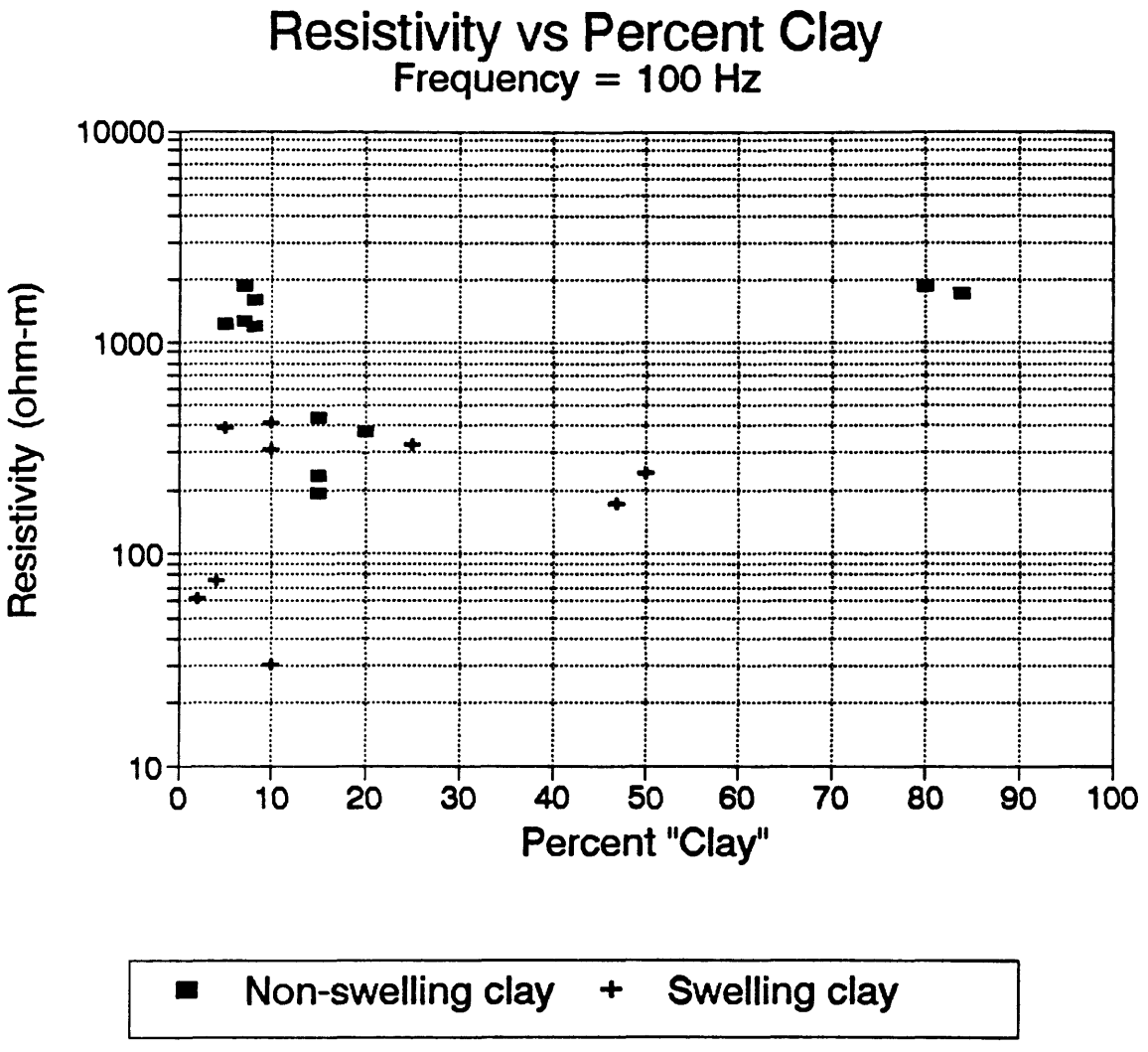

Figure 21. A plot of phase angle vs percent clay, measured at a frequency of 1 Hz. The plot indicates that the phase of the "as received" samples is not dependent upon clay content.

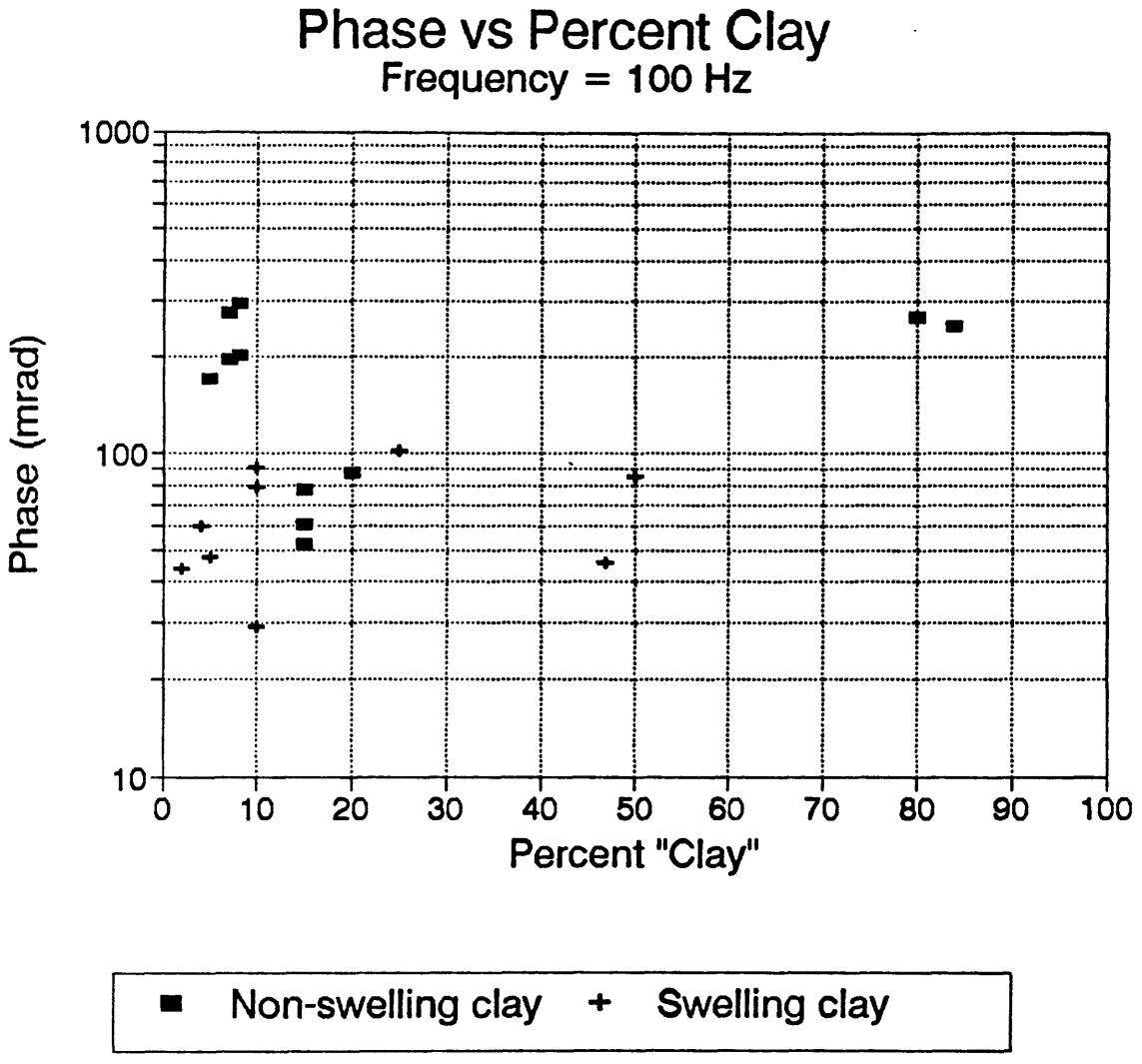

Figure 22. A plot of phase angle vs percent clay, measured at a frequency of 100 Hz. The plot indicates that the resistivity of the "as received" samples is not dependent upon clay content.

Appendix A

X-ray Diffraction Patterns of SRS Core Samples

Notes on XRD plots. All XRD data was plotted as raw, uncorrected, data. The file name of each XRD plot is in the upper left hand corner of each plot. The suffix of the file name ".rd" denotes raw data. The last two letters of the file name indicate the type of mount. File names of oriented samples end with "o" or "or". Files names of glycolated samples end with "g" or "og".

The bottom horizontal scale is the angle 2θ. The top horizontal scale is d-spacing in Å. The left vertical scale is the intensity of x-rays in counts per second (cps). The right vertical scale is percent. Peak labels are d-spacing/cps.

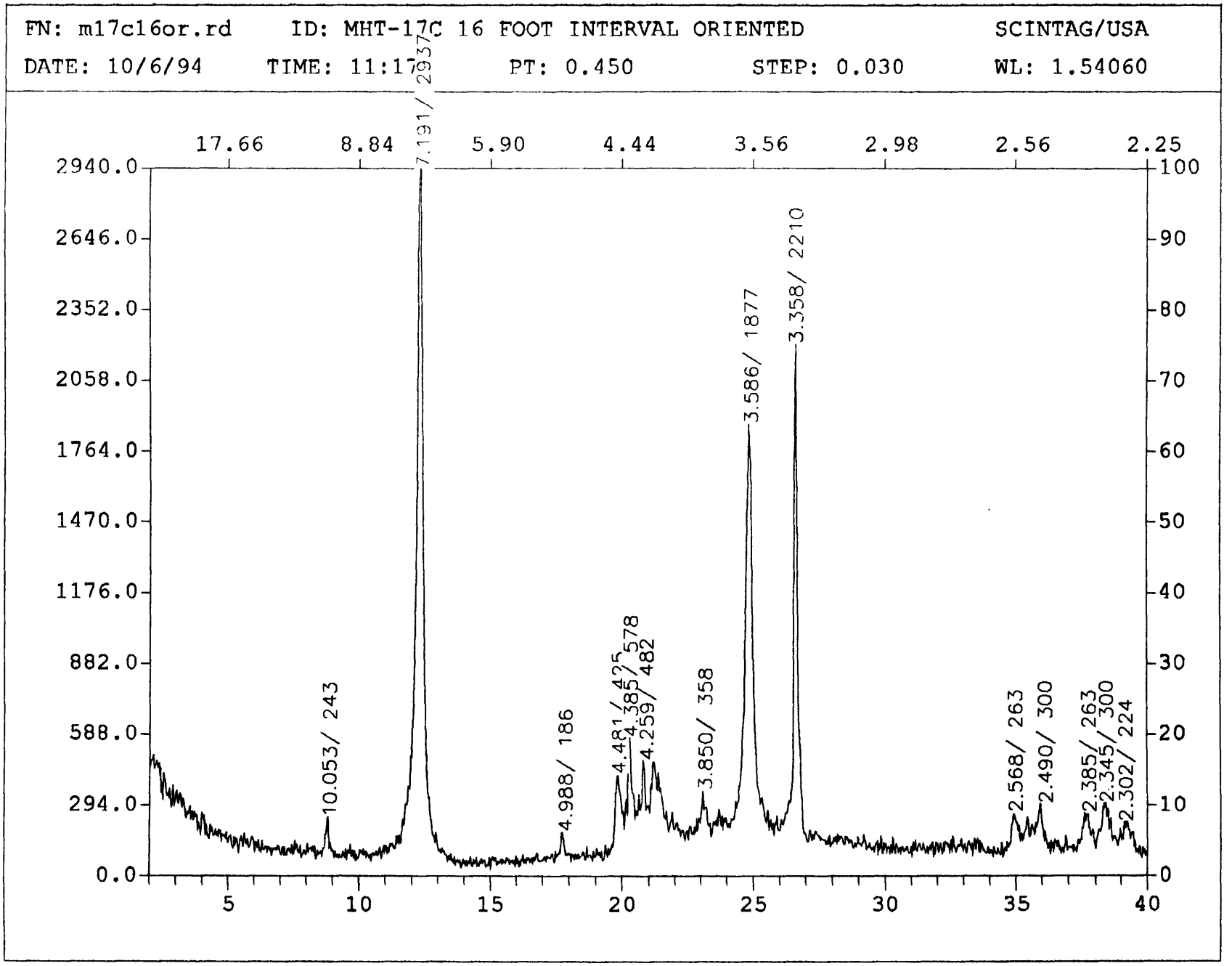
FN: m17c16or.rd
ID: MHT-17C 16 FOOT INTERVAL ORIENTED
SCINTAG/USA
DATE: 10/6/94
TIME: 11:17
PT: 0.450
STEP: 0.030
WL: 1.54060
17.66
8.84
5.90
4.44
3.56
2.98
2.56
2.25
2940.0
2646.0
2352.0
2058.0
1764.0
1470.0
1176.0
882.0
588.0
294.0
0.0
100
90
80
70
60
50
40
30
20
10
0
5
10
15
20
25
30
35
40
7.191/ 2937
10.053/ 243
4.988/ 186
4.481/ 425
4.385/ 578
4.259/ 482
3.850/ 358
3.586/ 1877
3.358/ 2210
2.568/ 263
2.490/ 300
2.385/ 263
2.345/ 300
2.302/ 224

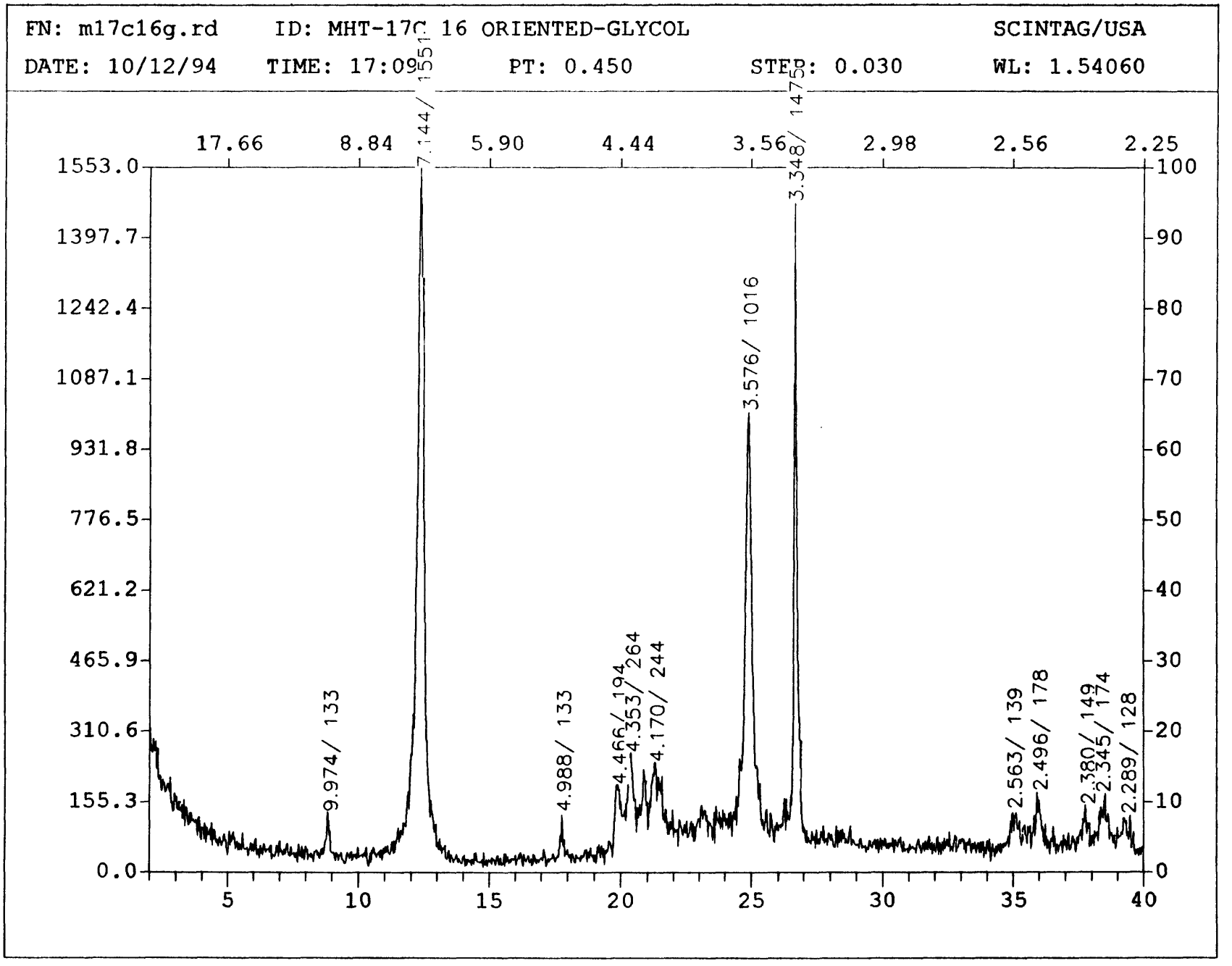
FN: m17c16g.rd
ID: MHT-17C 16 ORIENTED-GLYCOL
SCINTAG/USA
DATE: 10/12/94
TIME: 17:09
PT: 0.450
STEP: 0.030
WL: 1.54060
17.66
8.84
5.90
4.44
3.56
2.98
2.56
2.25
7.144/ 1551
3.348/ 1475
3.576/ 1016
9.974/ 133
4.988/ 133
4.466/ 194
4.353/ 264
4.170/ 244
2.563/ 139
2.496/ 178
2.380/ 149
2.345/ 174
2.289/ 128
1553.0
1397.7
1242.4
1087.1
931.8
776.5
621.2
465.9
310.6
155.3
0.0
100
90
80
70
60
50
40
30
20
10
0
5
10
15
20
25
30
35
40

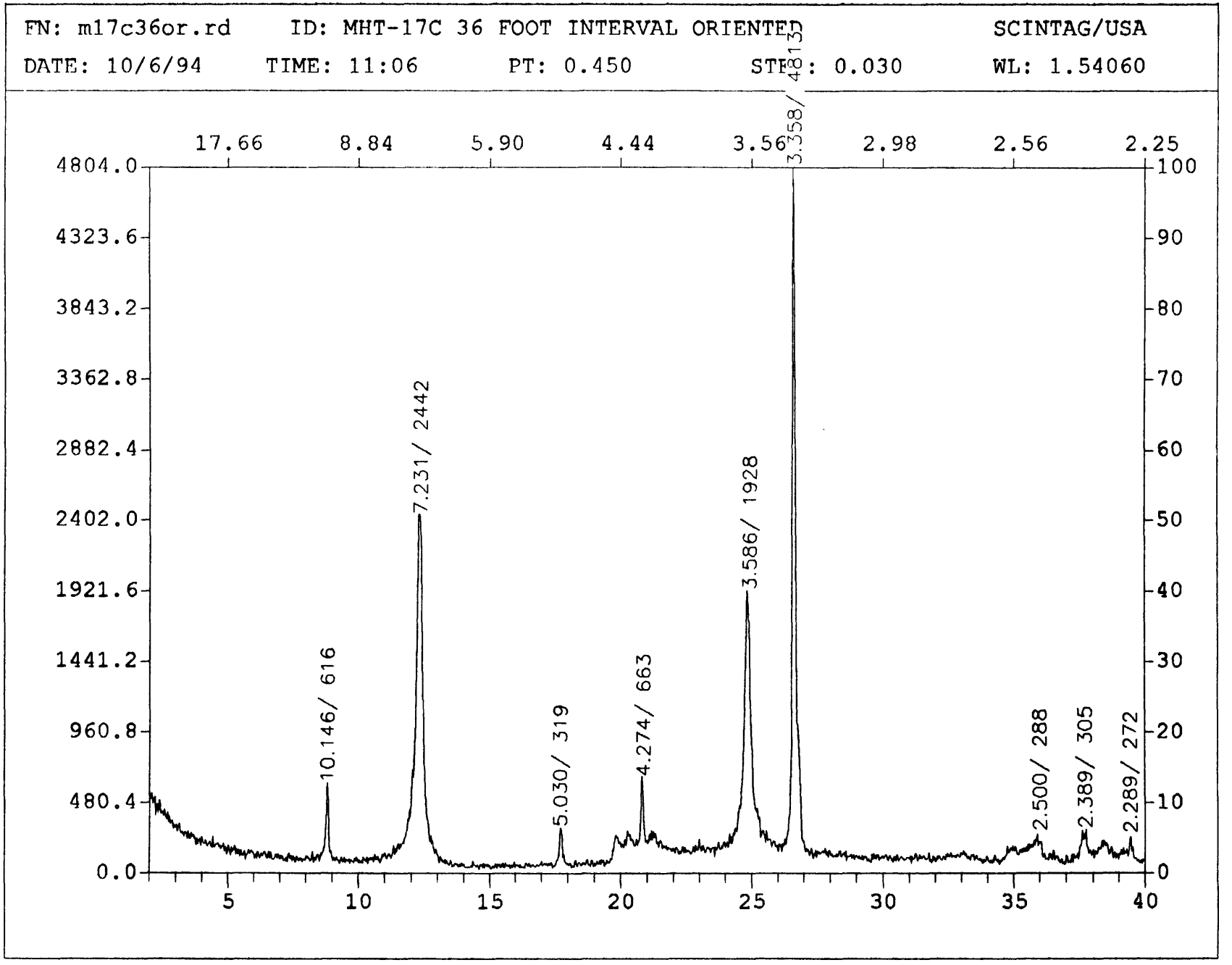
FN: m17c36or.rd
ID: MHT-17C 36 FOOT INTERVAL ORIENTED
SCINTAG/USA
DATE: 10/6/94
TIME: 11:06
PT: 0.450
STP: 0.030
WL: 1.54060
17.66
8.84
5.90
4.44
3.56
3.358/ 4813
2.98
2.56
2.25
4804.0
4323.6
3843.2
3362.8
2882.4
2402.0
1921.6
1441.2
960.8
480.4
0.0
100
90
80
70
60
50
40
30
20
10
0
10.146/ 616
7.231/ 2442
5.030/ 319
4.274/ 663
3.586/ 1928
2.500/ 288
2.389/ 305
2.289/ 272
5
10
15
20
25
30
35
40

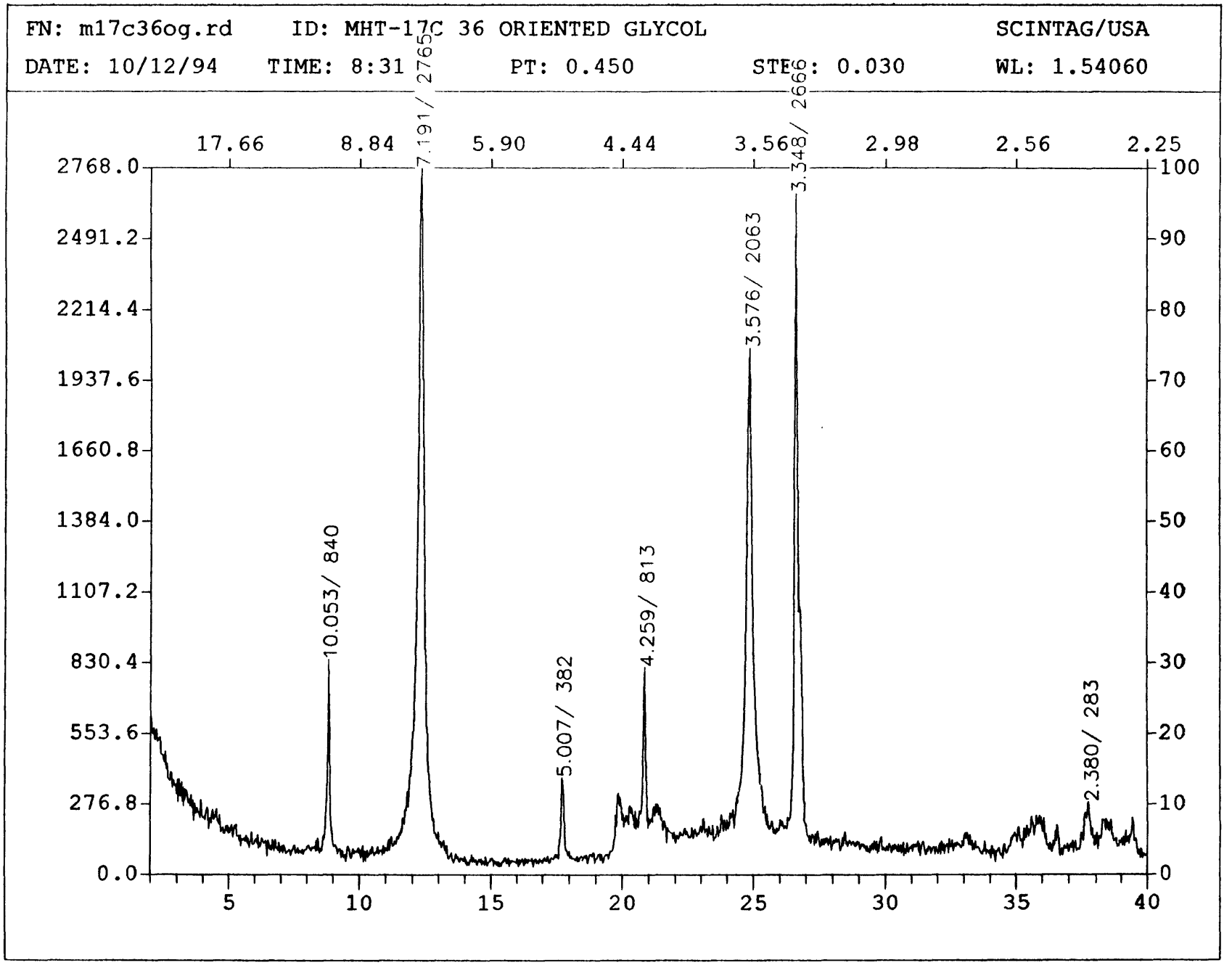
FN: m17c36og.rd
ID: MHT-17C 36 ORIENTED GLYCOL
SCINTAG/USA
DATE: 10/12/94
TIME: 8:31
PT: 0.450
STEP: 0.030
WL: 1.54060
17.66
8.84
5.90
4.44
3.56
2.98
2.56
2.25
7.191/ 2765
3.348/ 2666
3.576/ 2063
10.053/ 840
5.007/ 382
4.259/ 813
2.380/ 283
2768.0
2491.2
2214.4
1937.6
1660.8
1384.0
1107.2
830.4
553.6
276.8
0.0
100
90
80
70
60
50
40
30
20
10
0
5
10
15
20
25
30
35
40

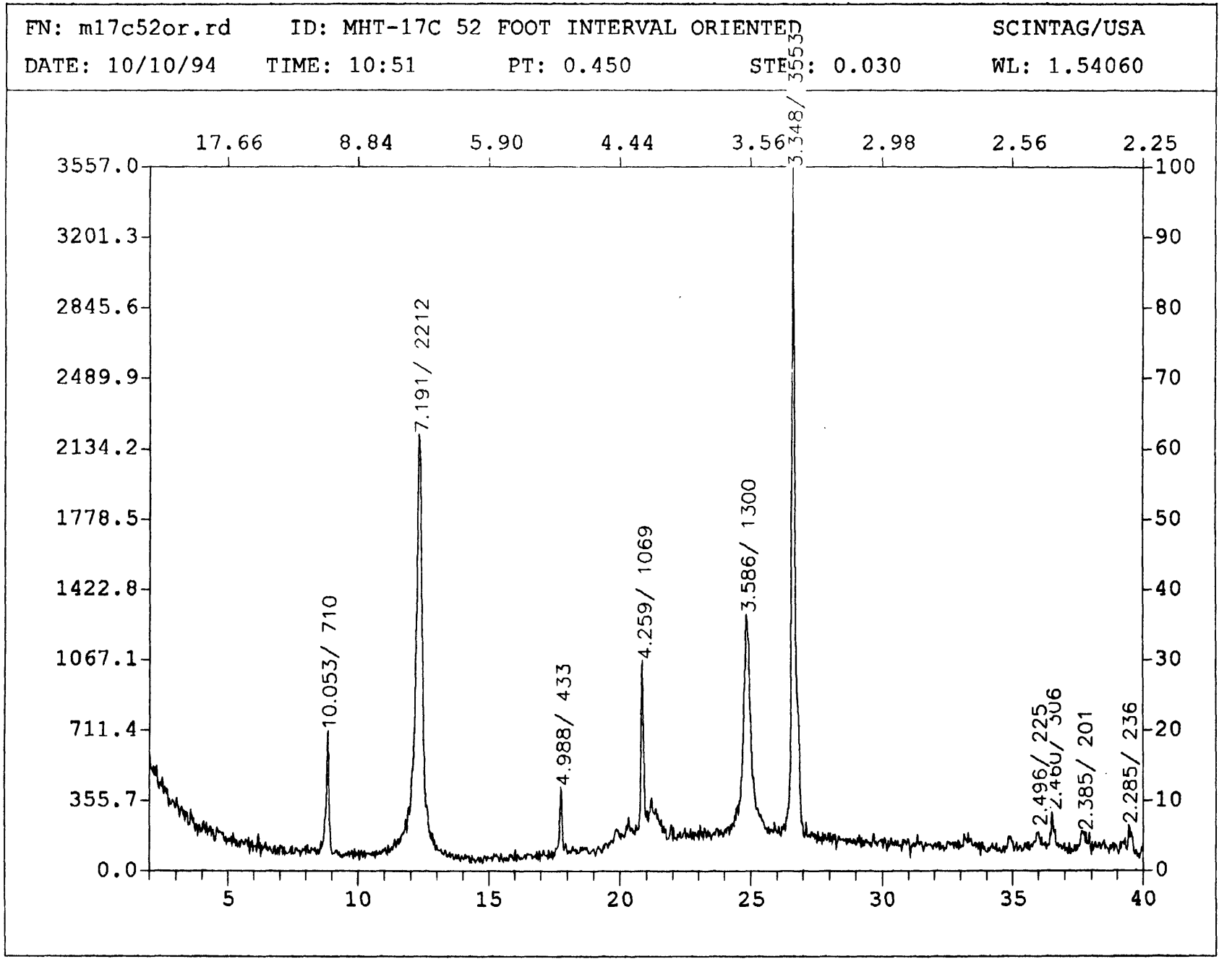
FN: m17c52or.rd
ID: MHT-17C 52 FOOT INTERVAL ORIENTED
SCINTAG/USA
DATE: 10/10/94
TIME: 10:51
PT: 0.450
STEP: 0.030
WL: 1.54060
17.66
8.84
5.90
4.44
3.56
3.348/ 3553
2.98
2.56
2.25
3557.0
3201.3
2845.6
2489.9
2134.2
1778.5
1422.8
1067.1
711.4
355.7
0.0
100
90
80
70
60
50
40
30
20
10
0
10.053/ 710
7.191/ 2212
4.988/ 433
4.259/ 1069
3.586/ 1300
2.496/ 225
2.460/ 306
2.385/ 201
2.285/ 236
5
10
15
20
25
30
35
40

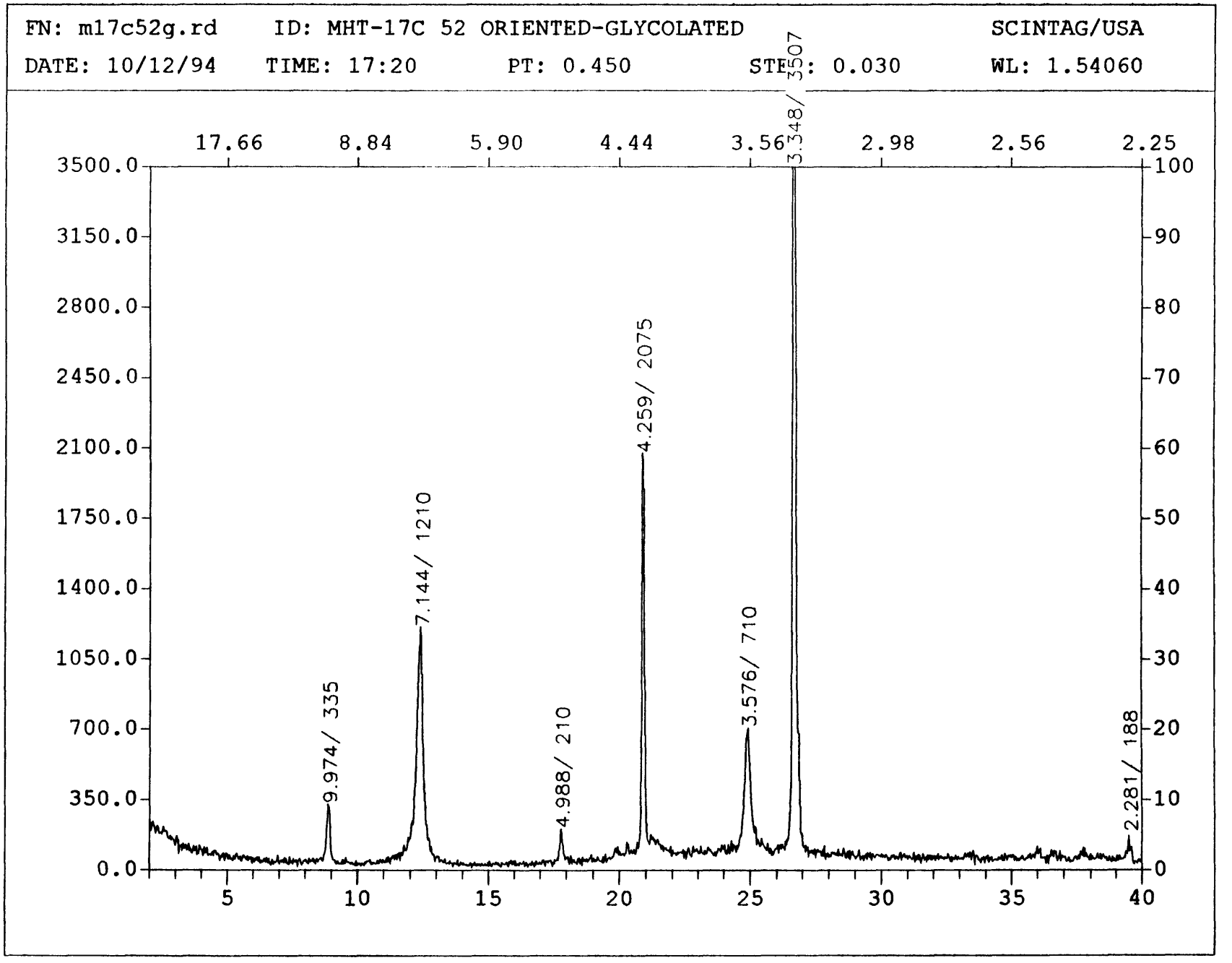
FN: m17c52g.rd
ID: MHT-17C 52 ORIENTED-GLYCOLATED
SCINTAG/USA
DATE: 10/12/94
TIME: 17:20
PT: 0.450
STP: 0.030
WL: 1.54060
17.66
8.84
5.90
4.44
3.56
3.348/ 3507
2.98
2.56
2.25
3500.0
3150.0
2800.0
2450.0
2100.0
1750.0
1400.0
1050.0
700.0
350.0
0.0
100
90
80
70
60
50
40
30
20
10
0
9.974/ 335
7.144/ 1210
4.988/ 210
4.259/ 2075
3.576/ 710
2.281/ 188
5
10
15
20
25
30
35
40

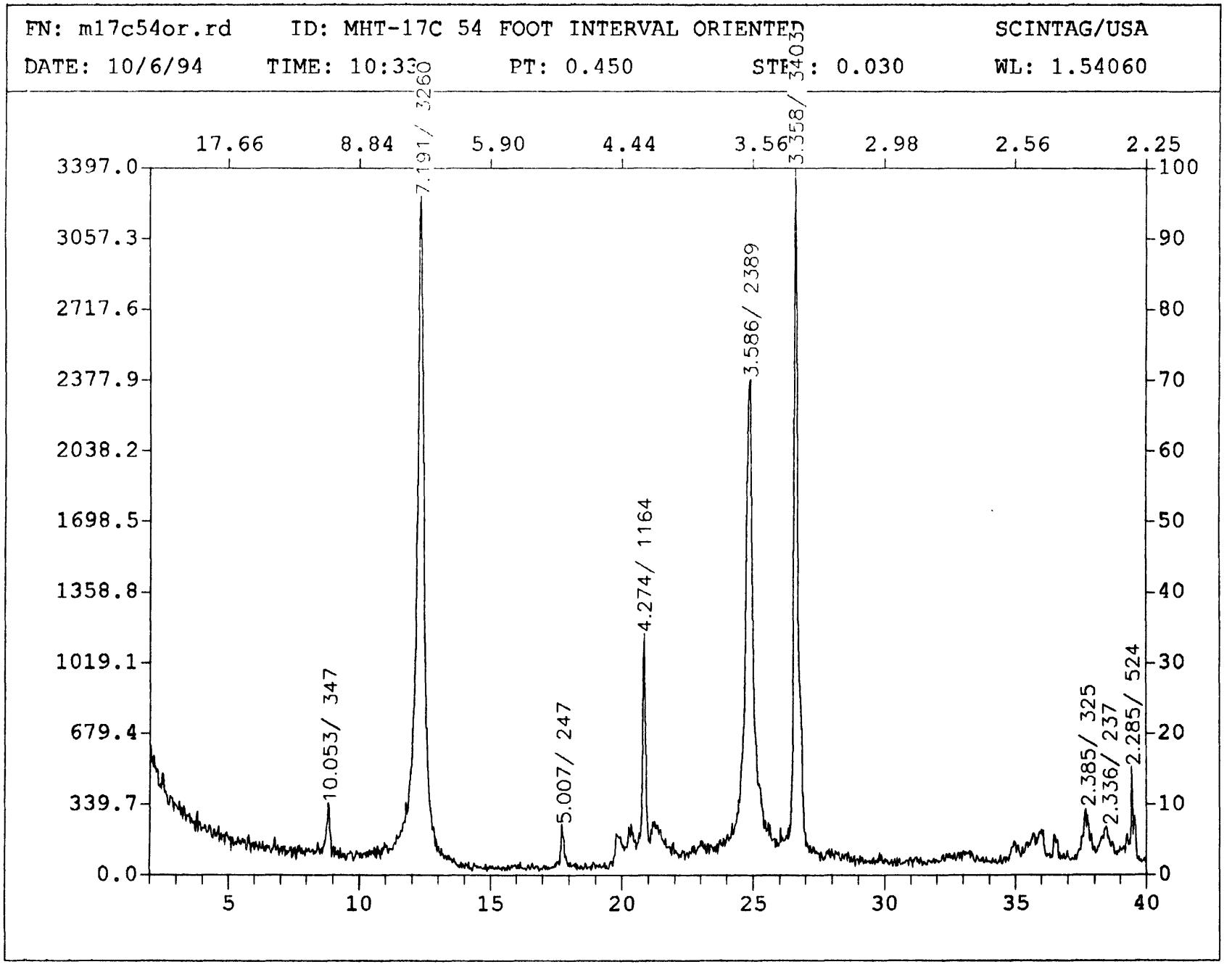
FN: m17c54or.rd
ID: MHT-17C 54 FOOT INTERVAL ORIENTED
SCINTAG/USA
DATE: 10/6/94
TIME: 10:33
PT: 0.450
STEP: 0.030
WL: 1.54060
17.66
8.84
5.90
4.44
3.56
2.98
2.56
2.25
3397.0
3057.3
2717.6
2377.9
2038.2
1698.5
1358.8
1019.1
679.4
339.7
0.0
100
90
80
70
60
50
40
30
20
10
0
5
10
15
20
25
30
35
40
7.191/ 3260
3.358/ 3403
3.586/ 2389
4.274/ 1164
10.053/ 347
5.007/ 247
2.385/ 325
2.336/ 237
2.285/ 524

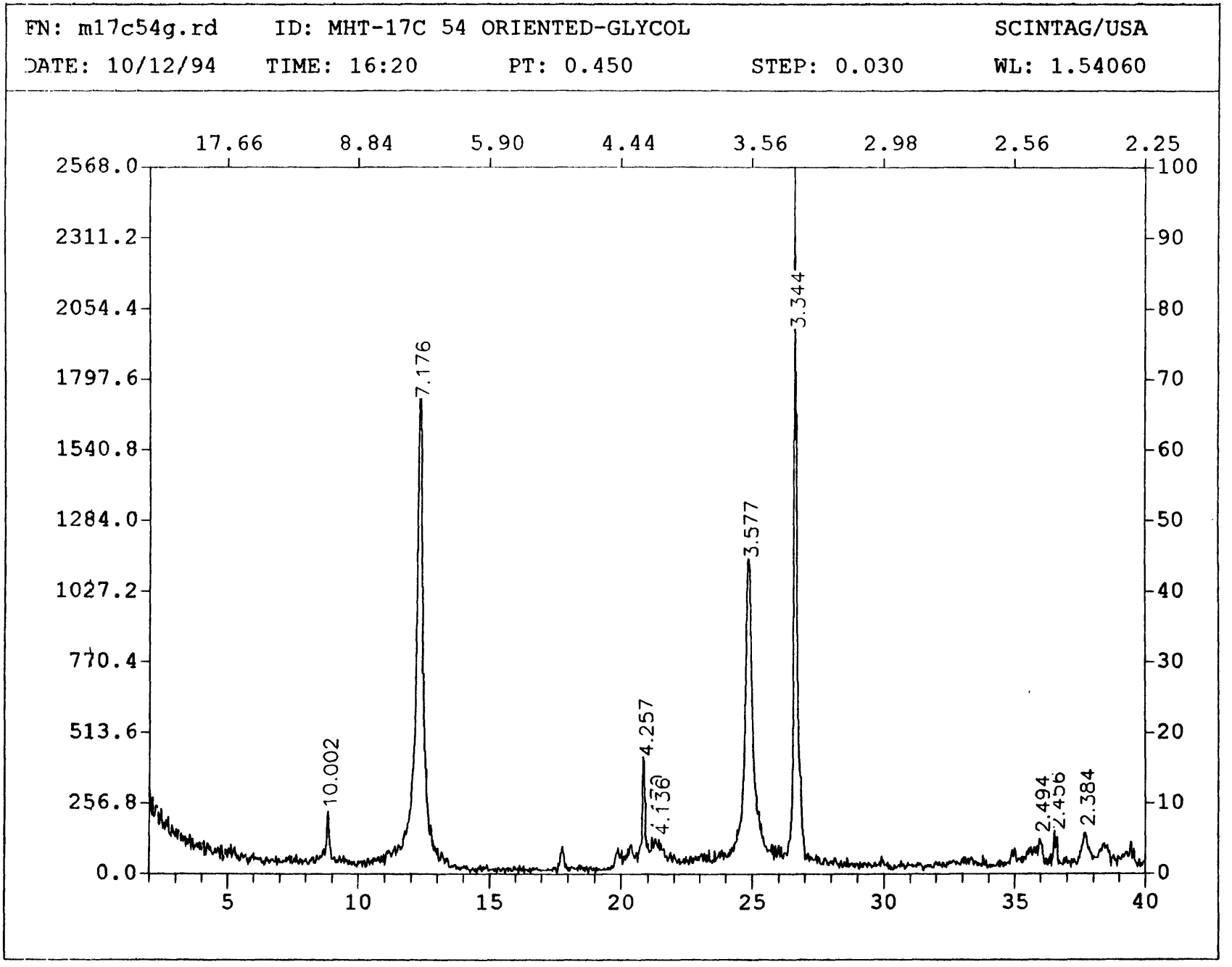
FN: m17c54g.rd
ID: MHT-17C 54 ORIENTED-GLYCOL
SCINTAG/USA
DATE: 10/12/94
TIME: 16:20
PT: 0.450
STEP: 0.030
WL: 1.54060
17.66
8.84
5.90
4.44
3.56
2.98
2.56
2.25
2568.0
2311.2
2054.4
1797.6
1540.8
1284.0
1027.2
770.4
513.6
256.8
0.0
100
90
80
70
60
50
40
30
20
10
0
10.002
7.176
4.257
4.136
3.577
3.344
2.494
2.456
2.384
5
10
15
20
25
30
35
40

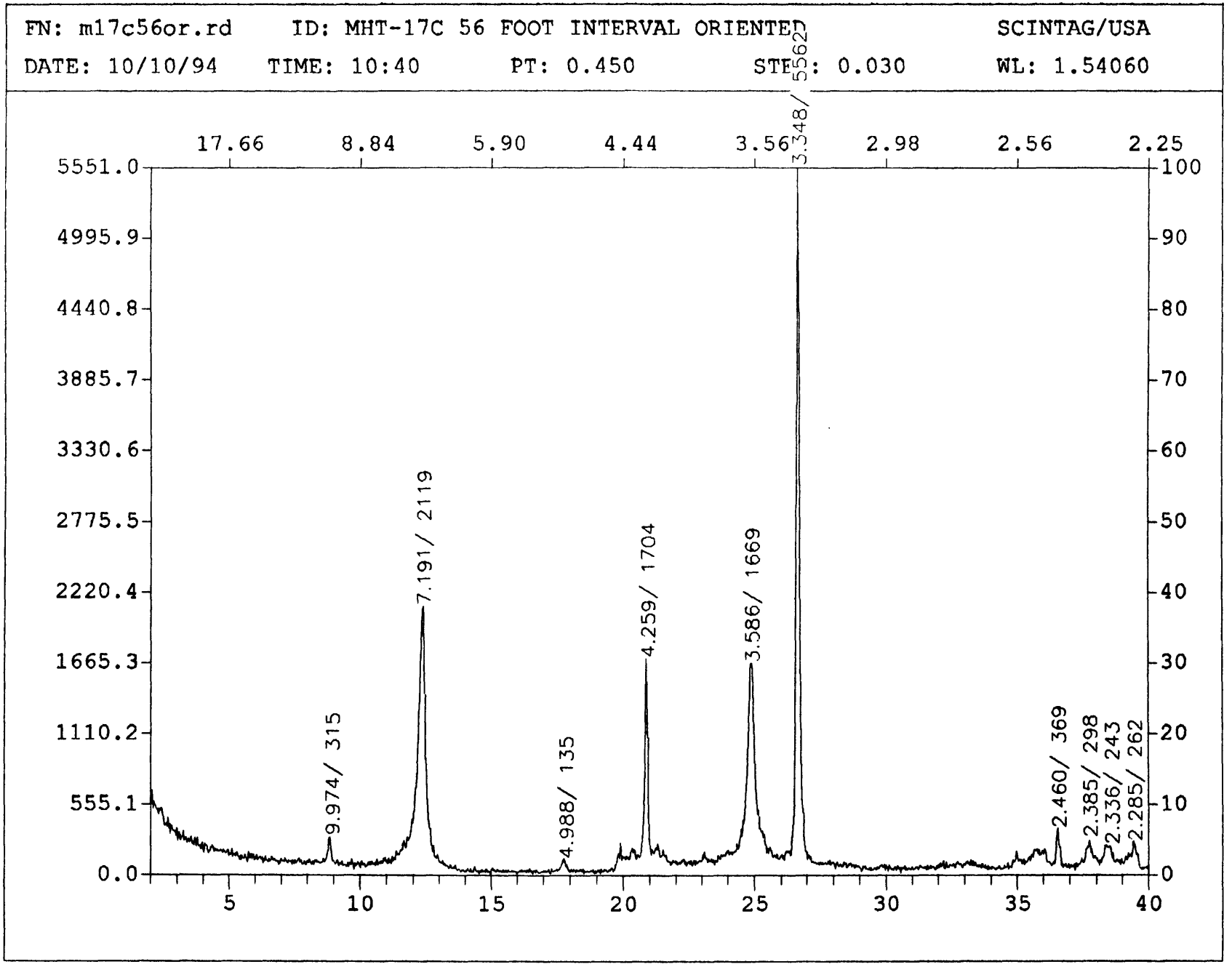
FN: m17c56or.rd
ID: MHT-17C 56 FOOT INTERVAL ORIENTED
SCINTAG/USA
DATE: 10/10/94
TIME: 10:40
PT: 0.450
STP: 0.030
WL: 1.54060
17.66
8.84
5.90
4.44
3.56
3.348/ 5562
2.98
2.56
2.25
5551.0
4995.9
4440.8
3885.7
3330.6
2775.5
2220.4
1665.3
1110.2
555.1
0.0
100
90
80
70
60
50
40
30
20
10
0
9.974/ 315
7.191/ 2119
4.988/ 135
4.259/ 1704
3.586/ 1669
2.460/ 369
2.385/ 298
2.336/ 243
2.285/ 262
5
10
15
20
25
30
35
40

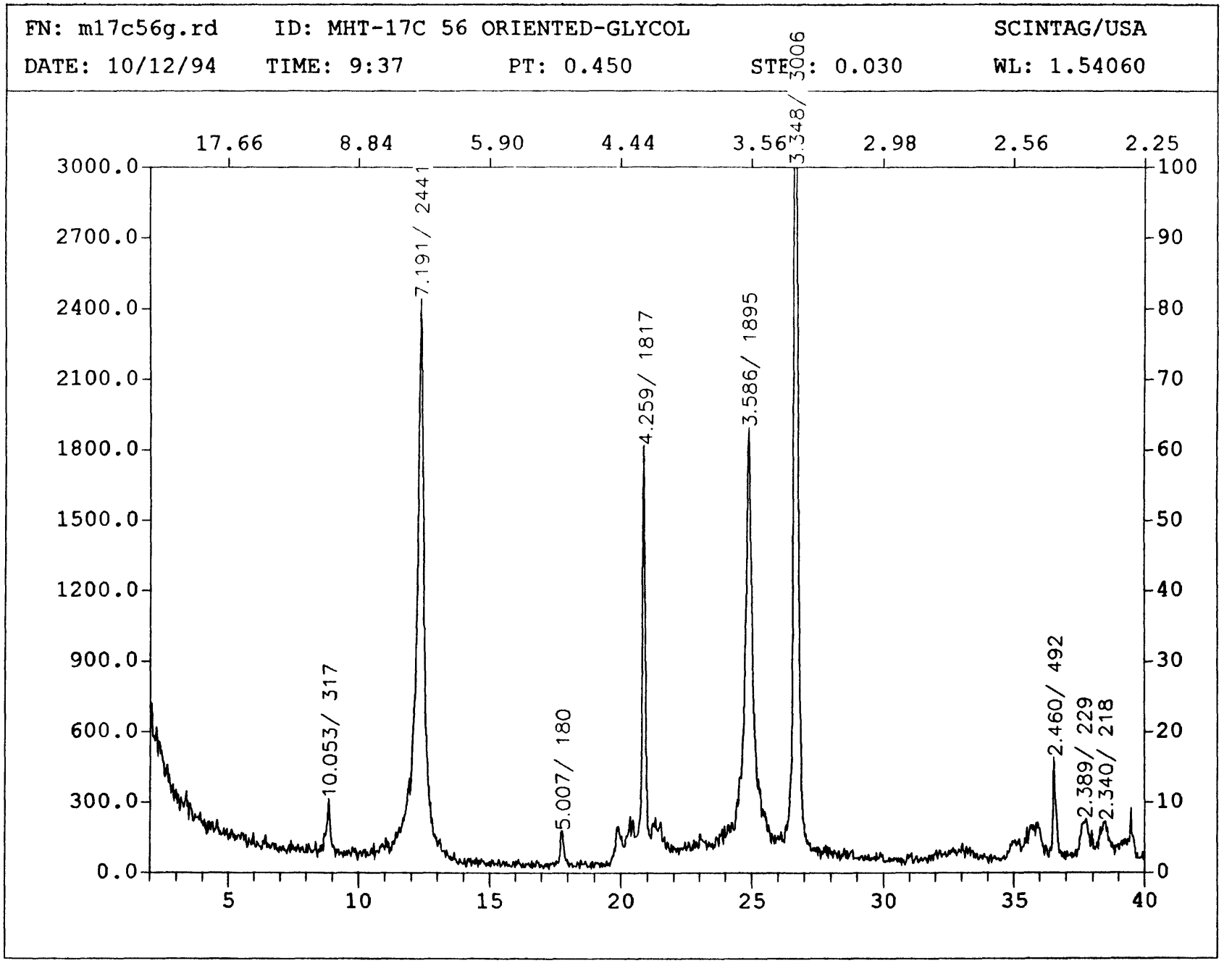
FN: m17c56g.rd
ID: MHT-17C 56 ORIENTED-GLYCOL
SCINTAG/USA
DATE: 10/12/94
TIME: 9:37
PT: 0.450
STE: 0.030
WL: 1.54060
17.66
8.84
5.90
4.44
3.56
2.98
2.56
2.25
3.348/ 3006
7.191/ 2441
4.259/ 1817
3.586/ 1895
10.053/ 317
5.007/ 180
2.460/ 492
2.389/ 229
2.340/ 218
3000.0
2700.0
2400.0
2100.0
1800.0
1500.0
1200.0
900.0
600.0
300.0
0.0
100
90
80
70
60
50
40
30
20
10
0
5
10
15
20
25
30
35
40

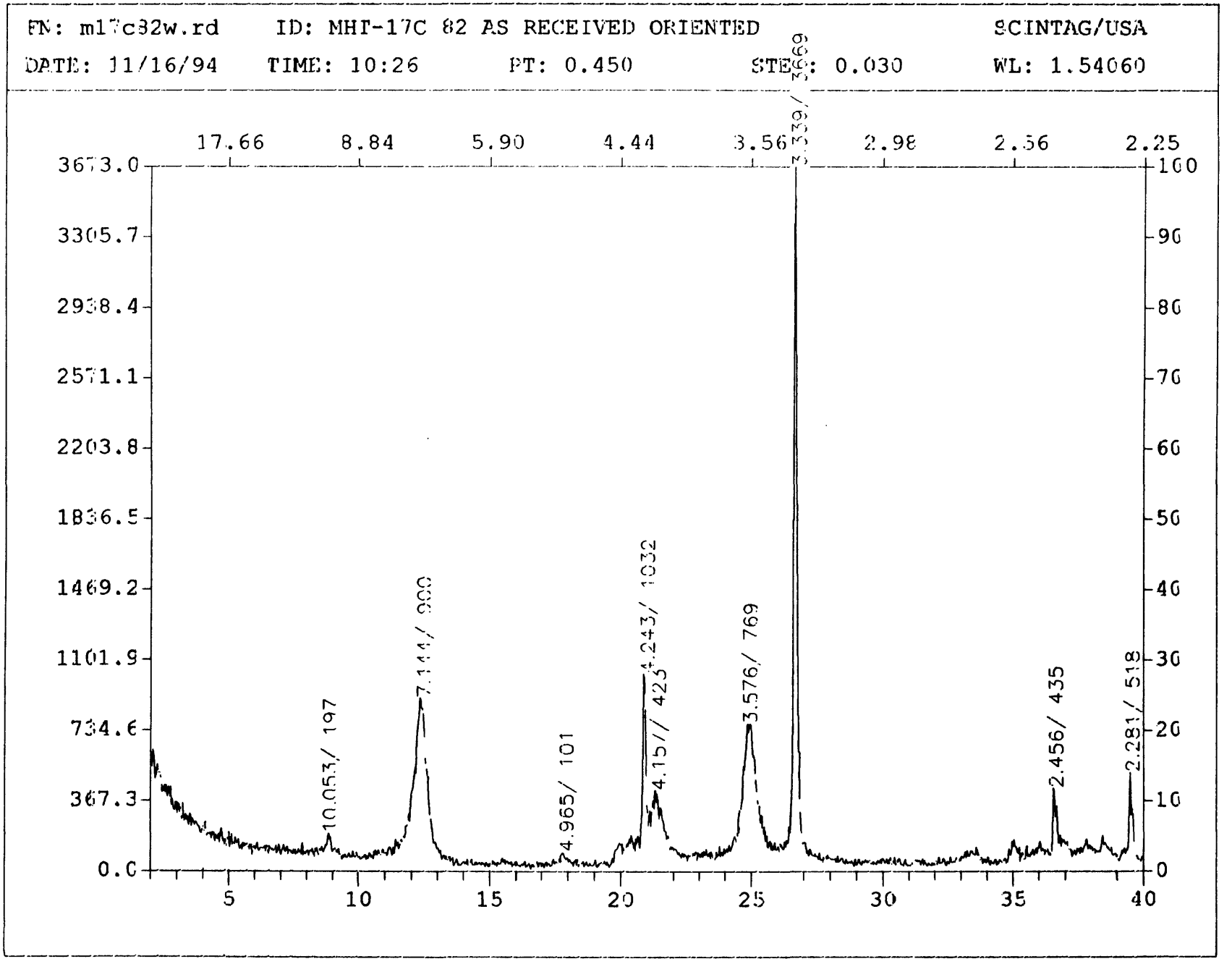
FN: m17c82w.rd ID: MHT-17C 82 AS RECEIVED ORIENTED SCINTAG/USA
DATE: 11/16/94 TIME: 10:26 PT: 0.450 STEP: 0.030 WL: 1.54060
17.66
8.84
5.90
4.44
3.56
2.98
2.56
2.25
3673.0
3305.7
2938.4
2571.1
2203.8
1836.5
1469.2
1101.9
734.6
367.3
0.0
100
90
80
70
60
50
40
30
20
10
0
5
10
15
20
25
30
35
40
10.053/ 197
7.144/ 900
4.965/ 101
4.243/ 1032
4.157/ 425
3.576/ 769
3.339/ 3669
2.456/ 435
2.281/ 518

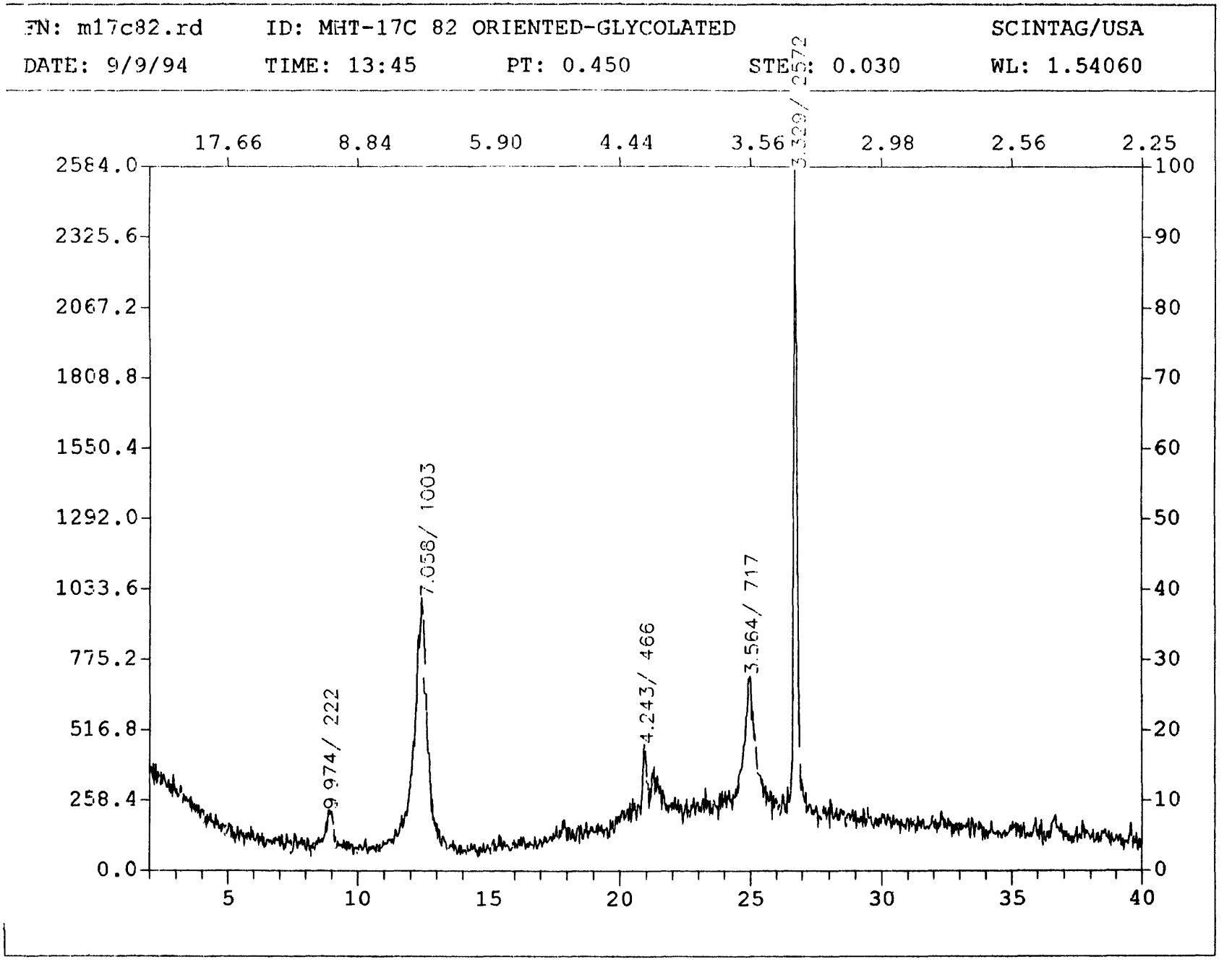
FN: m17c82.rd
ID: MHT-17C 82 ORIENTED-GLYCOLATED
SCINTAG/USA
DATE: 9/9/94
TIME: 13:45
PT: 0.450
STE: 0.030
WL: 1.54060
17.66
8.84
5.90
4.44
3.56
2.98
2.56
2.25
3.329/ 2572
2584.0
2325.6
2067.2
1808.8
1550.4
1292.0
1033.6
775.2
516.8
258.4
0.0
100
90
80
70
60
50
40
30
20
10
0
9.974/ 222
7.058/ 1003
4.243/ 466
3.564/ 717
5
10
15
20
25
30
35
40

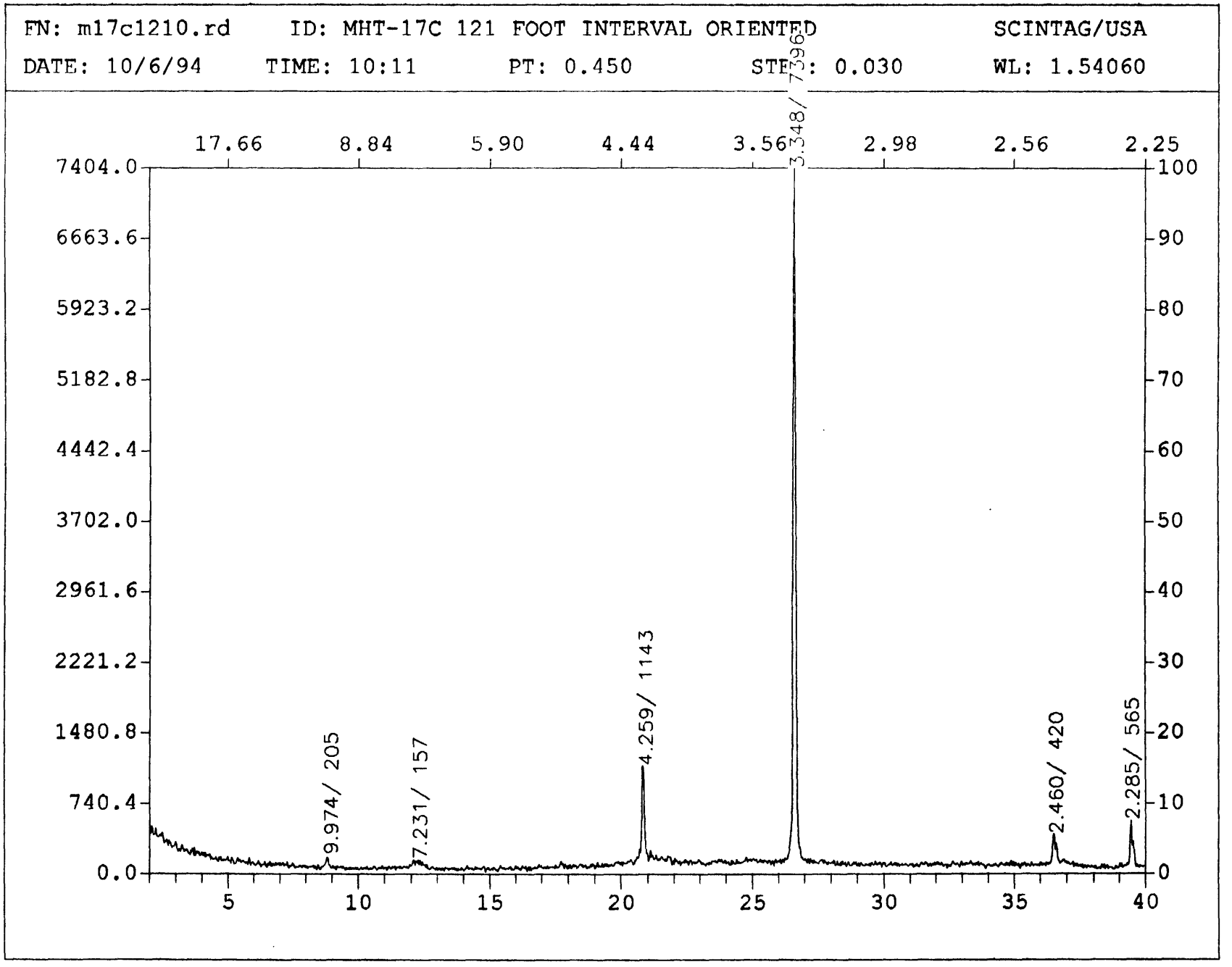
FN: m17c1210.rd
ID: MHT-17C 121 FOOT INTERVAL ORIENTED
SCINTAG/USA
DATE: 10/6/94
TIME: 10:11
PT: 0.450
STP: 0.030
WL: 1.54060
17.66
8.84
5.90
4.44
3.56
2.98
2.56
2.25
3.348/ 7396
7404.0
6663.6
5923.2
5182.8
4442.4
3702.0
2961.6
2221.2
1480.8
740.4
0.0
100
90
80
70
60
50
40
30
20
10
0
9.974/ 205
7.231/ 157
4.259/ 1143
2.460/ 420
2.285/ 565
5
10
15
20
25
30
35
40

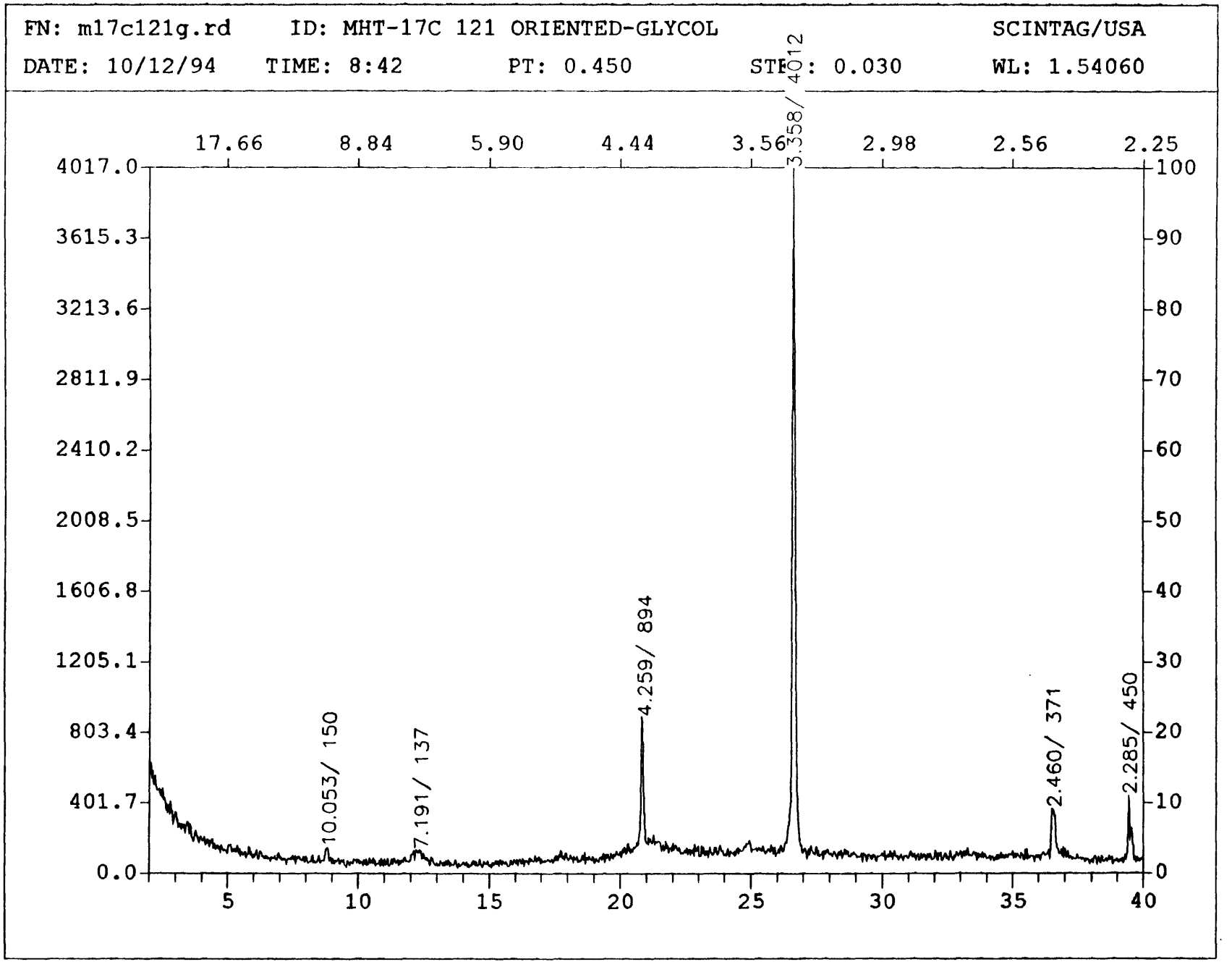
FN: m17c121g.rd
ID: MHT-17C 121 ORIENTED-GLYCOL
SCINTAG/USA
DATE: 10/12/94
TIME: 8:42
PT: 0.450
STP: 0.030
WL: 1.54060
17.66
8.84
5.90
4.44
3.56
2.98
2.56
2.25
4017.0
3615.3
3213.6
2811.9
2410.2
2008.5
1606.8
1205.1
803.4
401.7
0.0
100
90
80
70
60
50
40
30
20
10
0
5
10
15
20
25
30
35
40
3.358/ 4012
4.259/ 894
10.053/ 150
7.191/ 137
2.460/ 371
2.285/ 450

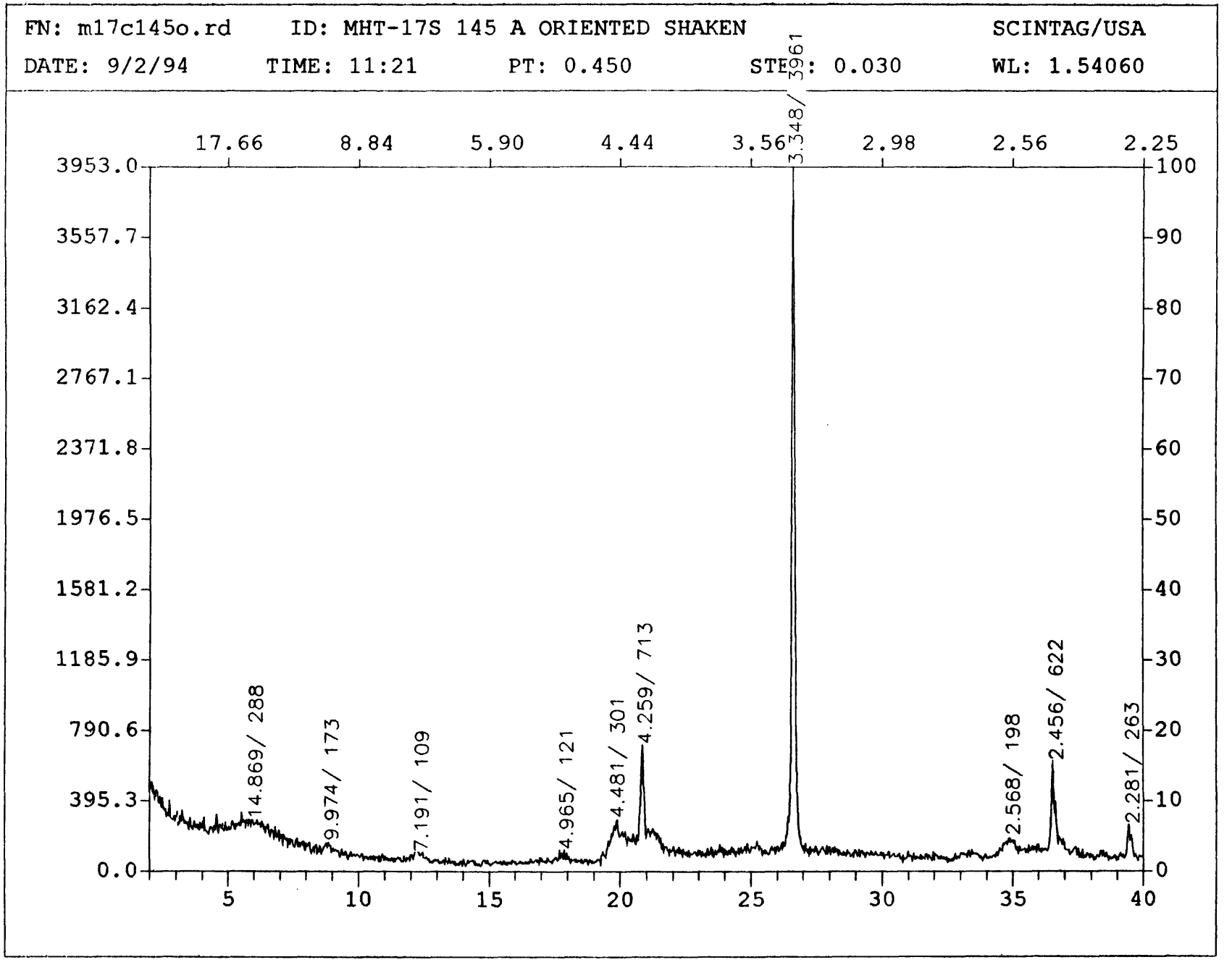
FN: m17c145o.rd
ID: MHT-17S 145 A ORIENTED SHAKEN
SCINTAG/USA
DATE: 9/2/94
TIME: 11:21
PT: 0.450
STEP: 0.030
WL: 1.54060
17.66
8.84
5.90
4.44
3.56
3.348/ 3961
2.98
2.56
2.25
3953.0
3557.7
3162.4
2767.1
2371.8
1976.5
1581.2
1185.9
790.6
395.3
0.0
100
90
80
70
60
50
40
30
20
10
0
5
10
15
20
25
30
35
40
14.869/ 288
9.974/ 173
7.191/ 109
4.965/ 121
4.481/ 301
4.259/ 713
2.568/ 198
2.456/ 622
2.281/ 263

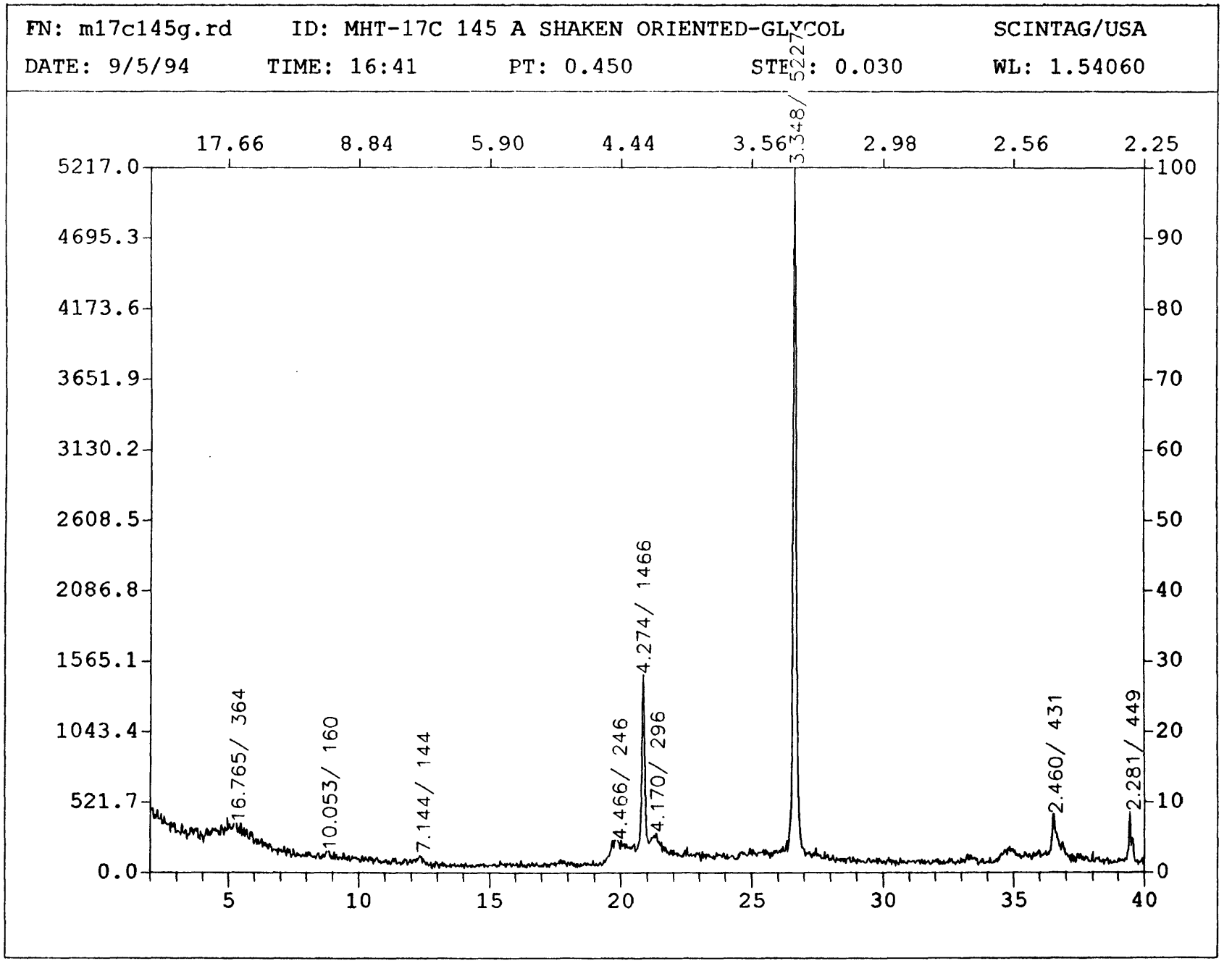
FN: m17c145g.rd
ID: MHT-17C 145 A SHAKEN ORIENTED-GLYCOL
SCINTAG/USA
DATE: 9/5/94
TIME: 16:41
PT: 0.450
STEP: 0.030
WL: 1.54060
17.66
8.84
5.90
4.44
3.56
2.98
2.56
2.25
5217.0
4695.3
4173.6
3651.9
3130.2
2608.5
2086.8
1565.1
1043.4
521.7
0.0
100
90
80
70
60
50
40
30
20
10
0
5
10
15
20
25
30
35
40
3.348/ 5227
16.765/ 364
10.053/ 160
7.144/ 144
4.466/ 246
4.274/ 1466
4.170/ 296
2.460/ 431
2.281/ 449

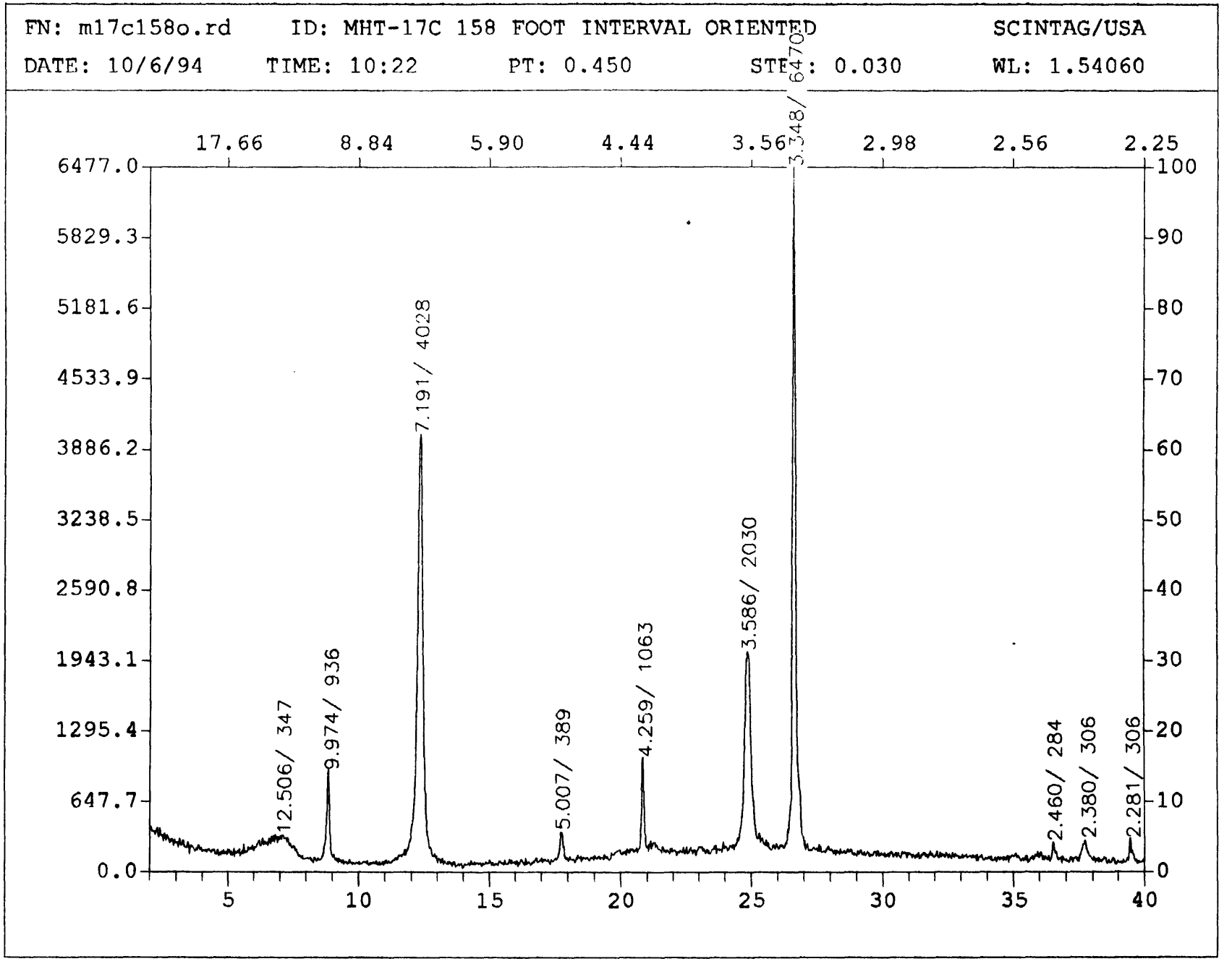
FN: m17c158o.rd ID: MHT-17C 158 FOOT INTERVAL ORIENTED SCINTAG/USA
DATE: 10/6/94 TIME: 10:22 PT: 0.450 STP: 0.030 WL: 1.54060
17.66
8.84
5.90
4.44
3.56
2.98
2.56
2.25
6477.0
5829.3
5181.6
4533.9
3886.2
3238.5
2590.8
1943.1
1295.4
647.7
0.0
100
90
80
70
60
50
40
30
20
10
0
5
10
15
20
25
30
35
40
12.506/ 347
9.974/ 936
7.191/ 4028
5.007/ 389
4.259/ 1063
3.586/ 2030
3.348/ 6470
2.460/ 284
2.380/ 306
2.281/ 306

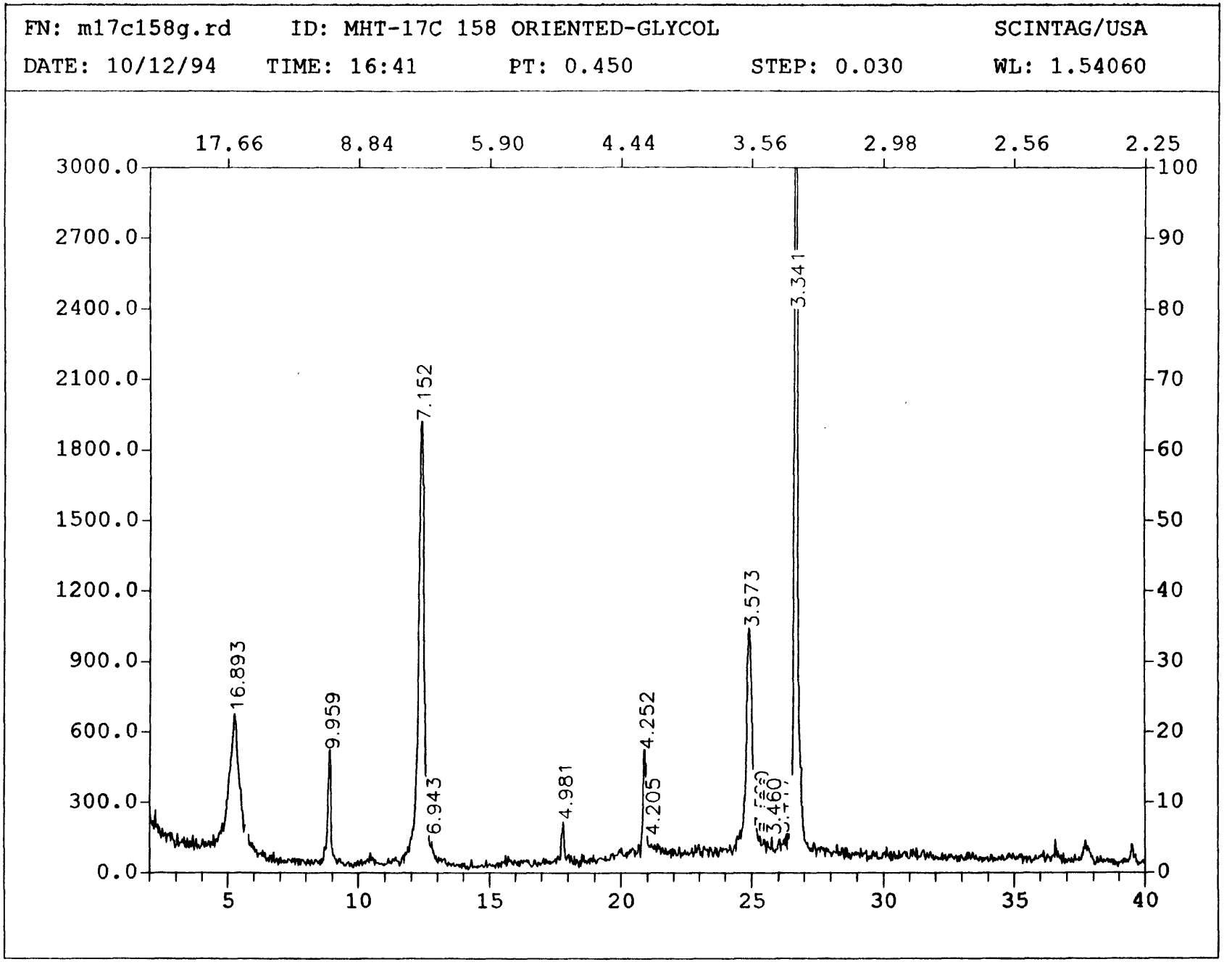
FN: m17c158g.rd
ID: MHT-17C 158 ORIENTED-GLYCOL
SCINTAG/USA
DATE: 10/12/94
TIME: 16:41
PT: 0.450
STEP: 0.030
WL: 1.54060
17.66
8.84
5.90
4.44
3.56
2.98
2.56
2.25
3000.0
2700.0
2400.0
2100.0
1800.0
1500.0
1200.0
900.0
600.0
300.0
0.0
100
90
80
70
60
50
40
30
20
10
0
16.893
9.959
7.152
6.943
4.981
4.252
4.205
3.573
3.460
3.341
5
10
15
20
25
30
35
40

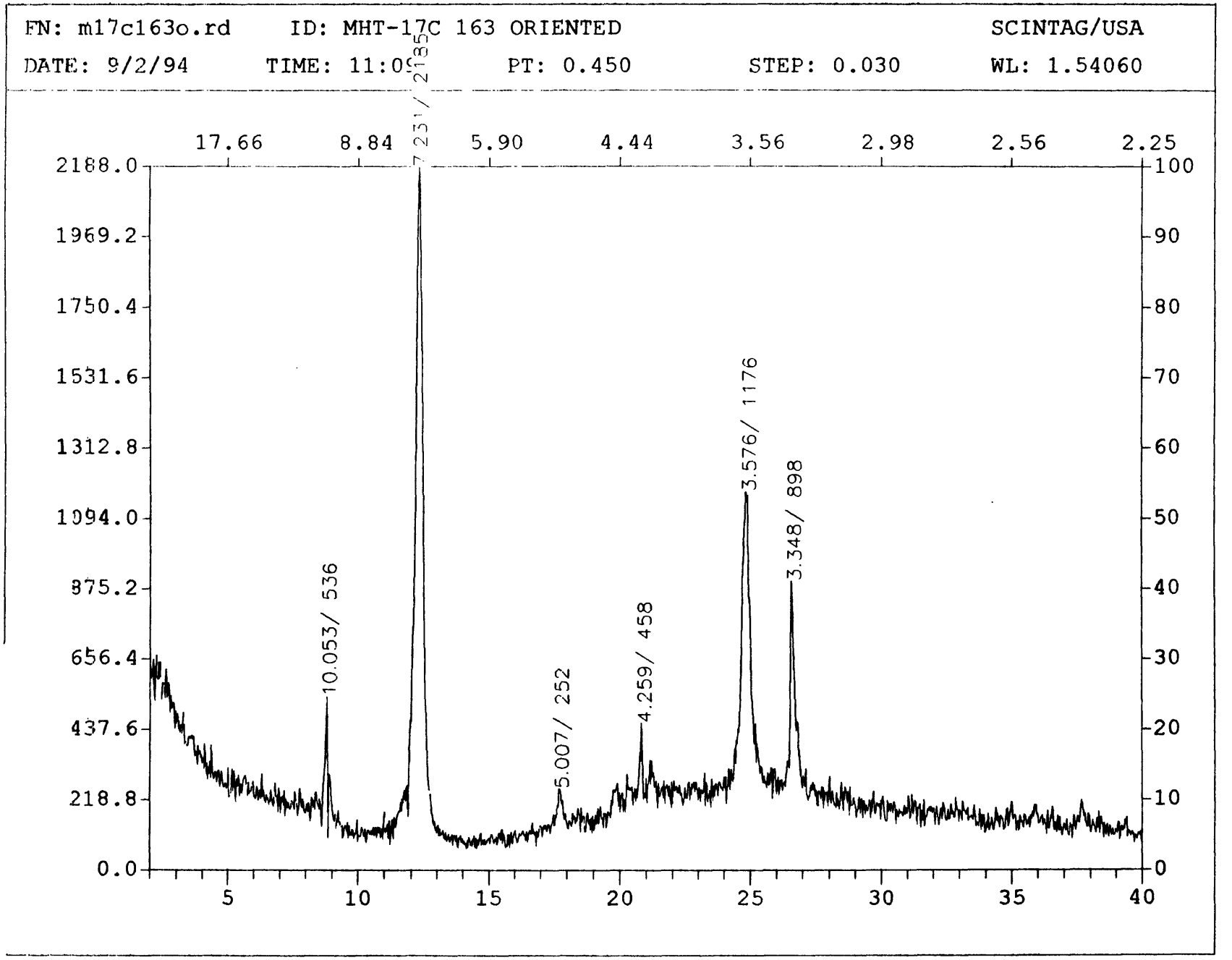
FN: m17c163o.rd
ID: MHT-17C 163 ORIENTED
SCINTAG/USA
DATE: 9/2/94
TIME: 11:0
PT: 0.450
STEP: 0.030
WL: 1.54060
17.66
8.84
7.231/ 2185
5.90
4.44
3.56
2.98
2.56
2.25
2188.0
1969.2
1750.4
1531.6
1312.8
1094.0
875.2
656.4
437.6
218.8
0.0
100
90
80
70
60
50
40
30
20
10
0
10.053/ 536
5.007/ 252
4.259/ 458
3.576/ 1176
3.348/ 898
5
10
15
20
25
30
35
40

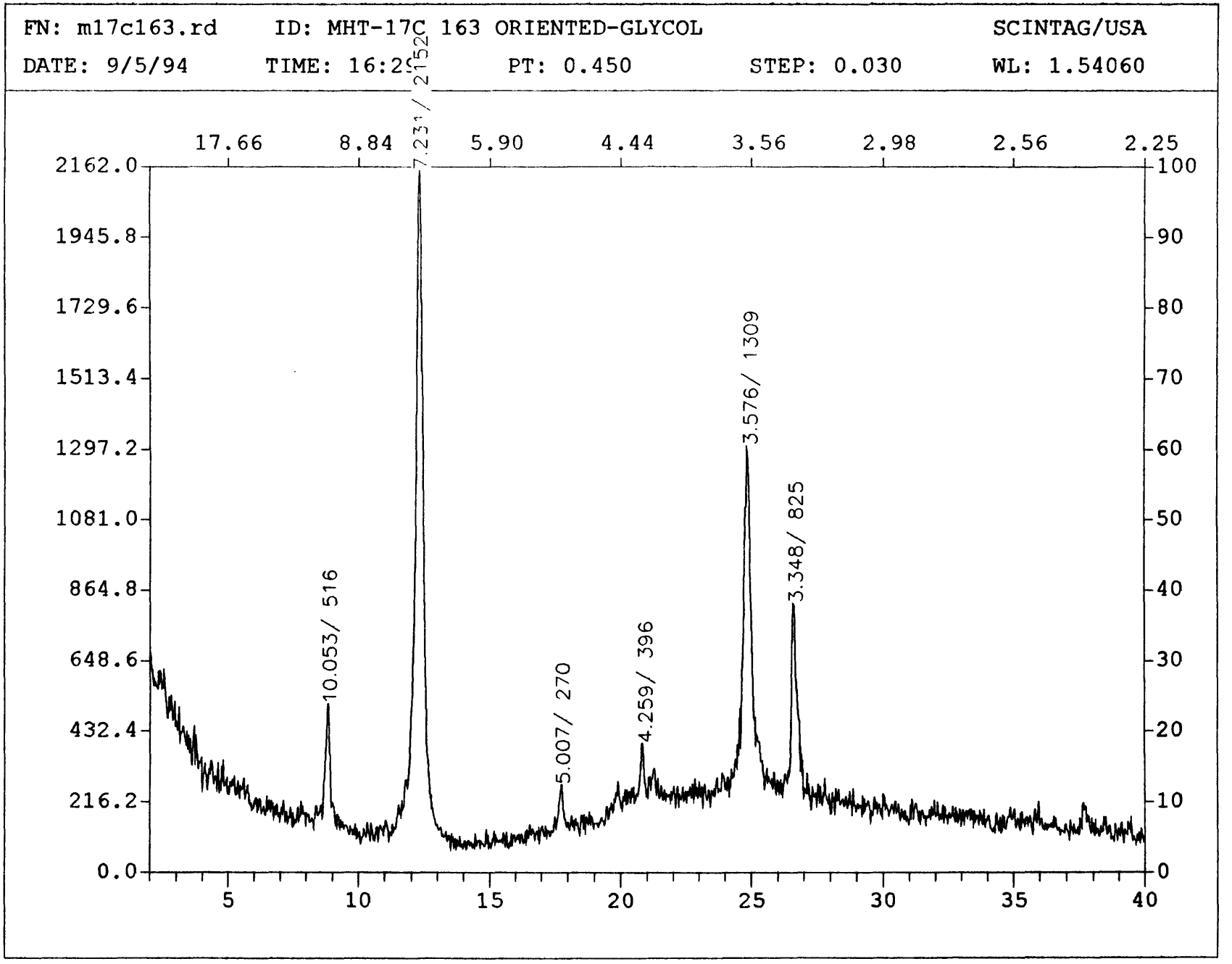
FN: m17c163.rd
ID: MHT-17C 163 ORIENTED-GLYCOL
SCINTAG/USA
DATE: 9/5/94
TIME: 16:2
PT: 0.450
STEP: 0.030
WL: 1.54060
17.66
8.84
5.90
4.44
3.56
2.98
2.56
2.25
2162.0
1945.8
1729.6
1513.4
1297.2
1081.0
864.8
648.6
432.4
216.2
0.0
100
90
80
70
60
50
40
30
20
10
0
5
10
15
20
25
30
35
40
7.231/ 2152
10.053/ 516
5.007/ 270
4.259/ 396
3.576/ 1309
3.348/ 825

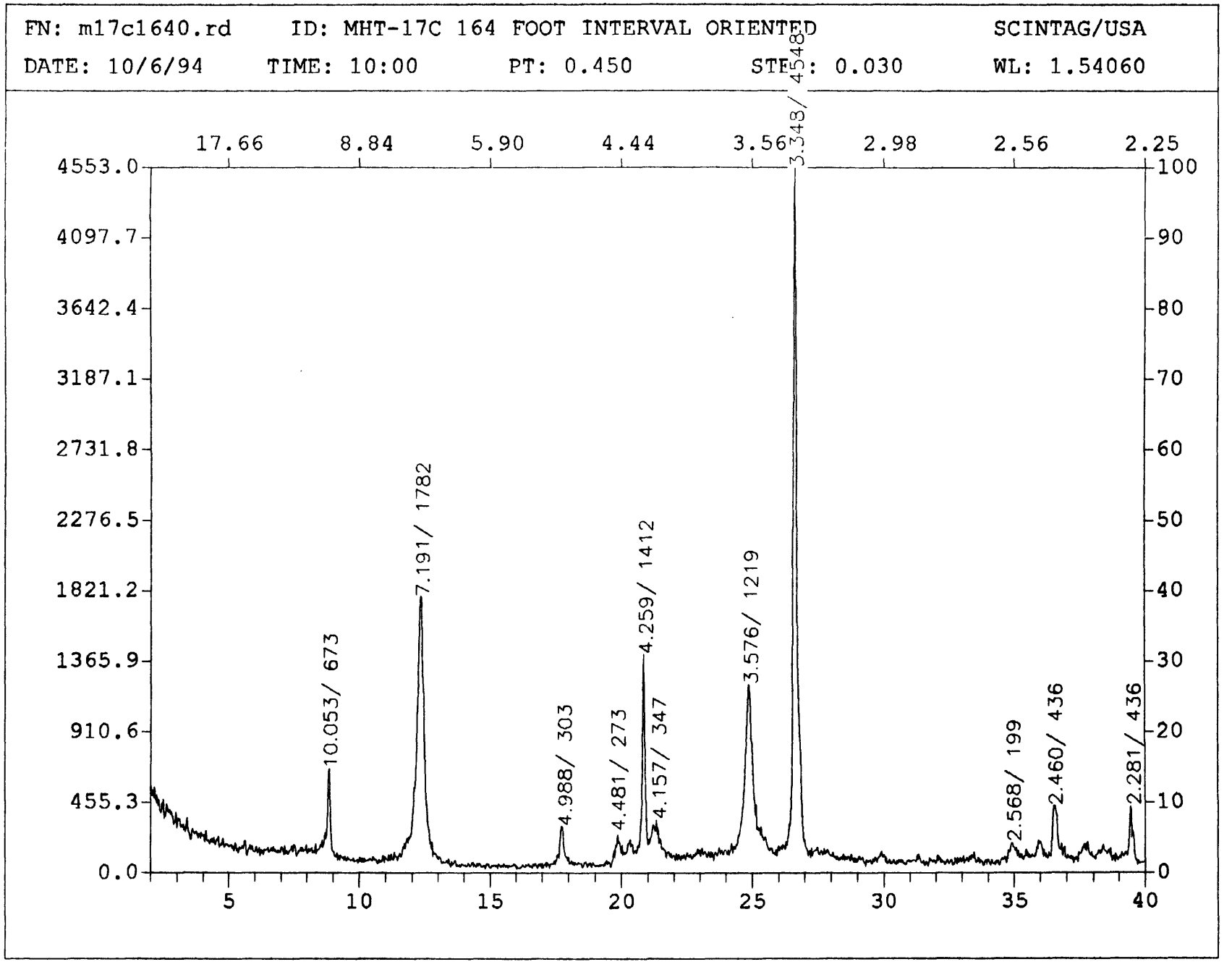
FN: m17c1640.rd
ID: MHT-17C 164 FOOT INTERVAL ORIENTED
SCINTAG/USA
DATE: 10/6/94
TIME: 10:00
PT: 0.450
STP: 0.030
WL: 1.54060
17.66
8.84
5.90
4.44
3.56
2.98
2.56
2.25
4553.0
4097.7
3642.4
3187.1
2731.8
2276.5
1821.2
1365.9
910.6
455.3
0.0
100
90
80
70
60
50
40
30
20
10
0
5
10
15
20
25
30
35
40
10.053/ 673
7.191/ 1782
4.988/ 303
4.481/ 273
4.259/ 1412
4.157/ 347
3.576/ 1219
3.348/ 4548
2.568/ 199
2.460/ 436
2.281/ 436

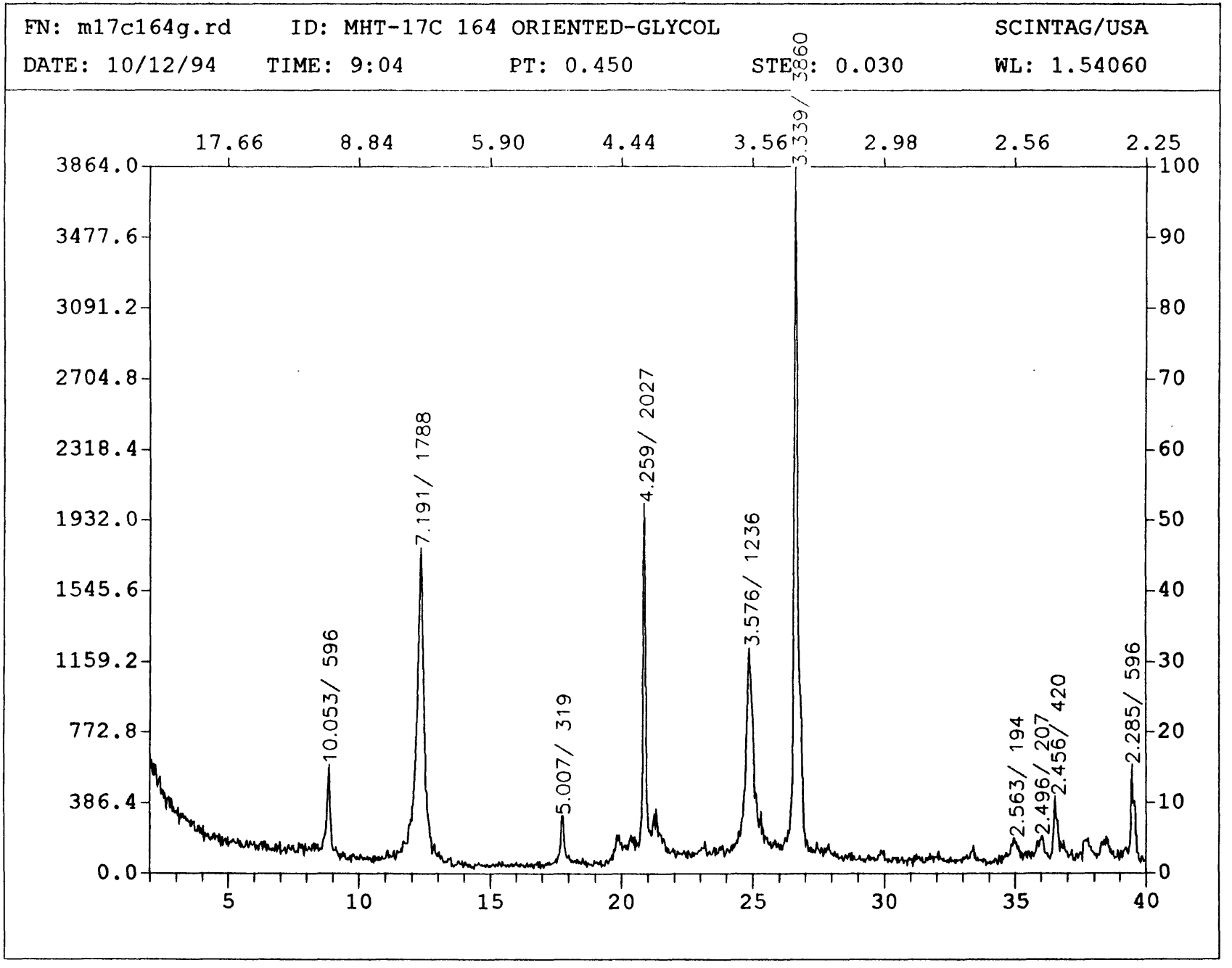
FN: m17c164g.rd
ID: MHT-17C 164 ORIENTED-GLYCOL
SCINTAG/USA
DATE: 10/12/94
TIME: 9:04
PT: 0.450
STE: 0.030
WL: 1.54060
17.66
8.84
5.90
4.44
3.56
2.98
2.56
2.25
3.339/ 3860
10.053/ 596
7.191/ 1788
5.007/ 319
4.259/ 2027
3.576/ 1236
2.563/ 194
2.496/ 207
2.456/ 420
2.285/ 596
3864.0
3477.6
3091.2
2704.8
2318.4
1932.0
1545.6
1159.2
772.8
386.4
0.0
100
90
80
70
60
50
40
30
20
10
0
5
10
15
20
25
30
35
40

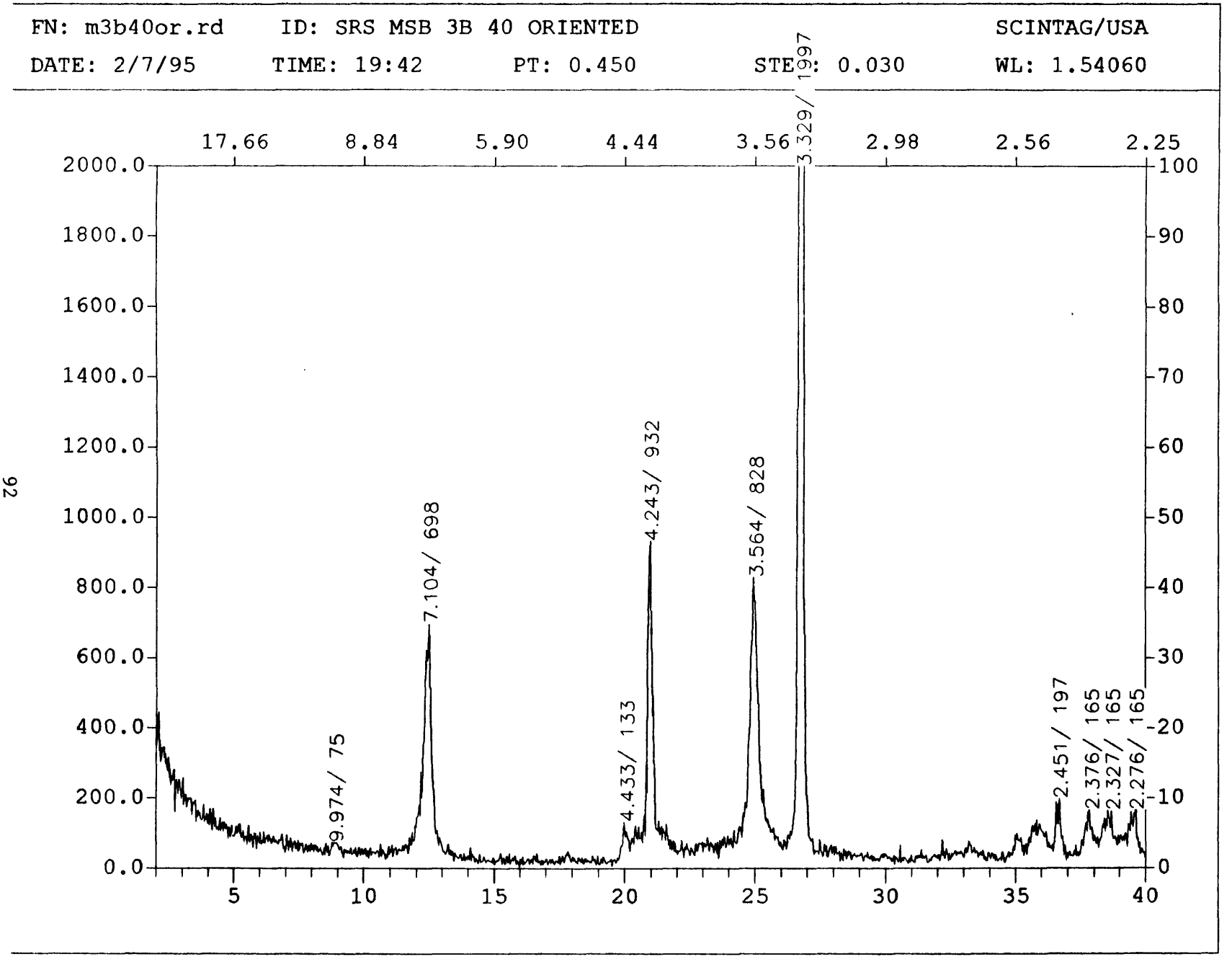
FN: m3b40or.rd
ID: SRS MSB 3B 40 ORIENTED
SCINTAG/USA
DATE: 2/7/95
TIME: 19:42
PT: 0.450
STEP: 0.030
WL: 1.54060
17.66
8.84
5.90
4.44
3.56
3.329/ 1997
2.98
2.56
2.25
2000.0
1800.0
1600.0
1400.0
1200.0
1000.0
800.0
600.0
400.0
200.0
0.0
100
90
80
70
60
50
40
30
20
10
0
9.974/ 75
7.104/ 698
4.433/ 133
4.243/ 932
3.564/ 828
2.451/ 197
2.376/ 165
2.327/ 165
2.276/ 165
5
10
15
20
25
30
35
40

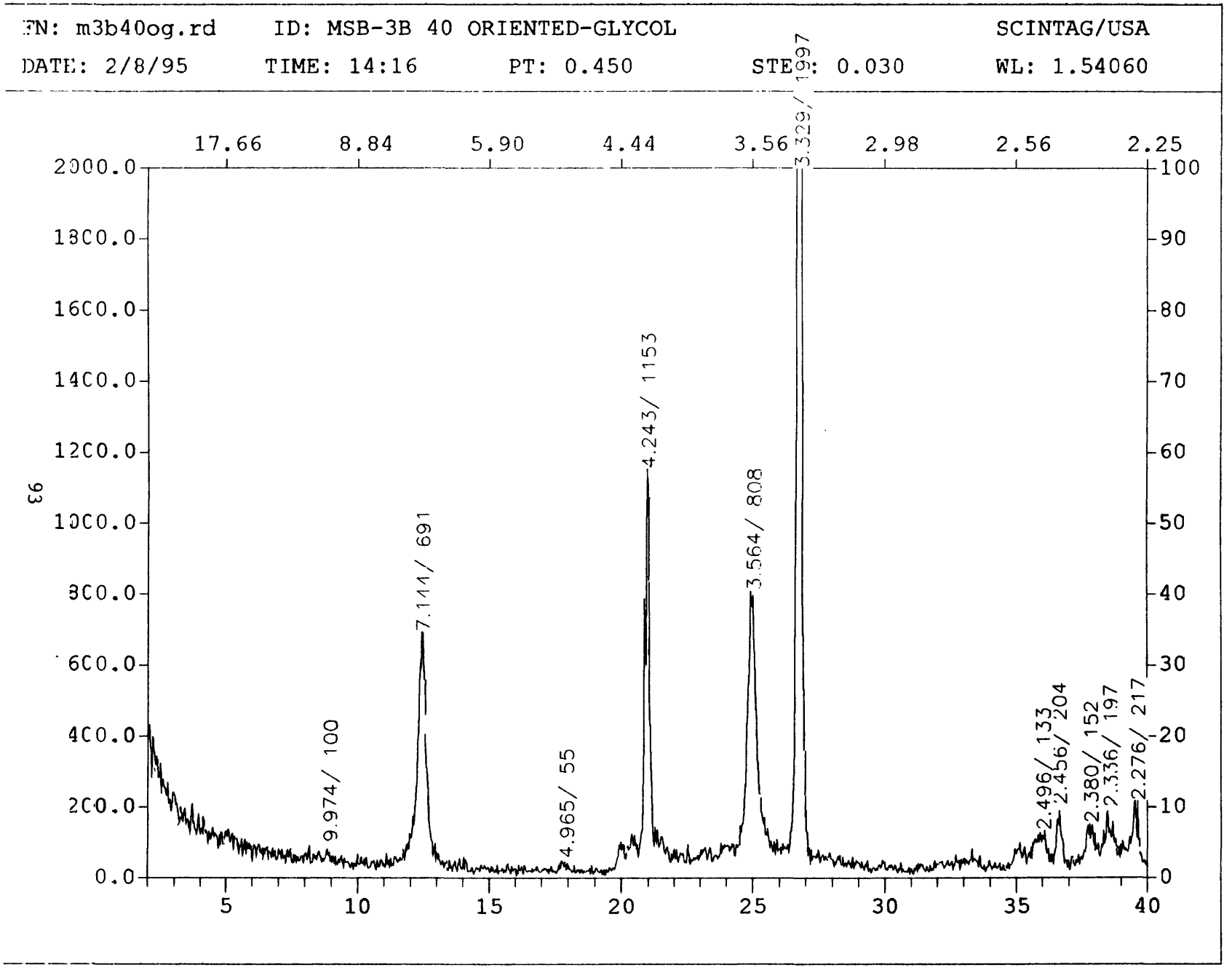
FN: m3b40og.rd
ID: MSB-3B 40 ORIENTED-GLYCOL
SCINTAG/USA
DATE: 2/8/95
TIME: 14:16
PT: 0.450
STEP: 0.030
WL: 1.54060
17.66
8.84
5.90
4.44
3.56
3.329/ 1997
2.98
2.56
2.25
2000.0
1800.0
1600.0
1400.0
1200.0
1000.0
800.0
600.0
400.0
200.0
0.0
100
90
80
70
60
50
40
30
20
10
0
93
9.974/ 100
7.111/ 691
4.965/ 55
4.243/ 1153
3.564/ 808
2.496/ 133
2.456/ 204
2.380/ 152
2.336/ 197
2.276/ 217
5
10
15
20
25
30
35
40

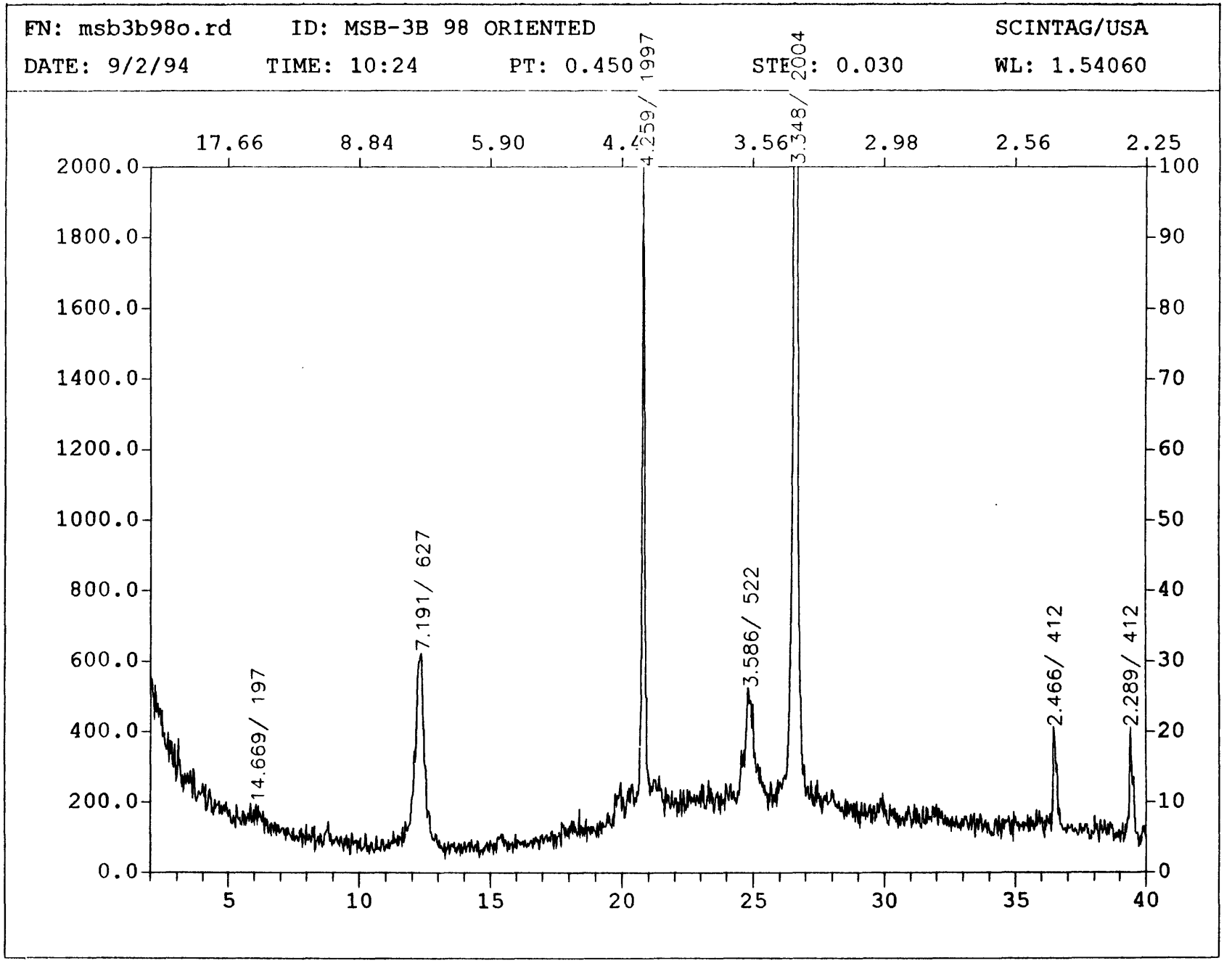
FN: msb3b98o.rd
ID: MSB-3B 98 ORIENTED
SCINTAG/USA
DATE: 9/2/94
TIME: 10:24
PT: 0.450
STEP: 0.030
WL: 1.54060
17.66
8.84
5.90
4.4
4.259/ 1997
3.56
3.348/ 2004
2.98
2.56
2.25
2000.0
1800.0
1600.0
1400.0
1200.0
1000.0
800.0
600.0
400.0
200.0
0.0
100
90
80
70
60
50
40
30
20
10
0
14.669/ 197
7.191/ 627
3.586/ 522
2.466/ 412
2.289/ 412
5
10
15
20
25
30
35
40

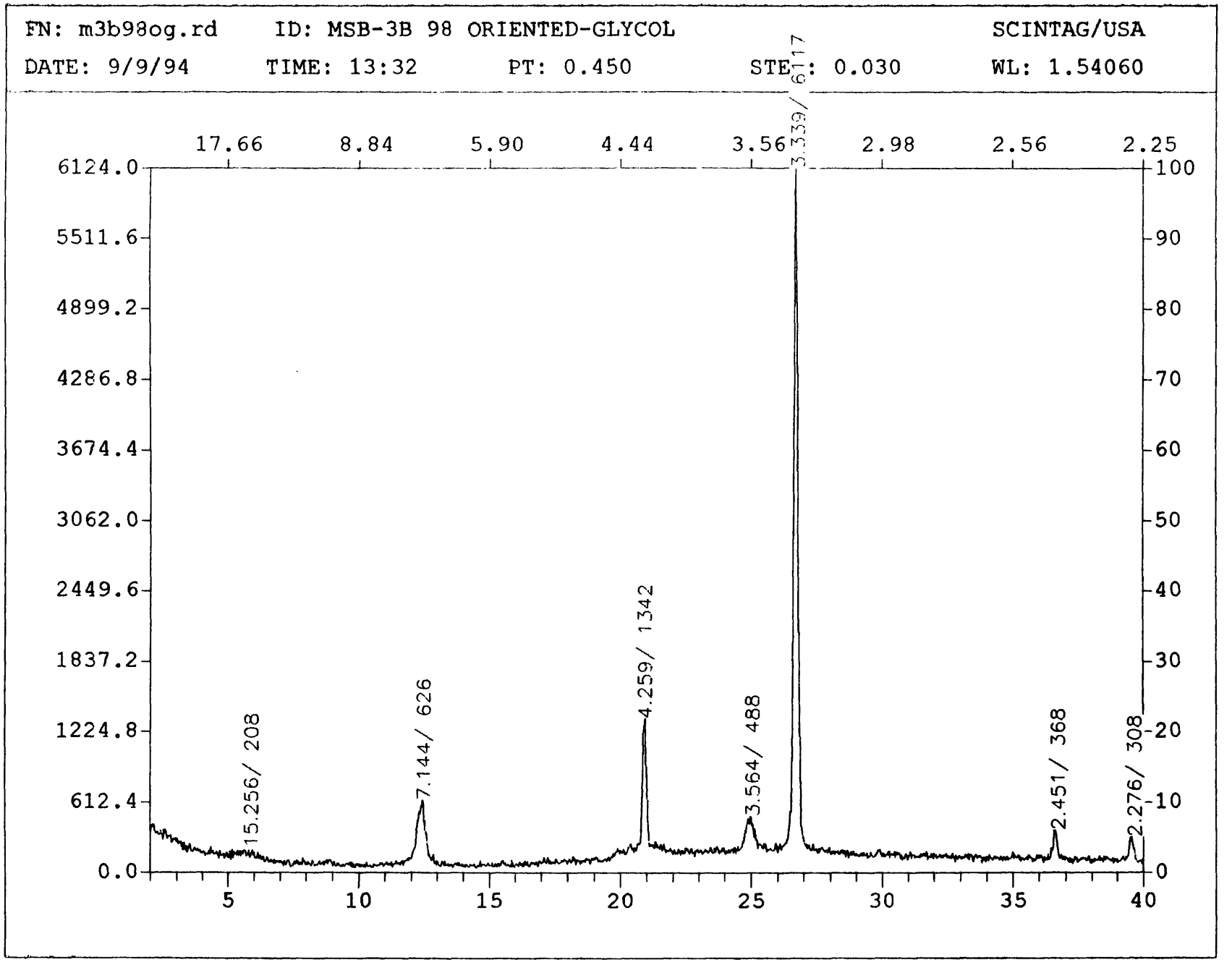
FN: m3b98og.rd
ID: MSB-3B 98 ORIENTED-GLYCOL
SCINTAG/USA
DATE: 9/9/94
TIME: 13:32
PT: 0.450
STE: 0.030
WL: 1.54060
17.66
8.84
5.90
4.44
3.56
2.98
2.56
2.25
6124.0
5511.6
4899.2
4286.8
3674.4
3062.0
2449.6
1837.2
1224.8
612.4
0.0
100
90
80
70
60
50
40
30
20
10
0
5
10
15
20
25
30
35
40
15.256/ 208
7.144/ 626
4.259/ 1342
3.564/ 488
3.339/ 6117
2.451/ 368
2.276/ 308

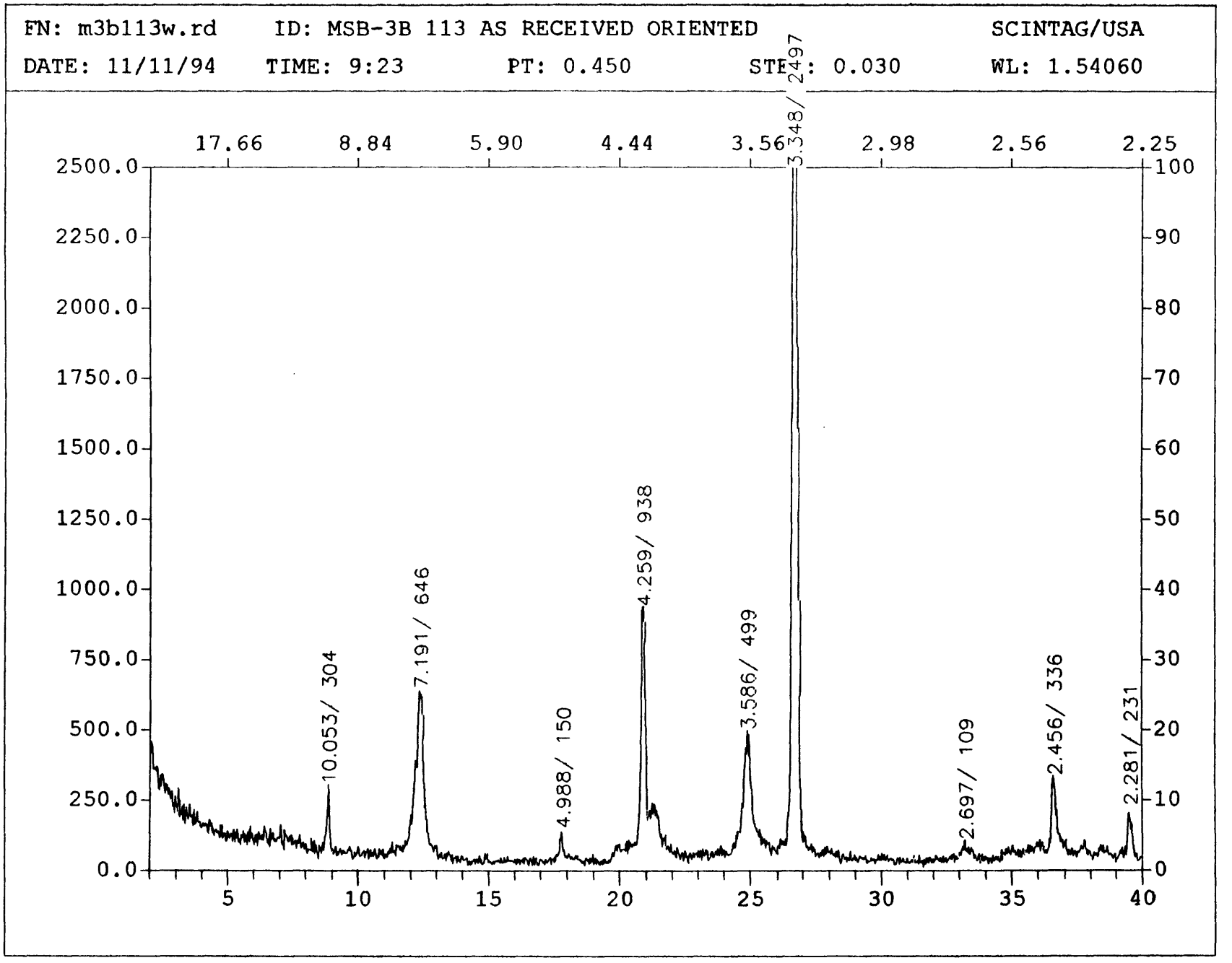
FN: m3b113w.rd
ID: MSB-3B 113 AS RECEIVED ORIENTED
SCINTAG/USA
DATE: 11/11/94
TIME: 9:23
PT: 0.450
STP: 0.030
WL: 1.54060
17.66
8.84
5.90
4.44
3.56
2.98
2.56
2.25
3.348/ 2497
10.053/ 304
7.191/ 646
4.988/ 150
4.259/ 938
3.586/ 499
2.697/ 109
2.456/ 336
2.281/ 231
2500.0
2250.0
2000.0
1750.0
1500.0
1250.0
1000.0
750.0
500.0
250.0
0.0
100
90
80
70
60
50
40
30
20
10
0
5
10
15
20
25
30
35
40

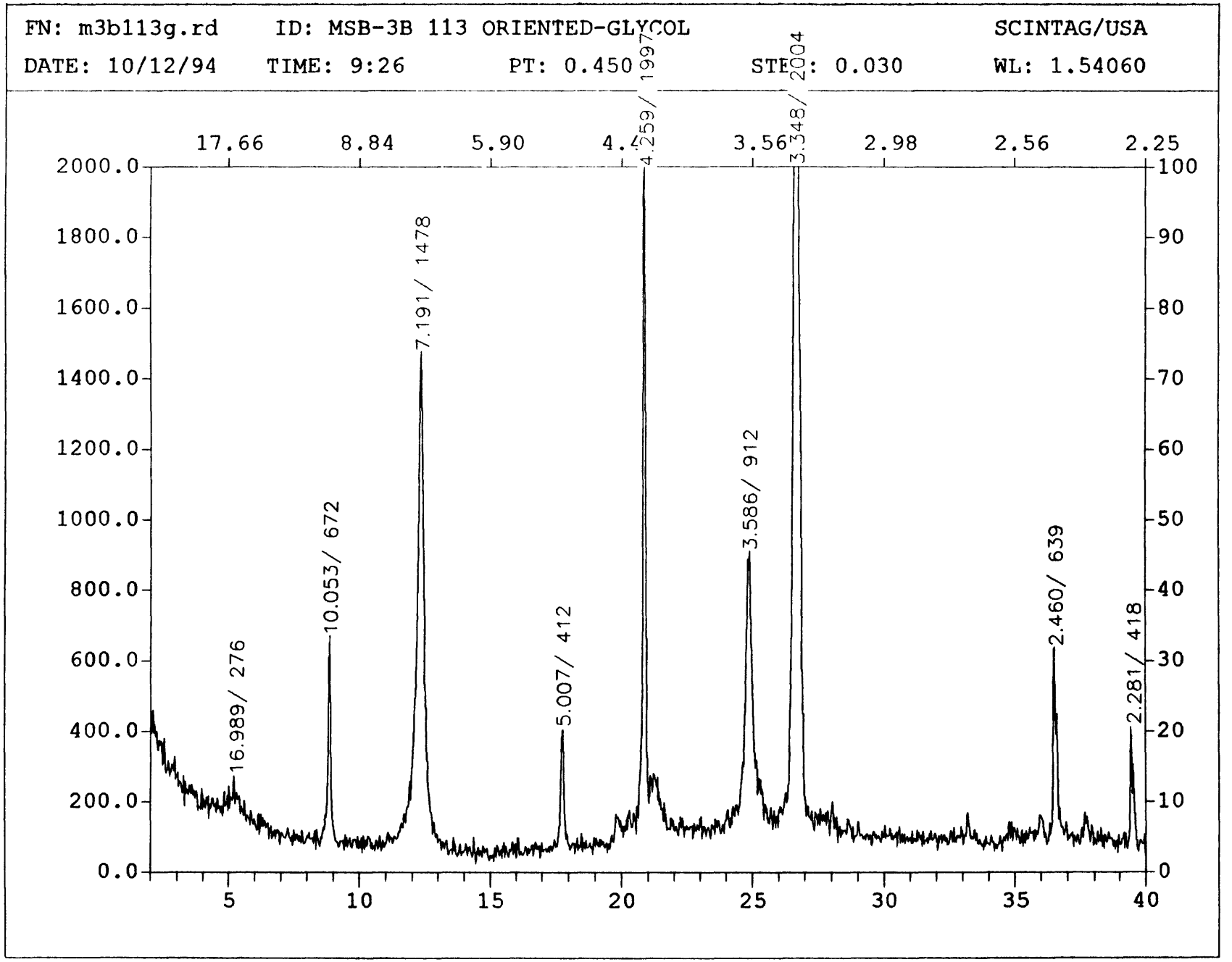
FN: m3b113g.rd
ID: MSB-3B 113 ORIENTED-GLYCOL
SCINTAG/USA
DATE: 10/12/94
TIME: 9:26
PT: 0.450
STEP: 0.030
WL: 1.54060
17.66
8.84
5.90
4.43
3.56
2.98
2.56
2.25
2000.0
1800.0
1600.0
1400.0
1200.0
1000.0
800.0
600.0
400.0
200.0
0.0
100
90
80
70
60
50
40
30
20
10
0
5
10
15
20
25
30
35
40
16.989/ 276
10.053/ 672
7.191/ 1478
5.007/ 412
4.259/ 1997
3.586/ 912
3.348/ 2004
2.460/ 639
2.281/ 418

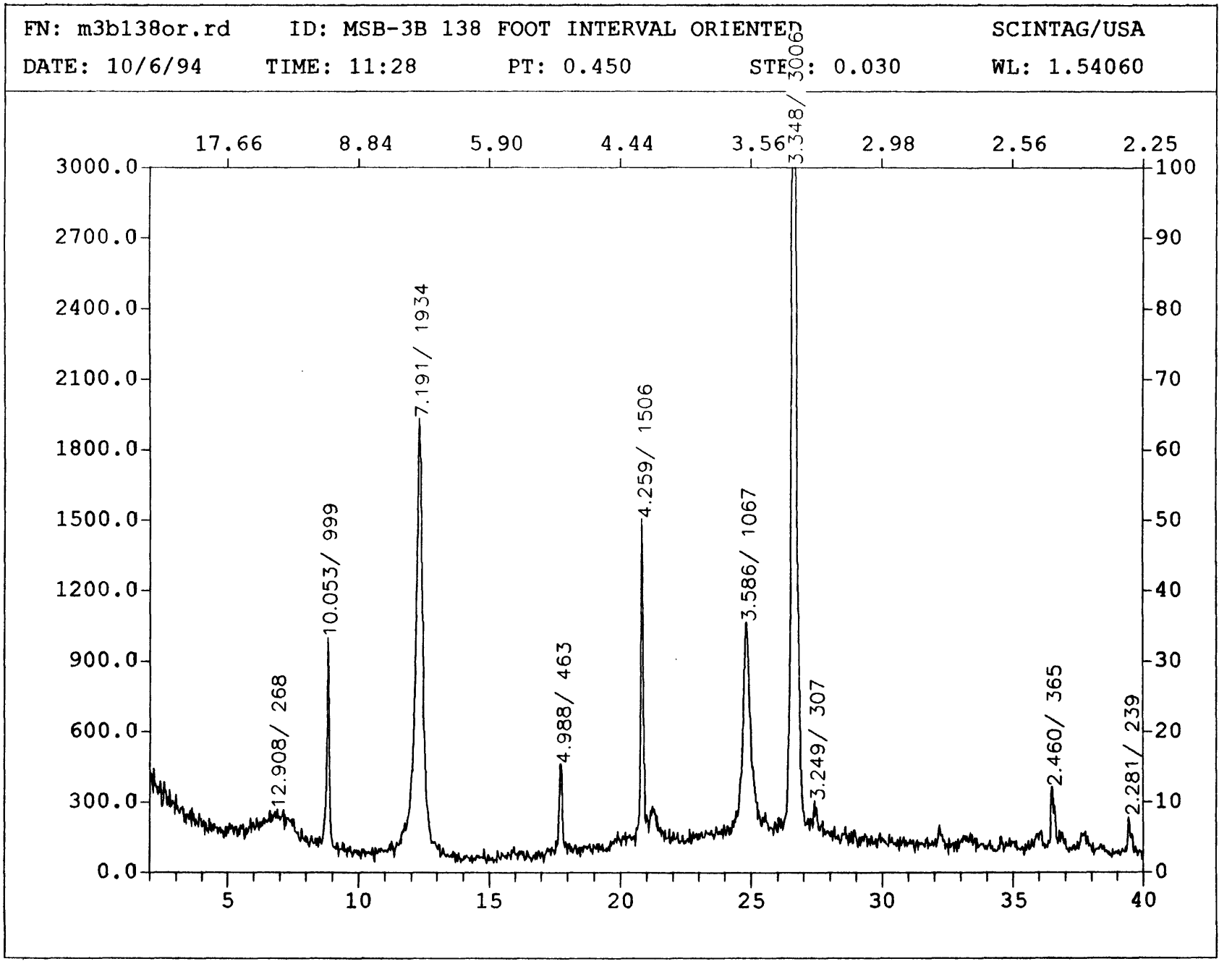
FN: m3b138or.rd ID: MSB-3B 138 FOOT INTERVAL ORIENTED SCINTAG/USA
DATE: 10/6/94 TIME: 11:28 PT: 0.450 STEP: 0.030 WL: 1.54060
17.66
8.84
5.90
4.44
3.56
2.98
2.56
2.25
3000.0
2700.0
2400.0
2100.0
1800.0
1500.0
1200.0
900.0
600.0
300.0
0.0
100
90
80
70
60
50
40
30
20
10
0
5
10
15
20
25
30
35
40
12.908/ 268
10.053/ 999
7.191/ 1934
4.988/ 463
4.259/ 1506
3.586/ 1067
3.348/ 3006
3.249/ 307
2.460/ 365
2.281/ 239

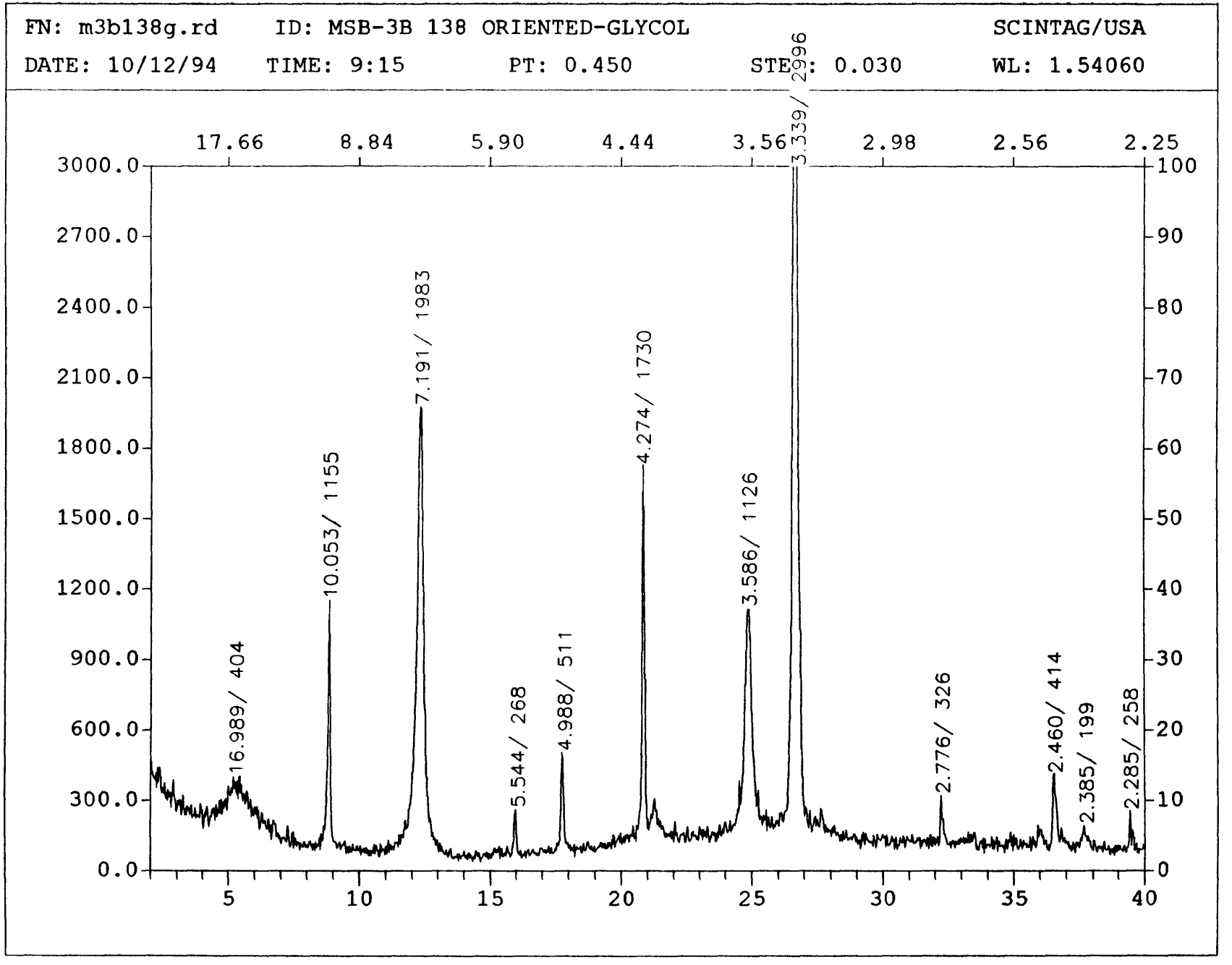
FN: m3b138g.rd
ID: MSB-3B 138 ORIENTED-GLYCOL
SCINTAG/USA
DATE: 10/12/94
TIME: 9:15
PT: 0.450
STEP: 0.030
WL: 1.54060
17.66
8.84
5.90
4.44
3.56
2.98
2.56
2.25
3000.0
2700.0
2400.0
2100.0
1800.0
1500.0
1200.0
900.0
600.0
300.0
0.0
100
90
80
70
60
50
40
30
20
10
0
5
10
15
20
25
30
35
40
16.989/ 404
10.053/ 1155
7.191/ 1983
5.544/ 268
4.988/ 511
4.274/ 1730
3.586/ 1126
3.339/ 2996
2.776/ 326
2.460/ 414
2.385/ 199
2.285/ 258

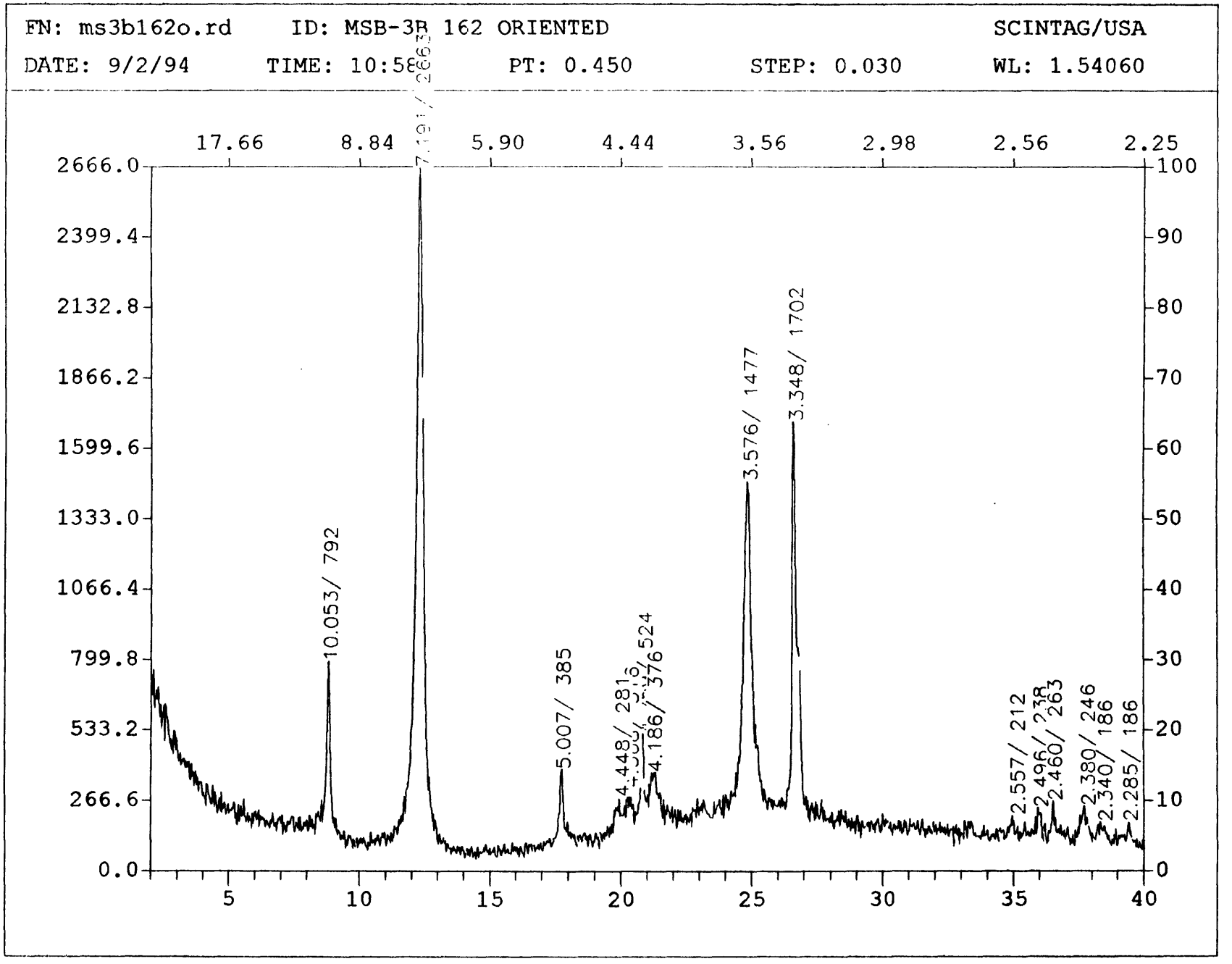
FN: ms3b162o.rd
ID: MSB-3B 162 ORIENTED
SCINTAG/USA
DATE: 9/2/94
TIME: 10:58
PT: 0.450
STEP: 0.030
WL: 1.54060
17.66
8.84
5.90
4.44
3.56
2.98
2.56
2.25
2666.0
2399.4
2132.8
1866.2
1599.6
1333.0
1066.4
799.8
533.2
266.6
0.0
100
90
80
70
60
50
40
30
20
10
0
5
10
15
20
25
30
35
40
10.053/ 792
5.007/ 385
4.448/ 281
4.186/ 376
3.576/ 1477
3.348/ 1702
2.557/ 212
2.496/ 238
2.460/ 263
2.380/ 246
2.340/ 186
2.285/ 186
I00

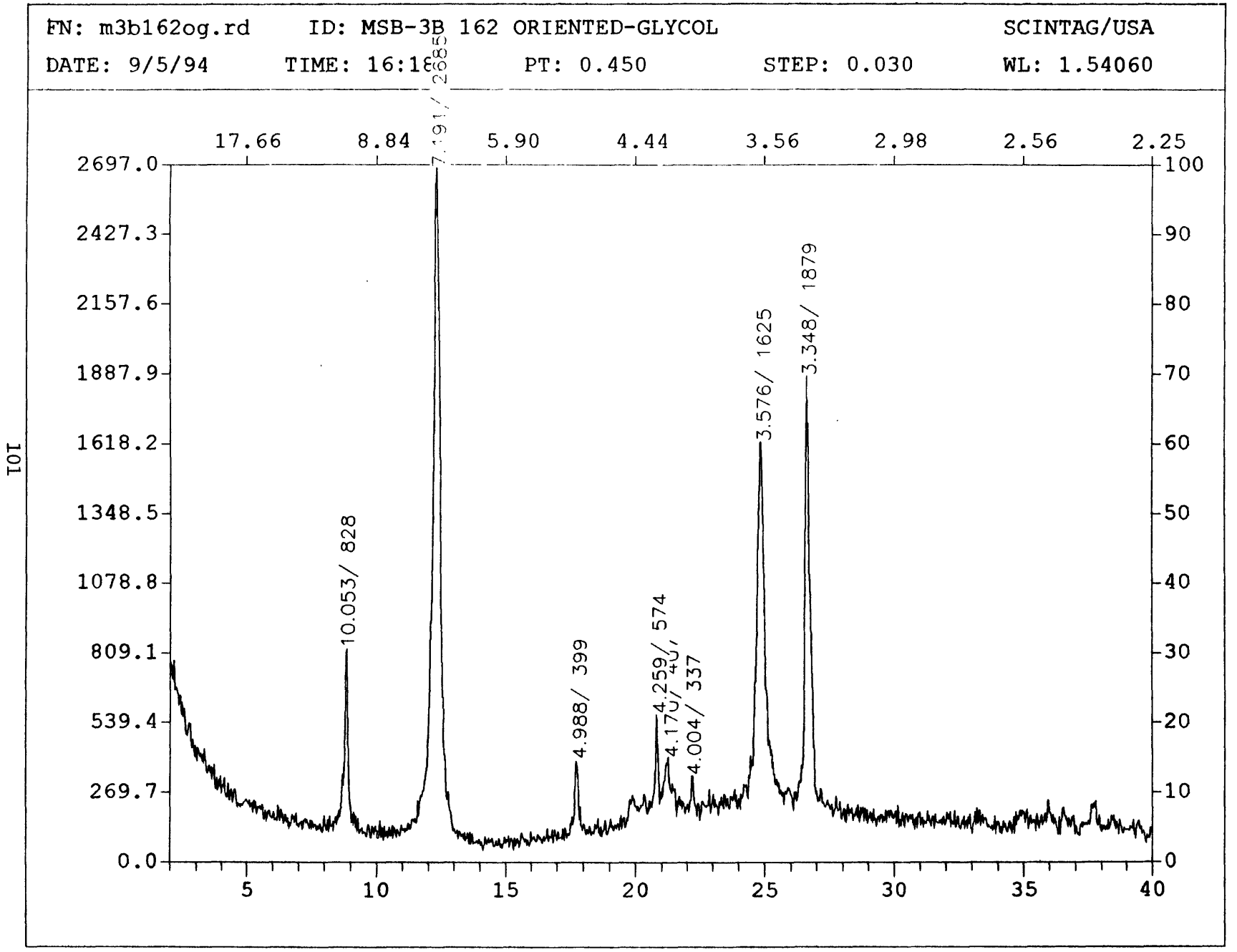
FN: m3b162og.rd
ID: MSB-3B 162 ORIENTED-GLYCOL
SCINTAG/USA
DATE: 9/5/94
TIME: 16:18
PT: 0.450
STEP: 0.030
WL: 1.54060
101
17.66
8.84
5.90
4.44
3.56
2.98
2.56
2.25
2697.0
2427.3
2157.6
1887.9
1618.2
1348.5
1078.8
809.1
539.4
269.7
0.0
100
90
80
70
60
50
40
30
20
10
0
5
10
15
20
25
30
35
40
7.191/ 2885
10.053/ 828
4.988/ 399
4.259/ 574
4.170/ 440
4.004/ 337
3.576/ 1625
3.348/ 1879

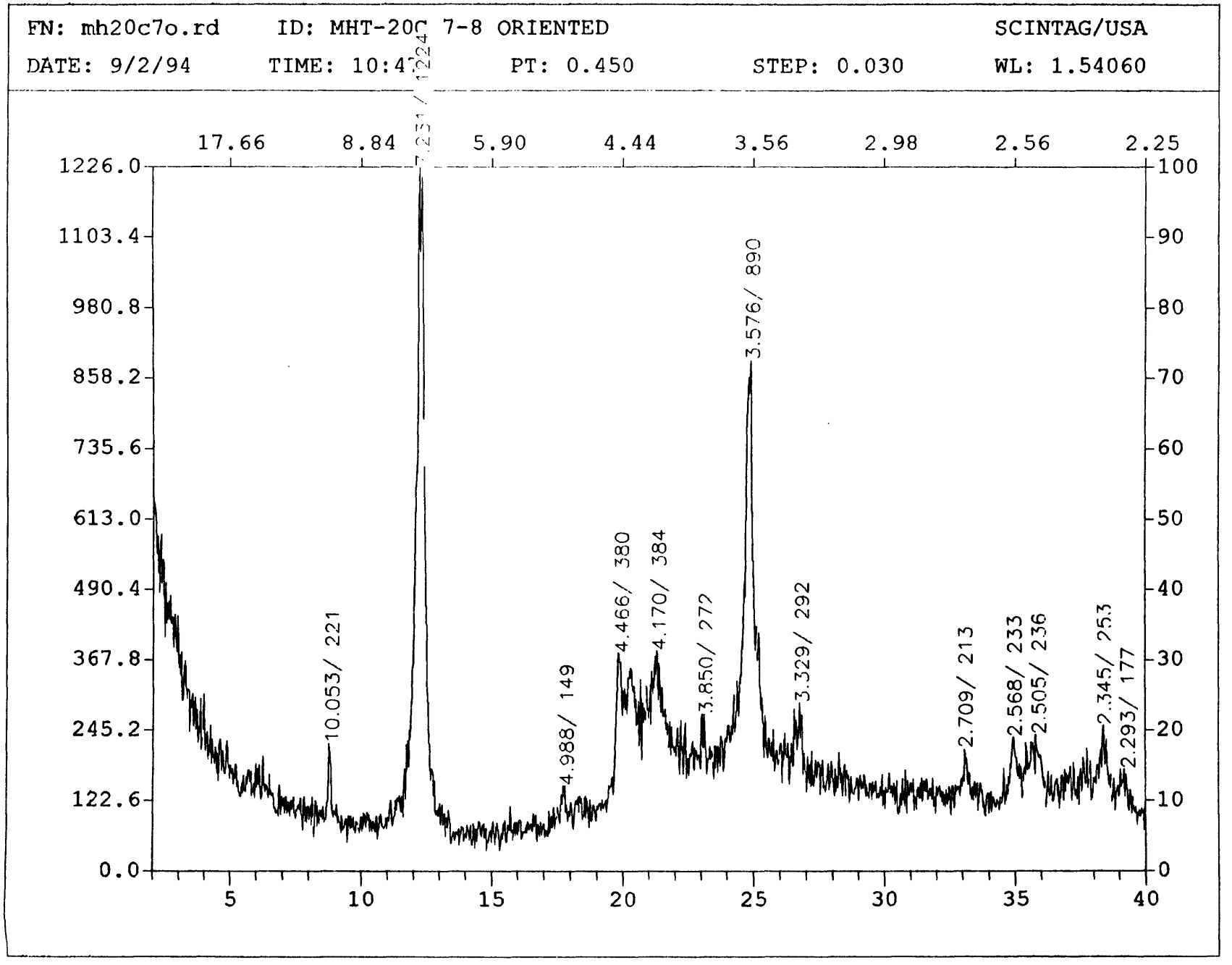
FN: mh20c7o.rd
ID: MHT-20C 7-8 ORIENTED
SCINTAG/USA
DATE: 9/2/94
TIME: 10:4
PT: 0.450
STEP: 0.030
WL: 1.54060
17.66
8.84
5.90
4.44
3.56
2.98
2.56
2.25
1226.0
1103.4
980.8
858.2
735.6
613.0
490.4
367.8
245.2
122.6
0.0
100
90
80
70
60
50
40
30
20
10
0
5
10
15
20
25
30
35
40
10.053/ 221
4.988/ 149
4.466/ 380
4.170/ 384
3.850/ 272
3.576/ 890
3.329/ 292
2.709/ 213
2.568/ 233
2.505/ 236
2.345/ 253
2.293/ 177

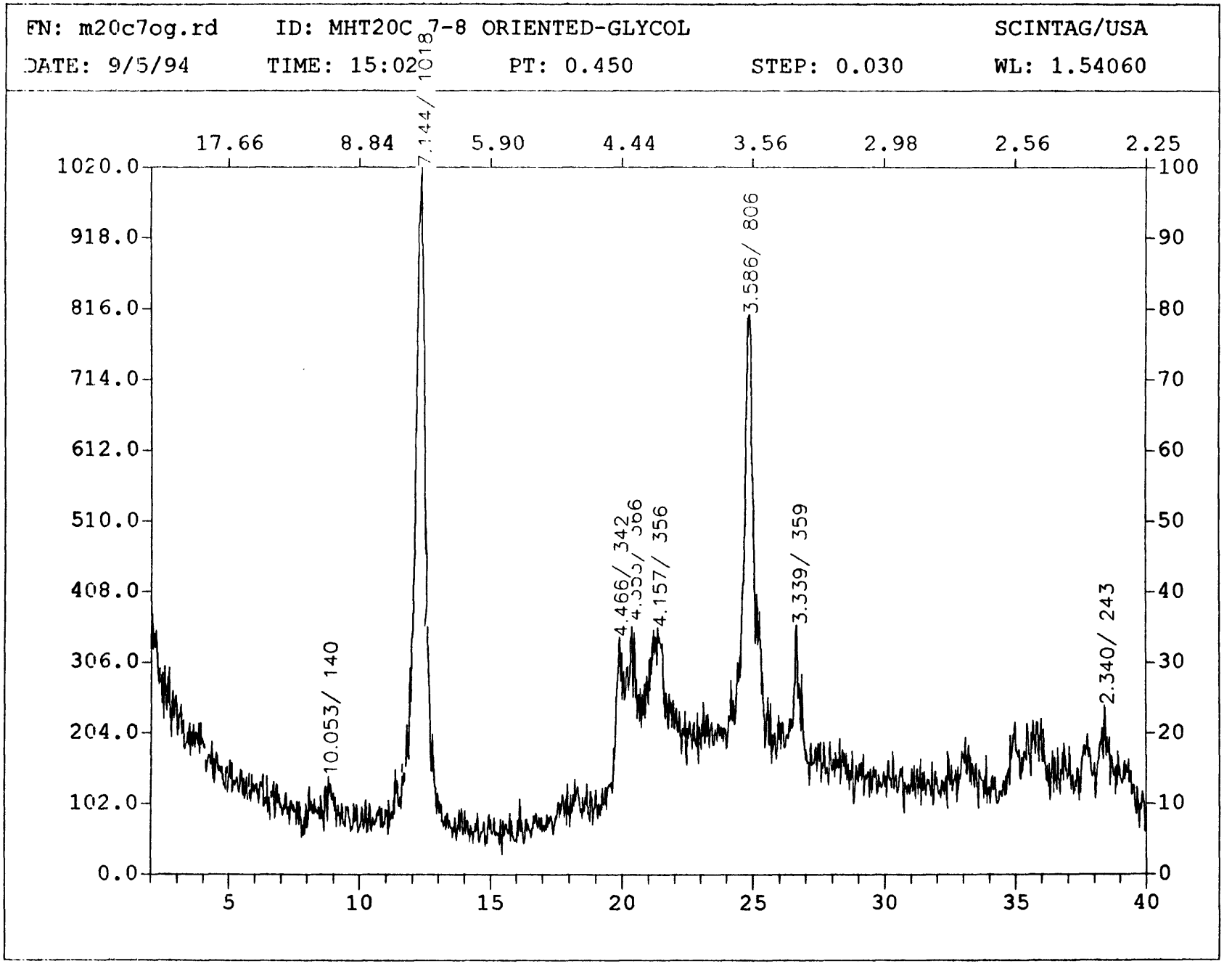
FN: m20c7og.rd
ID: MHT20C 7-8 ORIENTED-GLYCOL
SCINTAG/USA
DATE: 9/5/94
TIME: 15:02
PT: 0.450
STEP: 0.030
WL: 1.54060
17.66
8.84
5.90
4.44
3.56
2.98
2.56
2.25
1020.0
918.0
816.0
714.0
612.0
510.0
408.0
306.0
204.0
102.0
0.0
100
90
80
70
60
50
40
30
20
10
0
5
10
15
20
25
30
35
40
7.144/ 1018
10.053/ 140
4.466/ 342
4.353/ 366
4.157/ 356
3.586/ 806
3.339/ 359
2.340/ 243

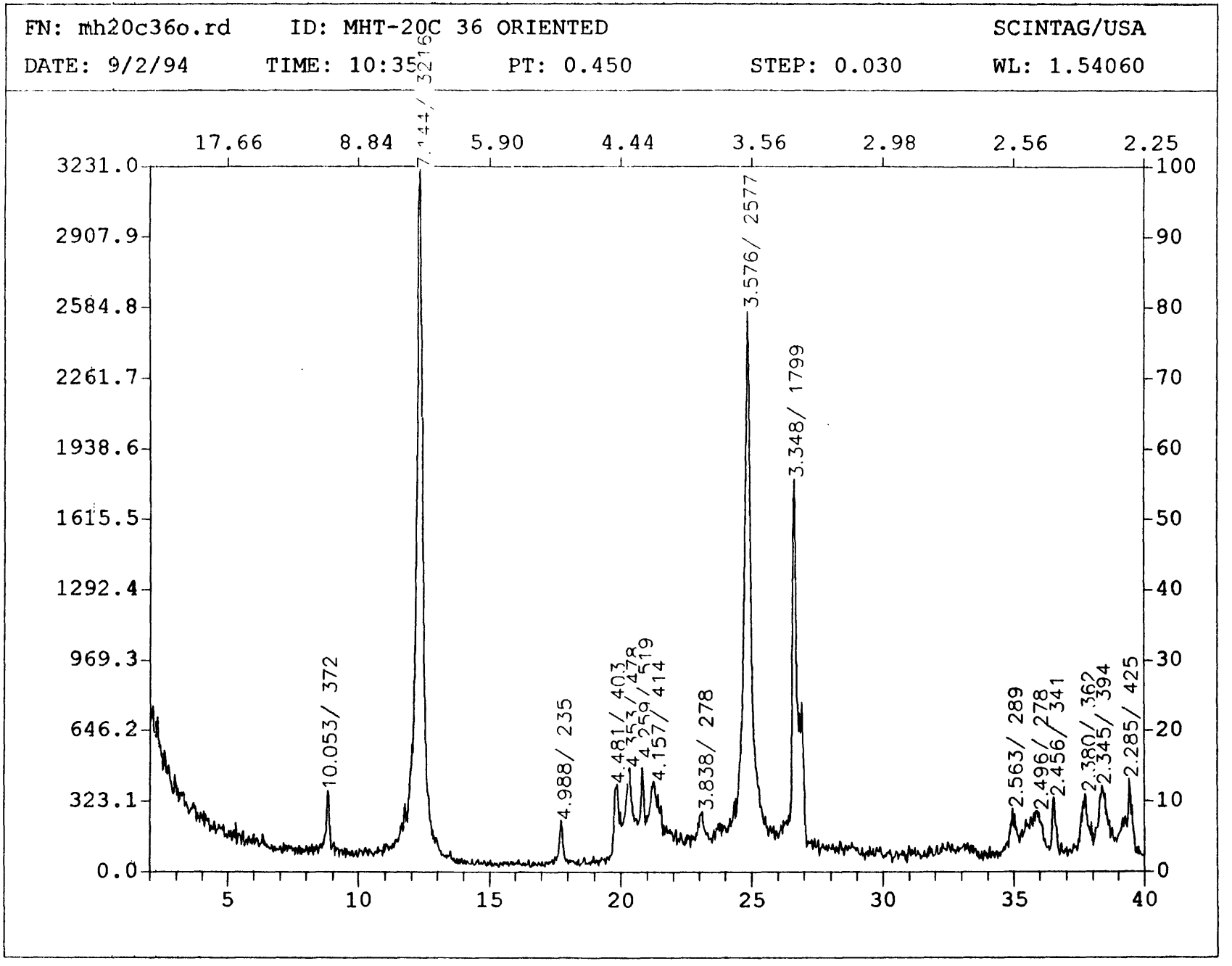
FN: mh20c36o.rd
ID: MHT-20C 36 ORIENTED
SCINTAG/USA
DATE: 9/2/94
TIME: 10:35
PT: 0.450
STEP: 0.030
WL: 1.54060
17.66
8.84
5.90
4.44
3.56
2.98
2.56
2.25
3231.0
2907.9
2584.8
2261.7
1938.6
1615.5
1292.4
969.3
646.2
323.1
0.0
100
90
80
70
60
50
40
30
20
10
0
5
10
15
20
25
30
35
40
10.053/ 372
4.988/ 235
4.481/ 403
4.157/ 414
3.838/ 278
3.576/ 2577
3.348/ 1799
2.563/ 289
2.496/ 278
2.456/ 341
2.380/ 362
2.345/ 394
2.285/ 425

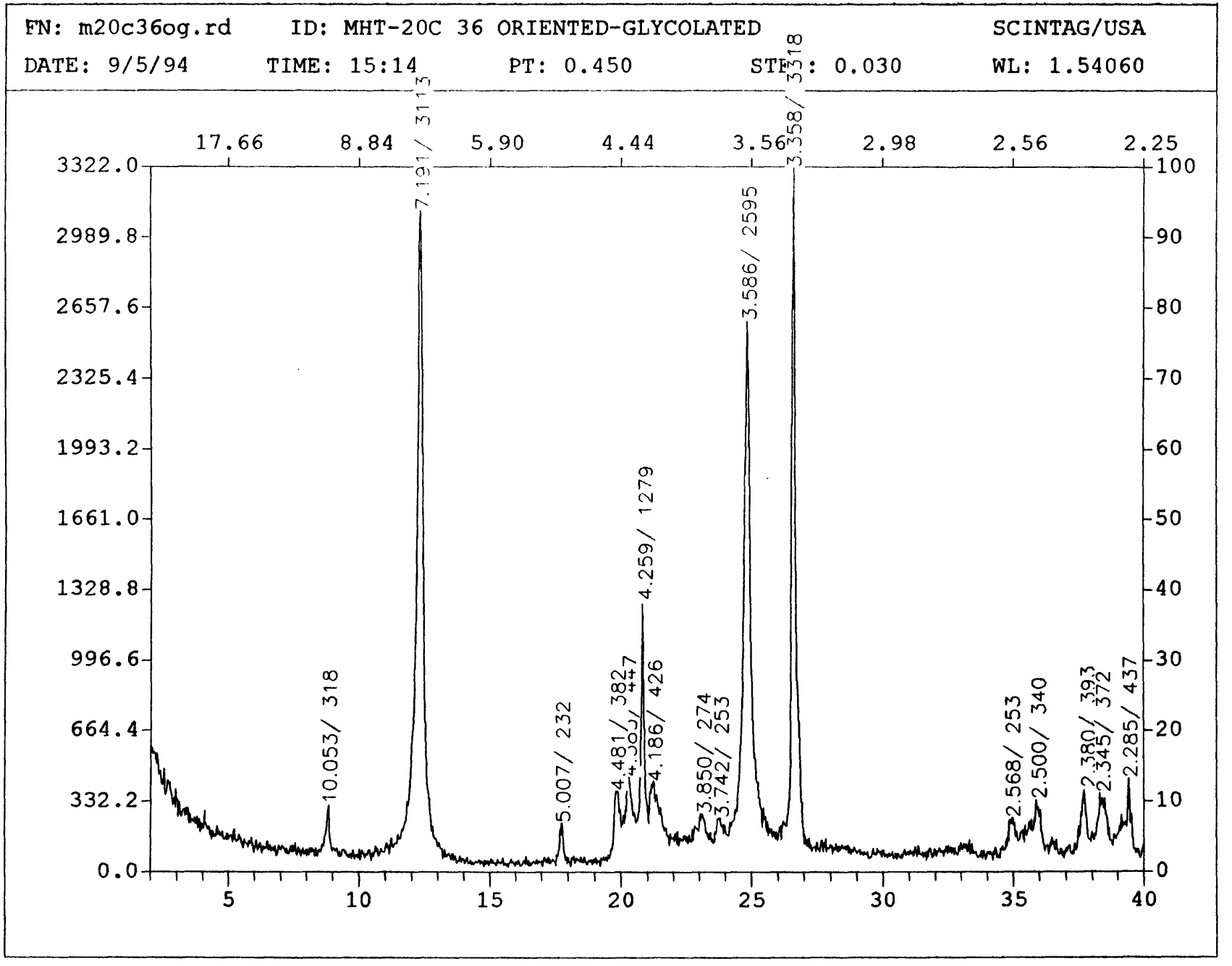
FN: m20c36og.rd
ID: MHT-20C 36 ORIENTED-GLYCOLATED
SCINTAG/USA
DATE: 9/5/94
TIME: 15:14
PT: 0.450
STP: 0.030
WL: 1.54060
17.66
8.84
5.90
4.44
3.56
2.98
2.56
2.25
3322.0
2989.8
2657.6
2325.4
1993.2
1661.0
1328.8
996.6
664.4
332.2
0.0
100
90
80
70
60
50
40
30
20
10
0
5
10
15
20
25
30
35
40
7.191/ 3113
3.358/ 3318
3.586/ 2595
4.259/ 1279
10.053/ 318
5.007/ 232
4.481/ 382
4.305/ 447
4.186/ 426
3.850/ 274
3.742/ 253
2.568/ 253
2.500/ 340
2.380/ 393
2.345/ 372
2.285/ 437

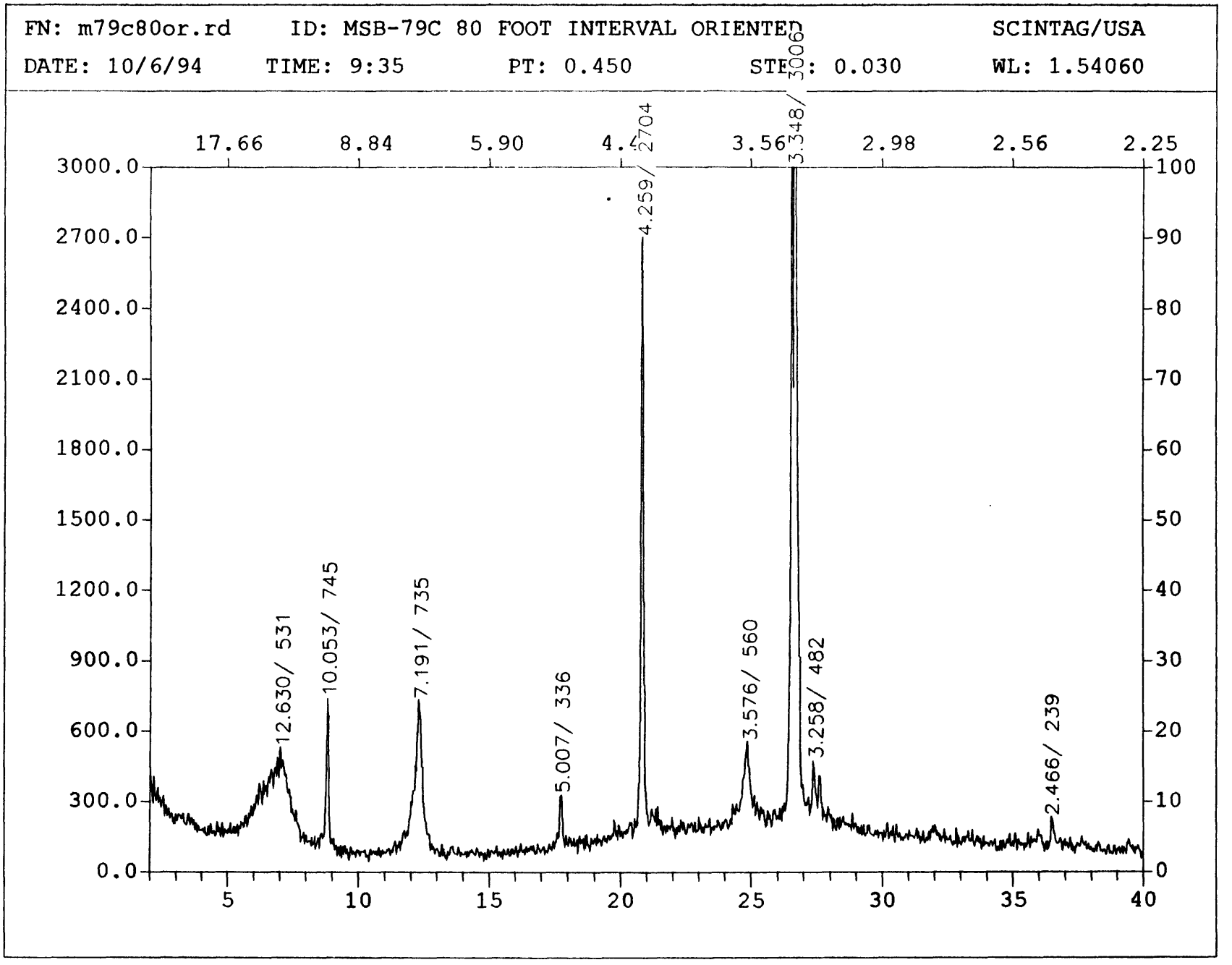
FN: m79c80or.rd
ID: MSB-79C 80 FOOT INTERVAL ORIENTED
SCINTAG/USA
DATE: 10/6/94
TIME: 9:35
PT: 0.450
STP: 0.030
WL: 1.54060
17.66
8.84
5.90
4.4
3.56
2.98
2.56
2.25
3000.0
2700.0
2400.0
2100.0
1800.0
1500.0
1200.0
900.0
600.0
300.0
0.0
100
90
80
70
60
50
40
30
20
10
0
5
10
15
20
25
30
35
40
12.630/ 531
10.053/ 745
7.191/ 735
5.007/ 336
4.259/ 2704
3.576/ 560
3.348/ 3006
3.258/ 482
2.466/ 239

106

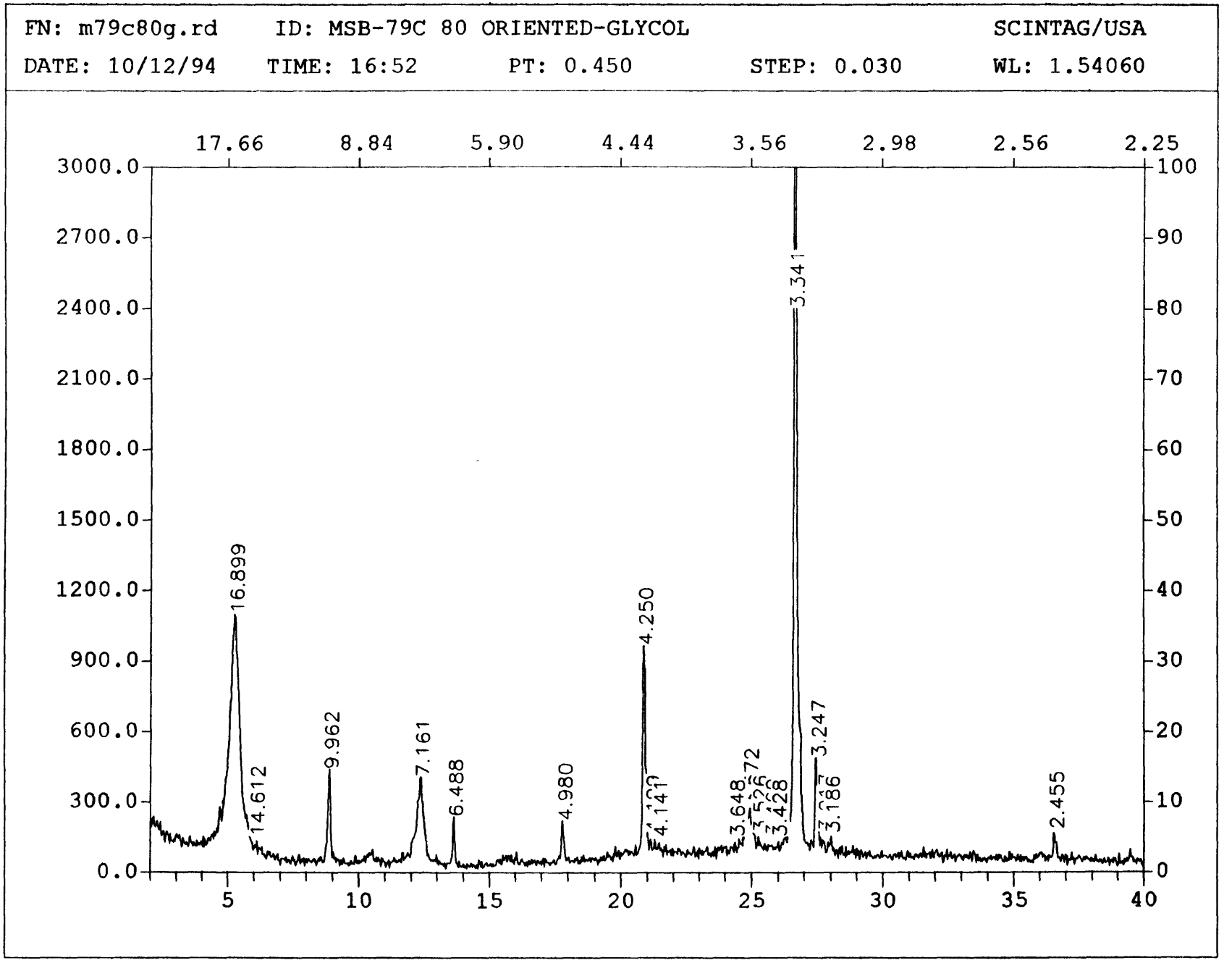
FN: m79c80g.rd
ID: MSB-79C 80 ORIENTED-GLYCOL
SCINTAG/USA
DATE: 10/12/94
TIME: 16:52
PT: 0.450
STEP: 0.030
WL: 1.54060
17.66
8.84
5.90
4.44
3.56
2.98
2.56
2.25
3000.0
2700.0
2400.0
2100.0
1800.0
1500.0
1200.0
900.0
600.0
300.0
0.0
100
90
80
70
60
50
40
30
20
10
0
5
10
15
20
25
30
35
40
16.899
14.612
9.962
7.161
6.488
4.980
4.250
4.141
3.648
3.572
3.526
3.428
3.341
3.247
3.186
2.455

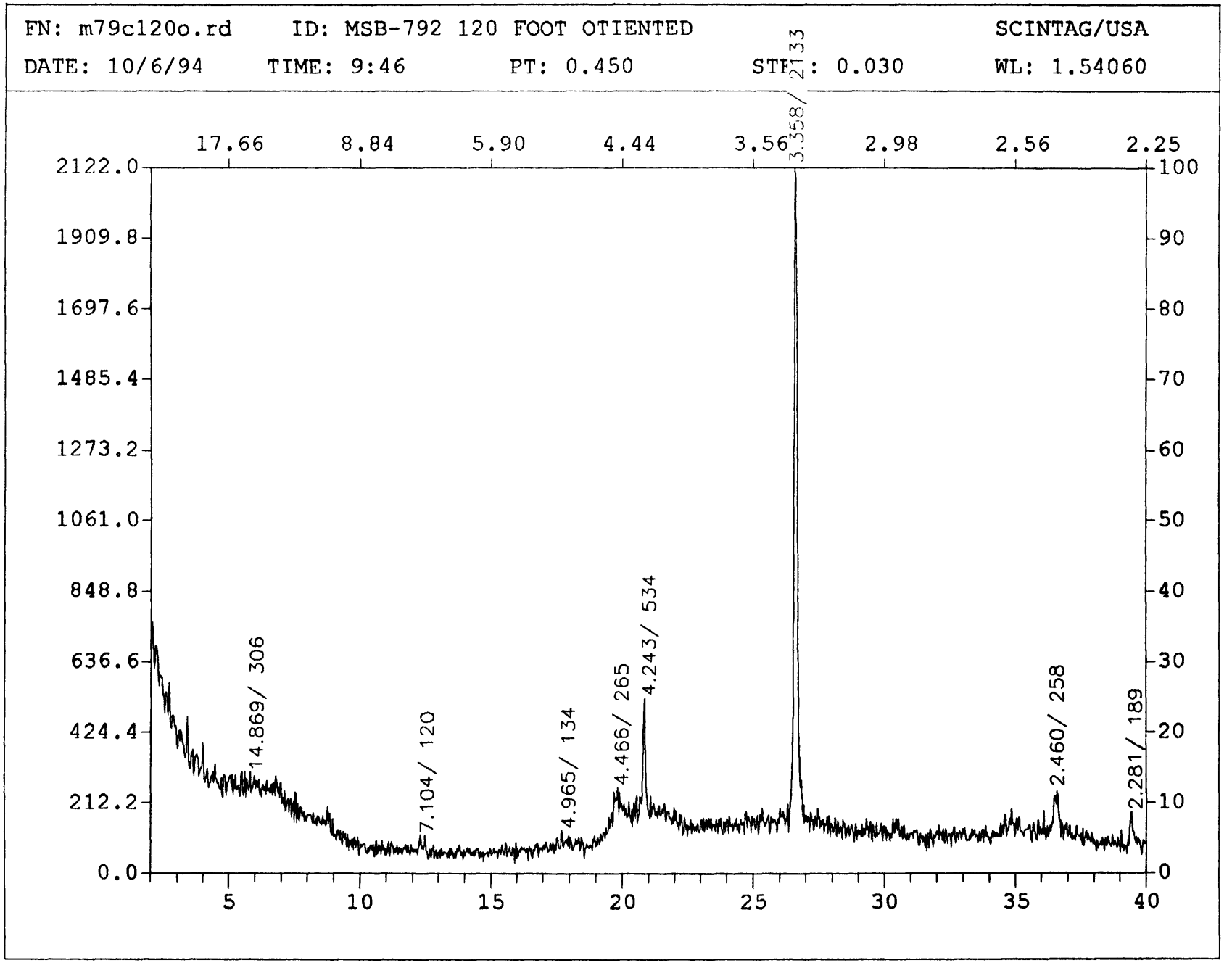
FN: m79c120o.rd
ID: MSB-792 120 FOOT OTIENTED
SCINTAG/USA
DATE: 10/6/94
TIME: 9:46
PT: 0.450
STP: 0.030
WL: 1.54060
17.66
8.84
5.90
4.44
3.56
2.98
2.56
2.25
2122.0
1909.8
1697.6
1485.4
1273.2
1061.0
848.8
636.6
424.4
212.2
0.0
100
90
80
70
60
50
40
30
20
10
0
5
10
15
20
25
30
35
40
3.358/ 2133
14.869/ 306
7.104/ 120
4.965/ 134
4.466/ 265
4.243/ 534
2.460/ 258
2.281/ 189

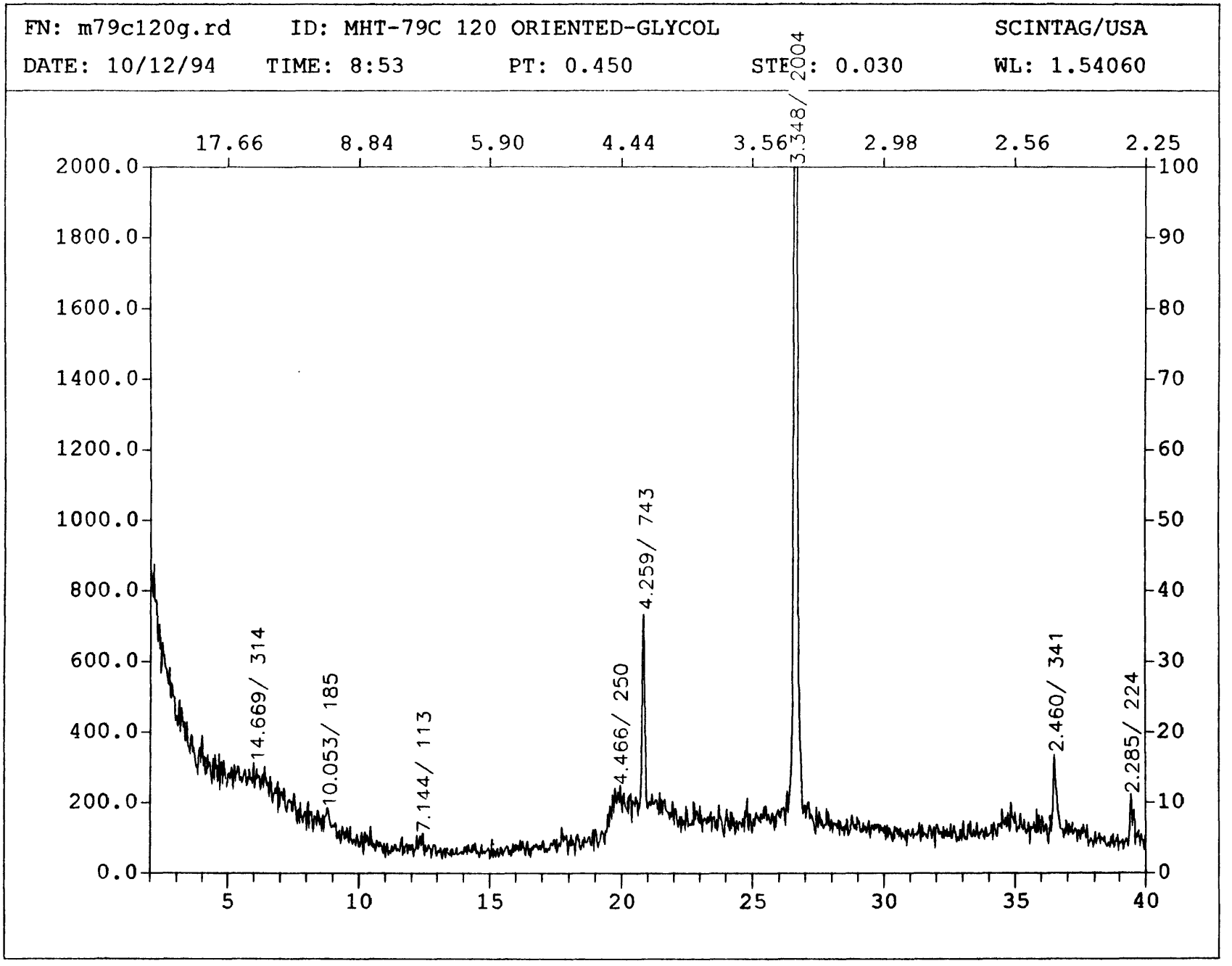
FN: m79c120g.rd
ID: MHT-79C 120 ORIENTED-GLYCOL
SCINTAG/USA
DATE: 10/12/94
TIME: 8:53
PT: 0.450
STEP: 0.030
WL: 1.54060
17.66
8.84
5.90
4.44
3.56
3.348/ 2004
2.98
2.56
2.25
2000.0
1800.0
1600.0
1400.0
1200.0
1000.0
800.0
600.0
400.0
200.0
0.0
100
90
80
70
60
50
40
30
20
10
0
5
10
15
20
25
30
35
40
14.669/ 314
10.053/ 185
7.144/ 113
4.466/ 250
4.259/ 743
2.460/ 341
2.285/ 224

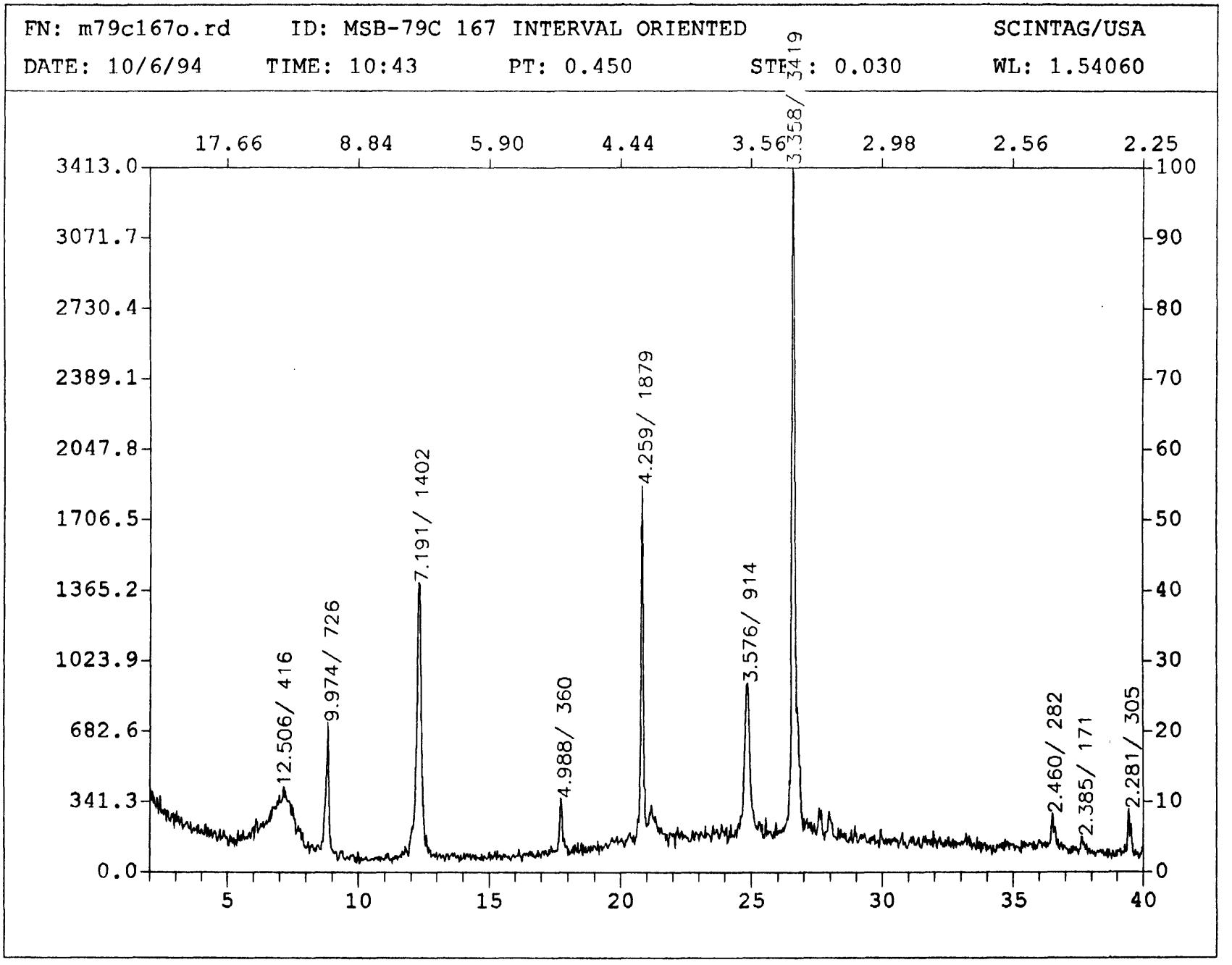
FN: m79c167o.rd ID: MSB-79C 167 INTERVAL ORIENTED SCINTAG/USA
DATE: 10/6/94 TIME: 10:43 PT: 0.450 STEP: 0.030 WL: 1.54060
17.66
8.84
5.90
4.44
3.56
3.358/ 3419
2.98
2.56
2.25
3413.0
3071.7
2730.4
2389.1
2047.8
1706.5
1365.2
1023.9
682.6
341.3
0.0
100
90
80
70
60
50
40
30
20
10
0
12.506/ 416
9.974/ 726
7.191/ 1402
4.988/ 360
4.259/ 1879
3.576/ 914
2.460/ 282
2.385/ 171
2.281/ 305
5
10
15
20
25
30
35
40

110

FN: m79c167g.rd ID: MSB-79C 167 ORIENTED-GLYCOL SCINTAG/USA

DATE: 10/12/94 TIME: 16:09 PT: 0.450 STEP: 0.030 WL: 1.54060

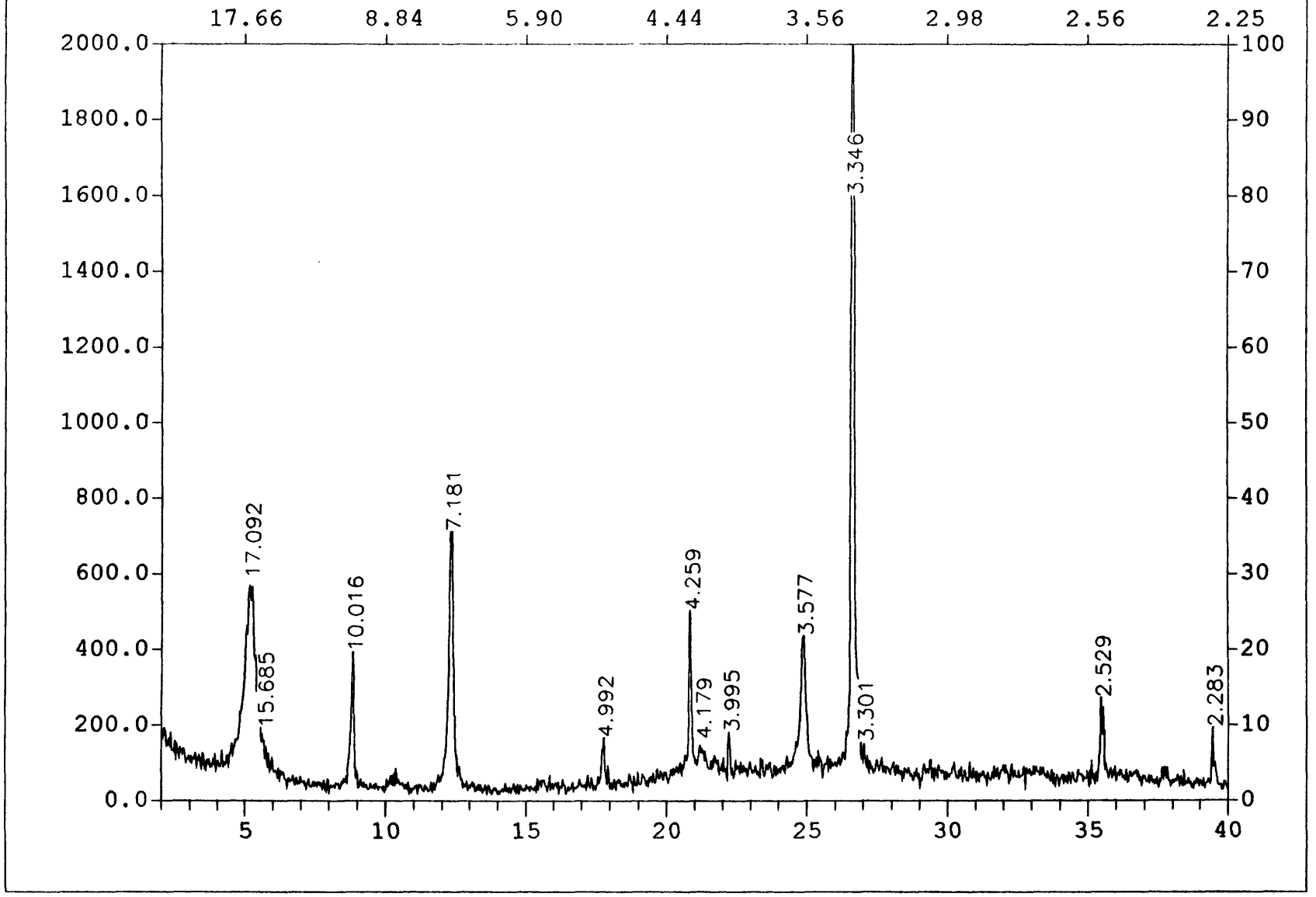

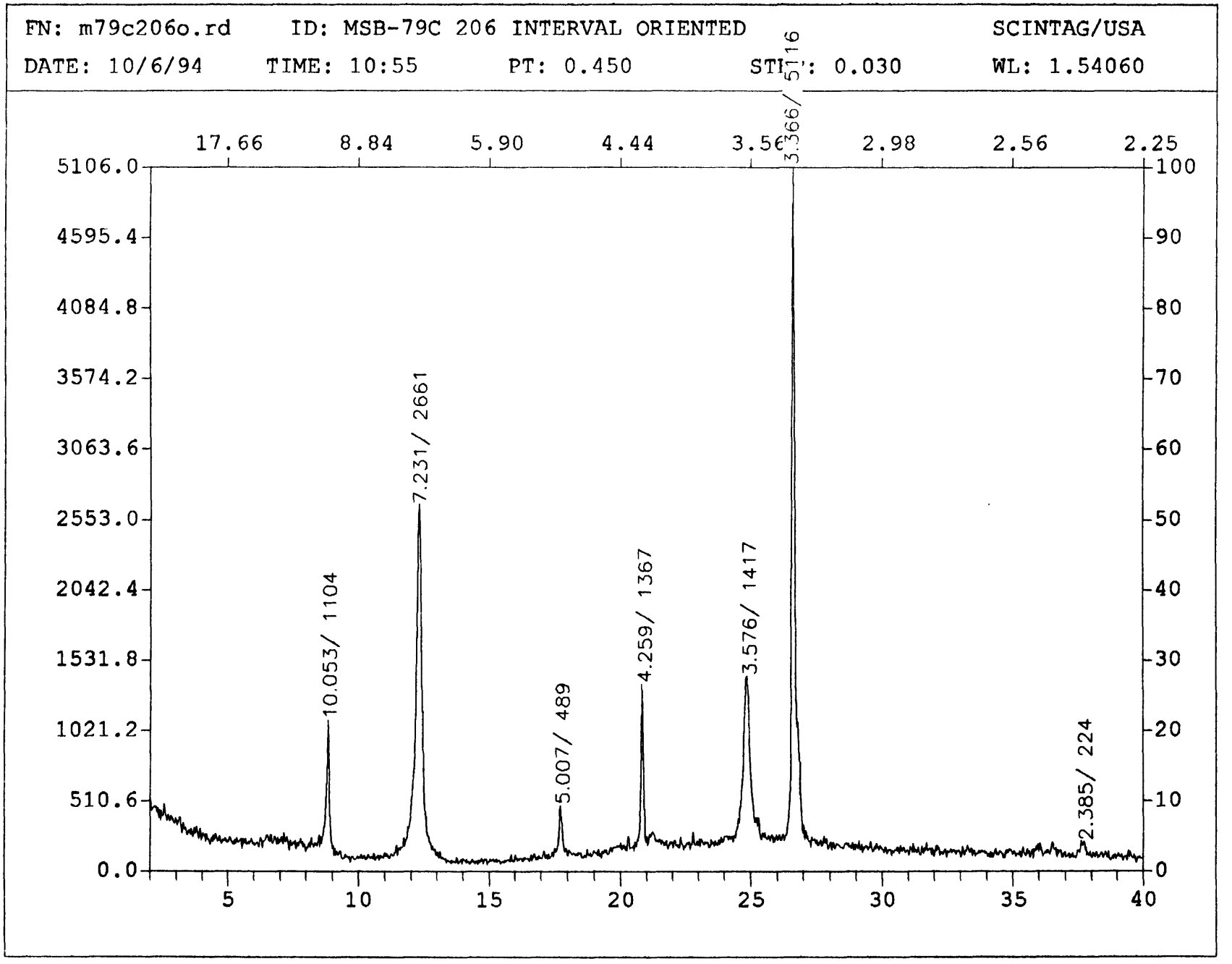
FN: m79c206o.rd
ID: MSB-79C 206 INTERVAL ORIENTED
SCINTAG/USA
DATE: 10/6/94
TIME: 10:55
PT: 0.450
STP: 0.030
WL: 1.54060
17.66
8.84
5.90
4.44
3.56
2.98
2.56
2.25
5106.0
4595.4
4084.8
3574.2
3063.6
2553.0
2042.4
1531.8
1021.2
510.6
0.0
100
90
80
70
60
50
40
30
20
10
0
5
10
15
20
25
30
35
40
10.053/ 1104
7.231/ 2661
5.007/ 489
4.259/ 1367
3.576/ 1417
3.366/ 5116
2.385/ 224

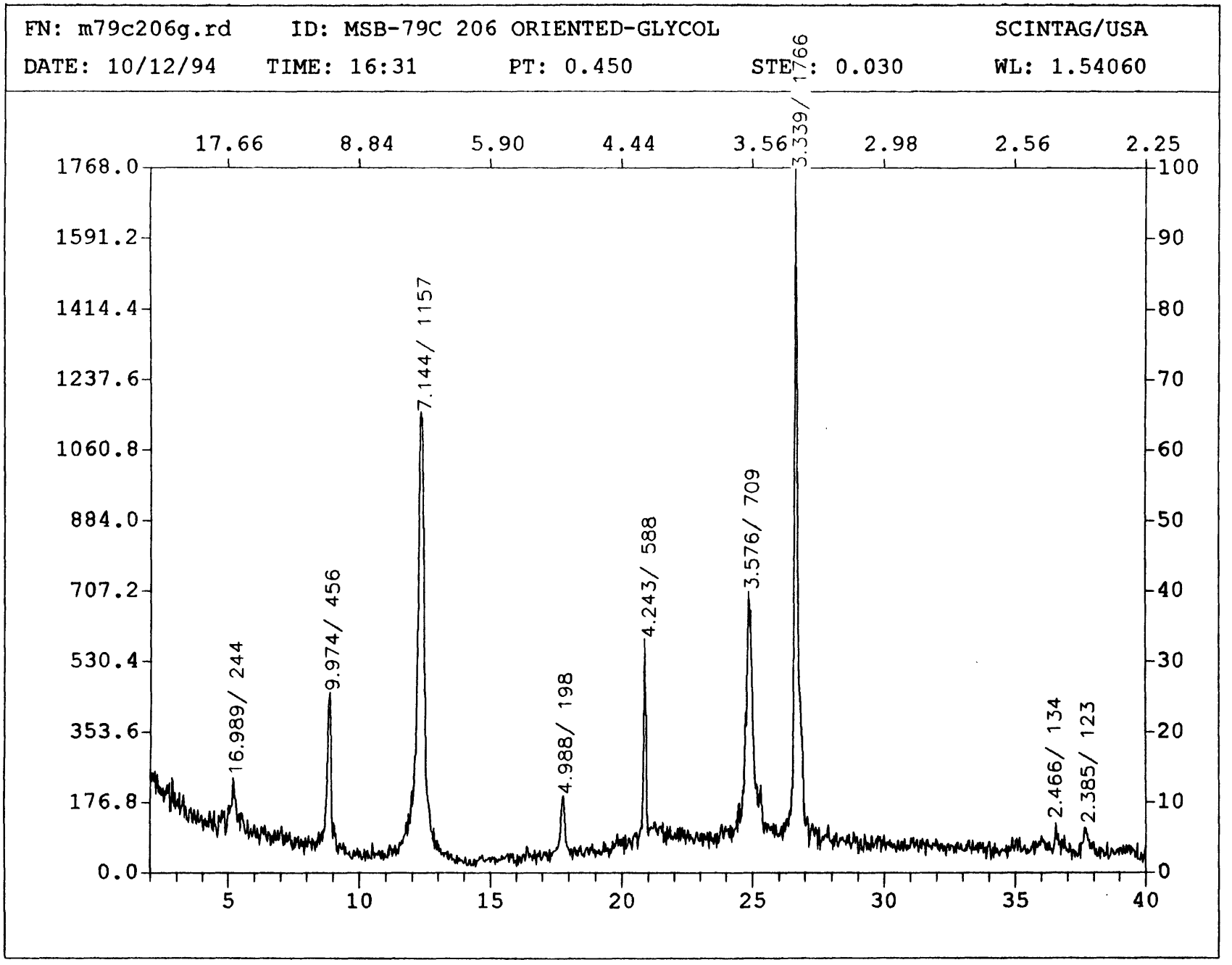
FN: m79c206g.rd
ID: MSB-79C 206 ORIENTED-GLYCOL
SCINTAG/USA
DATE: 10/12/94
TIME: 16:31
PT: 0.450
STEP: 0.030
WL: 1.54060
17.66
8.84
5.90
4.44
3.56
3.339/ 1766
2.98
2.56
2.25
1768.0
1591.2
1414.4
1237.6
1060.8
884.0
707.2
530.4
353.6
176.8
0.0
100
90
80
70
60
50
40
30
20
10
0
16.989/ 244
9.974/ 456
7.144/ 1157
4.988/ 198
4.243/ 588
3.576/ 709
2.466/ 134
2.385/ 123
5
10
15
20
25
30
35
40

Appendix B

Resistivity and Phase Spectra of SRS Core Samples

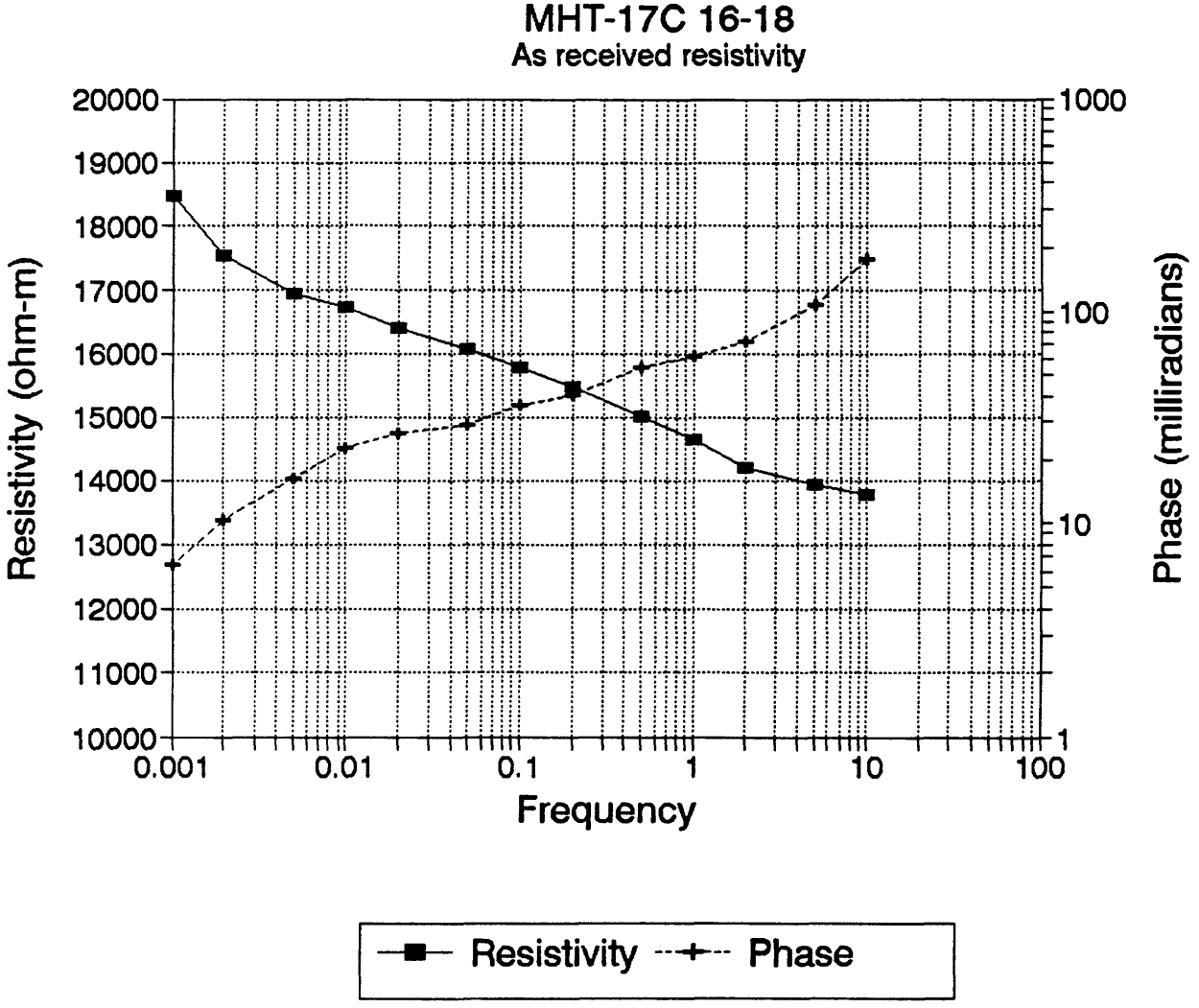
MHT-17C 16-18
As received resistivity
Resistivity (ohm-m)
20000
19000
18000
17000
16000
15000
14000
13000
12000
11000
10000
0.001
0.01
0.1
1
10
100
Frequency
1000
100
10
1
Phase (milliradians)
Resistivity
Phase

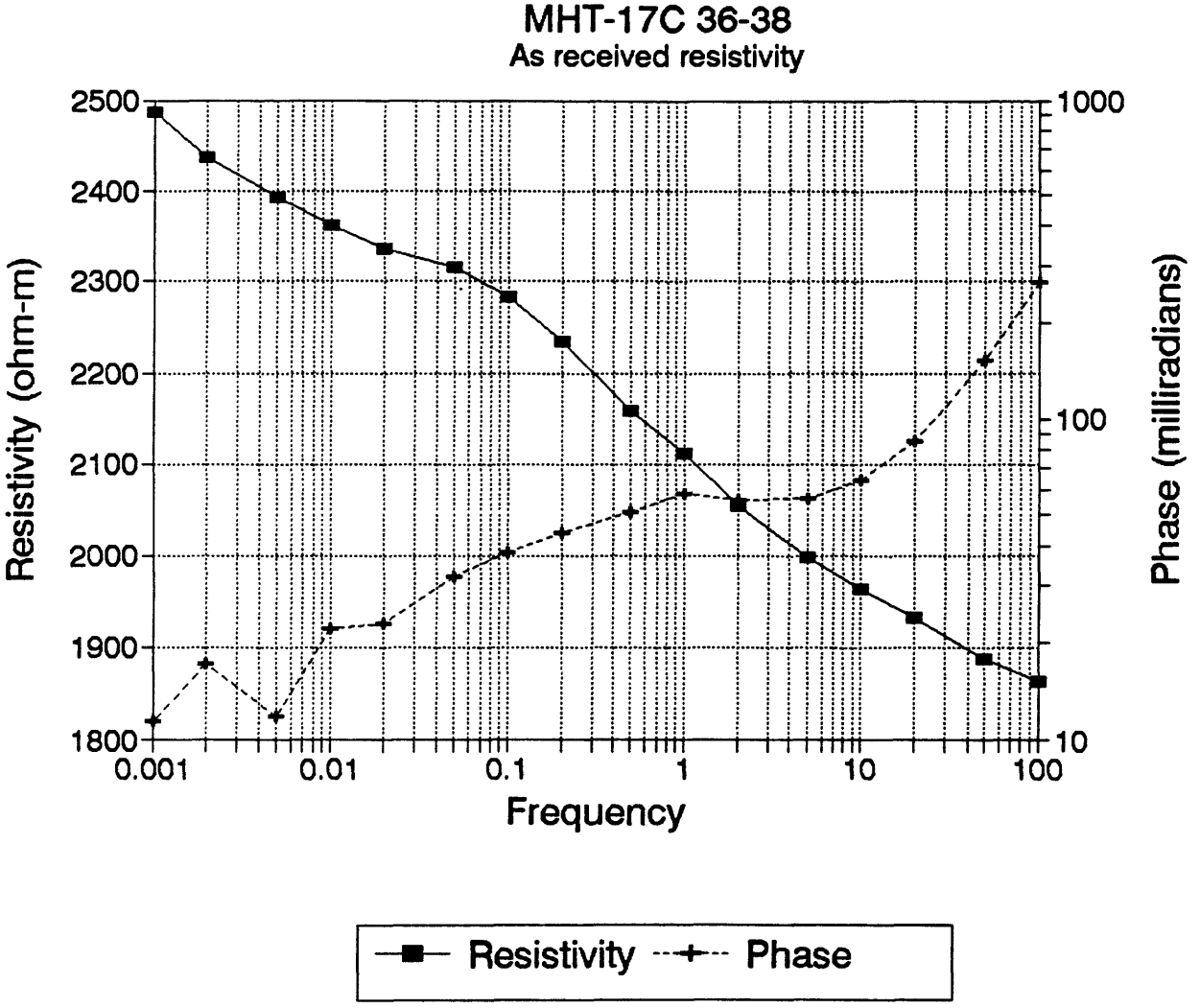
MHT-17C 36-38
As received resistivity
Resistivity (ohm-m)
2500
2400
2300
2200
2100
2000
1900
1800
Phase (milliradians)
1000
100
10
0.001
0.01
0.1
1
10
100
Frequency
Resistivity
Phase

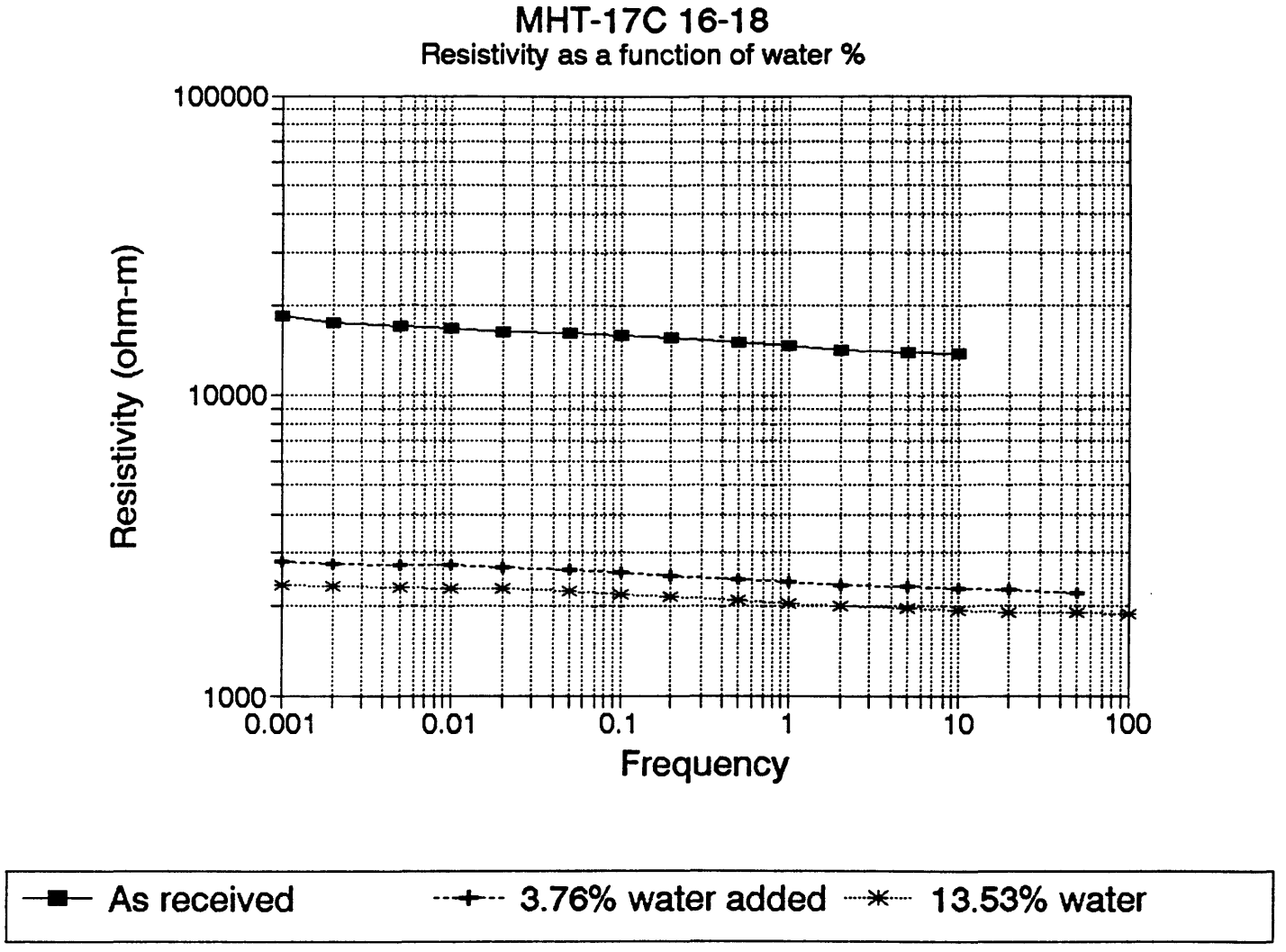
MHT-17C 16-18
Resistivity as a function of water %
Resistivity (ohm-m)
100000
10000
1000
0.001
0.01
0.1
1
10
100
Frequency
As received
3.76% water added
13.53% water

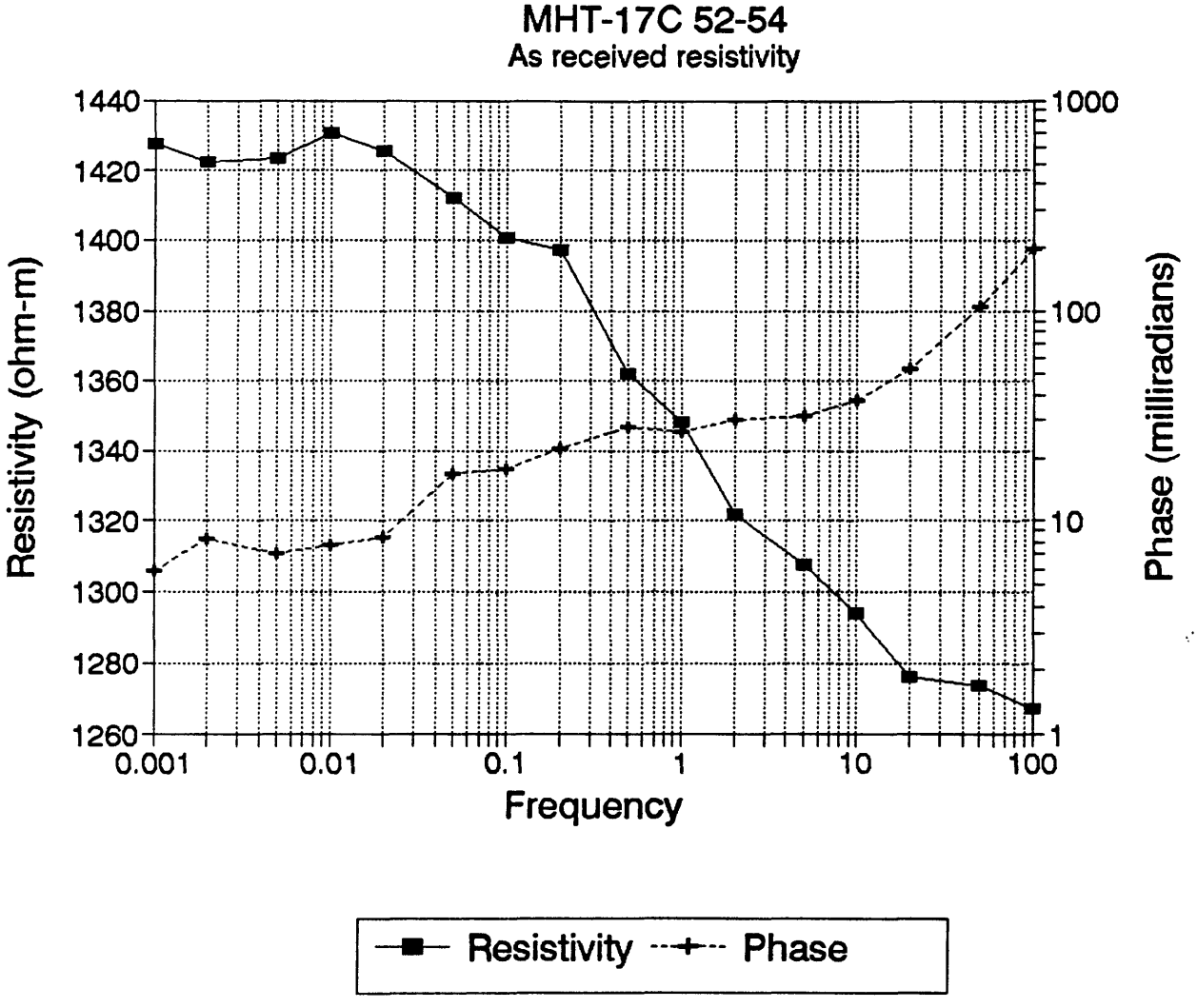
MHT-17C 52-54
As received resistivity
Resistivity (ohm-m)
1440
1420
1400
1380
1360
1340
1320
1300
1280
1260
Phase (milliradians)
1000
100
10
1
0.001
0.01
0.1
1
10
100
Frequency
Resistivity
Phase

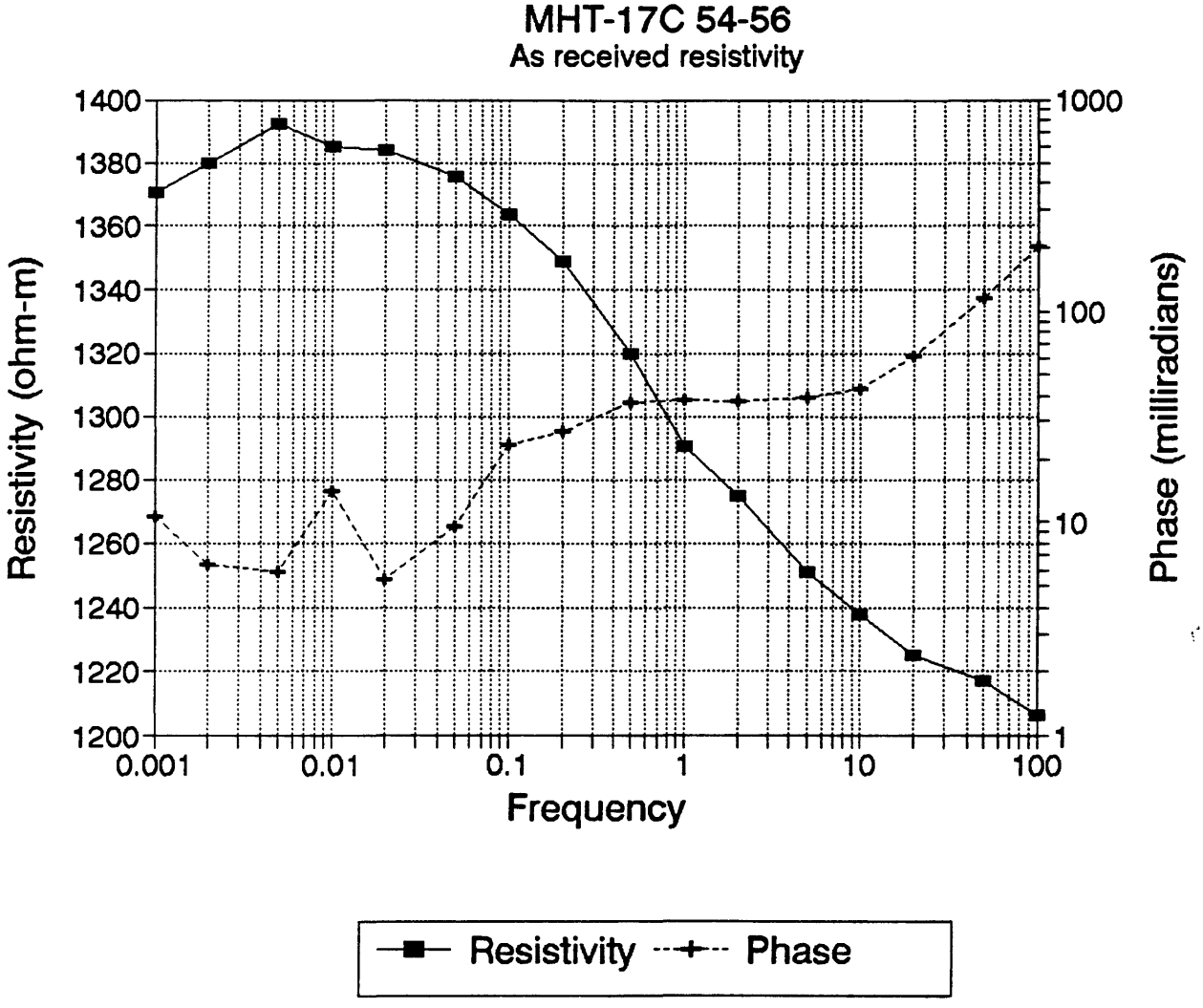
MHT-17C 54-56
As received resistivity
Resistivity (ohm-m)
1400
1380
1360
1340
1320
1300
1280
1260
1240
1220
1200
Phase (milliradians)
1000
100
10
1
0.001
0.01
0.1
1
10
100
Frequency
Resistivity
Phase

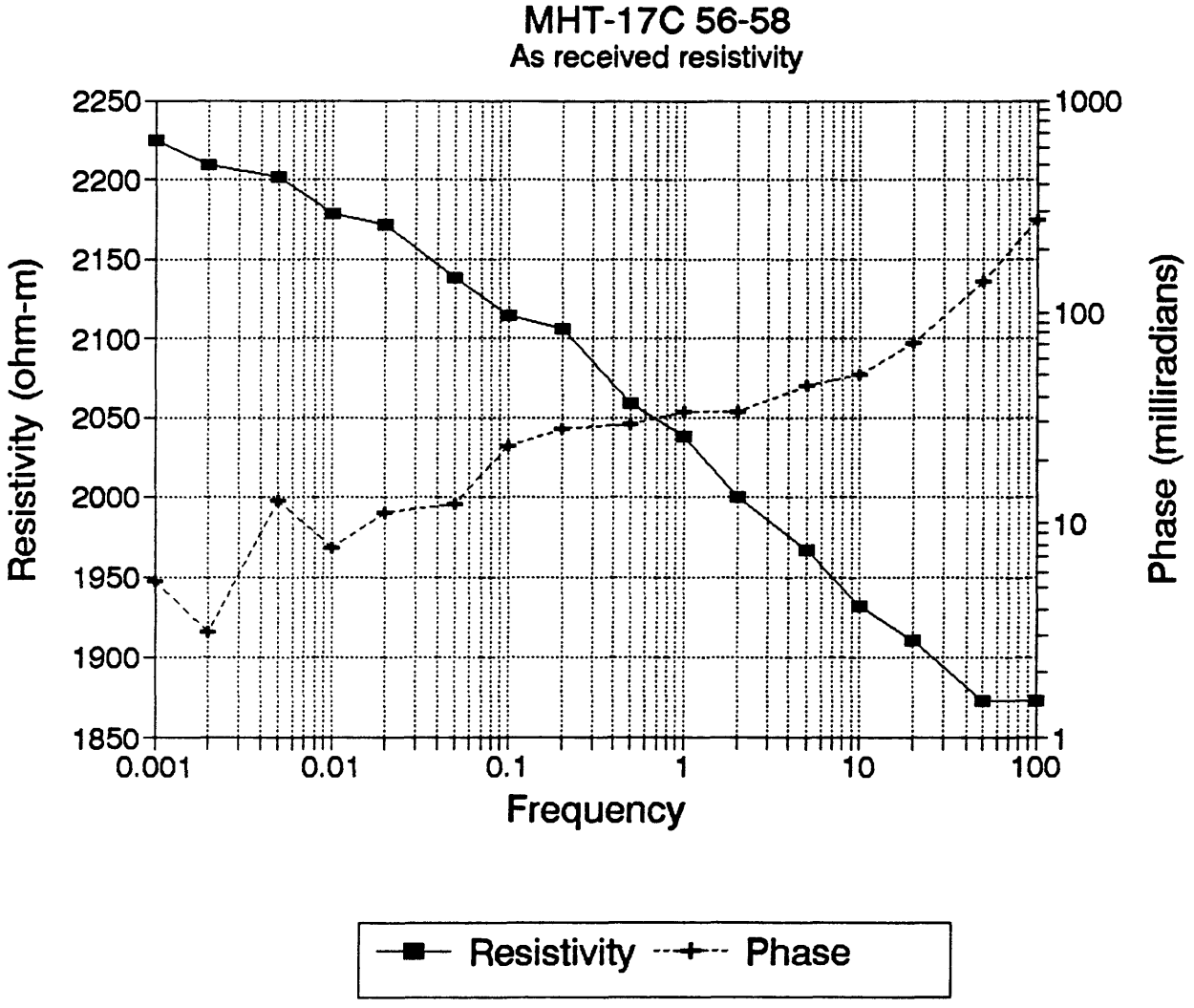
MHT-17C 56-58
As received resistivity
Resistivity (ohm-m)
2250
2200
2150
2100
2050
2000
1950
1900
1850
Phase (milliradians)
1000
100
10
1
0.001
0.01
0.1
1
10
100
Frequency
Resistivity
Phase

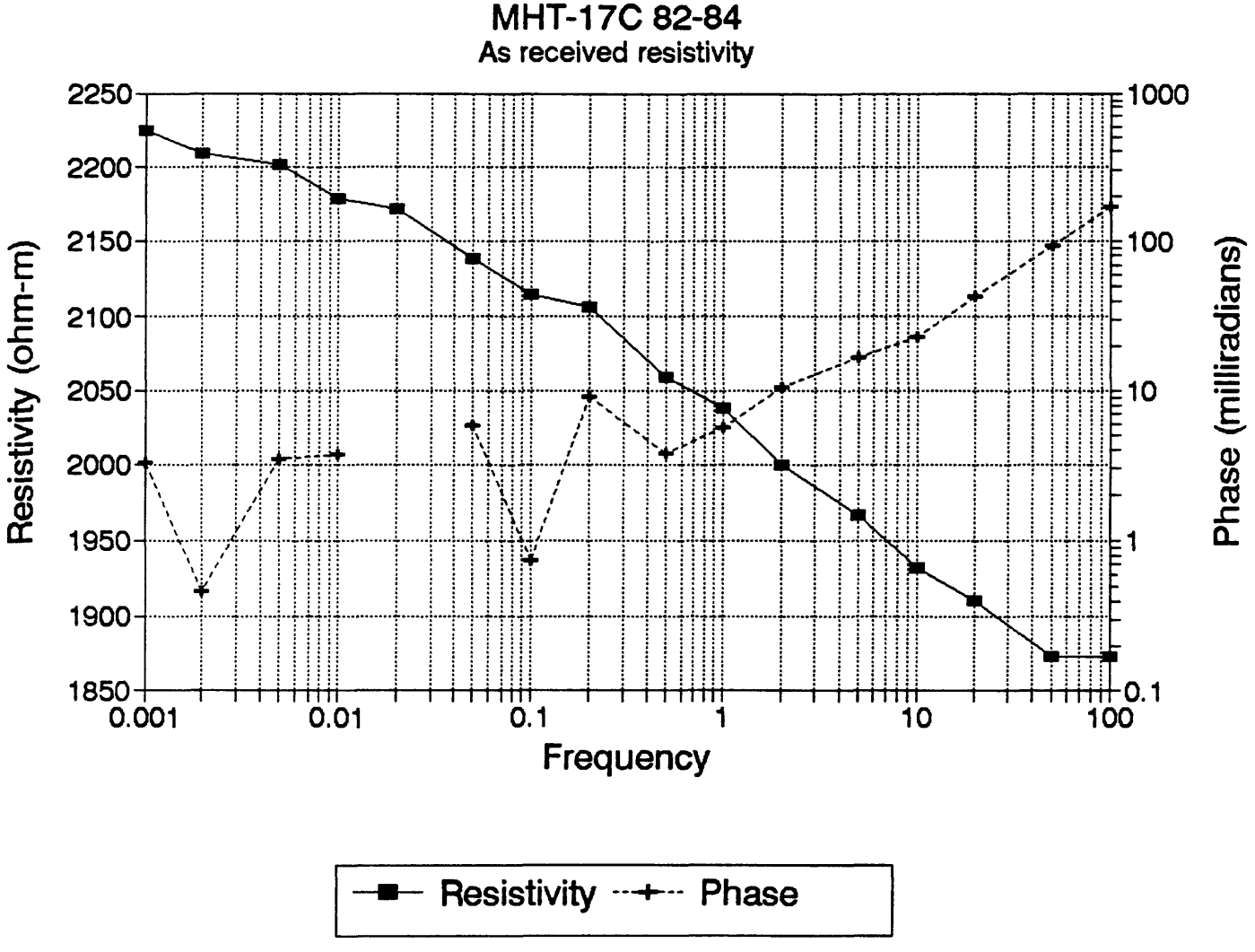
MHT-17C 82-84
As received resistivity
Resistivity (ohm-m)
2250
2200
2150
2100
2050
2000
1950
1900
1850
Phase (milliradians)
1000
100
10
1
0.1
0.001
0.01
0.1
1
10
100
Frequency
Resistivity
Phase

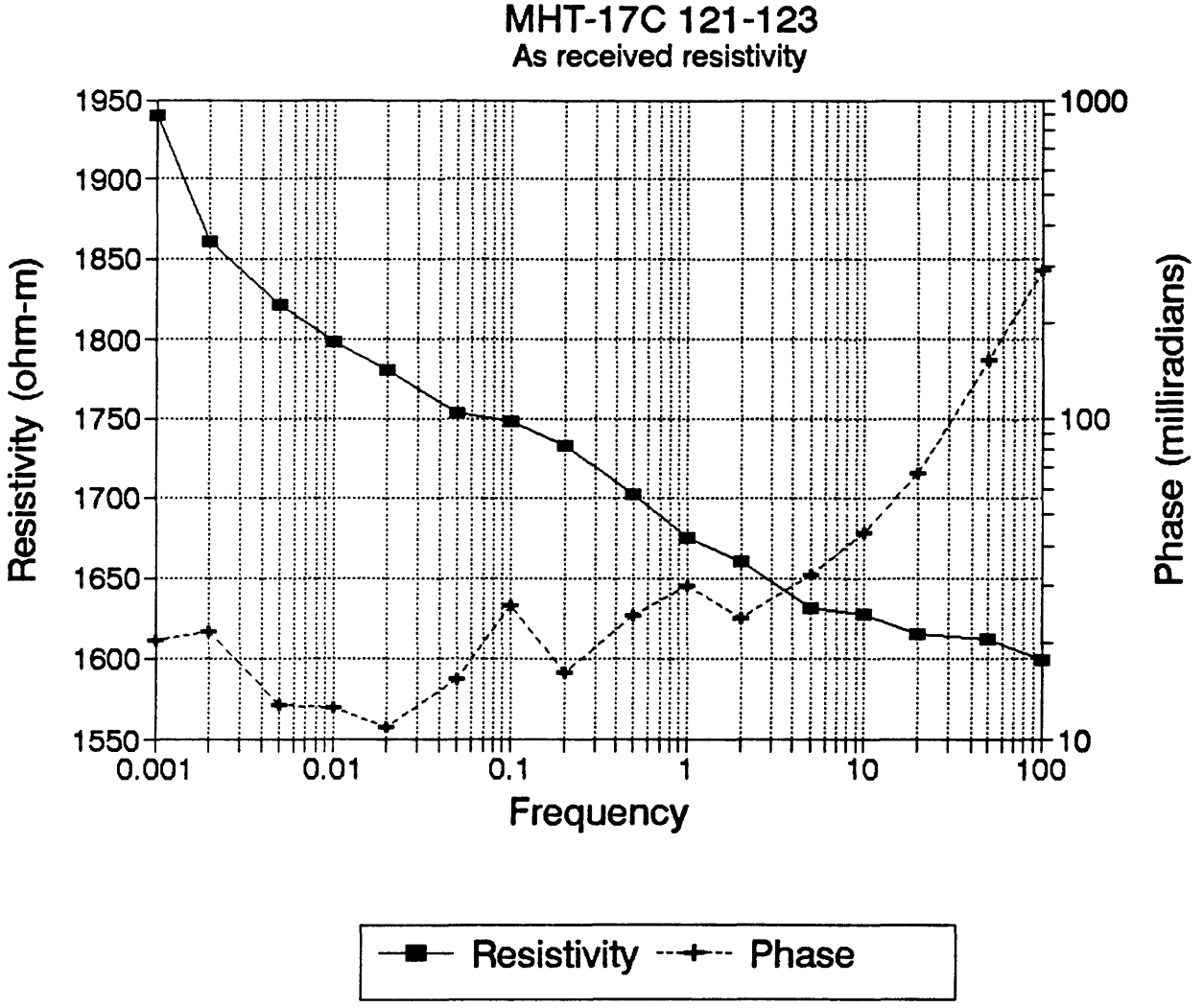
MHT-17C 121-123
As received resistivity
Resistivity (ohm-m)
1950
1900
1850
1800
1750
1700
1650
1600
1550
Phase (milliradians)
1000
100
10
0.001
0.01
0.1
1
10
100
Frequency
Resistivity
Phase

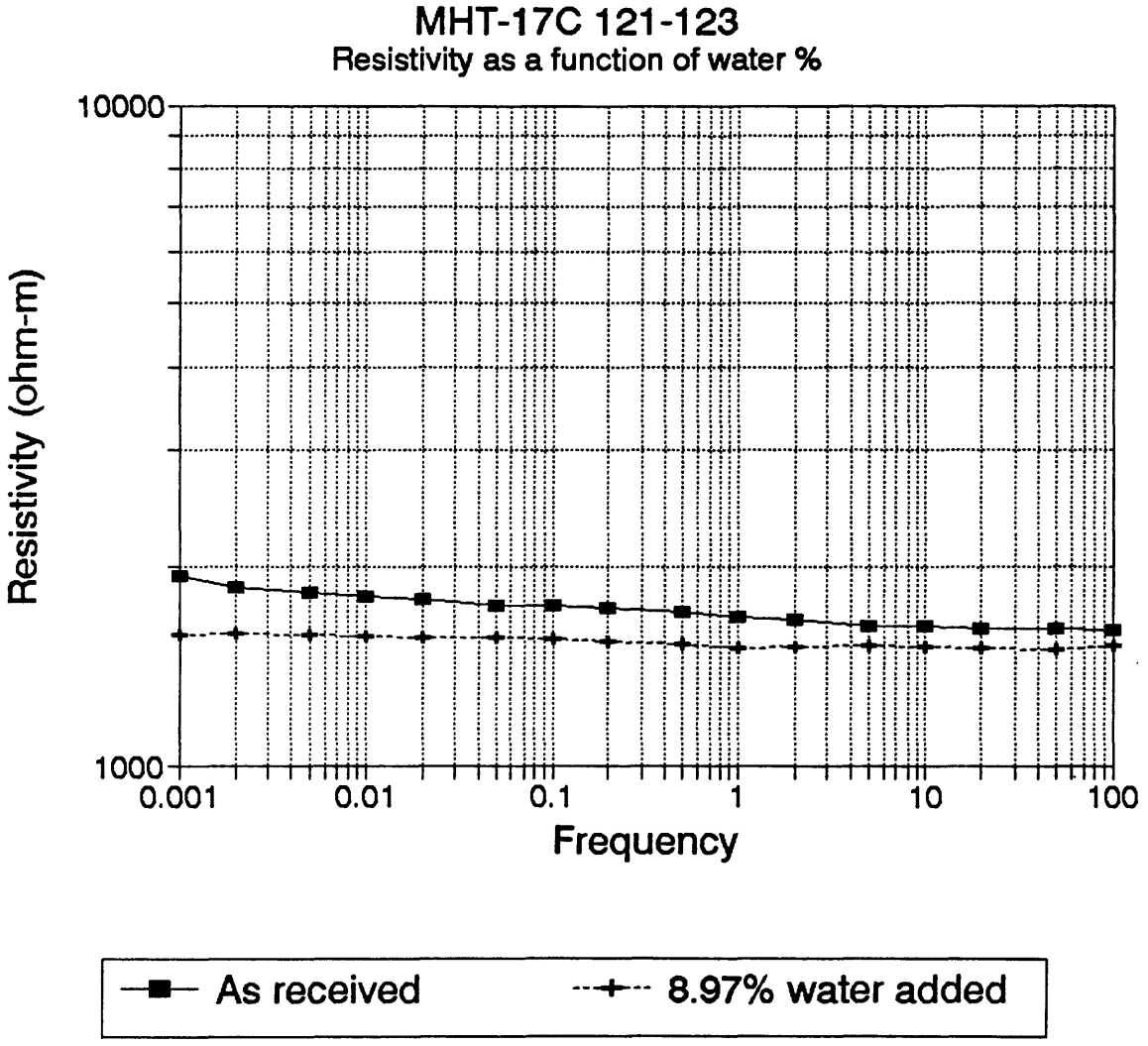
MHT-17C 121-123
Resistivity as a function of water %
10000
1000
Resistivity (ohm-m)
0.001
0.01
0.1
1
10
100
Frequency
As received
8.97% water added

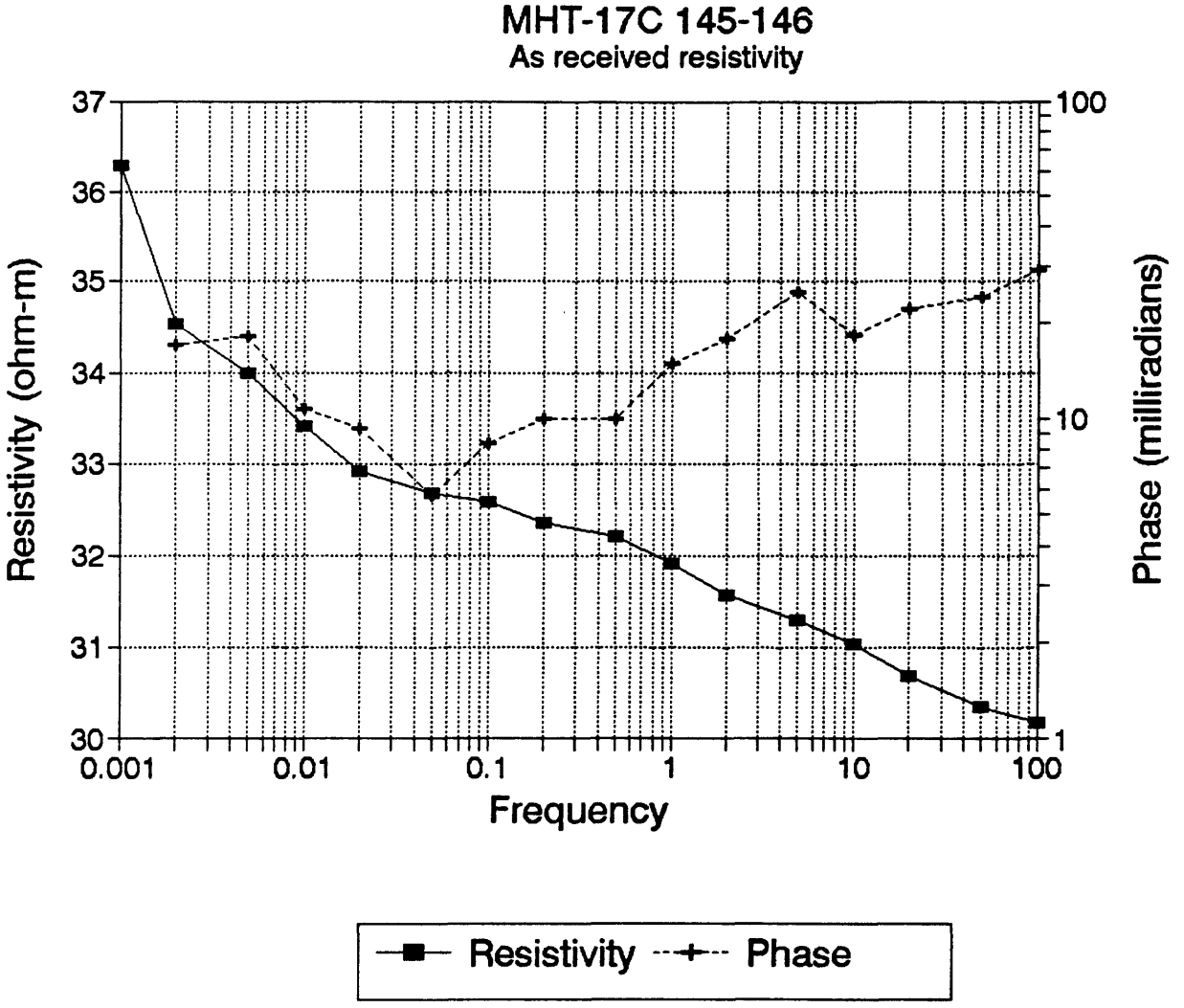
MHT-17C 145-146
As received resistivity
Resistivity (ohm-m)
37
36
35
34
33
32
31
30
Phase (milliradians)
100
10
1
0.001
0.01
0.1
1
10
100
Frequency
Resistivity
Phase

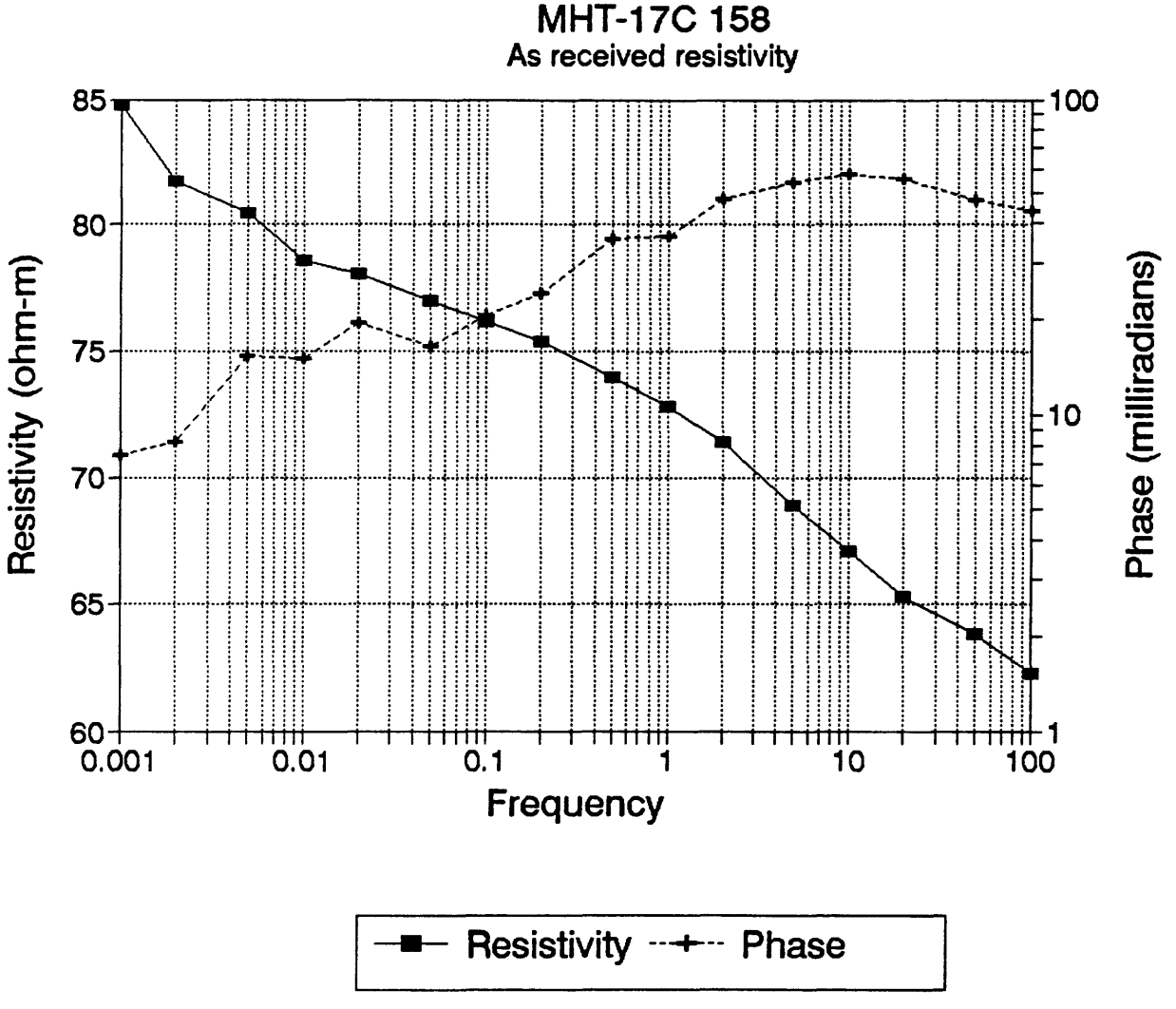
MHT-17C 158
As received resistivity
Resistivity (ohm-m)
85
80
75
70
65
60
0.001
0.01
0.1
1
10
100
Frequency
Phase (milliradians)
100
10
1
Resistivity
Phase

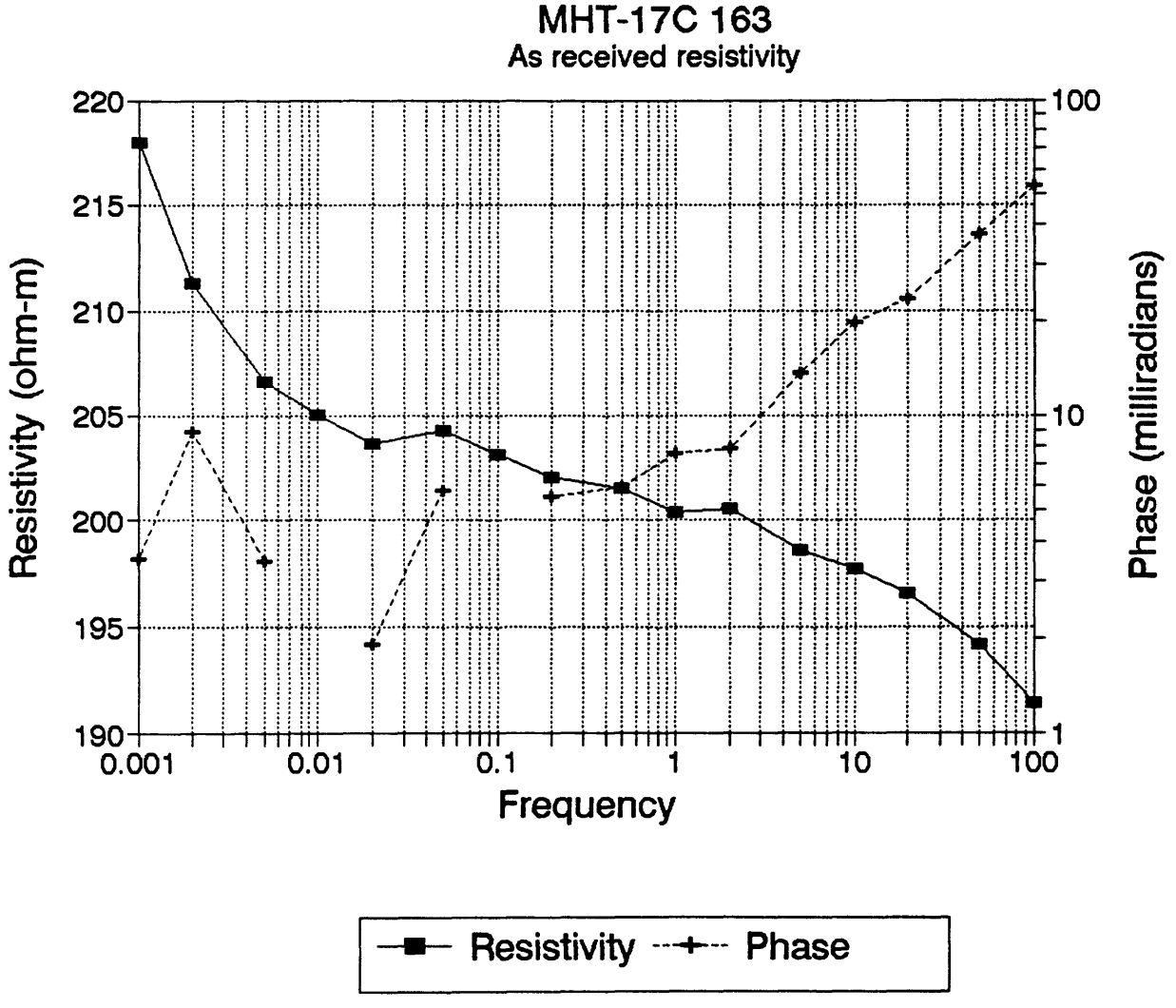
MHT-17C 163
As received resistivity
Resistivity (ohm-m)
220
215
210
205
200
195
190
Phase (milliradians)
100
10
1
0.001
0.01
0.1
1
10
100
Frequency
Resistivity
Phase

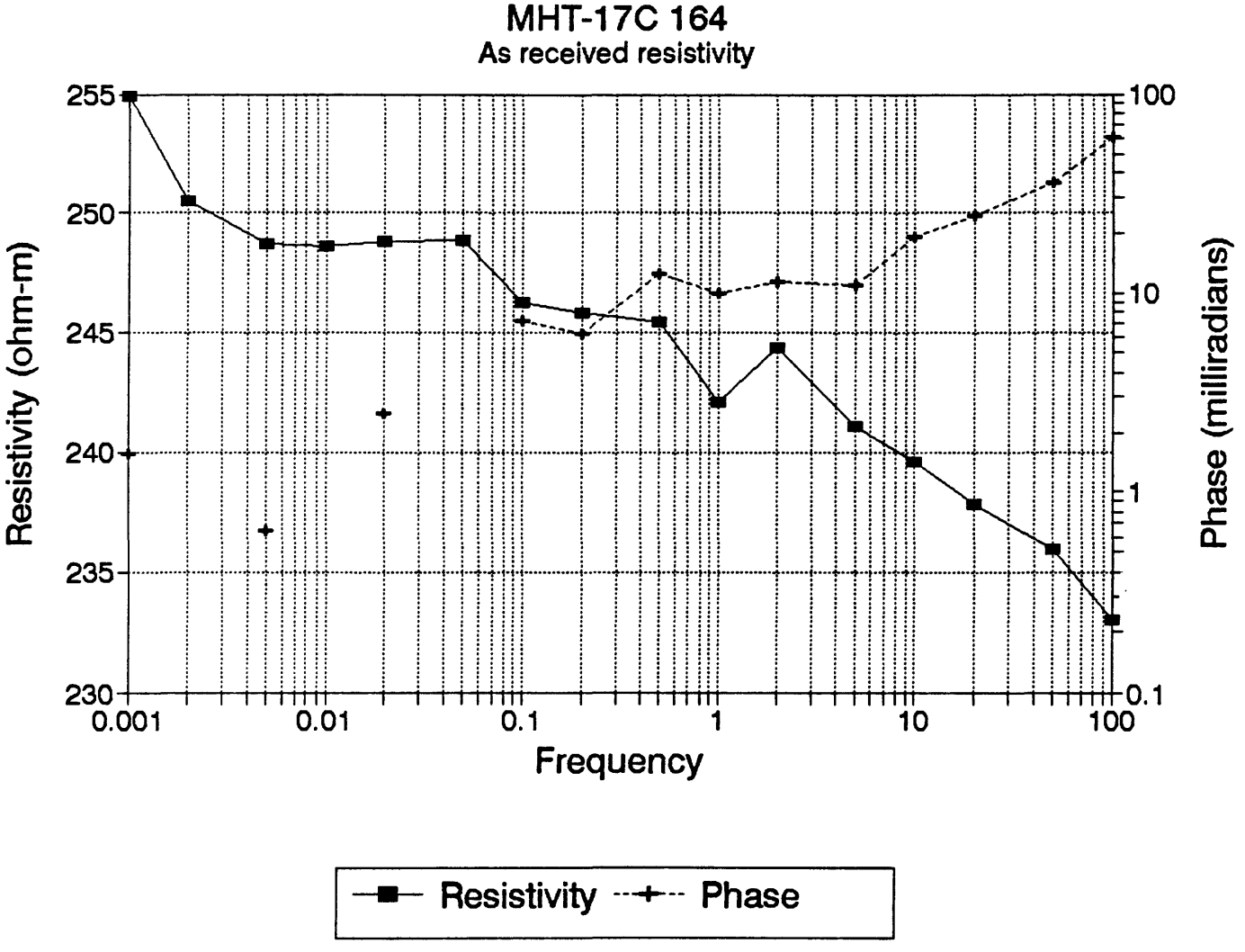
MHT-17C 164
As received resistivity
255
250
245
240
235
230
Resistivity (ohm-m)
100
10
1
0.1
Phase (milliradians)
0.001
0.01
0.1
1
10
100
Frequency
Resistivity
Phase

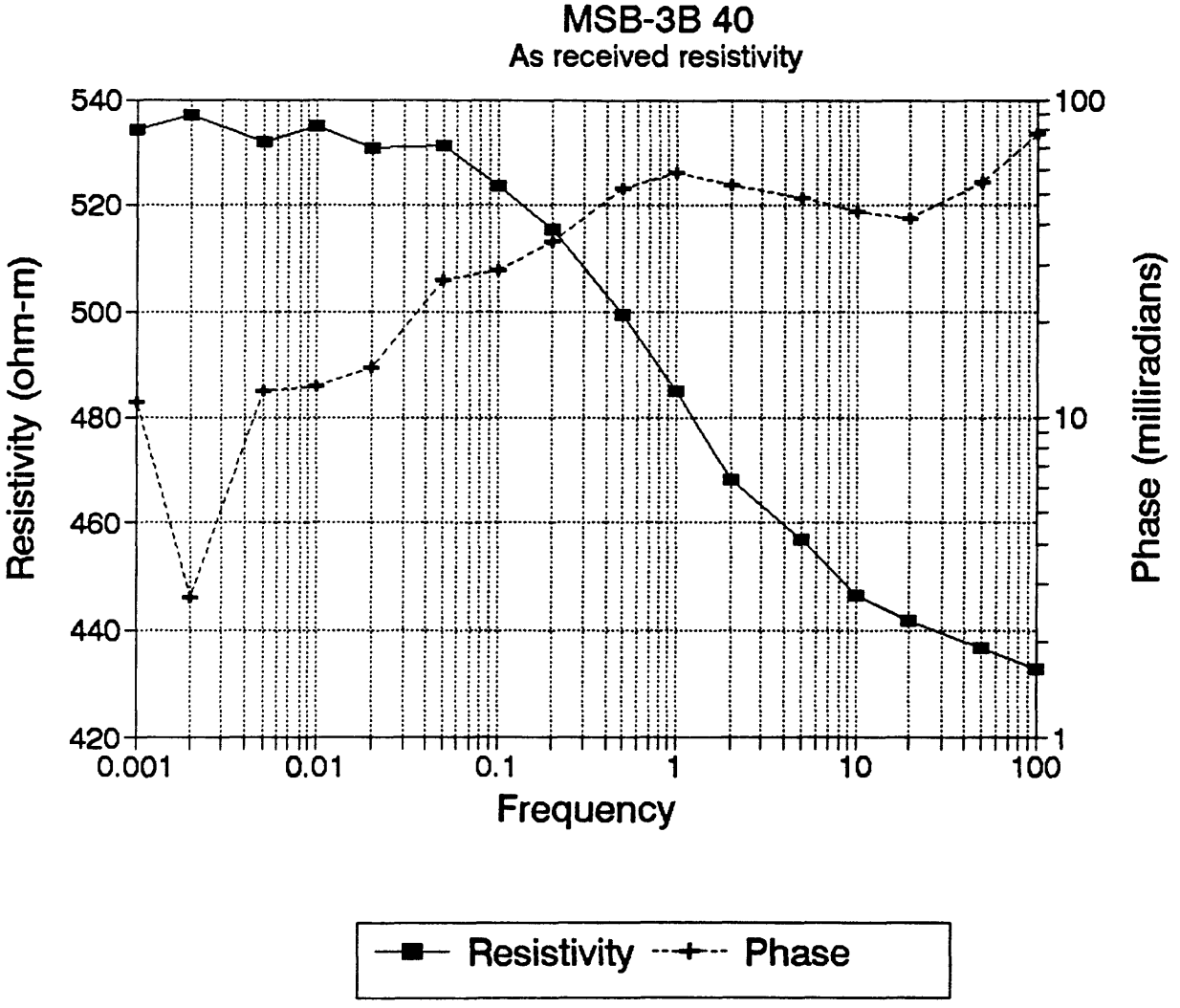
MSB-3B 40
As received resistivity
Resistivity (ohm-m)
540
520
500
480
460
440
420
Phase (milliradians)
100
10
1
0.001
0.01
0.1
1
10
100
Frequency
Resistivity
Phase

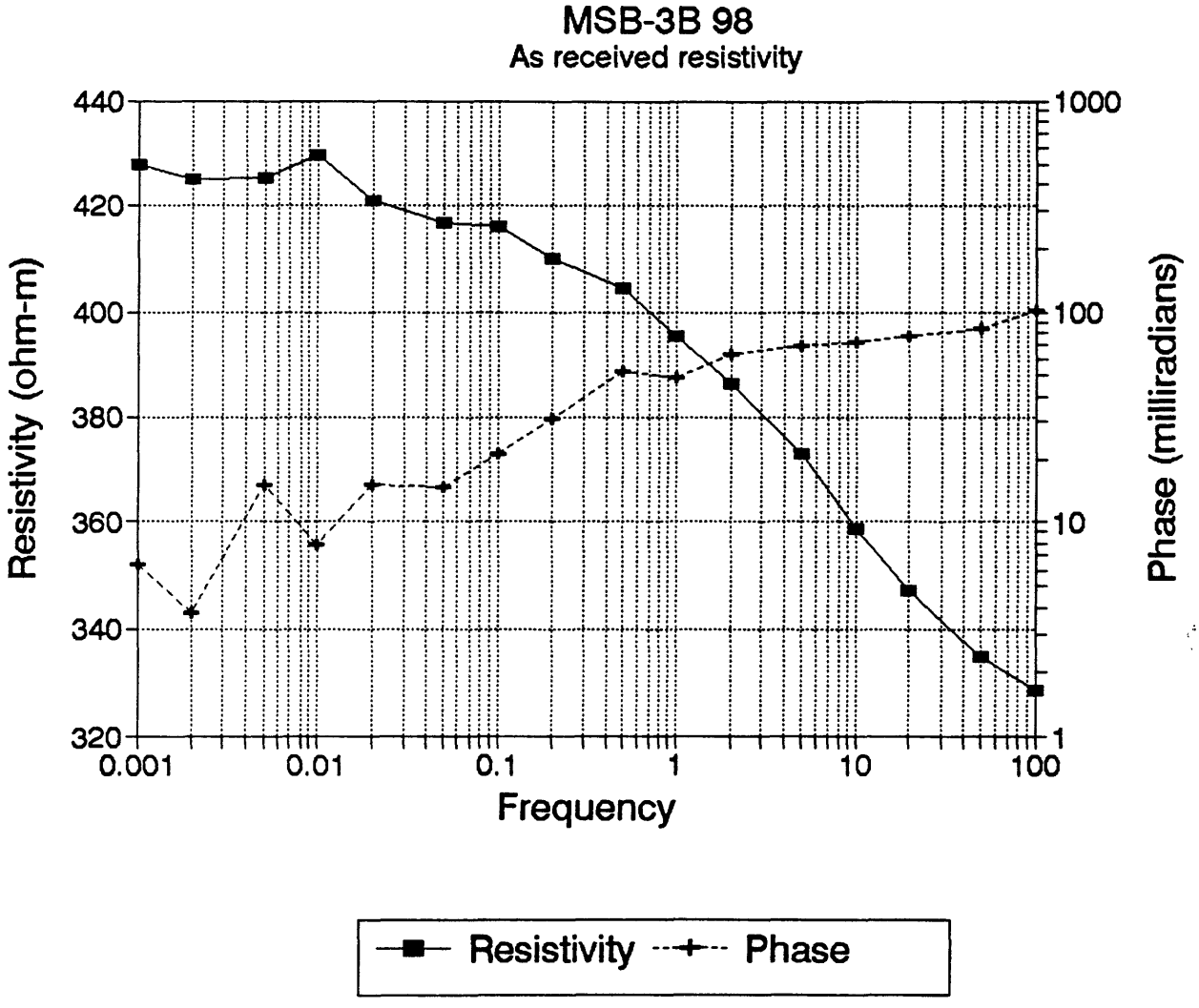
MSB-3B 98
As received resistivity
Resistivity (ohm-m)
440
420
400
380
360
340
320
Phase (milliradians)
1000
100
10
1
0.001
0.01
0.1
1
10
100
Frequency
Resistivity
Phase

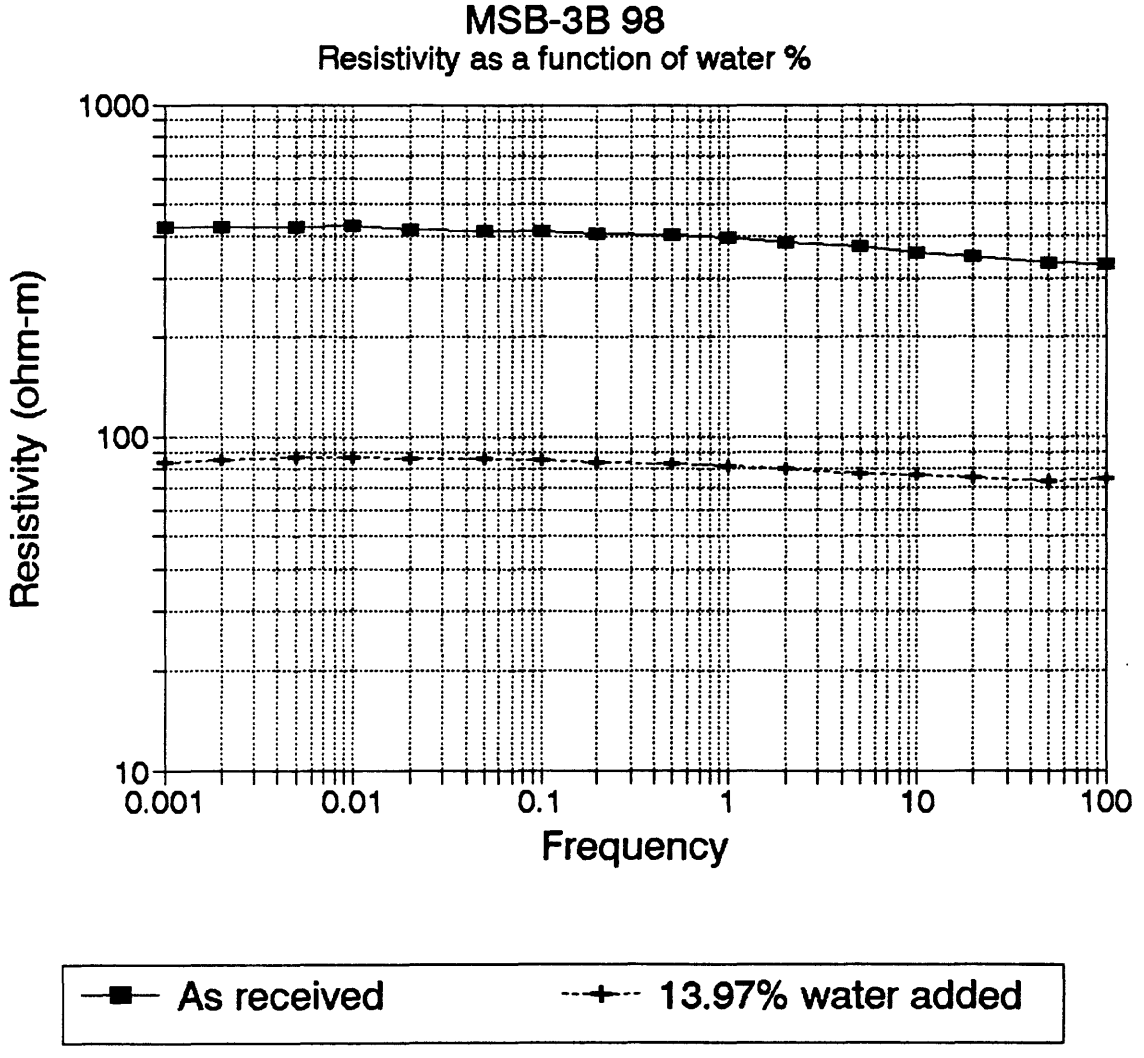
MSB-3B 98
Resistivity as a function of water %
1000
100
10
Resistivity (ohm-m)
0.001
0.01
0.1
1
10
100
Frequency
As received
13.97% water added

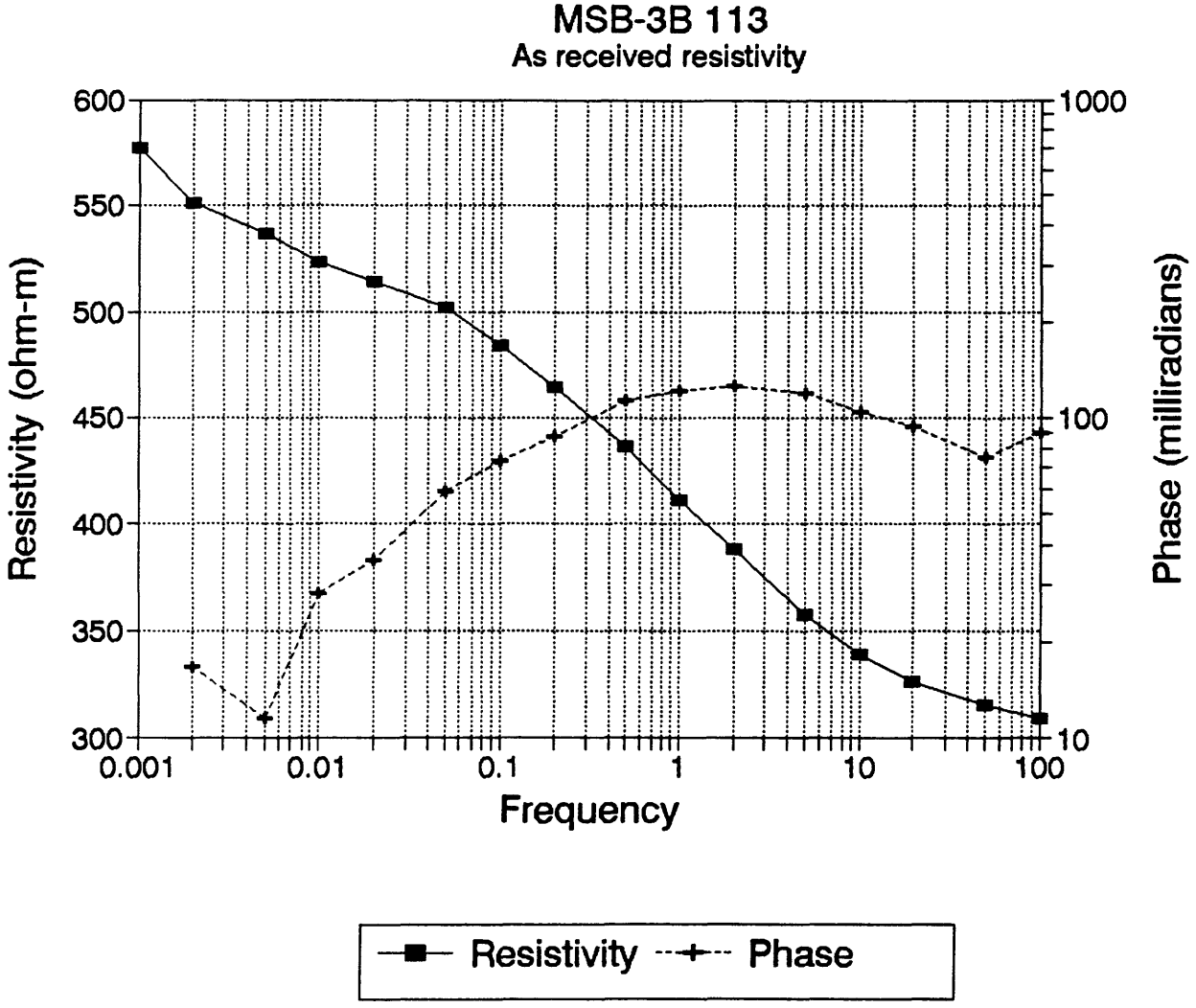
MSB-3B 113
As received resistivity
600
550
500
450
400
350
300
Resistivity (ohm-m)
1000
100
10
Phase (milliradians)
0.001
0.01
0.1
1
10
100
Frequency
Resistivity
Phase

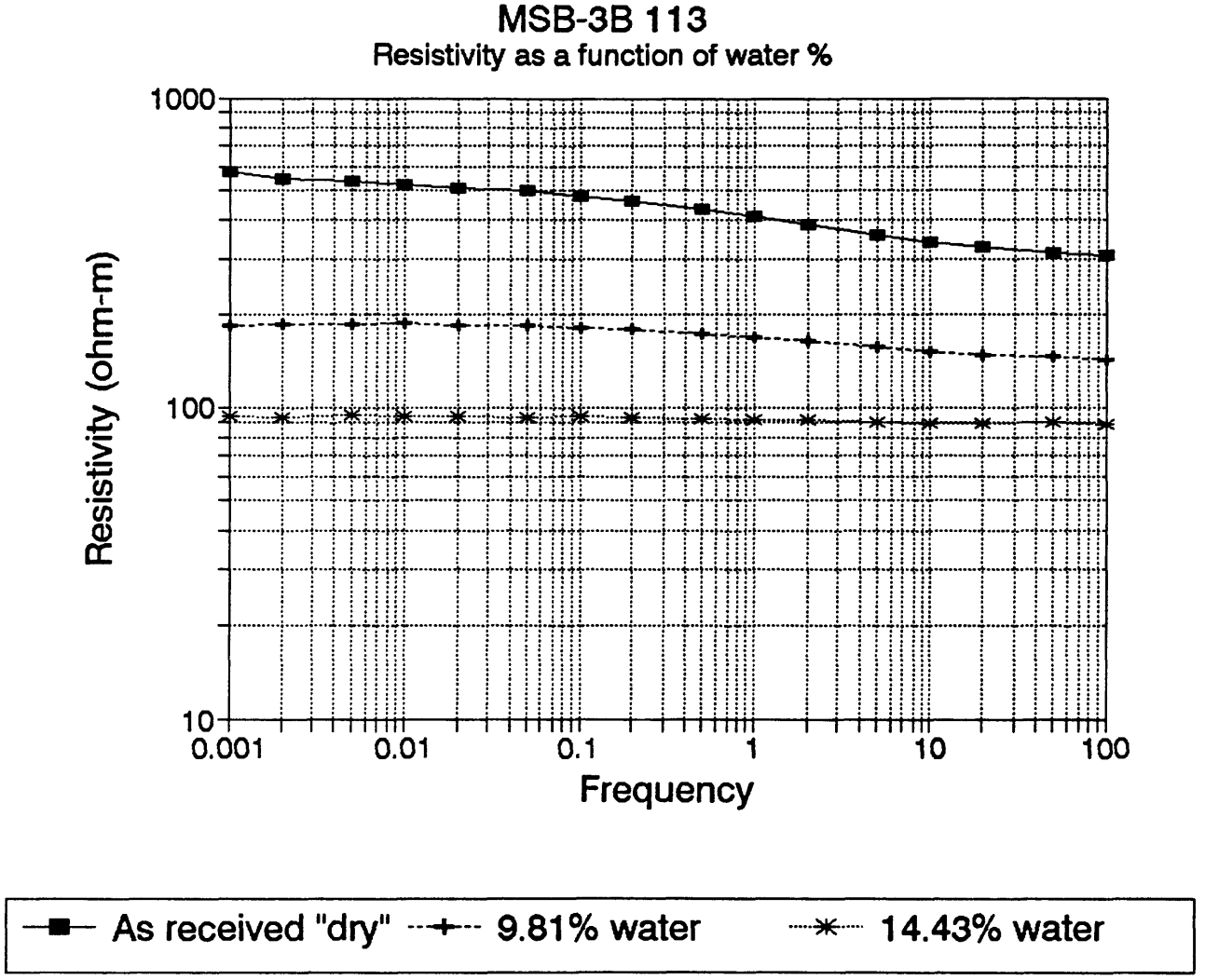
MSB-3B 113
Resistivity as a function of water %
1000
100
10
Resistivity (ohm-m)
0.001
0.01
0.1
1
10
100
Frequency
As received "dry"
9.81% water
14.43% water

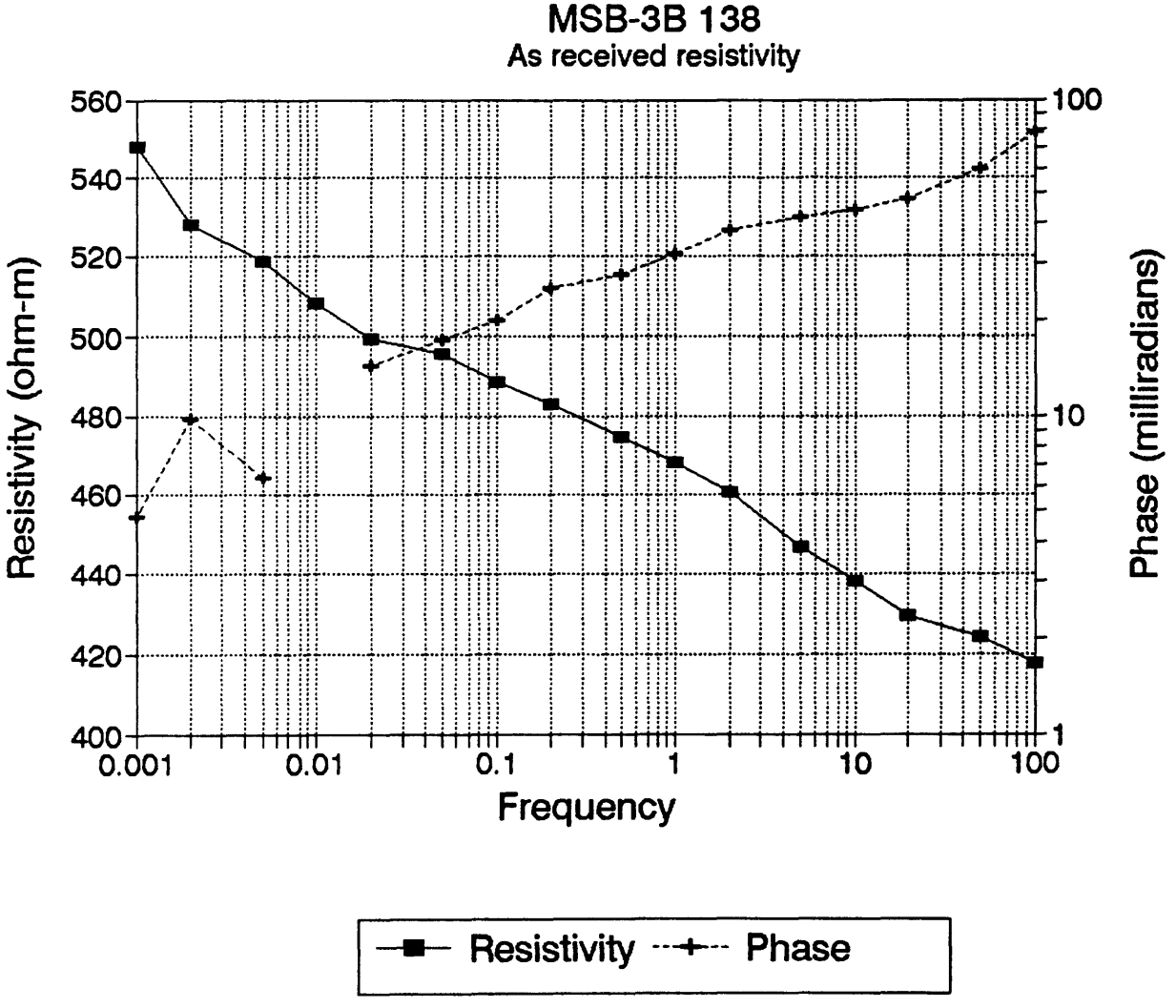
MSB-3B 138
As received resistivity
Resistivity (ohm-m)
560
540
520
500
480
460
440
420
400
0.001
0.01
0.1
1
10
100
Frequency
Phase (milliradians)
100
10
1
Resistivity
Phase

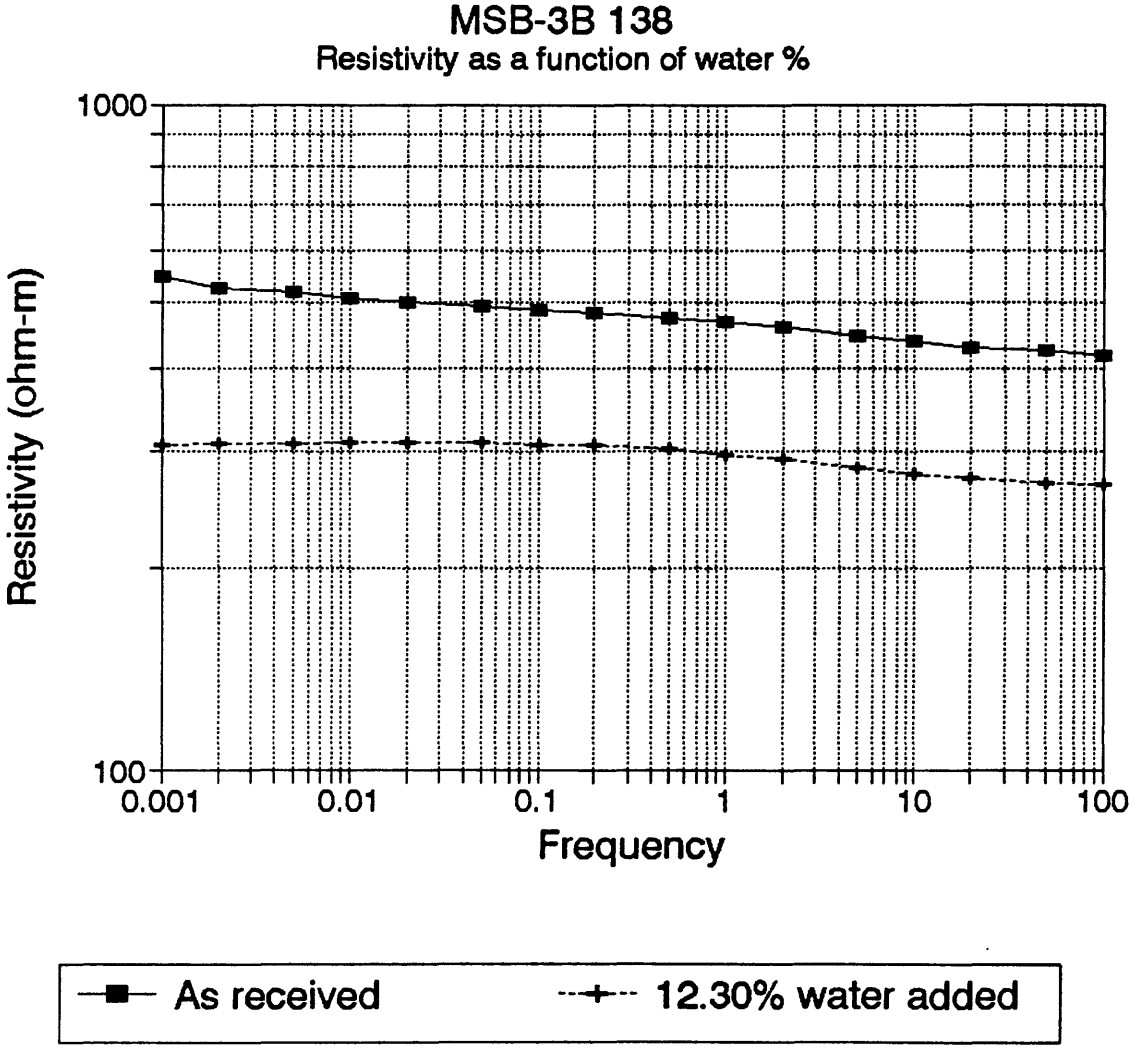
MSB-3B 138
Resistivity as a function of water %
1000
100
Resistivity (ohm-m)
0.001
0.01
0.1
1
10
100
Frequency
As received
12.30% water added

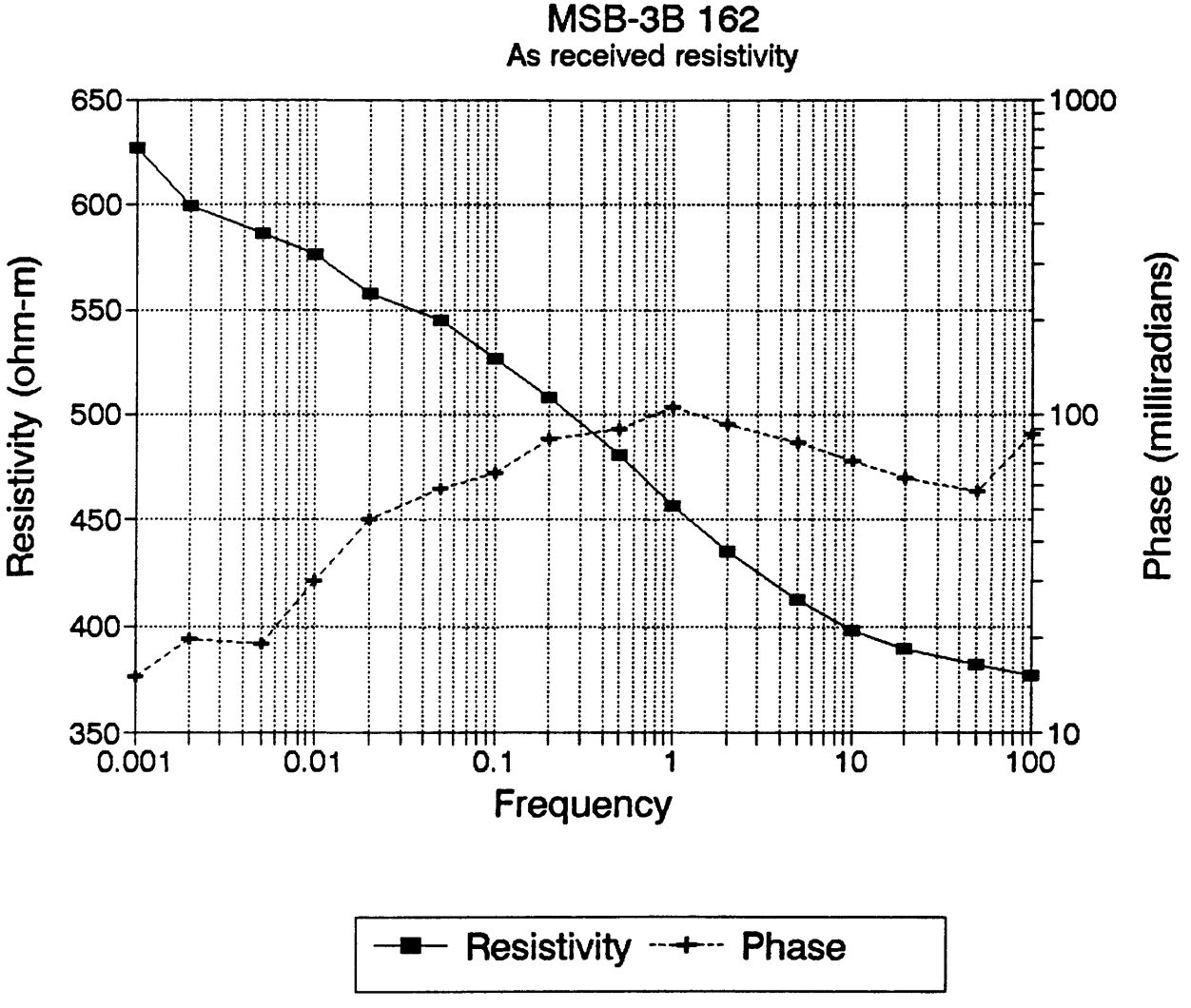
MSB-3B 162
As received resistivity
650
600
550
500
450
400
350
Resistivity (ohm-m)
1000
100
10
Phase (milliradians)
0.001
0.01
0.1
1
10
100
Frequency
Resistivity
Phase

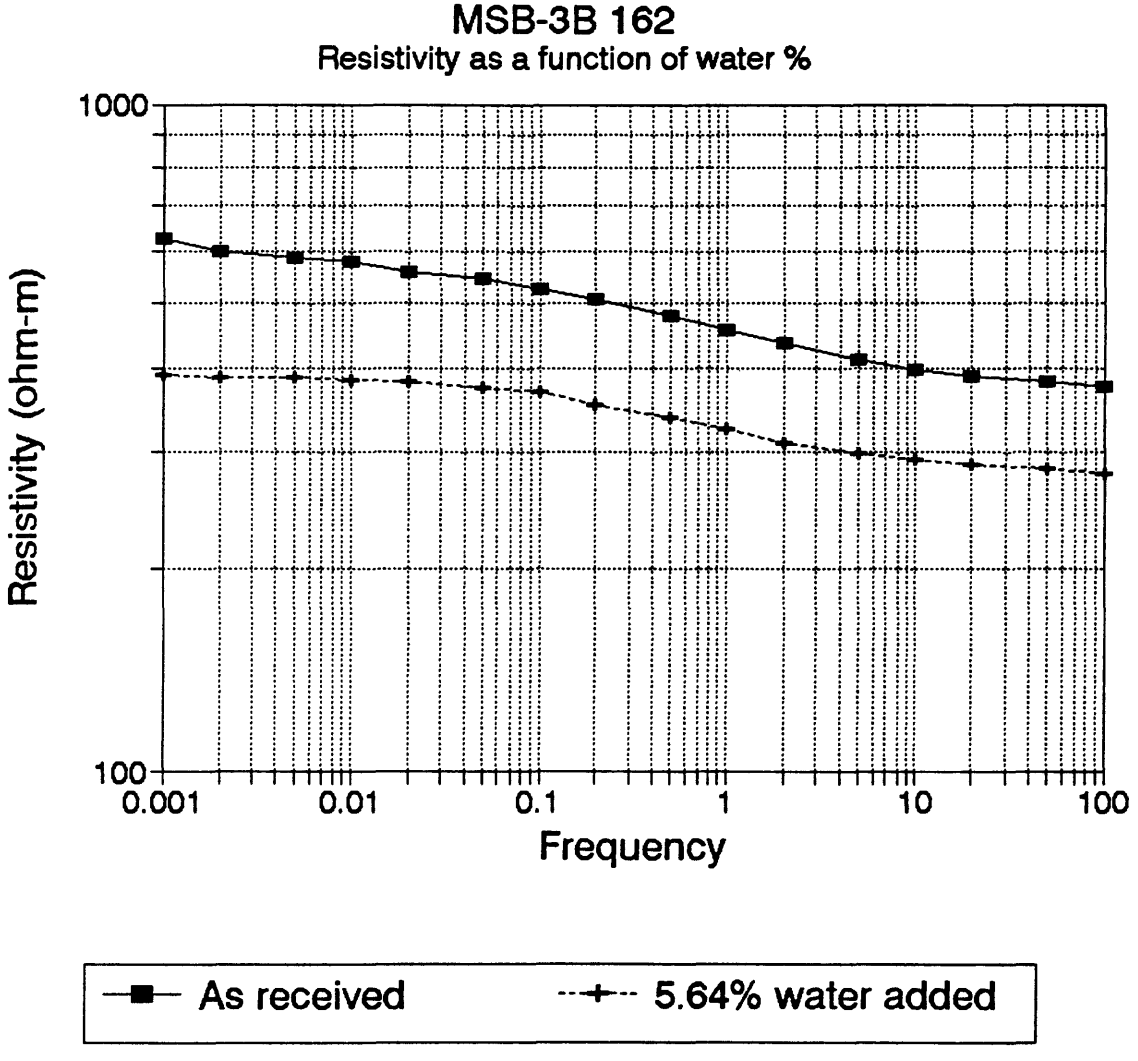
MSB-3B 162
Resistivity as a function of water %
1000
100
Resistivity (ohm-m)
0.001
0.01
0.1
1
10
100
Frequency
As received
5.64% water added

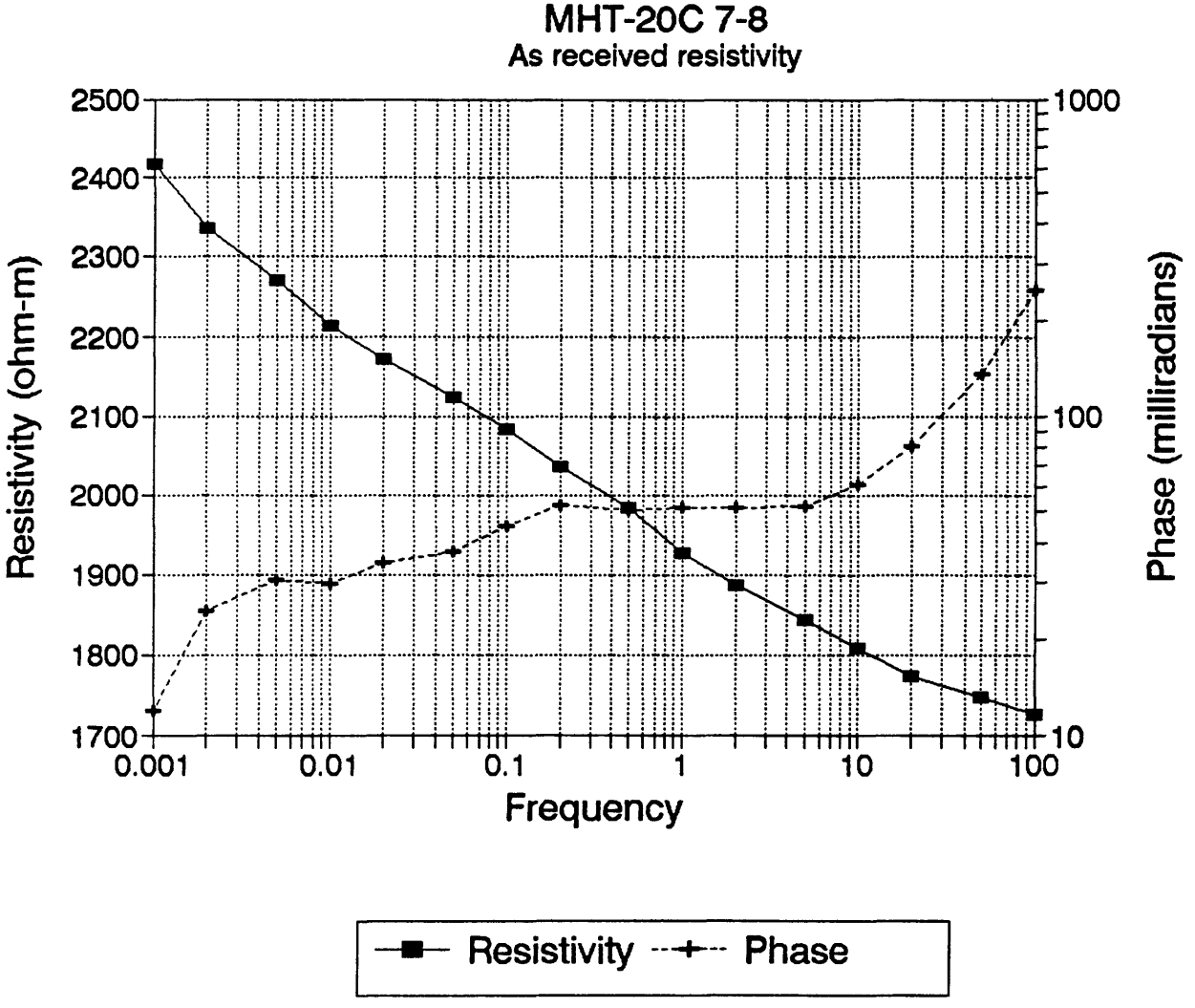
MHT-20C 7-8
As received resistivity
Resistivity (ohm-m)
2500
2400
2300
2200
2100
2000
1900
1800
1700
0.001
0.01
0.1
1
10
100
Frequency
1000
100
10
Phase (milliradians)
Resistivity
Phase

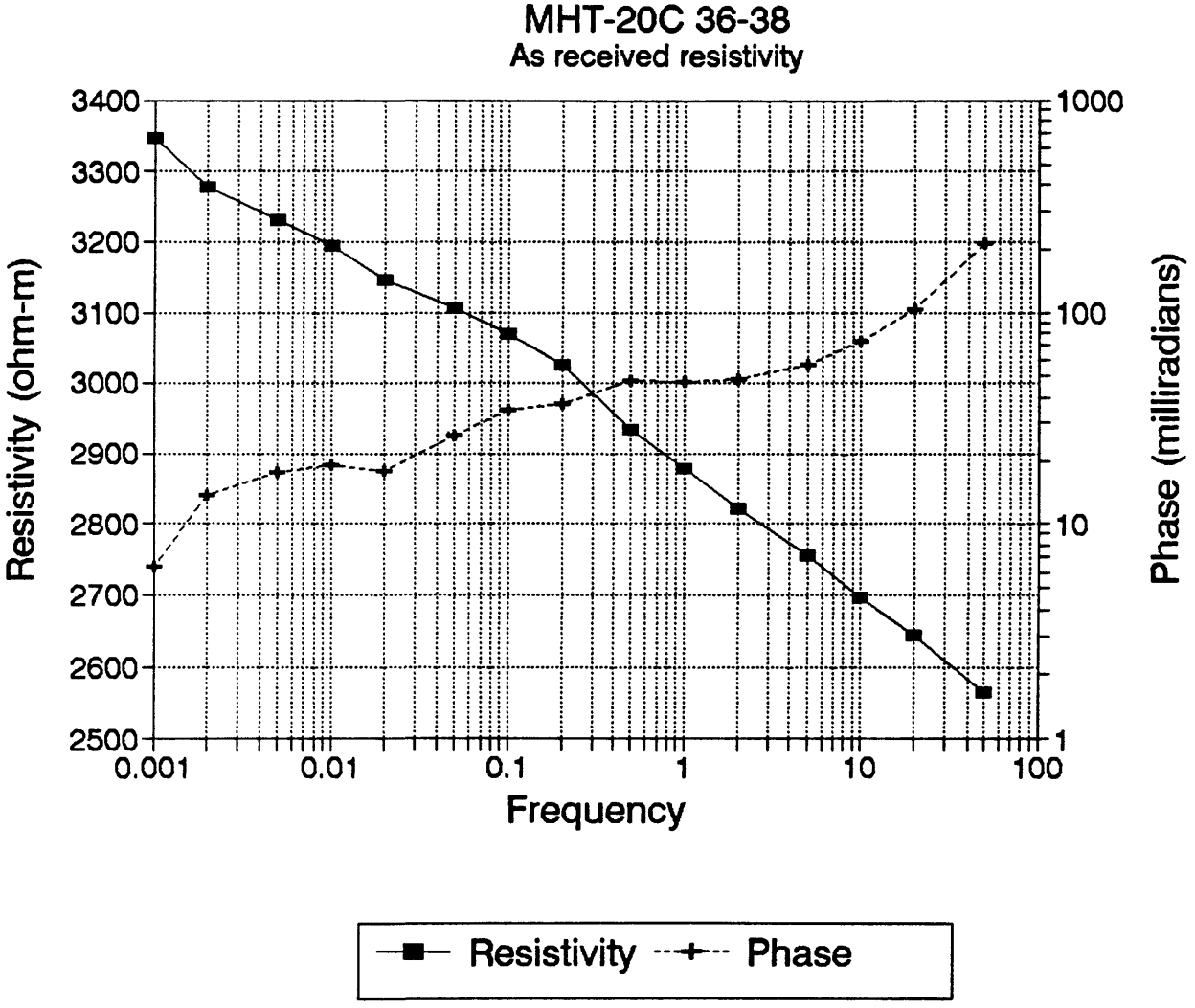
MHT-20C 36-38
As received resistivity
Resistivity (ohm-m)
3400
3300
3200
3100
3000
2900
2800
2700
2600
2500
Phase (milliradians)
1000
100
10
1
0.001
0.01
0.1
1
10
100
Frequency
Resistivity
Phase

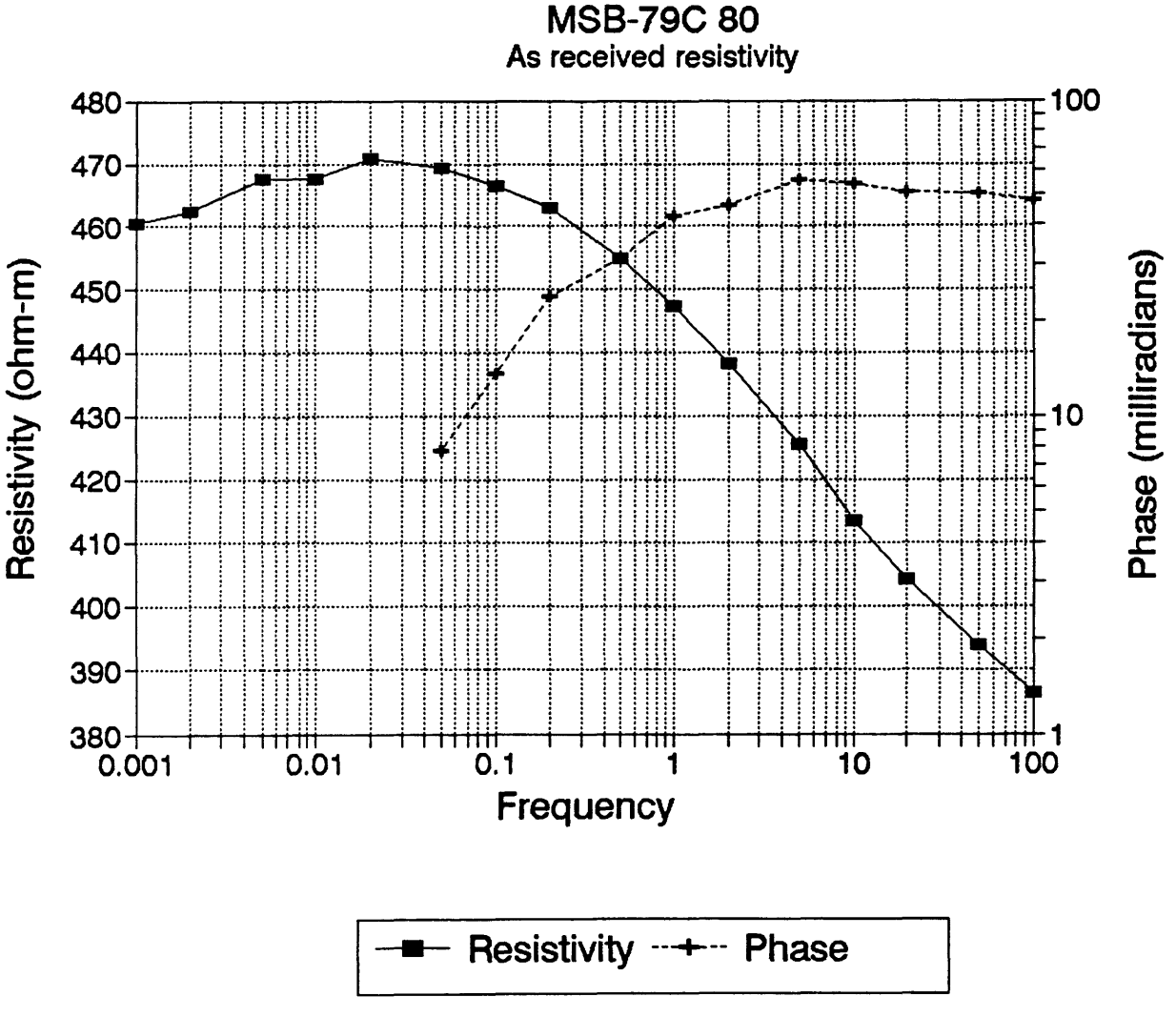
MSB-79C 80
As received resistivity
Resistivity (ohm-m)
480
470
460
450
440
430
420
410
400
390
380
0.001
0.01
0.1
1
10
100
Frequency
Phase (milliradians)
100
10
1
Resistivity
Phase

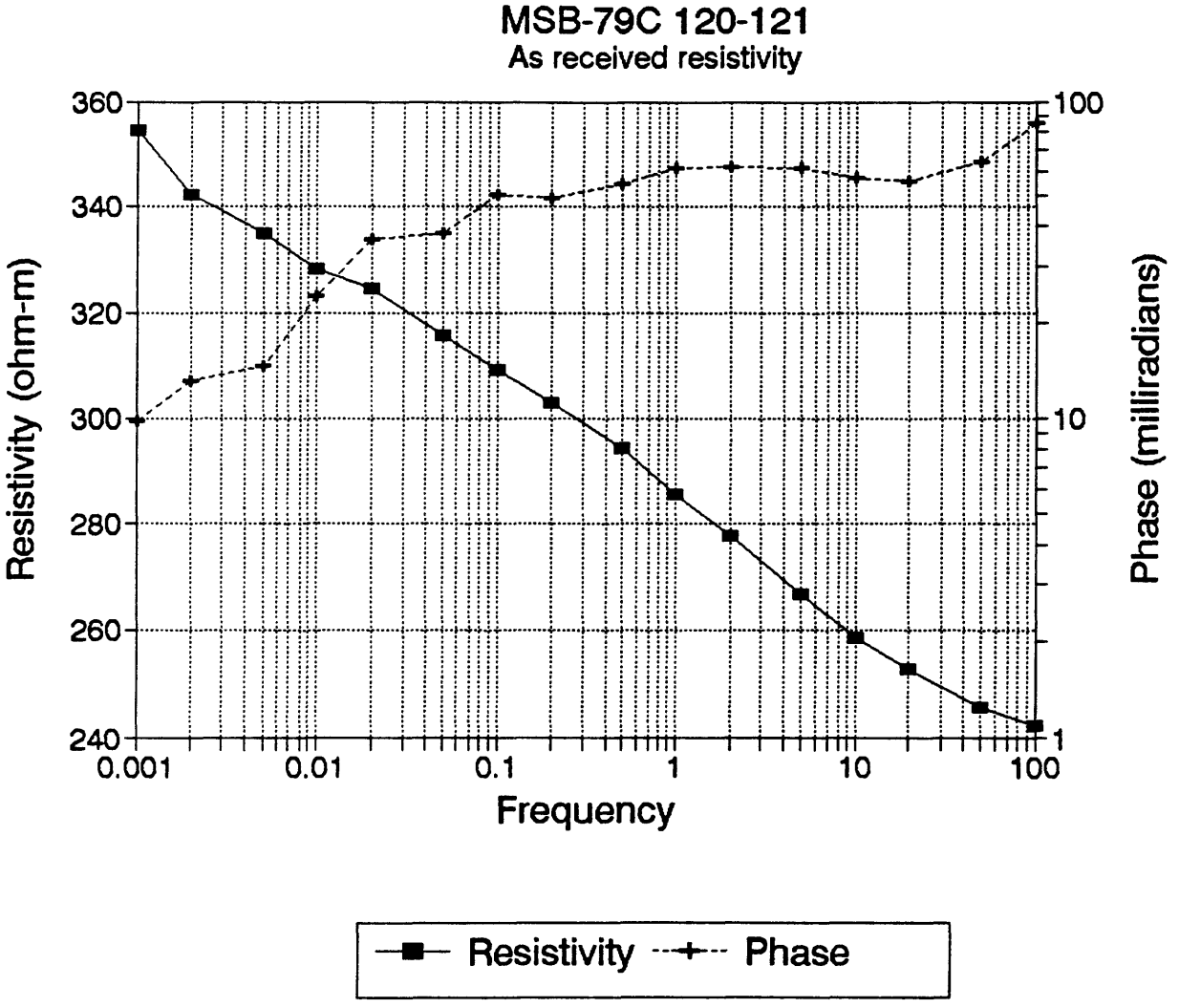
MSB-79C 120-121
As received resistivity
Resistivity (ohm-m)
360
340
320
300
280
260
240
Phase (milliradians)
100
10
1
0.001
0.01
0.1
1
10
100
Frequency
Resistivity
Phase

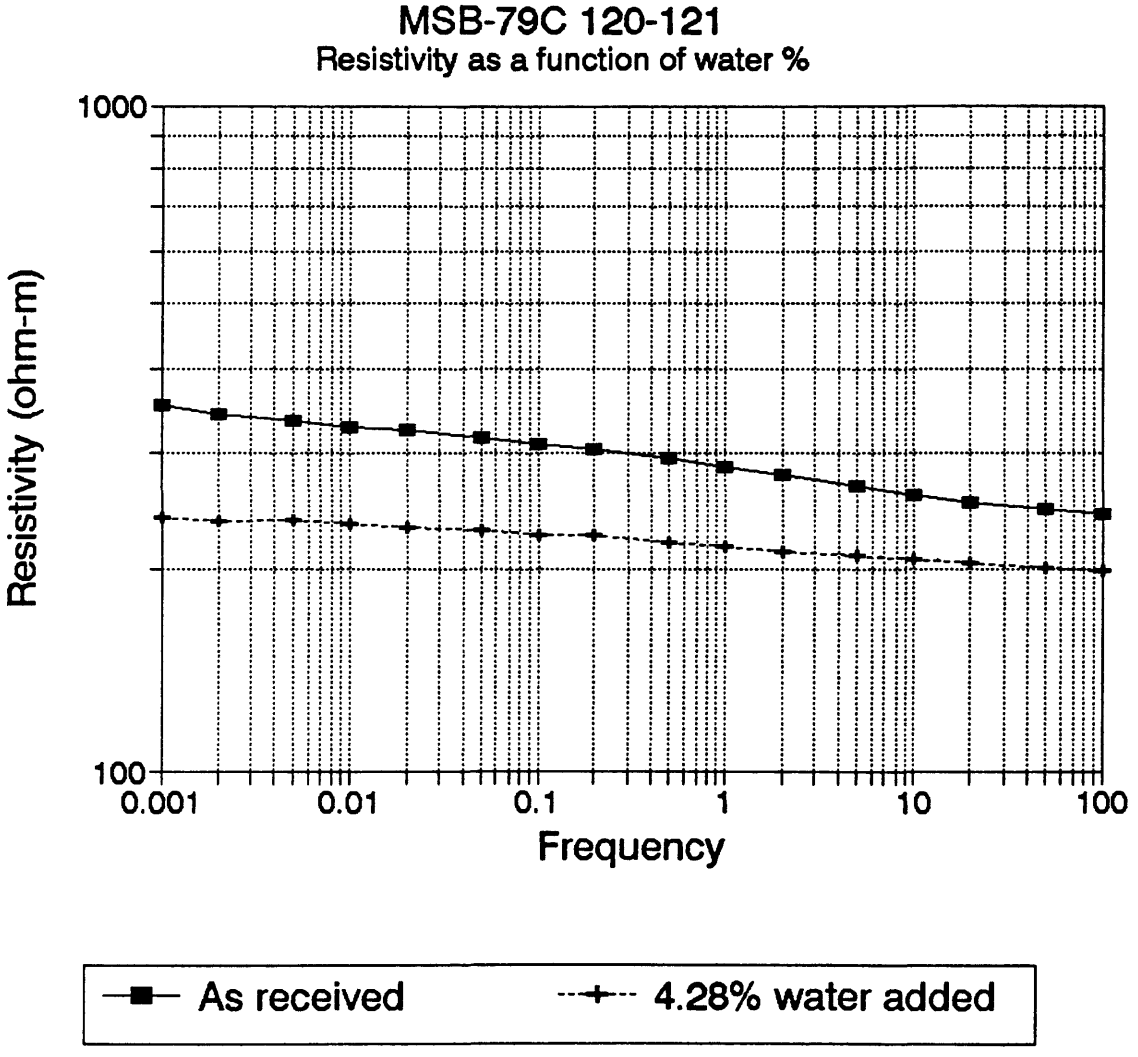
MSB-79C 120-121
Resistivity as a function of water %
1000
100
Resistivity (ohm-m)
0.001
0.01
0.1
1
10
100
Frequency
As received
4.28% water added

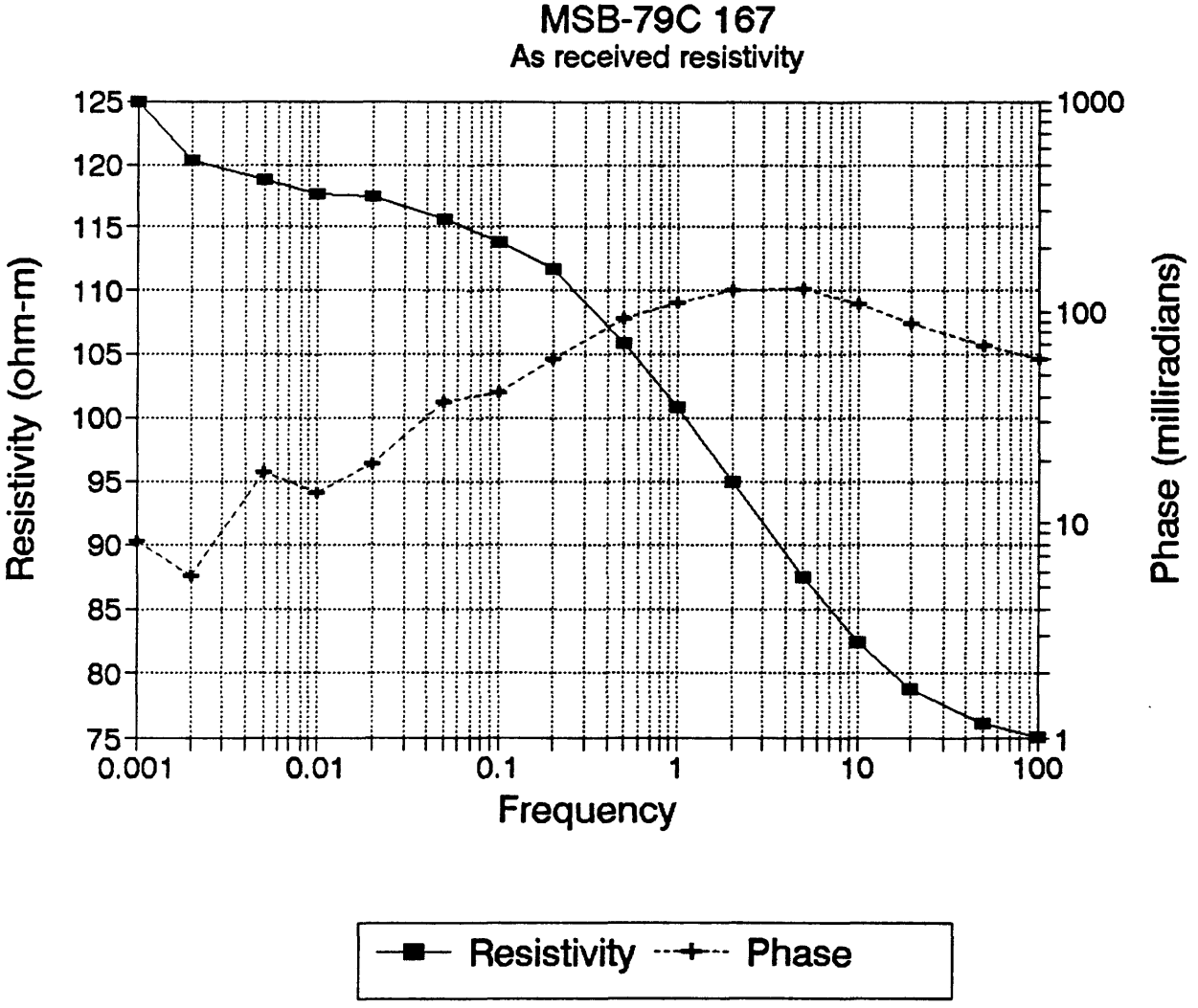
MSB-79C 167
As received resistivity
Resistivity (ohm-m)
125
120
115
110
105
100
95
90
85
80
75
0.001
0.01
0.1
1
10
100
Frequency
1000
100
10
1
Phase (milliradians)
Resistivity
Phase

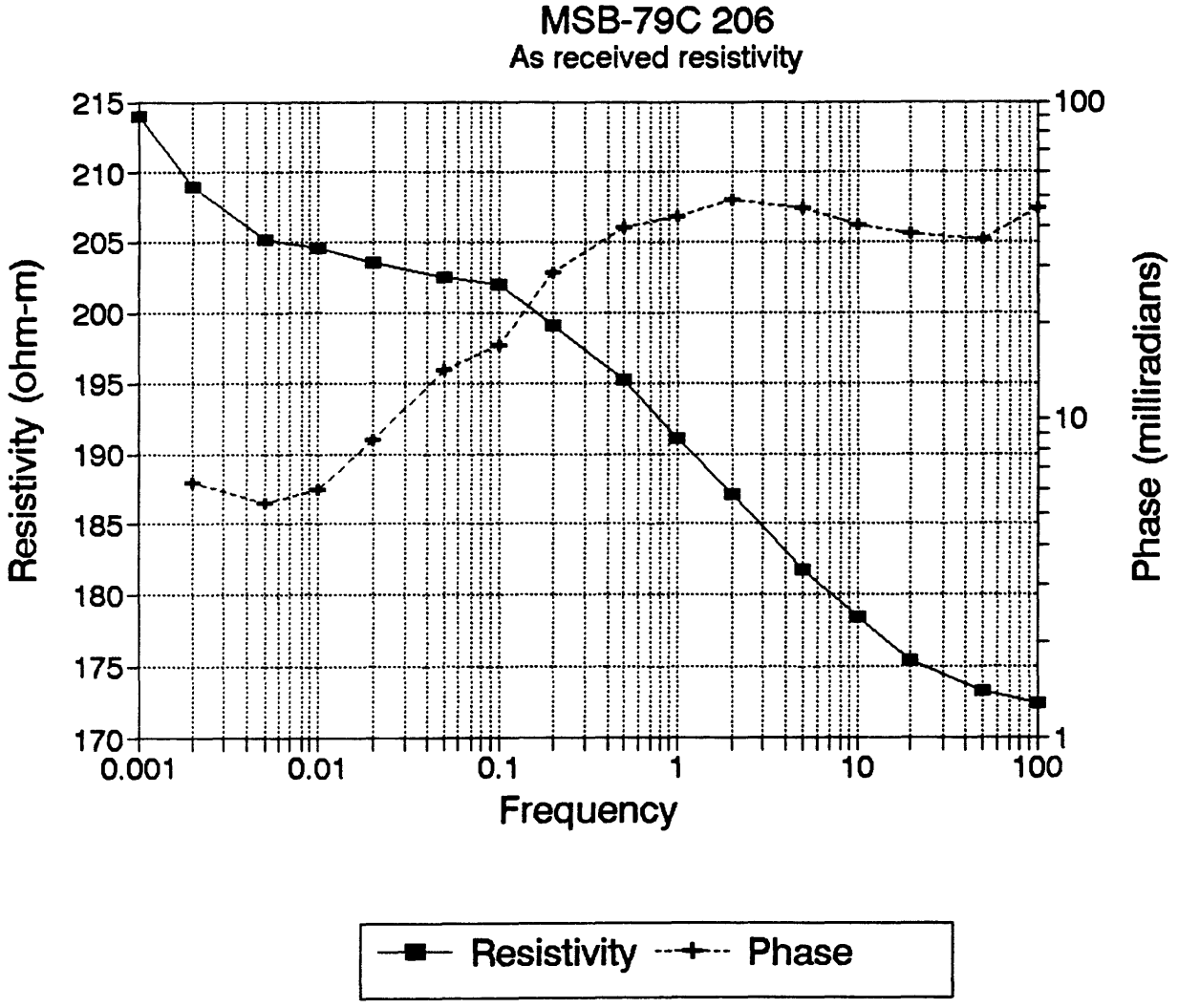
MSB-79C 206
As received resistivity
Resistivity (ohm-m)
215
210
205
200
195
190
185
180
175
170
0.001
0.01
0.1
1
10
100
Frequency
Phase (milliradians)
100
10
1
Resistivity
Phase